UNIVERSITAT DE BARCELONA

Deciphering the role of endothelial cells in the regulation of physiological and pathological white adipose tissue remodelling

Erika Monelli

Universitat de Barcelona

Facultat de Medicina

Programa de Doctorat en Biomedicina

Deciphering the role of endothelial cells in the regulation of physiological and pathological white adipose tissue remodelling

Memòria presentada per

Erika Monelli

per optar al títol de doctora per la Universitat de Barcelona.

Aquesta tesi ha estat realitzada sota la direcció de

Mariona Graupera i Garcia-Milà

en el Laboratori de Senyalització Vascular ubicat en l'Institut d'Investigació Biomedica de Bellvitge (IDIBELL)

Directora de tesi	Tutor	Doctoranda
Dra. Mariona Graupera i Garcia-Milà	**Dr. Fransesc Viñals Canals**	**Erika Monelli**

Barcelona, Junio 2017

This thesis work titled “Deciphering the role of endothelial cells in the regulation of physiological and pathological white adipose tissue remodelling” has been developed in the Vascular Signalling Laboratory at IDIBELL (L’Hospitalelt de Llobregat, Barcelona).

Financial Support:

• Gobierno de España - Ministerio de Ciencia e Inovación (MICINN). SAF2010-15661 and SAF2013-46542-P

• People Programme (Marie Curie Actions) of the European Union’s Seventh Framework Programme FP7/2013-2016/ under REA grant agreement 317250. VESSEL-317250. Title of the project: “Vascular Endothelial Interactions and Specialization”

• Instituto de Salud Carlos III (ISCIII). PIE13/00022 (ONCOPROFILE, 2014-2016)

• Generalitat de Catalunya - Agència de Gestió d’Ajust Universitaris i de Recerca (AGAUR) - 2014-SGR-725

During the present work Monelli Erika performed two secondments: one in Alexander Medvinsky laboratory, belting at the University of Edinburgh; and other in Kari Alitalo laboratory, under the supervision of Marius Robciuc, belting at University of Helsinki thanks to the financial support from Marie Curie Actions - VESSEL-317250 .

Alla mia famiglia

Acknowledgements

Lo más difícil es siempre comenzar,

the most difficult part is always to start,

la cosa più difficile è sempre iniziare.

Así que lo haré diciendo gracias, thanks, grazie, a todas las personas que me han acompañado en esta etapa de mi vida tan importante, to everyone that has been next to me in this very important part of my life e alle persone che sono sempre state al mio fianco e continuano ad esserci nonostante la distanza.

Dicho eso puedo empezar con la largaaaaaaa lista de personas que se merecen un sitio en estas primeras páginas de mi tesis.

La primera persona que quiero y debo agradecer es sin duda mi jefa…de hecho si no fuese por ella no estaría aquí ahora☺!! Muchas gracias ***Mariona*** *por haber confiado en mí y haberme dado la extraordinaria posibilidad de ser parte del grupo mas guai y divertido del mundo!! En estos 3 años y medio he aprendido mucho de ti, eres muy buena científica y te admiro tanto por eso. Gracias por dejarme la libertad de pensar, leer y discutir contigo sobre mi proyecto...no siempre nuestras opiniones han coincidido (y yo no soy nada fácil de convencer) pero al final mira que historia tan bonita ha salido!!☺ Eres muy buena jefa, siempre y cuando no entres en el lab ahahahahah ☺, a veces un poco exigente pero nadie es perfecto!! Fuera de bromas, muchas gracias de verdad por todo, por ser siempre positiva, por creer en mí y motivarme, gracias a ti he crecido mucho como científica y como persona y al final eso es lo más importante.*

Many thanks to ***Francesc Villarroya****,* ***Michael Potente*** *and* ***Arkaitz Carracedo*** *for being willing to read my thesis and be part of my thesis committee. Un gracias especial a ti* ***Arkaitz*** *por haberme dado la posibilidad de hacer parte de tu lab, aunque solo por una breve instancia, he aprendido mucho y me ha encantado estar allí...tanto que el*

tiempo se me pasó volando. Gracias también a tu grupo, y especialmente a ***Vero*** *y* ***Lorea****, por haberme ayudado con los experimentos y por ser todos tan amables y majos!! Gracias a* ***Cristina****,* ***Oriol*** *y* ***Pablo*** *por aceptar ser suplentes de mi tribunal y, más importante, por todas las ideas y las discusiones científicas que tanto han aportado a mi trabajo.*

Many thanks to the VESSELS team, it was a pleasure and a unique opportunity to be part of this network. I enjoyed all the meeting and workshop we had, and I learned something from each one of you. Thanks to the PI: ***Alexander Medvinsky****,* ***Elisabetta Dejana****,* ***Kari Alitalo****,* ***Tatiana Petrova****,* ***Christer Betsholtz****,* ***Ralf Adams*** *and* ***Adam Feiler****. And a special thanks to the fellows:* ***Sara****,* ***Anahi****,* ***Cecília****,* ***Surya****,* ***Markus****,* ***Lucia****,* ***Luana****,* ***Stefanie****,* ***Cansaran****,* ***Nebojsa****,* ***Marco*** *and* ***Rodrigo****; you made our meeting always funny!! I hope we will keep in touch. Thanks also to* ***Natalia*** *and* ***Sabrina*** *for organizing everything in a nice way! Many thanks to* ***Alexander Medvinsky*** *and* ***Kari Alitalo*** *that gave me the opportunity to stay in their lab and to experience a different scientific environment.* ***Marius****, many thanks for your help, valuable advises and the enthusiasm you showed for my project; I really enjoy the time I spent in Helsinky. Of course many thanks to* ***Essi*** *as well, you are a very nice person and it was a real pleasure to meet you.*

Muchas gracias a ***Marc Claret****, por las discusiones científicas y por tus consejos que han sido muy importantes por el desarrollo de este trabajo, y por supuesto muchas gracias por el material que unas cuantas veces he venido a coger☺!!*

Muchas gracias a ***Francesc*** *y* ***Oriol****, por vuestra ayuda y el interés que siempre habéis mostrado por cada uno de nuestro proyectos (el mío incluido aunque poco tenga a que ver con vuestra área de investigación!!). Gracias también a todas las personas que han pasado por Angio en estos años, gracias* ***Elisenda****,* ***Gabi****,* ***Lara****,* ***Agnès****,* ***Mar****,* ***Lydia****,* ***Roser****,* ***Susana****,* ***Nick****,* ***Iratxe****,* ***Patricia****,* ***Mariona****,* ***Álvaro*** *y* ***Júlia****. A ti* ***Laurita****, la reina de la puntualidad ahahhah, un gracias especial, eres una persona genial, llena de*

energía y determinada...fuiste la primera a acabar el doctorado y lo hiciste súper bien!! Gracias por las noches de fiestas, por el cotilleo y por ser una buena amiga (por supuesto cuento contigo el año que viene para volver al carnaval canario jajajajaj)!! Gracias ***Alba****, que haríamos sin ti?! Gracias por ser siempre disponible y ayudarnos (sin quejarte)…gracias por las PCR, los reactivos, los destetes…y mucho mas, gracias por ser siempre sonriente y amable aunque tengas mucho trabajo…eres muy buena persona y me alegro por haber compartido estos años contigo ☺.*

GRACIAS a tod@s l@s ONAs... de ahora y de cuando empecé... habéis hecho de mi doctorado una experiencia única que nunca olvidaré en mi vida. He aprendido mucho de cada uno de vosotros y sin duda habéis hecho de mi mejor persona. ***Helenita****, la persona más dulce y disponible al mundo...cuando llegué tú estabas en Londres pero todos me hablaban tan bien de ti, de lo estupenda que eras que no veía la hora de conocerte!! Gracias por todo lo que me enseñaste con tanta paciencia y claridad. Eres una persona muy trabajadora, pero lo que más admiro de ti es tu capacitad de ser siempre amable con todos y ayudar cualquier persona lo necesite, independientemente del tiempo de que dispongas. Me alegro mucho de haber compartido contigo mi primer año de doctorado, eres genial☺!* ***Adri****, la que siempre decía "ir tirando yo llego en 10 minutos" ajajajaj mas o menos!! Eres sin duda la mejor maestra que exista!! Muchas gracias por todo lo que me has enseñado. Gracias* ***Fonsequita****, mi compi de doctorado, de viaje, de escritura de tesis...y mucho más!! Eres simplemente única... te admiro mucho por tu forma de ser, amable, alegre, siempre sonriente, habladora, amiga con todos y dispuesta a escuchar los problemas no solo de tus amigos si no de quienquiera lo necesite. Tienes un dono especial...sabes ver lo que las personas no quieren mostrar, eres la única que siempre ha sido capaz de intuir cuando me pasaba algo y de hacerme hablar aunque yo no quisiera hacerlo...gracias de verdad por ser lo que eres. Todo el mundo te quiere y no me sorprende. Eres una buena amiga y te quiero mucho.* ***Angulita****, mi competidora en tono de voz... cuando hablamos las dos casi se rompen los cristales ahahahh!! Mil gracias por tus preciosos consejos (siempre acertados), por tu alegría y tu risa inconfundible que*

llenan el lab de vida. Eres un huracán de energía, bueno eso a partir del mediodía ajajajaj!! Gracias por tu ayuda y apoyo sobretodo en esta última etapa del doctorado...y gracias por creer en mi mucho más de cuanto lo haga yo misma. Eres una persona honesta, directa, luchadora, trabajadora, muy divertida (por supuesto) y feliz!! Ha sido un placer compartir contigo estos años, en el lab y sobretodo fuera del lab y aunque yo no sea muy buena para expresarlo te quiero mucho ☺ ! ***Iñigito****, un ONA forever!! Llegamos casi al mismo momento en el lab...tú el orden y yo el caos ajajaja!! Eres una persona increible... sensible, divertida y tan organizado, no sé como lo haces!! Muchas gracias por todo, y a ver cuando quedamos por la próxima carrera o triatlón☺...me encanta hacer deporte con un amigo como tú☺ !!!* ***Jordi****, has estado con nosotros muy poco tiempo pero aun así me has enseñado tanto. Fue un placer tenerte con nosotros ☺ !! Muchas gracias!!* ***An****, the sweetest animal lover I have ever met!! My first bench neighbour, poor you...I am a disaster I know it!! You have been part of our group only few months but it was a real pleasure to meet you and your crazy Puma!! I miss you, crazy party-girl :) ... but I am happy you find your way. I hope to see you soon and I can't wait to hear about your summer in Tanzania saving animals!!* ***Piotr****, the most sensitive person of the group. Many thanks for being so nice with me and for listening (patiently) anytime I was stressed and I complained about everything hihihih!! Many, many thanks for reading my thesis, I hope I can return it in the future somehow (although you don't really need me to revise your English because you are the best!). You are very smart, determined and super organized all qualities that make you a good scientist...and, most important, you are a very nice person maybe a bit negative but we have time to work on it ahahah ☺ !!! Besitos!!* ***Jazz****, la nuova italiana del gruppo! Sei arrivata in un momento molto difficile, con tre persone isteriche scrivendo la tesi...ma nonostante questo sei riuscita a portare energia, felicità e allegria nel lab!! Sei una persona solare e trasmetti serenità...grazie di cuore per il tuo sostegno!!* ***Pilar****, mi nueva compi de bench y de trabajo!! Has llegado hace poco pero ya has hecho mucho por mí, gracias de verdad por tu ayuda y comprensión.* ***Laia****, the best lab manager ever!! Que sería el lab sin ti?! Simplemente el reino del caos tal cual era antes de ti ajajajaj!!*

Gracias por tu alegría y energía positiva y gracias por habernos invitado en tu maravilloso castillo "princesa Laia" ajajajaja…a cuando la próxima!? ☺ ***Judit****, mi estudiante favorita☺, gracias por el empeño y determinación que has demostrado cada día, eres muy lista y seguramente tendrás un brillante futuro. Gracias por ayudarme con los experimentos, estás haciendo un gran trabajo y lo estás haciendo sola, lo que ya es un gran mérito.* ***Xica****, gracias a ti también!! Ha sido un placer tenerte con nosotros unos meses☺. Gracias también a* ***Maria*** *y* ***Eric****, sois unos craks!! Y* ***Alex****, a pesar de que no fue fácil enseñarte, y de que no nos hemos llevado muy bien, eres una buena persona y te deseo mucha suerte por tu futuro.*

Gaby*, la mamá de tod@s, gracias por los consejos, los abrazos, el "buenos día" que nunca te olvidas, y bueno por ser la maravillosa persona que eres. Gracias por haberme aguantado en los días malos y por haberme ayudado y escuchado cuando más lo necesitaba…eres una persona especial y te voy a echar de menos.*

Pau*, como ves no me olvido de ti ahahaha!! Muchas gracias por todos los experimentos que has hecho por mí, pero sobre todo por las risas que nunca faltan cuando nos vemos!! Eres una persona muy divertida y me encanta colaborar contigo!! ☺ Gracias también a* ***Josè Carlos*** *y* ***Petra*** *por haberme ayudado con unos cuantos experimentos y por ser siempre disponibles.*

Gracias también a los CMPs, nuestros compis de lab y de risas!! Los antiguos ***Raffa, Clara, Didac, Javi*** *y* ***Estefania*** *y los de ahora* ***Francy*** *y* ***Juan****.* ***Raffa****, la súper woman!! Lo tienes siempre todo bajo control, haces mil cosas a la vez y te salen perfectas...te admiro mucho por esa forma de gestionarlo todo sin pánico y con una eficiencia increíble. Eres una buena amiga y la mejor compañera de playa del mundo ☺ ahahah (tu y Simone también)!! PS: grazie mille per tutti i taralli (buonissimi) che ci hai portato tanto spesso in lab!!* ***Clarita****, gracias por tu amistad, alegría, locura y energía!! El lab sin ti ya no es lo mismo!* ***Javiiii****, cuanta paciencia has debido de tener con tantas chicas chillonas como nosotras (siempre me acordaré de ti y tus cascos!!)*

ahahahah!!! Muchas gracias por haberme motivado desde el principio a hablar castellano, ya ves, ahora casi se me ha olvidado el italiano!!! De verdad ha sido un placer compartir contigo un tiempo en el lab ☺. ***Estefania****, no te quedaste mucho pero lo suficiente para acostumbrarnos a tus abrazos y besos!! Gracias por la alegria y el cariño con que llenaste el lab ☺.* ***Francy****, many thanks for being so nice.* ***Juan****, muchas gracias a ti también, es divertido compartir lab contigo... nunca faltan las risas ahahah!!*

Gracias a toda la gente del COM, porqué sois los mejores compañeros de trabajo que se pueda imaginar!! Siempre me quedaré con un buen recuerdo de todos vosotros, de las novatadas, de las COMçotads y de lo bien que se trabaja en un ambiente tan alegre como el COM. Gracias a todos los OMs, ***Oscar****,* ***Olga****,* ***Roser****,* ***Silvia*** *(mi compañera de escritura),* ***David*** *y* ***Santi*** *(por ser siempre dispuesto ad ayudar). Muchas gracias también a* ***Maribel****,* ***Dani*** *y* ***Edu****. Muchísimas gracias a* ***Angels*** *y* ***Antonia*** *porqué sois el pilar del COM, sin vosotras no sé lo que haríamos! Muchas gracias por haberme ayudado cuando lo he necesitado y por ser tan disponibles y amables con migo. Gracias a los IFs,* ***Isabel****,* ***Esther****,* ***Dani*** *y* ***Joaquim****.* ***Judith,*** *un gracias especial va por ti ☺, eres una persona maravillosa, gracias por tu ayuda y ánimos en los momento de crisis máxima, y gracias también por las risas y por ser siempre tan dulce y amable.* ***Andrea****, el italiano DOC ahahah, que decirte...muchas muchas gracias por tu apoyo y tu amistad, por haberme escuchado cuando lo necesitaba y por tus sabios consejos (dall'alto della tua venerabile età!! ahahah ☺). E grazie per le chiacchiere e le risate, per i tuoi "que bonitooooo" e i "quindi" que tanto te encanta decir ahahah☺!!! Gracias también a otros compañeros de pasillo como* ***Giulio****,* ***Antonio*** *(grazie mille per la tua disponibilità e l'impegno con cui hai seguito il mio progetto in questi 3 anni e mezzo, e per essere stato sempre clemente nelle varie commissioni di seguimiento!!! ahahahah),* ***Pepelu****,* ***Pablo*** *y* ***Javi*** *(sin duda un gran secretario!).*

Un gracias especial a ***Catarina*** *y* ***Cala****, sois los mejores compis de piso que se pueda imaginar, este año con vosotros ha sido estupendo. Gracias por haberme aguantado y ayudado in estos meses tan complicados.* ***Catarina****, la portuguesa☺, es verdad que*

entre semana coincidimos poco pero cuando lo conseguimos es siempre divertido pasar un rato juntas y mirar nuestra serie favorida..."La que se avecina"...creo que ya somos adictos (los tres)!! También eres mi compi de sala VIP en Opium y Sutton...ahahahha y colarse a la entrada es un arte que conocemos muy bien!! Gracias de verdad por todo, te voy a echar de menos. ***Cala****, el canario loco que ha traído el caos en este piso (y que habla un idioma suyo un poco rarito ajajajaj ☺)!! Es difícil encontrar las palabras justas para agradecerte por todo lo que has hecho por mi...eres único por tu forma de ser, siempre alegre y cariñoso... ti voglio bene y lo sabes!! Gracias por los días inolvidable en Tenerife, las excursiones a esquiar y las fiestas...y básicamente por ser lo que eres... Conociéndote he ganado más que un amigo, una persona especial que, sin duda alguna, siempre tendrá un sitio en mi corazón. Gracias al equipo biotech. ,* ***Naty*** *y* ***Sara*** *sois estupendas!! Muy diferentes la una de la otra,* ***Naty*** *súper cariñosa todo abrazos y besos y* ***Sara*** *muy fuerte y independiente, pero ambas con un gran corazón y tanta alegría. Gracias* ***Marina****, tu igual que yo, la "compañera de piso" adoptada en el grupo del máster!! Una chica muy dulce y cariñosa que siempre cuida de las personas a la que quiere ☺. Chicas ha sido una suerte conoceros a las tres y independientemente de donde nos lleve el futuro espero no perderos!*

Un grazie di cuore al club delle zittelle... ***Elly****,* ***Emmina****,* ***Mery****,* ***Lalla*** *e* ***Fede*** *siete meravigliose e non potrei immaginare la mia vita senza di voi. NOI il club del venerdì sera allo Snoopy, il solito gradino, le dive della disco...quante risate e quanti bei ricordi!!* ***Elly****, la mia compagna di banco preferita dall'epoca delle medie...una vita insieme...eravamo delle bambine di 11 anni quando ci siamo conosciute e adesso si avvicinano i 30!! Quante avventure abbiamo passato insieme, soprattutto all'università...serate folli e indimenticabili!! Tu ci sei sempre stata e sai tutto di me, ti voglio un bene infinito e te ne vorrò sempre.* ***Emmina****, un tesoro di amica :) l'avvocatessa più fashion che conosca!! Pazzerella e dolcissima, ti voglio tanto bene...grazie per la tua energia e allegria sei una persona meravigliosa.* ***La Mery****, ti ho conosciuta come l'amica di pallavolo dell'Elly, all'epoca chi l'avrebbe mai immaginato*

che sarebbe nata un' amicizia così!! Grazie per avermi sempre ascoltato e sopportato nei momenti difficili...so che sono una testa dura e ci vuole molta pazienza con me!! Ti voglio bene. ***Lalla*** *e* ***Fede****, le due fruttine di mare più belle del mondo!! Evviva l'azienda "ragazze al top spa" ☺ !! Quante risate ci siamo fatte...la vostra fantasia è incredibile...e la gente che ci crede anche, se ci penso non riesco smettere di ridere!! Ambrogio dov'e l'elicottero?! Le donne del Pineta, seconda residenza MiMa!! Vi voglio troppo bene, grazie per esserci sempre state. Amiche, potrei scrivere un libro su voi 5 ma è il momento di smettere...semplicemente vi adoro e ringrazio il destino che ci ha fatto incontrare.*

Grazie ***Ele****, la mia compagna di uni, per 5 lunghi anni che in realtà sono volati!! Quante risate nelle ore di laboratorio di chimica, o con il fantastico Signor Bondi e i batteri con odore a mela golden!! Abbiamo condiviso momenti duri insieme, l'ansia degli esami, lo stress di ben due tesi anzi ormai 3 cara dottoressa...ma ci siamo sempre aiutate a vicenda e ce l'abbiamo fatta!! Grazie per esserci sempre stata, ti voglio bene e te ne vorrò sempre. E grazie per i pranzi in compagnia di Polach e Riki, mi hai presentato due persone stupende che mi hanno fatto ridere come una pazza con le loro imitazioni e aneddoti universitari!! E ovviamente grazie* ***Riki****, siamo persone molto diverse ma nonostante questo ti considero un buon amico, lo so ci vediamo molto poco ma è sempre piacevole far due chiacchiere con te. Grazie di cuore per i tuoi buoni consigli e per l'aiuto morale che mi hai dato soprattutto in questi ultimi mesi...so che mi capisci tanto come io capisco te...forza e coraggio che se sono sopravvissuta io puoi farlo anche tu!!*

Un GRAZIE anche a te ***Rachele****, la mia prima supervisor di lab, e la migliore che abbia mai avuto. Tu mi hai insegnato tantissimo, con tanta pazienza mi hai fatto diventare giorno dopo giorno sempre più autonoma e sicura di me stessa...senza di te non so se sarei arrivata dove sono. Grazie, grazie e ancora grazie di cuore, sei e continui ad essere un modello per me, non solo come scienziata ma anche come persona. Ti voglio bene e*

anche se vederci è difficile mi fa piacere sentirti ogni tanto e renderti partecipe della mia vita.

Grazie alle mie scurfette!! ***Chicca***, ***Ali*** *e* ***Chia*** *siete stupende ☺!! L'atletica ci ha fatto conoscere e la Puglia ci ha reso amiche inseparabili!!* ***Chicca***, *sei unica, energia allo stato puro...il primo anno di università insieme a te è stato incredibile! Quante serate indimenticabili nella mitica DUNA dei tempi d'oro...e come dimenticare il Mamma Orsa della domenica, e le occhiaie del giorno dopo a lezione!! Grazie per essere la persona meravigliosa che sei...ti voglio un mondo di bene.* ***Ali*** *e* ***Chia***, *posso dire un' amicizia nata per caso...non ricordo come nacque l'idea di andare in vacanza insieme ringrazio il caso per avermi dato l'opportunità di conoscervi. Siete due amiche stupende...Ali la donna dai mille impegni, ancora non so come tu faccia a fare tutto!! E Chia, la golosina di dolcetti più tenera che conosco!! Ragazze vi voglio troppo bene!*

Grazie mille anche a tutti i miei amici di Solara, quelli dell'infanzia, quelli che anche se non li vedi per mesi quando ci si rivede è come se il tempo non fosse passato...grazie ***Nicole***, ***Strava***, ***Gola***, ***Spezza***, ***Alle, Chicco***, ***Albi***, ***Pella***, ***Marty*** *e* ***Eli***.

Grazie alla mia famiglia, la mia ***mamma*** *e il mio* ***papi*** *che mi hanno sempre sostenuto nelle mie scelte e hanno fatto l'impossibile per aiutarmi a realizzare i miei sogni. Il mio spirito nomade mi ha portato lontano da casa ma non vi siete mai lamentati per questo, e ogni volta che torno a casa mi accogliete come una principessa...grazie di cuore per tutto quello che avete fatto per me, e anche se non ve lo dico spesso vi voglio tanto bene. Grazie* ***Elisa***, *la mia sister e rompi scatole come tutte le sorelle maggiori!! Siamo due persone molto diverse, quasi il giorno e la notte, ma nonostante le mille discussioni per motivi inutili sai che in realtà ti voglio bene...ti ho sempre adorato e ti vorrò sempre bene...sei mia sorella e farai sempre parte della mia vita. Grazie* ***nonnina Marta***, *ormai sei vecchietta ma sei sempre la mia nonna e ti voglio tanto bene anche se a volte ti strozzerei!! Un pensiero anche al* ***nonno Mondo***, *la* ***nonna Maria*** *e il* ***nonno Bassoli****...purtroppo non siete più qui fisicamente ma so che mi state guardando dal*

cielo e spero siate orgogliosi della persona che sono diventata. Grazie alla mia pazza cuginetta preferita...si ***Michi*** *parlo di te..la mia seconda sorella!! Grazie per essere sempre carica come una molla...quando ci sei tu è impossibile annoiarsi!! Ogni tanto ripenso al periodo di pazzia quando la frase tipica era <mamma esco con la Michi ma stasera non torniamo tardi>...no no infatti non tornavamo tardi ma la mattina presto ahahhaah ☺!! Ti voglio bene cuginetta e te ne vorrò sempre!! Si,* ***Marco****, adesso arriva anche il tuo turno, grazie "cuginetto" grande e anche tu pazzerello...siete due Bellodi che ci vuoi fare...avete il marchio di fabbrica!! Con voi due le risate non mancano mai e anche per questo vi adoro entrambi. Grazie* ***Marilena*** *e* ***Nubes****, non siete zii ma è come se lo foste...sempre presenti nei momenti importanti della mia vita da quando sono nata fino ad oggi, vi voglio bene. Grazie cuginetta* ***Giuli****, so che non sarai presente alla mia tesi ma sei sempre stata presente nelle occasioni importanti per cui ti posso perdonare ☺!! Scherzi a parte, sai che ti voglio bene e spero di vederti presto. Grazie anche allo* ***zietto Alberto*** *(uno sciatore provetto!!),* ***zia Nives****,* ***zio Gianni*** *e* ***tata Chiara****, vi voglio bene.*

Y así se acabaron los agradecimientos...si se me ha olvidado alguien pido perdón, y si os parecen muy largos y demasiado sentimental, pues lo siento pero me encanta escribir☺... además la tesis doctoral solo se hace una vez en la vida (por suerte) así que hay que aprovechar!! Y para acabar de la misma forma que empecé os agradezco otra vez en todos los idiomas que hace falta poner...

Muchas gracias a todos,

many thanks to everyone,

grazie mille a tutti.

Abstract

In response to nutritional variation, white adipose tissue (WAT) undergoes a physiological remodelling that involves qualitative and quantitative changes in resident cells and is coordinated with angiogenesis. In a condition of chronic over nutrition WAT expansion is associated to insufficient vascularisation which in turn leads to local hypoxia, inflammation and adipocytes death (hallmark of obesity). Currently, enhanced WAT angiogenesis is believed to be a promising intervention to ameliorate obesity associated metabolic dysfunctions. However, we still lack understanding of the cell intrinsic function of endothelial cells in WAT remodelling. Here we take advantage of our mouse model of PTEN (a dual lipid/protein phosphatase that counterbalance the activity of PI3K) deletion in ECs to promote vessel growth, in a cell autonomous manner. To this end, we crossed $Pten^{flox/flox}$ mice with $PdgfbiCreER^{T2}$ transgenic mice that express a tamoxifen-inducible Cre recombinase in ECs; 4-hydroxytamoxifen was administered *in vivo* at postnatal day 1 (P1) and P2 to activate Cre expression.

Increased ECs proliferation, induced by PTEN loss, promotes vascular hyperplasia exclusively in WAT and leads to a progressive loss of WAT mass. PTEN null ECs undergo a metabolic switch towards an oxidative metabolism; in vivo inhibition of β-oxidation is sufficient to revert both vascular hyperplasia and loss of WAT mass. Enhanced adipose vascularisation prevents from high fat diet induced WAT hypertrophy, limits body weight gain and improves glucose tolerance. Taken together our results suggest that, under obesogenic stimuli, more functional ECs prevent unhealthy WAT expansion and consequently the onset of obesity related comorbidity.

Contents

List of figures

Abbreviations

4E-BP1	Eukaryotic translation-initiation factor 4E binding protein 1
Acadm	Medium-Chain Specific Acyl-CoA Dehydrogenase
Acads	Short-Chain Specific Acyl-CoA Dehydrogenase
ACC1	Acetyl-CoA Carboxylase1
ACC2	Acetyl-CoA Carboxylase2
ACLY	ATP-Citrate LYase
ACS1	Acyl-CoA Synthetase
ACSL	Acyl-CoA synthetase
ADIPOR1,2	Adiponectin Receptor protein 1 and 2
AGPAT	Acylglycerol-3-phosphate acyltransferases
AJs	Adherent junctions
AMPK	5'-AMP-activated protein Kinase
Ang	Angiopoietin
AP1	Activating Protein-1
APC/C	Anaphase-Promoting Complex/Cyclosome
AS	Angiosarcoma
AT	Adipose Tissue
ATGL	Adipose TGs Lipase
ATMΦs	Adipose Tissue Macrophages
AVMs	Arteriovenous Malformations
BAT	Brown Adipose tissue
BM	Basement Membrane
BMI	Body Mass Index
C/EBPα,β,δ	CCAAT-Enhancer-Binding Proteins α,β,δ
CACT	Carnitine ACylcarnitine Translocase
CENP-C	Centromere-specific binding protein C
CEs	Cholesteryl Esters
CIDEA	Cell Death-Inducing DFFA-Like Effector A
CLS	Crown-Like Structures
CPT1	Carnityl Palmitoyl Transferase 1

CPT2	Carnitine Palmitoyl Transferase 2
DAG	Diacylglycerol
Dll4	Delta-like 4
DNL	De Novo Lipogenesis
Ebf1	Early B cell Factor 1
ECM	Extra Cellular Matrix
ECs	Endothelial Cells
EE	Energy Expenditure
EGF	Epidermal Growth Factor
EGFR-1	Early Growth Response protein 1
ER	Endoplasmic Reticulum
ERR-α	Estrogen-Related Receptor alpha
ESAM	Endothelial cell-Selective Adhesion Molecule
ETC	Electron Transport Chain
ETS	Electron Transport System
EVI-1	Ecotropic Virus Integration site 1
FABP4	Fatty Acid Binding Protein4
FABPpm	Plasma Membrane Fatty Acid-Binding Protein
$FADH_2$	Flavin adenine dinucleotide
FAO	FFAs oxidation
FAS	Fatty Acid Synthase
FAT/ CD36	Fatty Acid Translocase
FATPs	Fatty Acid Transporter Proteins
FBS	Fetal Bovine Serum
FFAs	Free Fatty Acids
FGFs	Fibroblast Growth Factors
FOXOs	Forkhead box O transcription factors
G0S2	G0/G1 switch gene 2
G3P	Glycerol-3-Phosphate
GPAT	Glycerol-3-Phosphate Acyltransferase
GPCRs	G protein-coupled receptors
GTT	Glucose Tolerance Test
Hes	Hairy Enhancer of Split

Hey	Hairy and enhancer-of-split related with YRPW motif protein
HFD	High Fat Diet
HIF	Hypoxia Inducible Factor
Hprt1	Hypoxanthine phosphoribosyltransferase 1
HSL	Hormon Sensitive Lipase
HUVECs	Human Umbilical Vein Endothelial Cells
IB4	Isolectin-B4
IHC	Immunohistochemistry
IL	interleukin
IM	Inner Membrane
IMS	Intermembrane space
iPLA2ζ	Calcium-independent phospholipase A2ζ
ITT	Insulin Tolerance Test
JAMs	Junctional Adhesion Molecules
KLF	Kruppel-Like protein Family
LA	Locomotor Activity
LCFAs	Very-long-chain fatty acids
Lcn2	Lipocalin2
LD	Lipid Droplet
LMs	Lymphatic Malformations
M/SCHAD	Medium and Short chain hydroxyacyl-CoA dehydrogenase
MAG	Monoacylglycerol
mAspAt	Mitochondrial aspartate aminotransferase
MCAD	Medium Chain acyl-CoA Dehydrogenase
MCKAT	Medium Chain 3-Ketoacyl-CoA Thiolase
MCP-1	Monocyte Chemoattractant Protein-1
MGL	Monoglyceride lipase
mlECs	Mouse Lungs endothelial cells
MMPs	Matrix MetalloProteinases
mTORC1	Mammalian target of rapamycin complex
MTP	Mitochondrial Trifunctional Protein
MΦs	Macrophages
NADH	Nicotinamide adenine dinucleotide

NF-κB	Nuclear Factor kappa B
NICD	Notch intracellular domain
Nrarp	NOTCH-Regulated Ankyrin Repeat Protein
Nrf-2	Nuclear Factor E2-related factor 2
OM	Outer Membrane
OxPhos	Oxidative Phosphorylation
p53	Tumour Protein 53
PA	Phosphatidic Acid
PAP2	Phosphohydrolase
PBD	PIP2-binding domain
PCR	Polymerase Chain Reactions
PDGFB	Platelet-Derived Growth Factor B
PDGFRβ	Platelet-derived growth factor receptor beta
PDK-1	Phosphoinositide-Dependent Kinase 1
PEPCK	Phosphoenolpyruvate carboxykinase
PFKFB3	Phosphofructokinase-2/fructose-2,6-bisphosphatase 3
PGC1-β	Proliferator-activated receptor-Gamma Coactivator 1β
PGC1-α	Proliferator-activated receptor-Gamma Coactivator 1α
PH	Pleckstrin homology
P_i	Inorganic Phosphate
PI3K	Phosphatidylinositol-3-Kinase
PIGF	Placenta growth factor
PPARα	Proliferator-Activated Receptor α
PPARβ	Proliferator-Activated Receptor β
PPARγ	Proliferator-Activated Receptor γ
PRDM16	PRD1-BF-1-RIZ1 homologous domain-containing protein-16
Pref-1	Preadipocyte factor-1
PtdIns	PhosphatidylInositol
PtdIns(3,4,5)P_3	PtdIns 3,4,5-trisphosphate (also named PIP3)
PtdIns(4,5)P_2	PtdIns- 4,5- bisphosphate (also named PIP2)
PtdIns4P	PtdIns- 4- phosphate
PTEN	Phosphatase and TENsin homolog deleted on chromosome 10
PX	Phox homology

qRT-PCR	Quantitative Real Time PCR
RBP4	Retinol Binding Protein 4
RBPJ	Recombining Binding Protein suppressor of hairless
REs	Retinyl Esters
ROS	Reactive Oxygen Species
RQ	Respiratoty Quotient
RT	Room Temperature
RTKs	Tyrosine kinase receptors
S6K	Ribosomal S6 protein (rS6) Kinase
SC	Subcutaneus
SCAD	Short Chain acyl-CoA Dehydrogenase
SREBP-1	Sterol Response Element–Binding Protein-1
SVF	Stromal Vascular Fraction
TGs	Triglycerides/ triacylglycerol
TJs	Tight junctions
TNFα	Tumor Necrosis Factor α
TSC-2	Tuberous Sclerosis Complex 2
UCP1	Uncoupling Protein 1
VAs	Vascular Anomalies
VEGF	Vascular Endothelial Growth Factor
VEGFR	Vascular Endothelial Growth Factor Receptor
VIS	Visceral
VLCAD	Chain acyl-CoA Dehydrogenase
VMs	Venous Malformations
vSMCs	Vascular Smooth-Muscle Cells
WAT	White Adipose Tissue
WHO	World Health Organization
Zfp423	Zinc Finger Protein 423
Zfp521	Zinc Finger Protein 521

1. Introduction

1.1 Adipose tissue

For decades Adipose Tissue (AT) was classified as a connective tissue merely dedicated to store lipids. This oversimplified thought began to change in the mid 1990s with the discovery of several adipocytes-derived serum factors (like leptin and adiponection). Suddenly, AT has been recognized as an endocrine organ essential to preserve whole body energy homeostasis. From this point forward, the number of publications related to AT development, function and pathophysiology, increased exponentially; a renewed interest that, not casually, has occurred in parallel with a dramatic increase in worldwide rate of obesity and diabetes (Rosen and Spiegelman, 2014). In mammals, AT is typically classified according to the color and location. Based on color, AT is divided into White Adipose Tissue (WAT) and Brown Adipose Tissue (BAT) which differ in both function and morphology. Regarding the anatomic location WAT is classified in Subcutaneus (SC) below the skin, and Visceral (VIS) in the trunk cavity. There is not a uniformly applied system for describing the anatomical location of each WAT depot and, therefore, depot names often vary between studies (Sanchez-Gurmaches and Guertin, 2014). This thesis is focused on two depots named Inguinal-WAT (ingWAT), which is dorsally attached along the pelvis to the thigh of the hindlimb, and Gonadal-WAT (gWAT) that surrounds the uterus and ovaries in females and the epididymis and testis in males. Other depots are shown in (Figure 1.1). An important point to keep in mind is the imperfect correlation between fat depots in rodents and humans; for example, a large percentage of VIS fat in humans is contained in the omentum, which is barely presents in rodents. Conversely the large gonadal fat in male mice, considered as the major VIS depot, does not exist in men (Rosen and Spiegelman, 2014).

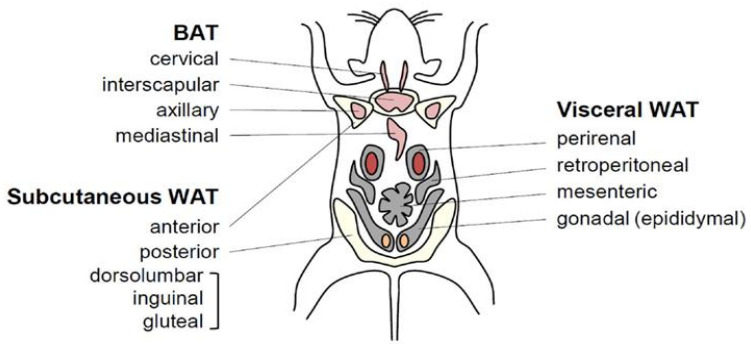

Figure 1.1: Anatomy of the major fat depots in rodents Adapted from (Choe et al., 2016).

1.1.1 WAT and BAT: morphology and function

WAT is the primary site of energy storage and it also functions as an endocrine organ secreting hormones and cytokines that regulate feeding and metabolism. WAT is composed of mature adipocytes and the, so called, Stromal Vascular Fraction (SVF) that includes adipocytes precursors, Endothelial Cells (ECs), immune cells and fibroblast. Mature white adipocytes are the major constituent cells of WAT; they have a very long half–life and the ability to store great amounts of energy in the form of triglycerides (TGs). In white adipocytes, TGs are packed in a single large Lipid Droplet (LD) that occupies almost all the cytoplasm and pushes the nucleus against the plasma membrane giving the characteristic signet-ring shape. Mitochondria in white adipocytes are thin and elongated, with randomly oriented cristae, and they vary number (F and M, 2013; Hassan et al., 2012; Saely et al., 2010). Whereas WAT stores an excess of energy as triglycerides, the function of BAT is to dissipate energy through the production of heat. This is referred to as nonshivering thermogenesis; a process meditated by the uncoupling protein 1 (UCP1). UCP1 is a BAT-specific protein, located within the mitochondria, that catalyzes a proton leak across the inner mitochondrial membrane, thus ‘‘uncoupling’’ fuel oxidation from ATP synthesis (Mattson, 2010; Rousset et al., 2004). BAT is abundant in small mammals and in newborns and helps them to survive cold temperatures. In adult humans, it had long been considered to be absent or at least irrilevant. Recent investigations, however, have shown that adults also have metabolically active BAT (in the neck and trunk) and that BAT may play an important role in energy homeostasis (Cypess et al., 2009, 2013). In rodents, BAT is located in discrete, highly innervated and vascularized depots: interscapular (iBAT), sub-scapular (sBAT), and cervical (cBAT). BAT is mainly composed of brown adipocytes which contain multiple small LDs (multilocular). Ultrastructurally, brown adipocytes have numerous, large and spherical mitochondria with densely packed laminar cristae (Saely et al., 2010). Interest is also growing in a third potential class of adipocyte called beige adipocyte (also known as “brite”, “inducible brown” or “recruitable brown” adipocyte). These, not yet, fully characterized cells reside within WAT and, in the basal or unstimulated state, are morphologically indistinguishable from its neighboring white adipocytes. However, upon chronic cold exposure or beta-adrenergic stimulation these cells become multilocular and begin to express UCP1. Whether beige adipocytes arise from transdifferentiation of existing mature white adipocytes or from a distinct precursor population is still under debate (Cinti, 2009; Rosenwald et al., 2013; Wu et

al., 2012). In rodents, the presence of beige adipocytes varies dramatically between depots, with the highest numbers found in inguinal and retroperitoneal fat and much lower numbers in gonadal fat. The effective contribution of beige adipocytes to thermogenesis is still not known (Cannon and Nedergaard, 2012; Cinti, 2011, 2012; Frontini and Cinti, 2010). With regard to humans an important issue is whether human BAT is more similar to beige fat or to classical BAT in mice. Recent studies suggest that there is a gradient of fat cell types in the neck, with deep neck fat being conventional BAT, intermediate cells possibly being more beige-like, and the most peripheral adipocytes being conventional white adipocytes (Cypess et al., 2013) (Figure 1.2).

	White adipocytes	Brown adipocytes	Beige adipocytes
Morphology	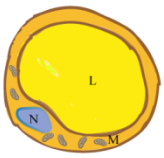	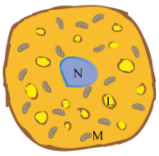	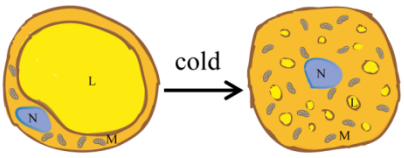
Functions	Energy storage Endocrine organ	Thermogenesis (UCP1)	Contribute significantly to thermogenesis?
Main Localisation	Inguinal Gonadal Mesenteric Retroperitoneal	Interscapular Sub-scapular Cervical	Within inguinal WAT

Figure 1.2: White brown and beige adipocytes. Schematic representation, main function and localization of adipocytes (L= lipid droplet; N= nucleus; M= mitochondria).

1.1.2 AT development

1.1.2.1 White Adipose Tissue

The developmental timing of WAT varies between species; in rodents WAT largely develops after birth with relevant differences between fat depots. In VIS depots, committed precursors are not detectable before postnatal day 4 (P4) and adipocytes only become visible by P7 and are fully matured at P14 (Han et al., 2011). Conversely expression of adipose specific markers in SC fat can be detected as early as embrionic day 16.5-17.5 and developing adipocytes rapidly accumulate lipid, becoming visible by P2 with the subsequent acquisition of a clear unilocular structure by P5 (Birsoy et al., 2011). In human WAT development occurs by the 14th weeks of gestation, the precise timing may depend on fetal size, with larger fetus developing visible adipocytes earlier (Poissonnet et al., 1983, 1984). The marked cell proliferation observed in the early

gestation is then arrested and AT growth is achieved by filling with lipids the pre-existing adipocytes. Later on, another period of increased proliferation, between childhood and adolescence, sets the total adipocytes number that an individual will have as an adult, although new cells are constantly being created and destroyed throughout life (Knittle et al., 1979). In humans, roughly 8% of adipocytes are turned over approximately every year, whereas in mice 0.6% of adipocytes are renewed each day (Rigamonti et al., 2011; Spalding et al., 2008).

1.1.2.2 Brow Adipose Tissue

BAT has a different developmental pattern than WAT. The onset of non-shivering thermogenesis is essential in newborns mammals to face and adapt in the cold extrauterine environment; so it is not a surprise that BAT develops early before birth. However, there are fundamental differences in the maturation of BAT between species: the so called altricial mammals, such as mice and rats, which are born after a short gestation with an immature hypothalamic-pituitary-adrenal (HPA) axis, stay warm by huddling in the nest rather than by using nonshivering thermogeneis. Therefore, BAT is presents at the time of birth but it does not express UCP1 until it matures during postnatal life. Conversely, precocial mammals, such as humans, born after a long gestation, can rapidly switch on nonshivering thermogenesis at birth. The cold extrauterine environment quickly induces UCP1 expression, whose level peaks after birth and then slowly decreases as brown adipocytes are replace with white fat cells (Symonds, 2013).

1.1.2.3 Adipogenesis: stem cell determination and terminal differentiation

From a cellular perspective, adipogenesis can be divided into two phases: determination and terminal differentiation (Figure 1.3). Determination refers to the commitment of a mesenchymal stem cell to the adipocyte lineage, whereas terminal differentiation is the process by which committed preadipocytes are converted into mature adipocytes and progressively acquire properties and morphology of fully differentiated fat cells (Rosen and MacDougald, 2006). Although the transcriptional cascade that promotes adipogenesis has been studied at length, we know much more about the process of terminal differentiation than we do about determination. Recently, little progress has been done in our knowledge on cell determination: a quantitative transcriptomic analysis of proliferating adipogenic and non-adipogenic fibroblasts identified Zinc Finger Protein 423 (Zfp423) as a transcriptional determinant of the adipose lineage.

Zfp423 promotes adipose lineage commitment by inducing Peroxisome Proliferator-Activated Receptor gamma (PPARγ) expression, a master regulator of adipocytes differentiation (Gupta et al., 2010). Conversely, a close paralog of Zfp423, Zfp521, has been found to negatively regulate adipogenesis. Zfp521 exerts its actions by binding to Early B cell Factor 1 (Ebf1), a transcription factor required for the generation of adipocyte progenitors (Jimenez et al., 2007), and inhibiting the expression of Zfp423. Interestingly, because Zfp521 is known to promote bone development, it has been suggested that it acts as a critical switch between adipogenic and osteogenic lineages (Kang et al., 2012). The development of fully differentiated mature adipocytes from committed precursor cells (terminal differentiation) is an elegant process driven by the sequential activation of a battery of transcription factors. In white adipocytes, this sequence begins with the activation of members of the Activating Protein-1 (AP-1) and continues with the activation of PPARγ, the "master regulator" of preadipocytes differentiation. PPARγ is both necessary and sufficient for adipogenesis, indeed it is so efficient that it can stimulate non-adipogenic cells to become adipocytes (Hu et al., 1995; Tontonoz et al., 1994). Consistent with murine studies, humans carrying mutations in PPARγ gene develop severe insulin resistance and lipodystrophy (Garg, 2004). Many other transcription factors promote adipocytes maturation, including STATs, members of the C2H2 zinc finger Kruppel-Like family (KLF) of proteins (KLFs 4, 5, 6, and 15), Sterol Response Element–Binding Protein-1 (SREBP-1), and members of the CCAAT-enhancer-binding proteins (C/EBP) family (C/EBPα, C/EBPβ and C/EBPδ). There are also potent negative repressors of adipocytes differentiation, including Preadipocyte factor-1 (Pref-1) and members of the GATA (GATA2 and 3) and Wnt (Wnt10b and 5a) families. Most of these factors exert their actions at least in part by inducing or repressing PPARγ expression (Sarjeant and Stephens, 2012).

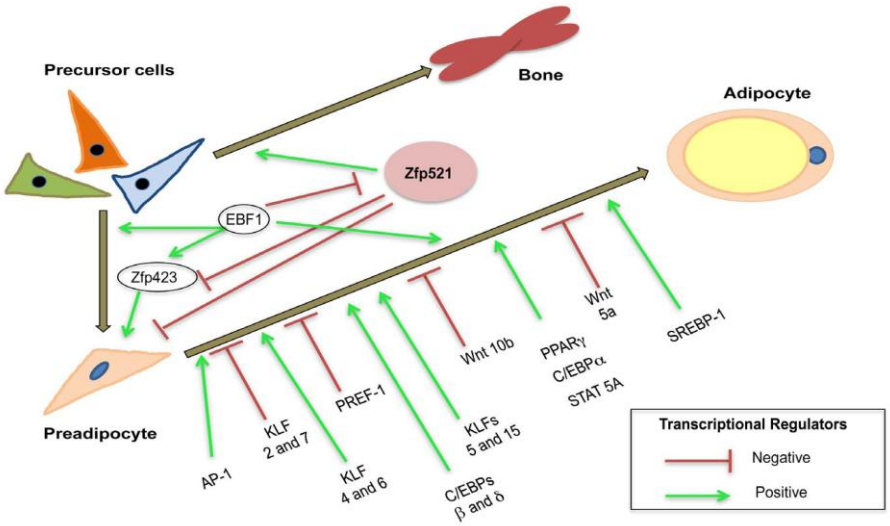

Figure 1.3: Adipocytes determination and terminal differentiation. Many transcription factors are induced during adipocytes differentiation. Some of these, like members of the AP-1 family, are induced early during adipocytes development. Other transcription factors like PPARγ promote terminal differentiation. Adipocytes development is also influenced by several transcription factor families that negatively regulate adipogenesis. Adapted from (Stephens, 2012).

Several established key factors that regulate white adipocytes differentiation (PPAR-γ, C/EBP-α, C/EBP-β and C/EBP-δ), also control brown adipogenesis. Accordingly the "molecular contest" that determines the brown-, beige- or white-cell fate during adipogenesis has remained elusive for a long time (Hansen and Kristiansen, 2006; Peirce et al., 2014). Lately, it has been suggested that cell fate determination requires three levels of control involving transcription factors and co-activators, epigenetics and miRNAs (Figure). The most important transcription factors that activate and orchestrate the brown fat differentiation program are the co-factors Peroxisome Proliferator-activated receptor-Gamma Coactivator 1 alpha (PGC1-α) and PRD1-BF-1-RIZ1 homologous domain-containing protein-16 (PRDM16). PGC1-α regulates mitochondrial biogenesis, oxidative metabolism and thermogenesis mainly via interaction with transcription factors like ERRα, Nrf-2, PPARα, and PPARγ (Puigserver and Spiegelman, 2003). PRDM16 seems to be a more specific driver of thermogenic genes and it controls a bidirectional cell fate switch between skeletal myoblasts and brown fat cells during brown adipogenesis (Seale et al., 2008). This transcriptional control is integrated with epigenetic modification that can interfere with the availability of the targeted promoters. Finally, miRNAs have been recently recognized as important regulators of cell differentiation and metabolism in several tissues, including AT (Trajkovski and Lodish, 2013). For example, miR-155 is involved

in a feedback loop with C/EBP-β, that controls adipocytes precursor proliferation and differentiation (Chen et al., 2013). miR-27 is a negative regulator of the brown and beige differentiation in BAT and WAT, whereas miR-196a expression in WAT increases upon cold exposure or β-adrenergic stimulation to induce browning (Mori et al., 2012; Sun and Trajkovski, 2014).

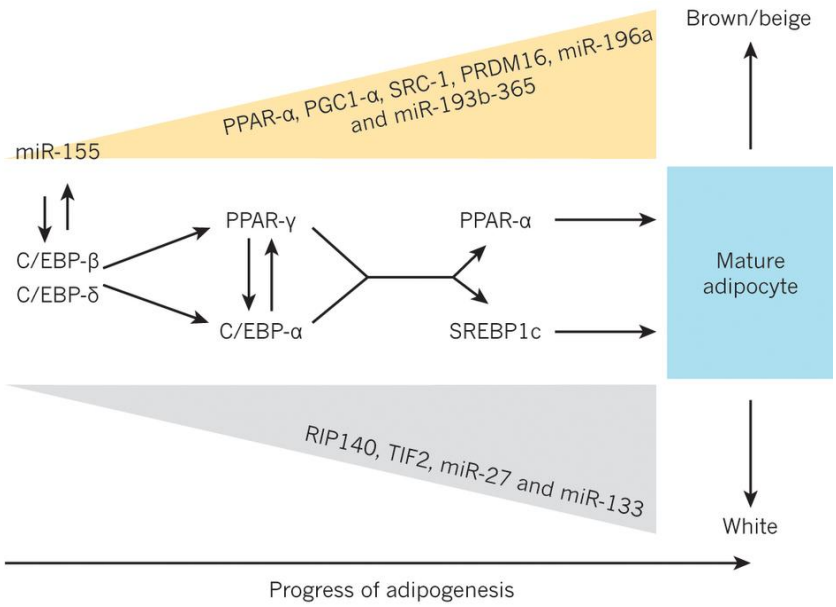

Figure 1.4: Factors regulating white, and brown or beige adipogenesis. Adipogenesis is driven by a cascade of transcription factors (C/EBP-δ, C/EBP-β, C/EBP-α, PPAR-γ, PGC1-α and SREBP1c) that establishes and maintains the stable differentiation of the adipocyte. This transcriptional cascade interacts with other transcription factors, co-activators and microRNAs during the decision to proliferate or differentiate and the decision to adopt a brown or beige 'thermogenic' cell fate or a white 'non-thermogenic fate. Adapted from (Peirce et al., 2014).

1.1.2.4 Adipocytes precursors reside in the vascular niche

The first recognizable structure that will become a fat pad is a cluster of blood vessels originally called a "primitive organ" (Rosen and Spiegelman, 2014). This observation, together with ultrastructural data showing a close juxtaposition of the vasculature and the developing AT (Cinti et al., 1984), led to hypothesizes that adipocyte precursors may reside in the vascular niche; hypothesis now supported by several lineage tracing studies. However, a unified opinion with regard to which cell type, within the blood vessel, give birth to adipocytes precursors is still missing. For example one study claimed that some PDGFRβ+ mural cells have adipogenic potential (Tang et al., 2008a) and others suggested that a subpopulation of endothelial cells might give rise to adipocytes (Gupta et al., 2012a; Tran et al., 2012a). Nevertheless, a more recent studies

failed to detect any adipocyte progenitors in either the perivascular or endothelial compartment, instead they identified a PDGFRα+, CD24+ population, dispersed throughout WAT, that generate all white adipocytes (Berry and Rodeheffer, 2013). In addition it has also been proposed that some adipocytes could derive from hematopoietic precursors (Majka et al., 2010).

1.2 White adipose tissue

1.2.1 WAT as an endocrine organ regulating energy homeostasis

Since the early 1990s, after leptin had been discovered, WAT has been considered as an endocrine organ at the center of whole body energy homeostasis. So far, many other cytokines, peptides and hormones have been indentified and collectively named adipokines (Choe et al., 2016). These bioactive molecules, through their autocrine, paracrine and endocrine functions, influence a number of organs critical for energy homeostasis. A dysregulation of these adipokines is observed in situations of both excessive adipose tissue as well as lack of adipose tissue. This altered adipokine profile leads to profound changes in insulin sensitivity, and other biochemical alterations of metabolites, making an individual more prone to metabolic disorders. The normalisation of the adipokines profile usually correlates well with the normalization of metabolic parameters, confirming the important role of this molecules as regulators of whole body energy homeostasis (Deng and Scherer, 2010). Up to date a huge number of adipokines has been identified with several new molecules being discovered every year. These include factors that improve or impair insulin sensitivity and glucose tolerance as well as factors that modulate local inflammation and angiogenesis. Here is a brief description of some of the most known and better characterized adipokines.

Leptin

Discovered in 1990 by Friedman's group, leptin was the first and likely the most studied adipocyte-derived cytokine (Choe et al., 2016). Leptin is a 16-kDa nonglycosylated peptide that belongs to the cytokine class 1 super family (Zhang et al., 1994); it is mainly produced by white adipocytes and its circulating levels are directly proportional to WAT mass. Leptin once secreted, in response to food intake, stimulates satiety and increases energy consumption by acting on hypothalamic neurons (Choe et al., 2016; Lago et al., 2009). It can also act on peripheral tissues such as muscles, where it promotes fatty acid oxidation by activating 5'-AMP-activated protein kinase (AMPK)

(Minokoshi et al., 2002). Congenital leptin deficiency is associated with severe obesity in both humans and mice due to unlimited appetite and reduced energy expenditure; in this specific case replacement of leptin alone efficiently reduce food intake and body weight (Montague et al., 1997; Pelleymounter et al., 1995). Circulating leptin level is often very high in obese people (directly proportional to WAT mass), however they are completely leptin-insensitive (Blüher and Mantzoros, 2009; Myers et al., 2010).

Adiponectin

Adiponectin is a 30kDa protein, quite abundant in the plasma and specifically secreted by adipocytes. It circulates in serum as trimers, hexamers and more complex structures, the latter being the most biologically active form. Adiponectin signalling is principally mediated by ADIPOR1 and ADIPOR2 receptors, which are ubiquitously expressed in all tissues, and it promotes metabolic health by enhancing peripheral insulin sensitivity and inducing fatty acid oxidation in liver (Turer and Scherer, 2012). Adiponectin has also a cardio-protective activity mainly accomplished through a non-signalling receptor called T-chaderin (Denzel et al., 2010). Although it is secreted by adipocytes, circulating adiponectin level is inversely proportional to WAT mass and it decreases under unfavorable metabolic conditions (Turer and Scherer, 2012).

Resistin

Resistin is a 12kDa peptide that circulates either in the form of high-molecular-weight hexamer or a less abundant but more bioactive trimer (Ouchi et al., 2011). In mice, it is primarily produced by white adipocytes and its serum levels are higher in obese mice (Steppan and Lazar, 2004). Resistin modulates glucose metabolism in mice: it has been found that high circulating levels of resistin induce insulin resistance, and mice lacking resistin have lower basal blood glucose levels (Banerjee et al., 2004). Moreover, resistin-deficient ob/ob mice are severely obese, but they have improved glucose tolerance and insulin sensitivity (Qi et al., 2006). However, it has been difficult to demonstrate a direct relationship between resistin and glucose metabolism in humans, where resistin seems to be primarily secreted by monocytes (Savage et al., 2001).

Retinol binding protein 4 (RBP4) and Lipocalin2 (Lcn2)

RBP4 and Lcn2 belong to the lipocalin family proteins and have been broadly studied with respect to their negative effects on glucose homeostasis and insulin sensitivity. RBP4, a 21kDa protein, is the major retinol (vitamin-A) transporting protein in the serum where it transports vitamin-A from the liver to peripheral tissues (Newcomer and Ong, 2000). It is preferentially expressed in VIS-WAT and it circulates at higher concentration in the serum of insulin-resistant humans and mice (Choe et al., 2016). Lcn2 is an iron-traffiking protein secreted by several tissues. Lcn2 induces insulin resistance in cultured adipocytes (Yan et al., 2007), but its effects in vivo remain controversial.

1.2.2 TG synthesis and breakdown

1.2.2.1 Lipogenesis

Fat build-up is determined by the balance between TGs synthesis (lipogenesis) and breakdown (lipolisis). Lipogenesis preferentially takes place in WAT, but also in liver, muscles, pancreas and heart. Many nutritional and hormonal factors influence the rate of fat mobilisation and storage. For example, a diet rich in carbohydrates or polyunsaturated fatty acids, respectively, stimulates and inhibits lipogenesis. Fasting reduces lipogenesis and increases lipolisis in AT; conversely, in liver, due to high amounts of Free Fatty Acids (FFAs) coming from the AT, it promotes TGs synthesis. Fasting is associated with important changes in plasma hormones concentration, such as a decrease in plasma insulin and leptin, and an increase in plasma growth hormone and glucagone. Insulin is one of the most important hormone that influences lipogenesis. It promotes lipogenesis by increasing glucose uptake in AT and activating lipogenic and glycolitic enzymes; it also has a long term effects on the expression of lipogenic genes likely mediated by the transcription factor SREBP-1. Conversely, growth hormone dramatically reduces lipogenesis in AT, resulting in significant fat loss with a concomitant gain of muscle mass (Kersten, 2001). TGs can be synthesized either from circulating FFA derived from the diet, peripheral lipogenesis, or by excess of carbohydrates, De Novo Lipogenesis (DNL).

Peripheral lipogenesis refers to a crucial and strictly regulated process that take place in adipose tissue and liver. It begins with the activation of FFA into acyl-CoA by the enzyme Acyl-CoA synthetase (ACSL), then FFA-CoA and Glycerol-3-Phosphate (G3P)

are transformed to Phosphatidic Acid (PA) by the subsequent action of Glycerol-3-Phosphate Acyltransferase (GPAT) and acyl-CoA acylglycerol-3-phosphate acyltransferases (AGPAT). Thus, PA is dephosphorylated by phosphohydrolase (PAP2) to give rise to diacylglycerol (DAG); finally the enzyme diacylglycerol acyltransferase (DGAT) catalyses the conversion of DAG into TGs (Ahmadian et al., 2007; Saponaro et al., 2015). G3P might come either from glycolysis or from non-carbohydrate substrates by the activity of the enzyme phosphoenolpyruvate carboxykinase (PEPCK), through a process named glyceroneogenesis (Figure 1.5).

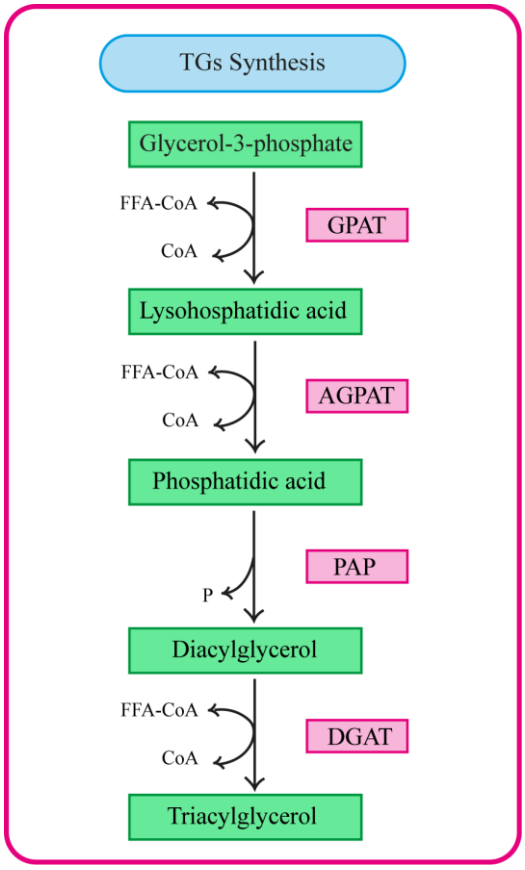

Figure 1.5: Schematic representation of triacylglycerol synthesis.

DNL is a complex and highly regulated metabolic pathway that converts excess carbohydrates into fatty acids, which are then esterified to storage TGs. DNL is primarily active in liver and adipose tissue especially after high-carbohydrate meal, when only a limited amount of carbohydrates can be stored as glycogen. The flow of carbon molecules from glucose to fatty acids includes a coordinated series of enzymatic reactions. The first step is the conversion of citrate to acetyl-CoA by ATP-Citrate LYase (ACLY). The resulting acetyl-CoA is carboxylated to malonyl-CoA by Acetyl-CoA Carboxylase (ACC). Finally Fatty Acid Synthase (FAS), which is the rate limiting

enzyme of DNL, converts malonyl-CoA into palmitate. After a series of reactions palmitate is further converted into more complex fatty acids (Ameer et al., 2014; Saponaro et al., 2015) (Figure 1.6).

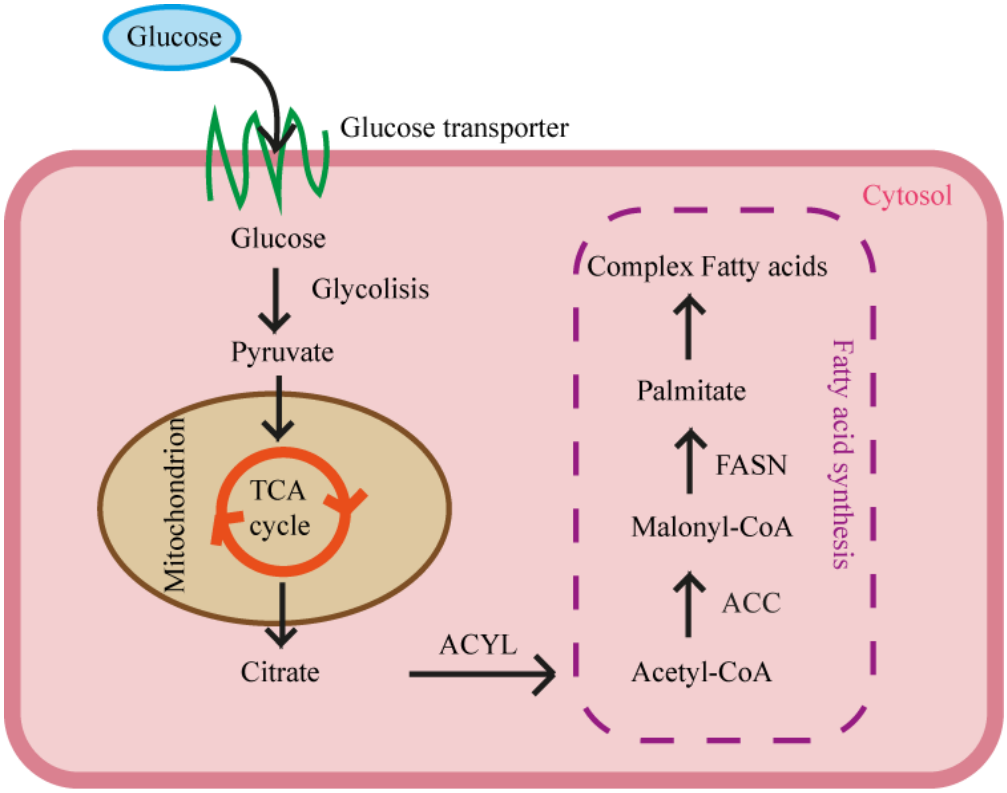

Figure 1.6: De Novo Lipogenesis. DNL is activated especially after a carbohydrate rich meal and convert carbohydrate into TGs which are a more efficient way to store surplus energy. Glucose, taken up by the glucose transporter, enters the glycolytic pathway and generates pyruvate. This pyruvate is converted into acetyl-CoA that feeds the tricarboxylic acid (TCA) cycle. The citrate produced exits the mitochondrion and is converted back into acetyl-CoA by the enzyme ATP-citrate lyase (ACLY). Acetyl-CoA carboxylase (ACC) acts on this acetyl-CoA yielding malonyl-CoA which is then utilized as a substrate for the production of 16-carbon saturated palmitate by the main biosynthetic enzyme fatty acid synthase (FASN).

1.2.2.2 Lipolisis and β-oxidation

1.2.2.2.1 Lipolisis

WAT, the major energy reservoir in mammals, stores excess of lipids in the form of chemical inert TGs. During periods of nutrient deprivation, stress, or physical exercise, TGs are cleaved by TGs hydrolases to generate FFAs, a process called lipolisis. Then FFAs enter the blood stream to reach peripheral tissues where they are oxidized inorder to produce ATP. Lipolisis proceeds in a sequential and regulated manner, with one FFA released at each step: the first cleavage is done by Adipose TGs Lipase (ATGL), which

forms DAG that is subsequently hydrolized by Hormon Sensitive Lipase (HSL) to generate monoacylglycerol (MAG); then the monoglyceride lipase (MGL) complete the process by producing glycerol and the final FFA (Figure 1.7). Together, these three enzymes account for over 90% of the lipolytic activity in adipocytes (Duncan et al., 2007; Lass et al., 2011).

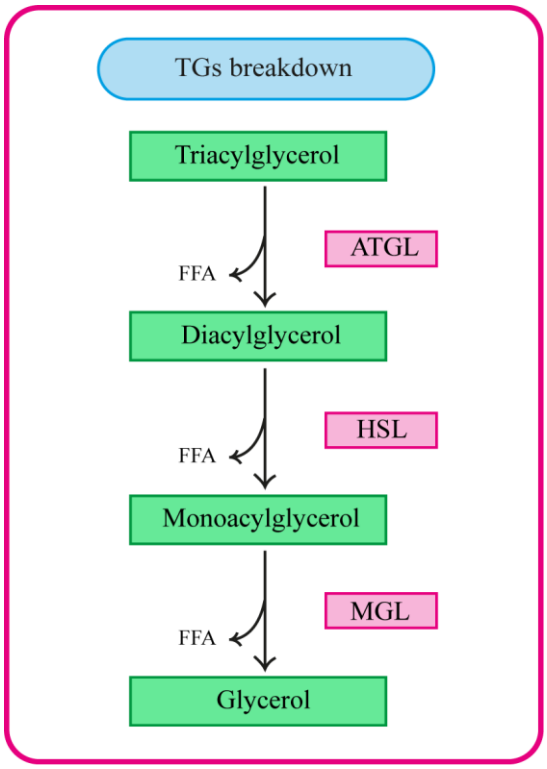

Figure 1.7: Schematic representation of triacylglycerol breakdown.

ATGL

ATGL is the rate-limiting enzyme for TGs hydrolysis. It was identified in 2004 by three different groups that named it ATGL (Zimmermann et al., 2004), desnutrin (Villena et al., 2004), and calcium-independent phospholipase A2ζ (iPLA2ζ) (Jenkins et al., 2004). The relative importance of ATGL in lipolysis was stressed by the observation that genetic inactivation of ATGL in mice causes an increase of fat mass and a dramatic ectopic fat deposition, especially in the heart, which eventually results in premature death (Haemmerle et al., 2006). Similarly, ATGL mutations in humans are associated with systemic TGs accumulation and cardiac myopathy (Fischer et al., 2007). ATGL is a 54kDa protein that contains an N-terminal patatin-like domain, is mainly expressed in AT and its primary structure is well conserved among humans and mice. The transcriptional control of ATGL is complex, besides, numerous studies have reported

that changes in mRNA and protein levels are often reciprocal, suggesting that ATGL is subjected to extensive post-transcriptional regulation (Nielsen et al., 2014). The lipolytic activity of ATGL is primary regulated by interaction with the co-activator CGI-58 (also known as α/β hydrolase domain-containing protein). CGI-58 is a 40 kDa protein that binds to lipid droplets by interaction with perilipin A in hormone-dependent fashion. In the basal state, CGI-58 is tightly associated with the lipid droplets and is unable to activate ATGL. Following hormonal stimulation, perilipin is phosphorylated at several serine residues, including serine 517, whereupon CGI-58 dissociates from perilipin, interacts with ATGL, and activates TGs breakdown. In concomitant with ATGL activation, HSL translocates from the cytosol to the lipid droplets where it hydrolyzes DAGs. Perilipin phosphorylation is strictly necessary for ATGL/CGI-58 mediated hydrolysis of TGs. Perilipin is a lipid droplet surface protein exclusively expressed in AT, but lipolysis of TGs is required also in other tissues (such as muscles and liver); therefore, alternative mechanisms (still unknown) must exist in order to control TGs hydrolysis in non-adipose tissues (Zechner et al., 2009). Recently, a protein called G0/G1 switch gene 2 (G0S2) was identified as an inhibitor of ATGL. G0S2 is highly expressed in adipose tissue, where it can directly bind to ATGL and suppress ATGL hydrolytic activity independently of CGI-38 (Yang et al., 2010).

HSL

HSL was discovered in the early 1960s (Vaughan et al., 1964) and for a long time it was believed to be the only and consequently the rate limiting enzyme for lipid catabolism in AT. This view change after several independent groups reported that HSL-deficiency in mice is associated with male sterility, but does not cause obesity or any metabolic disease. Despite being leaner and resistant to diet-induced obesity, HSL null mice accumulate high amounts of DAGs in several tissues, indicating that HSL is rate-limiting for DAGs hydrolysis (Haemmerle et al., 2002; Osuga et al., 2000; Wang et al., 2001). HSL is an 84 kDa cytoplasmic protein, highly expressed in AT, with demonstrated activity against a broad variety of substrates including TGs, DAGs, MAGs, cholesteryl esters (CEs) and retinyl esters (REs); the relative maximal hydrolysis rates are in the range of 1: 10: 1: 4: 2 for TGs: DAGs: MAGs: CEs: REs indicating that the TGs and DAGs are respectively the worst and the best substrate for HSL. According to the HSL structure model, three regions can be distinguished: 1) the N-terminal domain, believed to mediate the interaction with Fatty Acid Binding

Protein4 (FABP4), a protein that enhances HSL activity, 2) the catalytic domain, located at the C-terminal end, 3) the regulatory domain containing several HSL phosphorylation sites (Zechner et al., 2009). Two major mechanisms determine HSL activity: enzyme phosphorylation and the interaction with auxiliary proteins. HSL can be phosphorylate by several kinases at 5 different residues: PKA (Ser563, Ser565, Ser659 and Ser660), ERK (Ser 600), glycogen synthase kinase-4 (Ser563), Ca^{2+}/calmodulin-dependent kinase II (Ser565) and AMPK (Ser565). However, in response to β-adrenergic stimulation, phosphorylation alone is not enough to properly activate HSL. This observation led to the discovery of perilipin (Brasaemle, 2007; Tansey et al., 2004). During hormone stimulation, perilipin helps in the translocation of HSL to the lipid droplets surface and its phosphorylation by PKA is absolutely crucial for the hydrolytic activity of HSL (Miyoshi et al., 2006).

1.2.2.2.2 FFAs uptake and β-oxidation

To produce energy and biomass, an organism can use three principal substrates: glucose, amino acids and fatty acids. Under normal well-fed conditions, glucose represents the first substrate choice for oxidation; however, during fasting periods, when glucose level goes down, FFAs oxidation (FAO) becomes the most important energy source. This reciprocal relationship between the oxidation of fatty acids and glucose is also known as the Randle cycle. The rationale behind this glucose-fatty acid cycle is to save glucose exclusively for the brain, which cannot metabolize FFAs. Furthermore, in fasting condition, FAO is indispensable for the liver to convert FFAs into ketone bodies, which serve as an additional energy source available for all tissues including the brain. Although both mitochondria and peroxisomes harbor all the enzymes required for FAO, mitochondria β-oxidation is the principal pathway responsible for FFAs degradation (Bartlett and Eaton, 2004; Hue and Taegtmeyer, 2009).

1.2.2.2.2.1 FFAs uptake

Membrane uptake of FFAs, released from AT through lipolisis, is the first step in cellular fatty acid utilization and it is mediated by Fatty Acid Transporter Proteins (FATPs), Plasma Membrane Fatty Acid-Binding Protein (FABPpm), and Fatty Acid Translocase (FAT or CD36). In mammals, FATPs comprise a family of six highly homologous transmembrane proteins, FATP1–FATP6, well conserved among species. FATPs are not homogeneously distributed among tissues: FATP1 is expressed in WAT, BAT, skeletal muscles and heart; FATP2 is highly expressed in kidney and liver;

FATP3 has been described in lungs, liver, pancreas and in ECs of capillary in several organs; FATP4 is broadly distributed; FATP5 expression is liver-specific whereas FATP6 is only expressed in the heart (Kazantzis and Stahl, 2012; Stahl et al., 2001). The precise mechanism through which FATPs mediate FFAs uptake has not been described yet, but it seems that FATPs act in coordination with acyl-CoA synthetase (ACS1), as a functional complex, to take up and convert fatty acids into long chain acyl-CoA (Glatz et al., 2010). FABPpm is a 40kDa protein anchored to the outer layer of the plasma membrane. It was originally identified in rat liver and later in the adipose tissue and cardiac myocytes. It was found to be identical to the mitochondrial aspartate aminotransferase (mAspAt) (Stump et al., 1993), encoded by the same gene but with different functions depending on cellular localization. FABPpm implication in FFAs uptake has been proved by antibody inhibition experiments as well as transfection studies (Glatz et al., 2010; Stremmel et al., 2001). CD36 is 88kDa membrane protein that belongs to the class B scavenger receptor family. It is ubiquitously expressed in many tissues and cells, including endothelial cells, platelets, and macrophages, and is involved in angiogenesis, atherosclerosis, inflammation, and lipid metabolism (Glatz et al., 2010). CD36 is composed of two transmembrane domains, a short intracytoplasmatic domain (which is highly glycosylated) and a large extracellular domain; it resides in cholesterol-rich lipid raft domains and, in some tissues, copurifies with caveolae (Silverstein and Febbraio, 2009). In muscles there is an evidence of two other localizations of CD36: i) an intracellular pool, that can be mobilized to the plasma membrane to increase FFAs uptake, and ii) a mitochondria pool, where it positively interacts with Carnityl Palmitoyl Transferase 1 (CPT1), a key enzyme regulating mitochondrial β-oxidation, (Campbell et al., 2004; Su and Abumrad, 2009). Several studies indicate that CD36 regulates the uptake of very-long-chain fatty acids (LCFAs) in AT and highly oxidative tissues like heart and skeletal muscles but it is absent in the liver (Febbraio et al., 2001). Once lipids get inside the cells, intracellular lipid chaperones known as Fatty Acid Binding Proteins (FABPs) bind and lead them to specific cell compartment such as lipid droplets (for storage) or mitochondria (for oxidation) (Furuhashi and Hotamisligil, 2008). The entry of acyl-CoAs into the mitochondria is a well regulated process: it is mediated by the carnitine shuttle and constitutes the major point of control for β-oxidation rate (Figure 1.8). The first step of this shuttle is performed by CPT1, which converts acyl-CoA into an acylcarnitine, then the Carnitine ACylcarnitine Translocase (CACT) exchanges acylcarnitine for a free

carnitine molecule from the inside; thus, CPT2, located in the inner mitochondrial membrane, reconverts the acylcarnitine into acyl-CoA which is now ready to undergo FAO. There are three isoforms of CPT1: CPT1A expressed in liver, brain, kidney, lungs, spleen, intestine, pancreas, ovary and adipose tissue; CPT1B expressed almost only in muscles and CPT1C, which is brain-specific and of unknown function. Both CPT1A and CPT1B are located in the mitochondria membrane and, being sensitive to inhibition by malonyl-CoA, represent the rate-controlling element for β-oxidation (Bartlett and Eaton, 2004; Houten and Wanders, 2010).

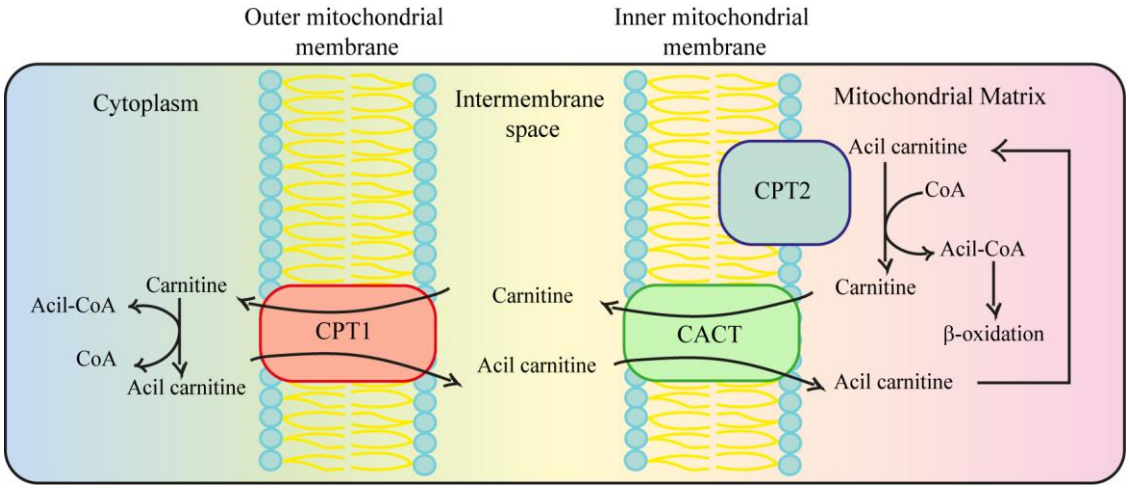

Figure 1.8: Transport of FFAs into mitochondria. The mitochondrial imports of long chain acil-CoA molecules require the carnitine shuttle system. This transport system converts acyl-CoA to acylcarnitine by the action of carnitine palmitoyltransferase 1 (CPT1); acylcarnitine is shuttled into the matrix by the carnitine: acylcarnitine translocase (CACT) and converted back to acyl-CoA by carnitine palmitoyl transferase 2 (CPT2). Next acil-CoA enters the β-oxidation cycle.

1.2.2.2.2.2 The β-oxidation cycle

FFAs β-oxidation is a cyclic process that breaks down long acyl-CoA molecules into acetyl-CoA units (Figure 1.9). This process is catalyzed by four enzymes: acyl-CoA dehydrogenase, enoyl-CoA hydratase, hydroxyacyl-CoA dehydrogenase, and ketoacyl-CoA thiolase. At first, acyl-CoA is dehydrogenated to yield trans-2-enoyl-CoA, and then the double bound is being hydrated to produce L-3-hydroxy-acyl-CoA which in turn is dehydrogenated to 3-keto-acyl-CoA. Finally, thiolytic cleavage of the 3-keto-acyl-CoA produces a two-carbon chain-shortened acyl-CoA plus acetyl-CoA. There are different enzyme isoforms for each step of the pathway, which vary in their chain-length specificity. The first cycles, directly after acyl-CoA import, take place in the mitochondrial membrane and are catalyzed by long chain acyl-CoA dehydrogenase

(VLCAD) and the long chain isoform of 2-enoyl-CoA hydratase, 3-hydroxyacyl-CoA dehydrogenase and 3-oxoacyl-CoA thiolase, which are constituents of a single protein of the inner mitochondrial membrane named Mitochondrial Trifunctional Protein (MTP). After 2-3 FAO cycles, the resulting medium chain acyl-CoA are metabolized in the mitochondrial matrix, where the first step of the cycle is performed first by medium chain acyl-CoA dehydrogenase (MCAD, encoded by ACADM gene) and after other 3-4 FAO cycles by short chain acyl-CoA dehydrogenase (SCAD, encoded by ACADS gene). The second, third and fourth step are catalyzed by the enoyl-CoA hydratase named crotonase (encoded by ECHS1gene), the medium and short chain hydroxyacyl-CoA dehydrogenase (M/SCHAD, encoded by HADH gene) and medium chain 3-ketoacyl-CoA thiolase (MCKAT, encoded by ACAA2 gene). Each β-oxidation cycle results in one acyl-CoA shortened by two carbon atoms, an acetyl-CoA, one nicotinamide adenine dinucleotide (NADH) and one flavin adenine dinucleotide ($FADH_2$) being produced. The acyl-CoA enters again in the β-oxidation process; the acetyl-CoA can enter the Krebs cycle or can be used to form ketone bodies (in ketogenic tissues like liver); the $FADH_2$ and NADH are used by the electron transport chain to produce ATP (Bartlett and Eaton, 2004; Houten and Wanders, 2010).

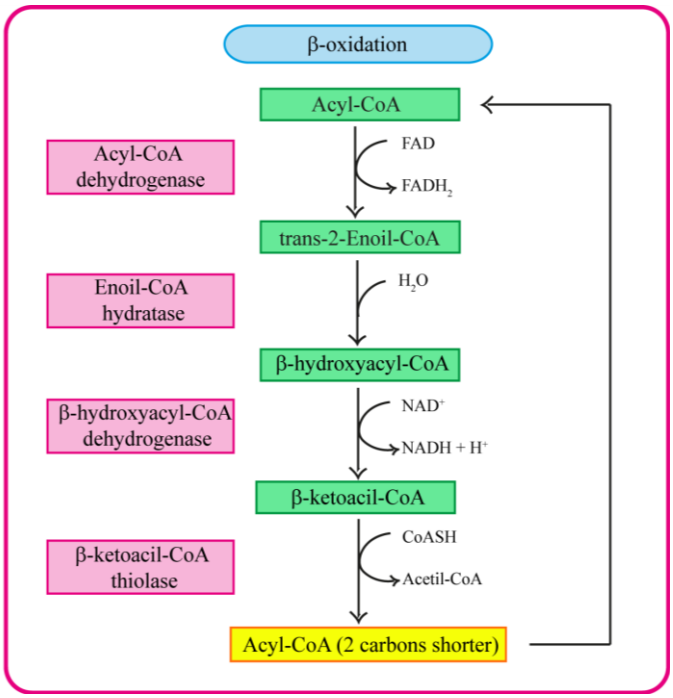

Figure 1.9: β-oxidation cycle. Schematic representation of the four steps of the β-oxidation cycle.

1.2.2.2.2.3 Regulation of β-oxidation

The uptake of acyl-CoA mediated by CPT1 represents the most important checkpoint to control β-oxidation rates. CPT1 activity is regulated by its inhibitor malonyl-CoA, which is synthesized by two different enzymes: Acetyl-CoA Carboxylases 1 and 2 (ACC1 and ACC2). ACC1 and ACC2 are encoded by separate genes, that share 80% identity in amino-acid sequence, but differ in several aspects: i) cell localization, with ACC1 being cytosolic and ACC2 bound to the mitochondrial membrane in close proximity with CPT1; ii) tissue distribution, with ACC1 highly expressed in lipogenic tissues (liver and AT), whereas ACC2 in oxidative tissue (heart and muscle, but not liver); iii) function, ACC1 promotes fatty acid synthesis while ACC2 exerts a negative control on β-oxidation. The malonyl-CoA molecules produced by ACC1 and ACC2 within the cell do not mix and are highly separated: the ACC1-generated malonyl-CoA is utilized by FAS in the cytosol, on the contrary the ACC2-generated malonyl-CoA functions as inhibitor of CPT1 activity (Schreurs et al., 2010; Stahl et al., 2001). The activity of both ACC isoforms is highly regulated in a similar way by allosteric modulation (being activated by citrate and inhibited by long-chain acyl-CoA) and phosphorylation/dephosphorylation mechanisms. When ATP is needed, both ACC1 and ACC2 are turned off by phosphorylation, in order to increase ATP level by a simultaneous decrease in FA synthesis and increase in β-oxidation. The AMPK, a master sensor for energy level in the cell, is the major kinase responsible for both ACC1 and ACC2 phosphorylation and inactivation (Hardie and Pan, 2002; Wakil and Abu-Elheiga, 2009). Transcriptional regulation is also involved in regulating fatty acid β-oxidation. The PPARγ coactivators-1 (PGC-1) family, especially PGC1α and PGC1β, are considered the master regulators of oxidative energy metabolism, able to activate gene programs that increase energy production to equip the cell to face an increase energy demand. PGC1α and PGC1β act by directly targeting Nuclear Receptor (NR) and non-NR transcription factors involved in the control of cellular metabolism, including PPARα, PPARβ, PPARγ, ERRα and many others. These transcription factors, in turns, increase gene expression of the enzymes involved in many steps of oxidative metabolism including FA uptake, β-oxidation, Krebs cycle, electron transport, and oxidative phosphorylation (Finck and Kelly, 2006; Huss and Kelly, 2004; Vega et al., 2000).

1.2.2.3 Mitochondria and oxidative phosphorylation

Mitochondria are the primary energy-generating systems in most eukaryotic cells. In addition to their central role in ATP synthesis, mitochondria accommodate central metabolic pathways, such as the Krebs cycle and the β-oxidation of fatty acids. Because of their endosymbiotic origins, mitochondria still contain their own small genome (mtDNA), which is organised in a closed-circular double strand structure encoding 37 genes, of which 22 encode for tRNAs (transfer RNAs) and two for rRNAs (ribosomal RNAs), so that, together with some nuclear-encoded factor, it provides mitochondria with their own replication, translation and transcription system. The other 13 mtDNA genes encode proteins that are located in the inner mitochondrial membrane as components of the oxidative phosphorylation (OxPhos) machinery (Taanman, 1999). Mitochondria are surrounded by two separate and functional diverse phospholipids bilayers: the outer (OM) and the inner (IM) membranes, which confine two aqueous compartments, the intermembrane space (IMS) and matrix compartments (Figure 1.10 A). The OM is permeable by small molecules and includes specific proteins to facilitate the import of mitochondrial proteins that have been synthesized in the cytoplasm (Dudek et al., 2013). The IM presents many tubular invaginations, named cristae, where all the components of OxPhos system (with the exception of the cytochrome c which is located in the IMS) are localised. The OxPhos system is composed of the electron transport chain (ETC) and the ATP synthase (or complex V), and it combines electron transport with the ATP production. The ETC comprises NADH-dehydrogenase (complex I), succinate dehydrogenase (complex II), ubiquinone, bc1 complex (complex III), cytochrome c (Cyt c), and cytochrome c oxidase (CcO; complex IV). Electrons, that enter the ETC, are donated to complex I from NADH or to complex II from $FADH_2$, then are moved from one complex to the next one until they reach complex IV, where they are required to combine hydrogen ions (H^+) and molecular oxygen (O_2) to form water (H_2O). The movement of electrons across the complexes I, III and IV is coupled with H^+ being pumped from the matrix to the IMS. This generates an electrochemical gradient used by complex V to generate ATP from ADP and inorganic phosphate (Pi) (Figure 1.10 B). The OxPhos system activity is regulated at several levels in order to match cellular energy demands with the ATP production. First of all, OxPhos activity is limited by the availability of the substrate required to generate ATP (that is ADP and Pi), a mechanism called respiratory control; secondly, there is a tissue-specific expression of different isozymes that are adapted to the requirement of the

particular tissue; third, it is subjected to an allosteric control by small molecules and finally, there is a cell signalling-mediated control (Hüttemann et al., 2007).

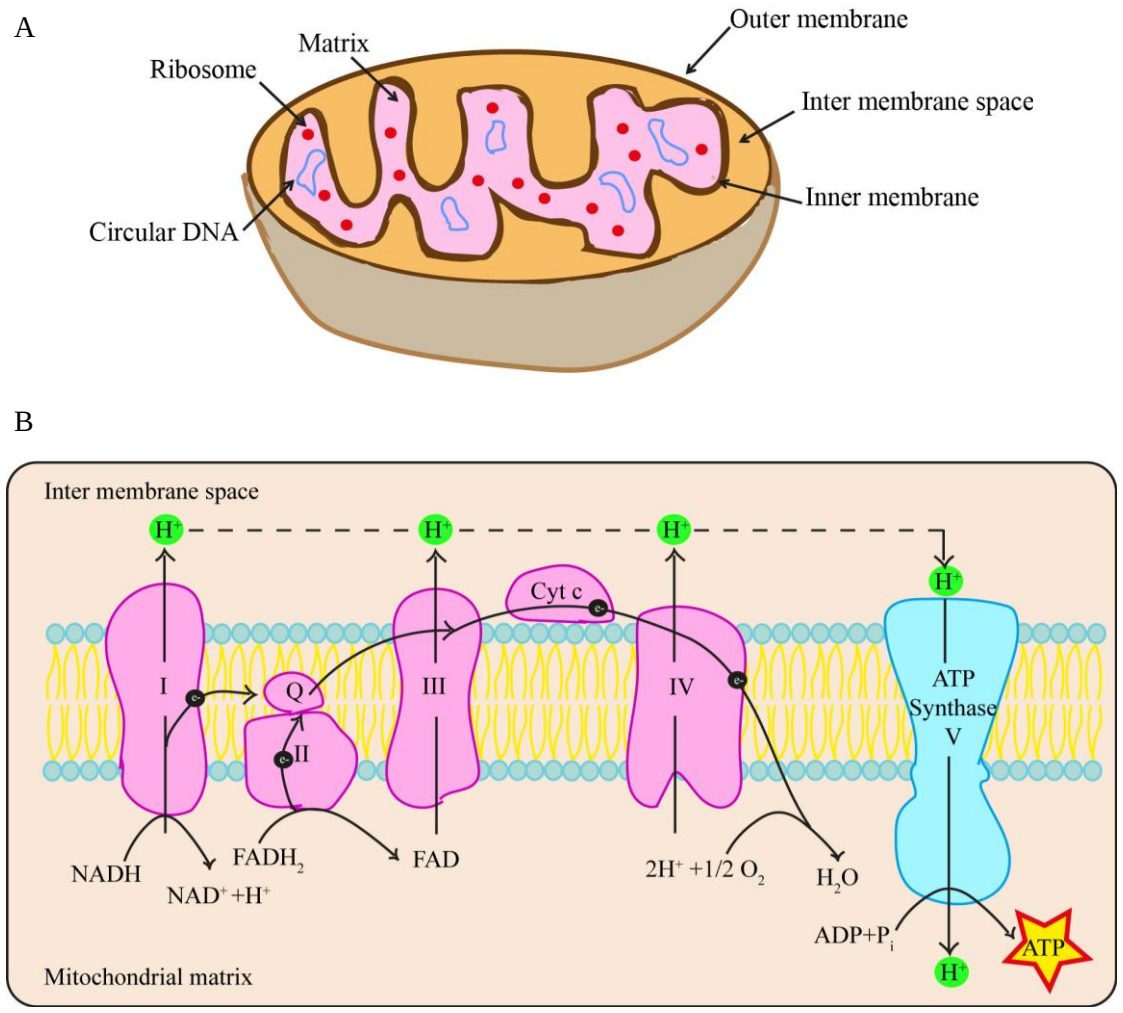

Figure 1.10: Structure of a mitochondrion and the electron transport chain. A) Schematic representation of mitochondrion structure. B) Schematic representation of the four complexes of the electron transport chain (I-IV) and the ATP synthase. As electrons flow along the electron transport chain, protons (H+) are pumped from the matrix into the intermembrane space through complexes I, III, and IV. Protons then flow back into the matrix through complex V, producing ATP.

1.3 Angiogenesis

De novo blood vessel formation occurs early during embryogenesis through a process, named vasculogenesis, in which mesoderm-derived endothelial precursors (angioblasts) differentiate into ECs and assemble into a primitive vascular "labyrinth". Subsequently, all further vessels growth is being done through angiogenesis. Although the term "angiogenesis" classically refers to the generation of new blood vessels from already established ones, it is now commonly used to indicate the growth and remodeling of the

primitive blood plexus into a complex and organized network (Carmeliet, 2000). Angiogenesis may happen through different mechanisms, but the most important and well studied one is the sprouting angiogenesis.

1.3.1 Sprouting angiogenesis

Sprouting angiogenesis strictly refers to the sprouting of new vessels from the wall of preexisting ones, and likely accounts for the majority of vascular growth (Carmeliet, 2000; Chung and Ferrara, 2011; Potente et al., 2011). Sprouting angiogenesis is a complex process that requires Endothelial Cells (ECs) proliferation, directional migration, establishment of the appropriate junction, lumen formation, recruitment of perivascular cells and anastomosis (Figure 1.11).

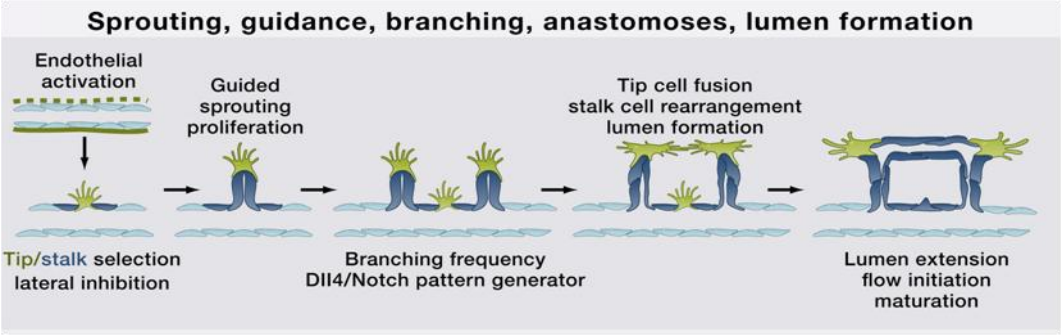

Figure 1.11: Sprouting angiogenesis: a multi-step process. Schematic representation of the principal steps of sprouting angiogenesis. Adapted from, (Potente et al., 2011).

The induction of a new sprout in a quiescent vessel is initiated by several pro-angiogenic factors (such as the vascular endothelial growth factor, VEGF-A), that are expressed by the surrounding hypoxic tissues, and is followed by changes in the endothelial cells polarity and junctions together with the degradation of the surrounding Extra Cellular Matrix (ECM) (Potente et al., 2011) (Figure 1.12).

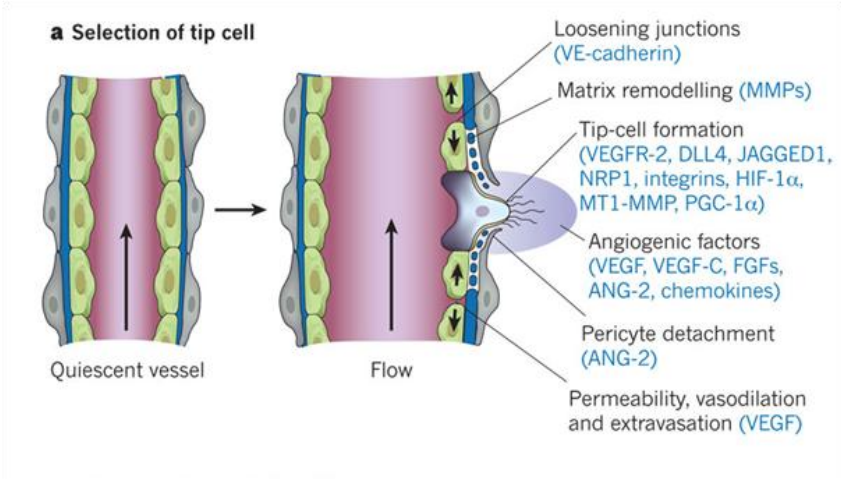

Figure 1.12: Initiation of a new vessel sprout. Upon pro-angiogenic stimulation, basement membrane (BM) is degraded, pericytes detach and ECs junctions are loosened. Only the BM of ECs is represented but pericytes also are embedded in this BM. Adapted from (Carmeliet and Jain, 2011).

1.3.1.1 Tip and stalk cell determination

Within a new vessel sprout, two different ECs populations can be distinguished: so-called tip cells and stalk cells. Tip and stalk cell specification is coordinated by the interplay between VEGF-A and Notch signalling. When angiogenesis is required, VEGF-A interacts with VEGFR2, expressed on the surface of the quiescent ECs, which results in increased Dll4 expression. Following VEGF-A stimulation, all ECs upregulate Delta-like 4 (Dll4), but the ones that express it quickly enough and at higher level have a competitive advantage to become a tip cells (Eilken and Adams, 2010). The cells that acquire the tip position induce Notch activation in the neighbouring ECs (a process known as lateral inhibition), that leads to the down-regulation of Dll4 expression and the up-regulation of the canonical Notch target genes, Hes, Hey and Nrarp. Dll4 stimulated ECs inhibit their tip cell behavior and differentiate into stalk cells. In addition, activation of Notch signalling in stalk cells inhibits VEGFR-2 expression, making those cells less sensitive to further VEGF stimulation. The phenotypic characterization of the tip and stalk cells is transient, in fact ECs at the sprouting front dynamically compete for the tip position (Jakobsson et al., 2010; Potente et al., 2011) (Figure 1.13).

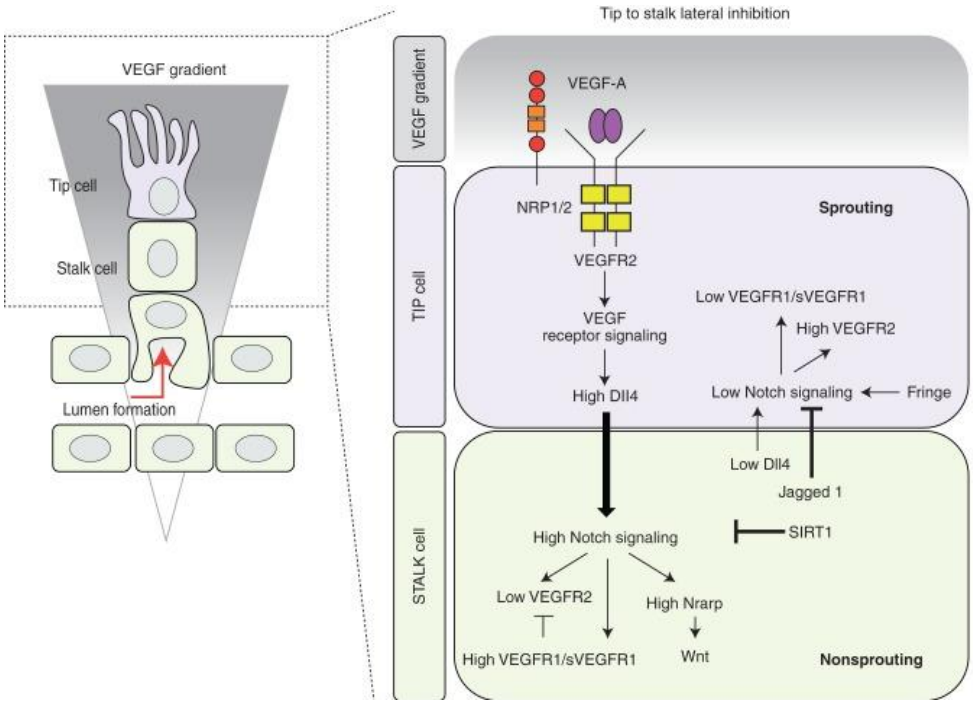

Figure 1.13: Tip/stalk cell specification during sprouting angiogenesis. Schematic representation of the crosstalk between Notch and VEGFR signalling pathways to control tip/stalk specification. Adapted from (Blanco and Gerhardt, 2013).

1.3.1.2 Lumen formation

Once new sprouts are generated the immature vessels need to establish a lumen, that occurs via different mechanisms depending on the vascular plexus that is being formed and/or the type of vessel that is being lumenized (Iruela-Arispe and Davis, 2009). As a tubular organ, the endothelial vasculature shares common features with epithelial tubes found in a number of other organs, such as lung, kidney, salivary glands and pancreas. A considerable amount of work has been carried out to elucidate epithelial tubulogenesis during the past several decades. Eventually, five different mechanisms by which epithelial cells could form lumens and tubular structures during morphogenetic processes have been proposed: wrapping, budding, cavitation, cord hollowing and cell hollowing (Lubarsky and Krasnow, 2003). In analogy, during sprouting angiogenesis lumen formation is thought to occur primarily by two mechanisms: cell hollowing (formation of intracellular luminal spaces initiated by vesicle formation and assembly in large vacuoles that later fuse together) and cord hollowing (a set of compact cells undergoes shape changes to create a central lumen) (Xu and Cleaver, 2011) (Figure 1.14).

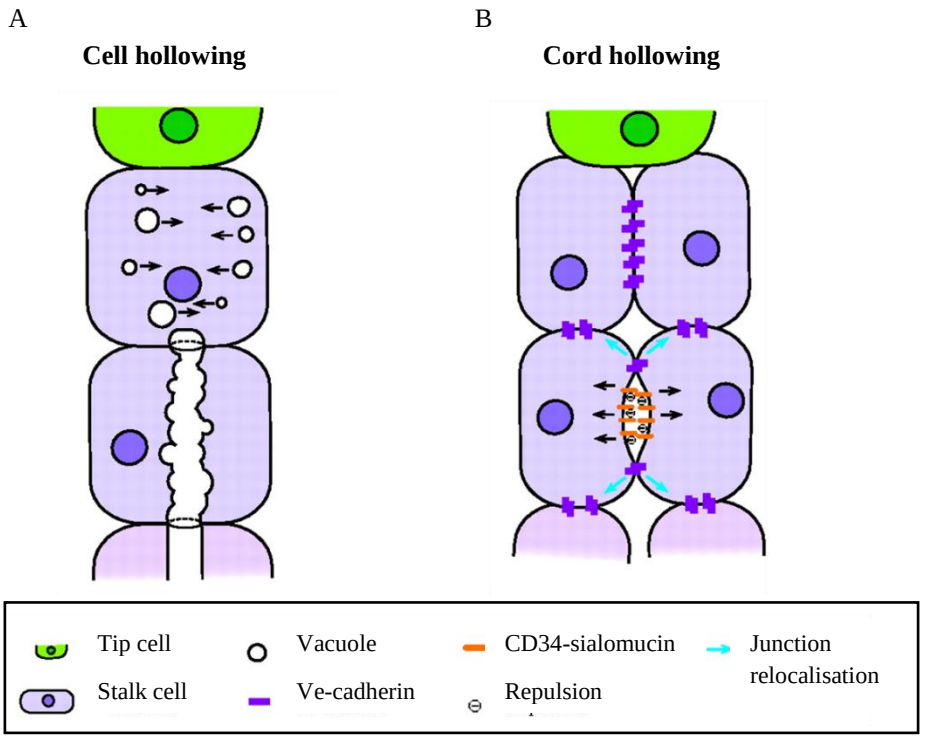

Figure 1.14: Principal models of vascular lumen formation. A) ECs can form a lumen by forming intracellular vacuoles that coalesce and connect with each other and with vacuoles in neighbouring cells. B) An intercellular lumen can be created by apical membrane (luminal) repulsion. VE-cadherin establishes the initial apical-basal polarity in ECs and localises CD34-sialomucins to the cell-cell contact sites. The negative charge of sialomucins induces electrostatic repulsion and initial separation of the apical membranes, thereby relocalising the junctional proteins to the lateral membranes and opening a vascular lumen. Adapted and modified from (Geudens and Gerhardt, 2011).

1.3.1.3 Anastomosis and vascular maturation

Vascular anastomosis is the process by which neighbor tip cells contact each other to add new vessel circuits to the existing network. For a proper anastomosis, tip cells have to suppress their motile and explorative behaviour and establish strong adhesive interactions and EC-EC junctional contacts at the joining points (Adams and Alitalo, 2007). It has been described that machrophages can facilitate this process by accumulating at the site of vessel anastomosis and interacting with filopodia of neighbouring tip cells (Fantin et al., 2010); however, anastomosis does not strictly require macrophages. Once anastomosis is completed, the newly formed capillaries are connected with the rest of the vascular network, but still need to undergo further maturation and stabilization. Three main processes contribute to generate mature and stable vessels: the formation of tight junctions between ECs, the deposition of

extracellular matrix into the basement membrane and the recruitment of supporting mural cells (Potente et al., 2011).

EC-EC junctions

ECs constituting vessel walls need to assure vessel integrity by maintaining a monolayer of contiguous endothelial cells that prevent areas of vascular damage and extravasation. Accordingly, neighbouring ECs establish junctional structures, formed by transmembrane adhesive proteins that not only connect ECs with ECs but also with surrounding cells and the ECM. In the endothelium, junctional complexes principally comprise adherent junctions and tight junctions. Adherent junctions (AJs) are ubiquitously distributed along the vascular tree and are formed by transmembrane adhesion proteins of the cadherin family. Vascular endothelial (VE)-cadherin is the principal, and endothelial specific, AJs protein expressed in all endothelial cells of all types of vessels (Bazzoni and Dejana, 2004). VE-cadherin is essential during the embryo development for the organisation of a stable vasculature, whereas in the adult it controls vascular permeability and it prevents unlimited vessel growth by promoting cell-contact inhibition (Giannotta et al., 2013).

Tight junctions (TJs) mediate adhesion and communication between adjacent cells. Specifically, TJs control two processes: 1) paracellular permeability, exhibiting a barrier function that restricts the diffusion of solutes across intercellular spaces, and 2) cell polarity by restricting the movement of membrane molecules between the apical and basolateral domains of the plasma membrane (Bazzoni and Dejana, 2004). TJs show considerable variability among different segments of the vascular tree; a disparity that has a strong impact on vascular permeability and leukocyte extravasation. The core components of TJs are members of the claudin family, principally Claudin-5, which is rather ubiquitous along the vascular tree. Other additional adhesion molecules within TJs include: occludins, junctional adhesion molecules (JAMs) and endothelial cell-selective adhesion molecule (ESAM). TJs are well developed in celebral vessels, where they contribute to the blood-brain barrier, but their role in early vascular development is not known (Wallez and Huber, 2008).

Mural cell recruitment and extracellular matrix deposition

A fundamental step during vessel maturation is the recruitment of mural cells, consisting of pericytes and vascular smooth-muscle cells (vSMCs), that stabilize the newly formed vessel. vSMCs principally cover big vessels, such as arteries and veins, forming an independent layer over the endothelium, which is separated from the vascular basal membrane (BM). Conversely, pericytes are located around small vessels, such as capillaries, and do not organize in a separate layer, but are embedded within the BM together with ECs. During vascular remodelling, ECs secrete several growth factors, partially to attract pericytes and promote vessels maturation. Among all, the most important for pericytes recruitment is the platelet-derived growth factor B (PDGFB), which, once released, binds to the extracellular matrix where it acts as a chemoattractant molecule for pericytes that express the PDGF receptor-β (PDGFR-β) (Bergers and Song, 2005). Pericytes do not serve solely as supporting scaffold, but communicate with ECs by direct physical contact and paracrine signalling pathways (Bergers and Song, 2005); in this way, pericytes exert an inhibitory effect on ECs proliferation and migration which allow the formation of stable and mature vessels (Gerhardt and Betsholtz, 2003). Another critical point to ensure vessel stability is the deposition of ECM. The vascular ECM is composed of laminins, type IV collagen, perlecan, nidogen/entactin, fibulins, type XVIII collagen and fibronectins among others (Senger and Davis, 2011).The regulation of ECM deposition and degradation is essential for all stages of angiogenesis. The ECM gives a structural support, protecting vessels from disruptive physical stresses, and provides an interactive interface between ECs and surrounding environment which mediates local and distant signals within and between these compartments (Carmeliet, 2003).

1.3.1.4 Vascular quiescence

Eventually, once vessels are stable and angiogenesis is not more required, external VEGF-A expression diminished, leading to a shift in the endothelial behavior towards a quiescent phenotype (Potente et al., 2011). In the majority of adults healthy tissues, vessels are quiescent and rarely form new branches, but ECs preserve a high plasticity to sense and respond to angiogenic signals (Carmeliet, 2000; Potente et al., 2011). In this quiescent status, ECs still need to maintain a prosurvival micro-environment to ensure vessel integrity. Accordingly, it has been described that ECs release VEGF-A that, in turn, activates pro-survival pathways such as the phosphatidylinositol-3-kinase

(PI3K) signalling cascade (Warren and Iruela-Arispe, 2010). Thereby, intracrine VEGF expression in blood vessels prevents ECs from becoming apoptotic and from disrupting vessel integrity. Other signalling pathways such as fibroblast growth factors (FGFs) and the Angiopoietin-1/Tie-2 signalling pathways can also help to maintain vessel quiescence and survival by stabilizing EC-EC junctions and suppressing mediators of the apoptotic pathway, respectively (Augustin et al., 2009; Beenken and Mohammadi, 2009).

1.3.2 Molecular regulator of angiogenesis: a brief overview

Angiogenesis is essential in many biological contexts, including development, reproduction and tissue repair, and it is tightly regulated through a fine balance between pro- and anti-angiogenic molecules. Uncontrolled angiogenesis is often associated with malignancy and retinopathies, while insufficient angiogenesis is a characteristic feature of disorders like ischemic tissue injury or cardiac failure (Bisht et al., 2010). Several signalling pathways strictly regulate different phases of the vascular development such as the PDGF-B / PDGFR-B, the Ephrin / Eph, the Semaphorins / Plexins, the Netrins / Unc5b, the TGF-β, or the PI3K. However, among all, the most important ones involved in the regulation of angiogenesis are the VEGF/VEGFR and Notch signalling pathways.

1.3.2.1 VEGF-VEGFR signalling pathway

One of the most specific and important key regulator of angiogenesis is VEGF-A (also known as VEGF). It belongs to a gene family that comprehends several secreted glycoproteins designated VEGF-A, VEGF-B, VEGF-C, VEGF-D and Placental Growth Factor (PIGF) (Ferrara et al., 2003; Houck et al., 1991). As a result of an alternative splicing, VEGF-A exists in multiple isoforms: the human isoforms are denoted VEGF-A121, VEGF-A145, VEGF-A148, VEGF-A165, VEGF-A183, VEGF-A189 and VEGF-A206 (Harper and Bates, 2008). The mouse isoforms are one residue shorter from the human equivalents, thereby VEGF-A120, etc. (Olsson et al., 2006). The indispensable role of VEGF-A signalling in early angiogenesis is emphasized by the fact that mice lacking a single VEGF-A allele die at embryonic day (E)9.5 (Carmeliet et al., 1996; Ferrara et al., 1996). VEGF ligands exert their biological effects through interactions with three transmembrane tyrosine kinases receptors (RTKs) named VEGFR1, VEGFR2 and VEGFR3 (Otrock et al., 2007). Distinct VEGF ligands display different affinities to each receptor: VEGF-A binds VEGFR1 and VEGFR2, VEGF-B and PIGF selectively tie to VEGFR1, whereas VEGF-C and VEGF-D primarily interact

with VEGFR-3 (Figure 1.15). Although VEGF-A has a 10-fold higher affinity to VEGFR1 than to VEGFR2, VEGFR-1 is a kinase-impaired RTK whereas VEGFR2 is an highly active kinase (Rahimi, 2006); therefore, VEGFR2 is considered the main mediator of VEGF-A angiogenic signal. VEGF-A promotes ECs survival both *in vivo* and *in vitro*, an activity mediated by the PI3K/Akt pathway (Gerber et al., 1998a). VEGF-A also induces the expression of anti-apoptotic proteins Bcl-2 and A1, that prevent apoptosis induced by serum starvation (Gerber et al., 1998b). *In vivo*, the prosurvival effect of VEGF-A is essential for ECs growth and survival in early postnatal life, but it is dispensable in adult mice (Gerber et al., 1999).

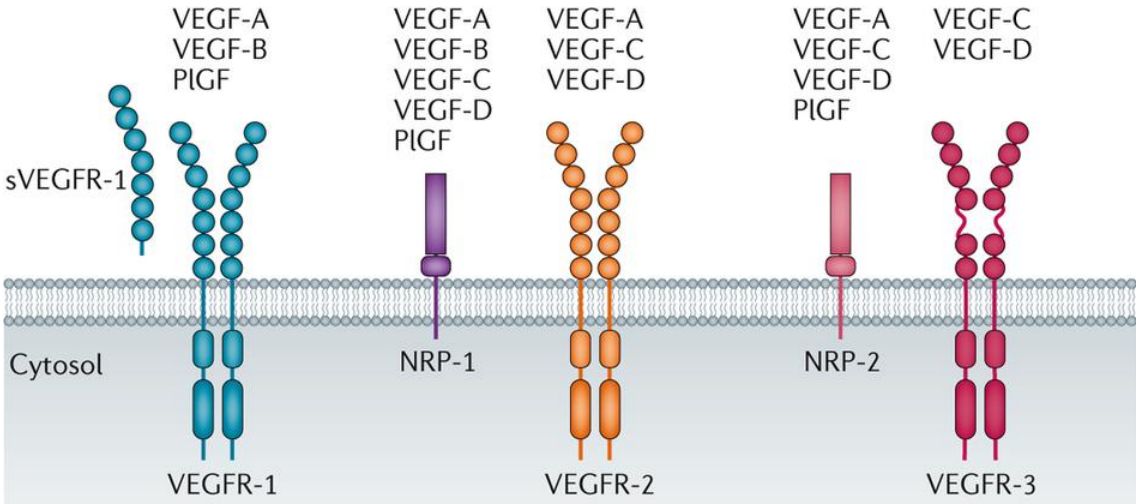

Figure 1.15: Receptor-binding specificity of VEGF family members. Schematic diagram representing the interaction between the different VEGF ligands (VEGF-A, -B, -C,-D and PlGF) and their tyrosine kinase receptors, VEGFR-1, VEGFR-2, and VEGFR-3. The co-receptors NRP1 or NRP2 are also shown. VEGFR-1 and VEGFR-2 activation is important in the regulation of both the vasculogenesis and angiogenesis. Adapted from (Lange et al., 2016).

1.3.2.2 Notch signalling pathway

Notch signalling is a well known pathway that regulates cell fate specification, growth and differentiation during the embryonic development, tissue homeostasis, and the maintenance of stem cell in adults (Kopan and Ilagan, 2009). In mammals, there are four Notch receptors (Notch1, Notch2, Notch3 and Notch4) and five ligands named Jagged1, Jagged2, Delta-like (Dll)1, Dll3 and Dll4. The pathway is activated when a signal-sending cell expressing a Notch ligand physically interacts with a receiving cell expressing a Notch receptor leading to several proteolytic cleavage of the receptor. The last cleavage is triggered by the γ-secretase complex that releases the Notch intracellular domain (NICD) that translocates to the nucleus. Once in the nucleus, NICD forms a

complex with the RBP-Jk protein, a sequence-specific DNA binding protein, activating the Notch transcriptional machinery that modulates the expression of multiple genes as Hairy/enhancer of split (HES), HES-related proteins (HEY/HRT/HERP) family genes and also Dll4 gene (Iso et al., 2003). This signalling mechanism is known as the "canonical Notch pathway". Many studies modulating the expression of the different Notch components in mice and zebrafish have revealed that this pathway has an essential role in angiogenesis, regulating different steps of the angiogenic process (Roca and Adams, 2007). During angiogenic expansion, reduced Dll4 expression or Notch inhibition by different strategies promotes sprouting, branching and filopodia formation (Benedito et al., 2012; Suchting et al., 2007). In contrast, activation of Notch signalling leads to the opposite vascular phenotype (Hellström et al., 2007).

1.3.3 The PI3Ks family

PI3Ks are an evolutionary conserved family of lipid kinases that play an important role in several cellular functions such as cell metabolism, proliferation and survival. Once activated by extracellular stimuli (like insulin, cytokines and growth factors), PI3Ks phosphorylate the 3'-hydroxyl group of the inositol ring of three species of phosphatidylinositol (PtdIns) lipid substrates: PtdIns, PtdIns-4-phosphate (PtdIns4P) and PtdIns-4,5-bisphosphate (PtdIns(4,5)P_2). These three phospho-inositides then modulate the activity of multiple effector proteins by binding to their FYVE, pleckstrin homology (PH) or phox homology (PX) domains (Vanhaesebroeck et al., 2010). According to their lipid substrate preference and sequence homology, PI3Ks have been divided into three classes (Figure 1.16). Class I PI3Ks is the most studied and understood among the others. Class I PI3Ks function as heterodimers, are composed of catalytic and regulatory subunits and can be divided into class IA and IB, depending on the ability to bind the p85 regulatory subunit. Class IA subfamily consists of three different catalytic (p110α, β, and δ) and five regulatory (p85α, p55α, p50α, p85β, and p55γ) subunits, all of which are able to bind each other. Class IB is only composed of one catalytic subunit (p110γ) that can bind to either p101 or p87 regulatory subunits, thath have no homology to p85 (Graupera and Potente, 2013).

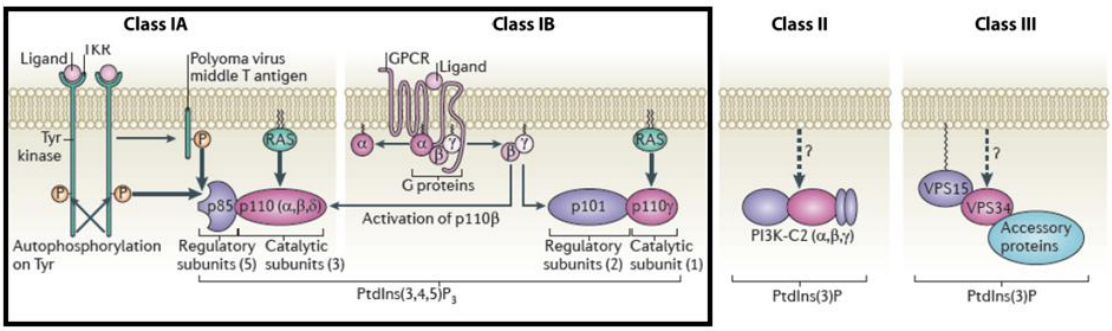

Figure 1.16: Class I mammalian PI3Ks. Class I PI3Ks are receptor-regulated PtdIns(4,5)P2-kinases that generate PtdIns(3,4,5)P3. The p110α, p110β and p110δ isoforms of the catalytic subunit are constitutively bound to a p85 regulatory subunit. The p110γ isoform does not bind to a p85 subunit, but binds to the unrelated p101 or p87 regulatory subunits, which link p110γ to Gβγ subunits released from heterotrimeric G proteins downstream of GPCRs. Adapted from (Vanhaesebroeck et al., 2012).

Class I PI3Ks signal mainly downstream RTKs, although they can also transduce signals downstream some G-protein-coupled receptors (GPCRs). One of the most important and broadly studied target of PI3Ks is the Ser/Thr kinase Akt. The Akt family consists of three isoforms: Akt-1, Akt-2 and Akt-3. All the Akt isoforms contain an N-terminal PH domain for phospholipid binding, followed by a short linker domain, a catalytic domain and a C-terminal regulatory tail domain (Zhou et al., 2006). The interaction with PtdIns(3,4,5)P_3 results in Akt translocation to the plasma membrane, what enables its phosphorylation by PDK1 (at Thr308) and mTORC2 (at Ser473), leading to full Akt activation. Then, Akt phosphorylates several downstream targets (for example eNOS, mTORC1, PFKFB2, TSC2, p21, GSK3 and FOXOs), thereby converting the upstream signal into many different cellular responses (Manning and Cantley, 2007) (Figure 1.17). Due to its extensive influence on many cell functions and overall pro-survival activity, the PI3K signalling needs to be strictly regulated; in fact uncontrolled activation of this pathway has been associated with various disease such as cancer, overgrowth syndromes, inflammation and autoimmunity (Vanhaesebroeck et al., 2016). The most important negative regulator of PI3Ks is PTEN (phosphatase and tensin homolog deleted on chromosome 10). It hydrolyzes the 3'-phosphate bond on PtdIns(3,4,5)P_3 to generate its precursor PtdIns(4,5)P_2, thereby counterbalancing the activity of PI3Ks. Not surprisingly PTEN is one of the most frequently mutated tumor suppressor gene in several human cancers (Salmena et al., 2008).

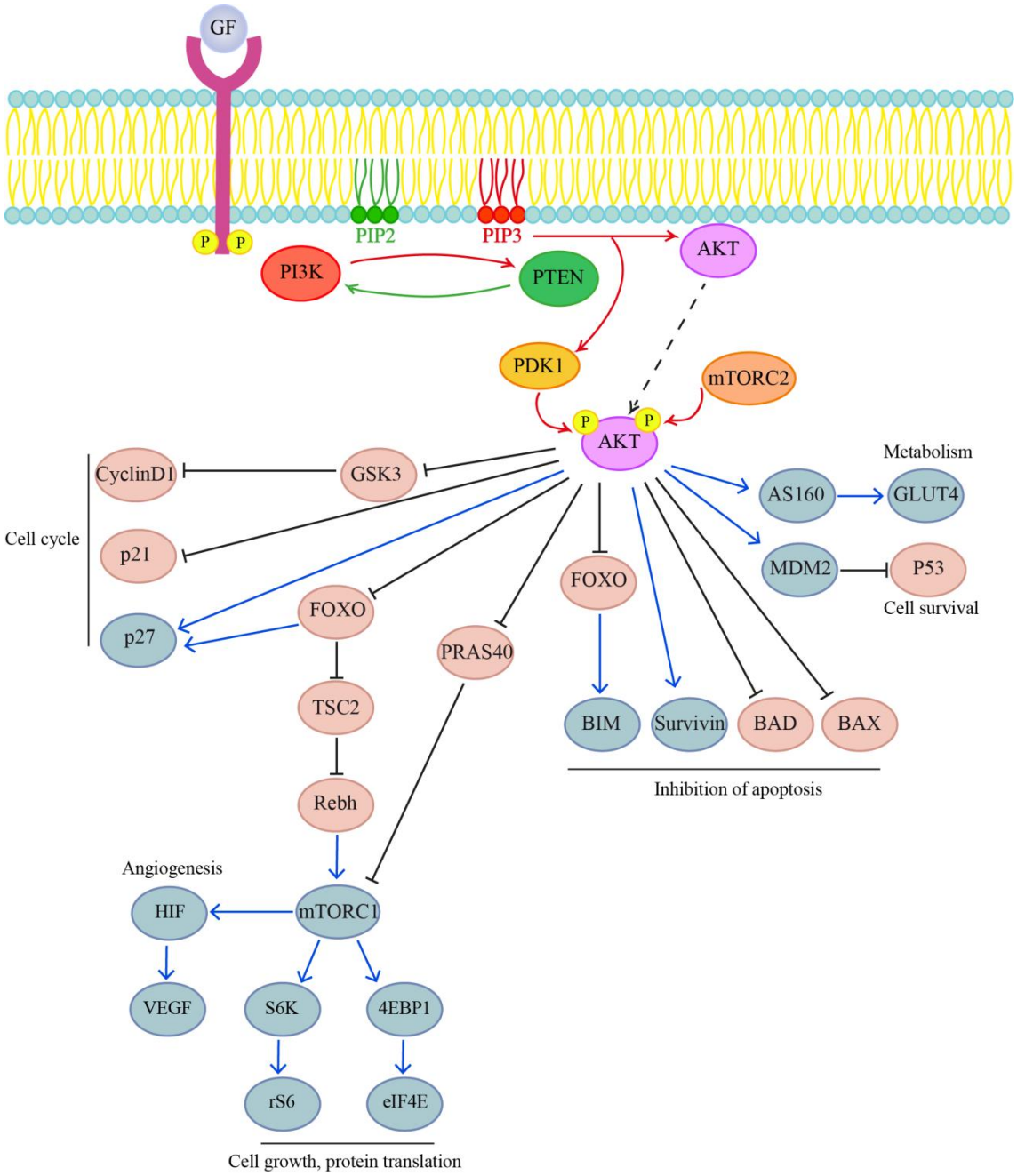

Figure 1.17: PI3K/Akt signalling transduction. Receptor-stimulated class I PI3Ks generate PtdIns(3,4,5)P3, which binds directly to the PH domain of Akt, driving translocation of Akt to the plasma membrane and allowing its phosphorylation of Thr308 by PDK1. Additional phosphorylation on Ser473 by mTORC-2 leads to full Akt activation, driving the phosphorylation of a plethora of downstream targets that ultimately regulate proliferation, cell growth, survival, apoptosis, metabolism and angiogenesis.

1.3.3.1 PI3K-Akt signalling transduction

The PI3K-Akt pathway controls many cellular functions including: survival, growth, proliferation and metabolism. Akt activation promotes cell survival through several mechanisms: i) Akt phosphorylation of Forkhead box O (FOXOs) determines FOXO

exclusion from the nucleus, which results in the inhibition of FOXO-mediated transcription of target genes that promote apoptosis, cell-cycle arrest and regulates metabolic processes (Oellerich and Potente, 2012; Tzivion et al., 2011). ii) Akt negatively regulates the function or expression of several Bcl-2 homology domain 3 (BH3)-only proteins, which exert their proapoptotic effects by binding to and inactivating prosurvival Bcl-2 family members (Manning and Cantley, 2007). iii) Activation of Akt results in diminished cellular levels of tumour protein 53 (p53), a tumour suppressor protein responsible for cell-cycle arrest and apoptosis. Mechanistically, Akt phosphorylates MDM2 leading to its nuclear translocation; once in the nucleus MDM2 decreases the transcriptional activity of p53. Reduced p53 levels upon Akt activation results in pro-growth and pro-survival signals (Mayo and Donner, 2001). Akt also controls cell growth, principally through activation of Mammalian target of rapamycin (mTOR) complex 1 (mTORC-1). Activated Akt can directly phosphorylate the tuberous sclerosis complex 2 (TSC-2), a tumor suppressor gene that acts as negative regulator of mTOR, which results in TSC-2 destabilisation and inactivation (Inoki et al., 2002). The Akt-mTORC-1 pathway is known to regulate cellular growth, protein synthesis and autophagy (Huang and Manning, 2008; Manning and Cantley, 2007). The principal downstream effectors of mTORC-1 are thought to be ribosomal S6 protein (rS6) kinase (S6K) and eukaryotic translation-initiation factor 4E (eIF4E) binding protein 1 (4E-BP1) (Bhaskar and Hay, 2007). Akt can directly stimulate proliferation by preventing the nuclear localization of the cell-cycle arresters p27 and p21 and thus attenuating its cell-cycle inhibitory effects, such as apoptosis and senescence (Manning and Cantley, 2007; Sekimoto et al., 2004; Shin et al., 2002). Besides, due to its position downstream the insulin receptor and IRS adaptor molecules, the PI3K-Akt pathway is also involved in the regulation of glucose metabolism. First, it enhances insulin-mediated glucose uptake and membrane translocation of the glucose transporter GLUT4 through the inhibition of the AS160 Rab GTPase activating protein; second, activation of mTORC1, through Akt, can contribute to both HIFα-dependent transcription and cap-dependent translation of GLUT1 (Manning and Cantley, 2007).

1.3.3.2 PI3K signalling in angiogenesis

Several well known pro-angiogenic growth factors like fibroblast growth factor (bFGF), epidermal growth factor (EGF) and VEGF can activate PI3K, thus linking the PI3K pathway to angiogenesis. Especially through VEGF/VEGFRs signalling, PI3K-Akt axis can be strongly induced in ECs where it promotes ECs survival, migration and proliferation. It has been described that VEGFR1 and VEGFR2 control PI3K activation by recruiting and interacting with the p85 regulatory subunit (Cunningham et al., 1995; Dayanir et al., 2001). The Angiopoietin (Ang) /Tie system is another important pathway that controls PI3K activation in ECs. The Ang–Tie signalling is essential during embryonic vessel assembly and maturation, and it functions as a key regulator of adult vascular homeostasis (Augustin et al., 2009). The Ang-Tie family consists of three ligands (Ang1, Ang2 and Ang3) and two receptors (Tie1 and Tie2). Activation of Tie2 receptor by its ligand Ang1 can activate PI3K signalling by binding of p85 subunit to the activated receptor (Jones et al., 1999). Ang1 is required for ECs survival and vessels stability, conversely, Ang2 acts as antagonist of Ang1, favouring vessel destabilization (Augustin et al., 2009). The physiological effects of PI3K activity in ECs during angiogenesis are principally mediated by Akt and its downstream targets. However, PI3K can also directly promote angiogenesis by regulating the expression of Hypoxia-Inducible Factor(HIF) HIF-1α and HIF-2α transcription factors, via mTORC-1, which in turn increases VEGF level (Semenza, 2003). Interestingly, analysis of class IA catalytic subunits mutant mice (p110α, p110β and p110δ) revealed that the different p110 isoforms are not equally important for a proper vascular development and remodeling; indeed only p110α has been found to be absolutely essential (Graupera et al., 2008).

1.3.4 PTEN

PTEN (phosphatase and tensin homolog deleted on chromosome 10) was first discovered in 1997 by two independent groups looking for tumor suppressor genes in the chromosome 10q23 (hot spot for loss of heterozygosity in many human tumors) (Li et al., 1997; Steck et al., 1997). PTEN is a dual lipid protein phosphatase that, unlike most of the protein tyrosine phosphatases, preferentially dephosphorylates phosphoinositide substrates (Cristofano and Pandolfi, 2000). Once located at the plasma membrane, PTEN dephosphorylates PtdIns(3,4,5)P_3 thereby negatively regulating the PI3K activity. The PI3K/AKT signalling cascade is critical in cancer as it promotes cell

survival and growth; several components of this pathway have been found altered in many tumors and they represent a target for cancer therapy (Wong et al., 2010). Therefore, its lipid phosphatase activity converts PTEN in a key tumour suppressor gene. Accordingly, PTEN is one of the most frequently mutated genes in human cancer, and PTEN inactivation occurs in multiple sporadic tumor types (Carracedo et al., 2011).

1.3.4.1 PTEN structure and localisation

The PTEN gene, mapped to 10q23.3, contains nine exons and encodes a 47 kDa protein with 403 amino acids. PTEN possesses multiple domains including the N-terminal phosphatase domain which consists of the first 185 amino acids, and the C-terminal domain, made up of the remaining amino acids (186-403), which is divided into a central C2 domain and a C-terminal tail. The N-terminal and C2 domains are responsible for PtdIns(3,4,5)P3 metabolism while the C-terminal tail is principally involved in PTEN regulation (Govender and Chetty, 2012; Shi et al., 2012) (Figure 1.18).

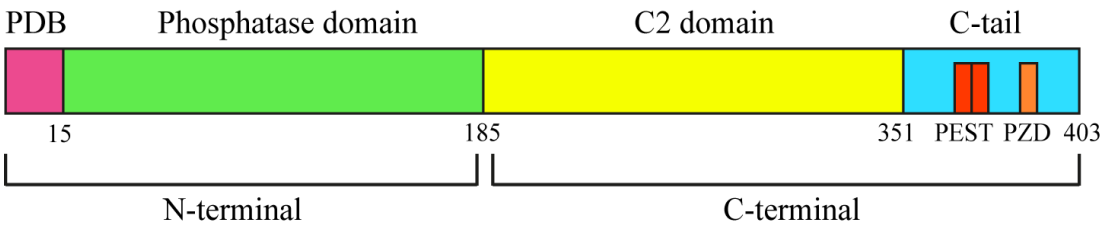

Figure 1.18: PTEN protein primary structure. The N-terminal region is composed by a PIP2-binding domain (PBD) and a phosphatase domain The C-terminal regionis is composed by a C2 domain and a C-terminal tail containing two PEST (proline, glutamic acid, serine, threonine) sequences, and a PDZ-interaction motif at the end.

Early studies showed that PTEN only localised at the cytoplasm and was able to transiently bind at the plasma membrane depending on PIP2 and PIP3 concentration (Iijima et al., 2004; Vazquez et al., 2006). However, later on, it has been demonstrated that PTEN can localize or associate with many organelles and subcellular compartment such as mitochondria, the nucleus, endoplasmic reticulum and mitochondria-associated membranes (Bononi et al., 2013; Trotman et al., 2007; Zhu et al., 2006). Moreover, PTEN can be exported or secreted from donor cells to recipient cells where it acts as tumour suppressor by inhibiting the PI3Ks signalling (Hopkins et al., 2013; Putz et al., 2012).

1.3.4.2 PTEN general functions

PTEN is involved in regulating many cellular processes; a significant portion of PTEN function is attributed to its well-known lipid phosphatase activity that antagonizes PI3K activity. However, PTEN also has several PI3K/Akt-independent activities. Interestingly, PTEN function is, at least partially, determined by its subcellular localisation.

Plasma membrane PTEN

In most mammalian cells, PTEN does not show an obvious association with the plasma membrane, being mostly localised in cytoplasm and nucleus. Once recruited at the plasma membrane, PTEN antagonizes the PI3K-Akt signalling pathway thereby inhibiting all the Akt dependent cellular processes such as proliferation, growth, survival and metabolism (described in 1.3.3.1) .

Nuclear PTEN

The first persuasive evidence suggesting a functional role of nuclear PTEN came from melanoma studies which showed that in quiescent cells PTEN was mainly confined in the nucleus, whereas in actively dividing cells it was mostly localized in the cytoplasm (Whiteman et al., 2002). Other studies observed a similar trends in different tissues (Gimm et al., 2000; Perren et al., 2000). These findings lead to the belief that PTEN in the nucleus have an important tumor-suppressive function. Later on it was found that PTEN entry in the nucleus is cell-cycle dependent, with higher and lower nuclear PTEN levels respectively in G0-G1 and S phase (Ginn-Pease and Eng, 2003). PTEN does not contain traditional nuclear import/export sequences; however, several putative mechanisms for the nucleo-cytoplasmic shuttling of PTEN have been identified and include: simple diffusion (Liu et al., 2005), active shuttling by the RAN GTPase or major vault protein (Gil et al., 2006; Yu et al., 2002), export/import dependent on a putative cytoplasmic localization signal or unconventional nuclear localization signal, respectively, (Chung et al., 2005; Denning et al., 2007) and monoubiquitylation-dependent import (Trotman et al., 2007). Within the nucleus, PTEN exerts an important role in chromosome stability, DNA repair and cell-cycle arrest. Recently, it has been reported that PTEN inhibits cell cycle progression by modulating the activity of the anaphase-promoting complex/cyclosome (APC/C) in the nucleus in a manner that is independent of PTEN phosphatase activity. Specifically, PTEN promotes the biding of

APC/C with its partner CDH1 thereby enhancing the tumor-suppressive activity of the APC-CDH1 complex (Song et al., 2011). Furthermore, PTEN plays a fundamental role in the maintenance of chromosomal stability through the physical interaction with the centromere-specific binding protein C (CENP-C) and it prevents double-strand DNA breaks (DSB) controlling the transcription of Rad51 (a protein required to repair DSB) (Shen et al., 2007).

1.3.4.3 PTEN levels of regulation

PTEN is involved in the regulation of a wide variety of cell functions, therefore, it requires tight regulatory mechanisms. Indeed, PTEN level and function are regulated transcriptionally, post-transcriptionally and post-translationally. PTEN is also sensitive to regulation by its interacting proteins and its localization. Intriguingly, subtle changes in PTEN gene expression, mRNA regulation and protein synthesis are sufficient to have a substantial impact on the normal physiology of potentially any tissue (Alimonti et al., 2010; Carracedo et al., 2011).

1.3.4.3.1 Transcriptional and post-transcriptional regulation

PTEN is positively and negatively regulated by many transcription factors that operate at specific times and in different cell types (Shi et al., 2012). Positive regulators include early growth response protein 1 (EGFR-1), PPAR-γ, and p53; these transcription factors were shown to directly bind to PTEN promoter region (Patel et al., 2001; Stambolic et al., 2001; Virolle et al., 2001). Negative regulators include the proto-oncogene c-Jun, nuclear factor kappa B (NF-κB), ecotropic virus integration site 1 (EVI-1), BMI-1, and SNAIL. NF-κB negatively regulates PTEN expression through sequestration of the transcriptional co-activator CBP/p300 (Vasudevan et al., 2004); EVI-1 binds directly to the PTEN promoter and represses its transcription in bone marrow cells (Yoshimi et al., 2011). BMI-1 is a polycomb-group protein that is deregulated in a variety of cancers; BMI-1 regulates PTEN transcription both directly (binding to PTEN locus) and indirectly by stabilizing SNAIL (a transcriptional repressor of PTEN, which is also involved in epithelial to mesenchymal transition) (Song et al., 2009). Notch signalling has also been reported to exert a cell-context dependent regulation on PTEN transcription. Specifically, Notch signalling might lead to up-regulation or down-regulation of PTEN by respectively inhibiting the Recombining Binding Protein suppressor of hairless (RBPJ) or activating the transcription factor Hairy and Enhancer of Split 1 (HES1), which are both PTEN down-regulators (Chappell et al., 2005;

Palomero et al., 2007; Whelan et al., 2007). In addition, at the post-transcriptional level, a variety of microRNAs (miRNAs) have been identified to repress PTEN mRNA translation; in fact, miRNAs deregulation has been associated with the development of different human cancers (Bermúdez Brito et al., 2015). An additional level of complexity is given by the presence of endogenous PTEN pseudogene (PTENp1), which encodes three different non-coding RNA that function like a miRNA sponge, sequestering them and therefore de-repressing PTEN expression and enhancing its tumor-suppressor activity (Johnsson et al., 2013; Poliseno et al., 2010) (Figure 1.19) .

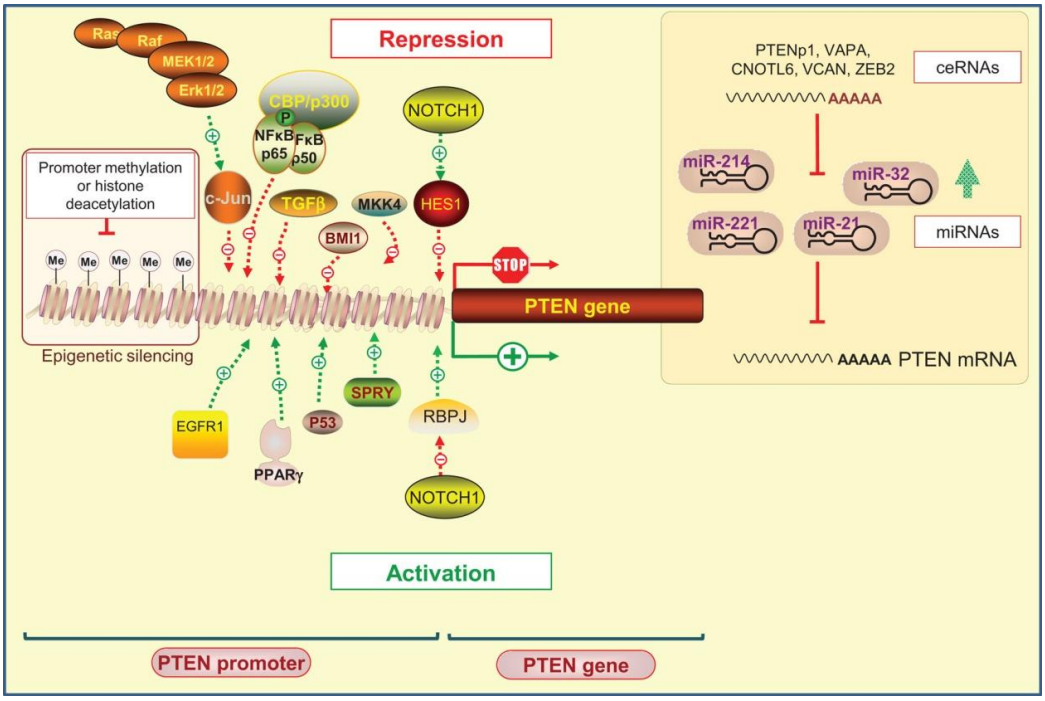

Figure 1.19: Regulation of PTEN expression by epigenetic, transcriptional and post-transcriptional mechanisms. PTEN regulation occurs at the transcriptional level by several proteins that positively or negatively modulate PTEN transcription. Epigenetic silencing by the gene promoter methylation and histone modifications may also negatively control PTEN expression. PTEN is also subjected to post-transcription regulation by numerous microRNAs. Additionally, the pseudogene (PTENP1) acts as a decoy for PTEN-targeting microRNAs and serves as an example of the many competitive endogenous RNAs that might function as trans-regulators of PTEN. Adapted from (Bermúdez Brito et al., 2015).

1.3.4.3.2 Post-translational regulation

PTEN is regulated post-translationally mainly through phosphorylation, acetylation, ubiquitylation, oxidization or s-nitrosylation.

PTEN phosphorylation mainly occurs at the C-tail and it interferes with the localization, the stability, and the activity of the protein. Phosphorylated PTEN acquires a compact

conformation which prevents PTEN recruitment to the membrane, and consequently it impairs PTEN phosphatase activity (Bermúdez Brito et al., 2015).

Acetylation is another well-known mechanism to regulate PTEN activity. Two acetylation sites have been identified till now. One is located in the phosphatase active domain (Lys 125–128) and is conferred by p300/calcium-binding PTEN-associated factor. Acetylation of this site was reported to downregulate PTEN activity (Okumura et al., 2006). The other acetylation event is driven by CREB-binding protein and results in the modulation of PTEN interaction with other PDZ-domain containing proteins (Ding et al., 2014).

Ubiquitination is an enzyme-catalyzed cascade well known to mark protein substrates for 26S proteasome-dependent degradation, but it can also modify protein localization, trafficking and/or activation. It is, actually, poly-ubiquitination that targets PTEN for proteasomal degradation whereas mono-ubiquitination regulates PTEN nuclear import (Tolkacheva et al., 2001; Trotman et al., 2007). In parallel, it was shown that both poly- and mono-ubiquitination of PTEN inhibit its phosphatase activity, thus interfering also with PTEN tumor-suppressive function (Maccario et al., 2007).

PTEN is also susceptible to direct oxidization by reactive oxygen species (ROS). Both exogenous H_2O_2 or endogenous ROS production have been reported to oxidize and inactivate PTEN (Kwon et al., 2004; Leslie et al., 2003).

Finally, s-nitrosylation has also been described to regulate PTEN activity. Nitric oxid (NO) signalling induces PTEN s-nitrosylation, thereby inactivating the lipid phosphatase activity of PTEN and leading to downstream activation of PI3K/Akt (Shi et al., 2012).

1.3.4.4 PTEN function in vascular development

Once established the indispensable function of PI3K in angiogenesis, other authors try to elucidate the role exerted in this process by its principal antagonist PTEN. The first studies were performed on global PTEN KO mice. This approach points out that constitutive null mutation of PTEN results in embryonic lethality (E9.5), due to bleeding and cardiac failure, whereas mice carrying only one functional PTEN allele are viable, but they develop, within a short time, different type of cancers and autoimmune diseases. Later on, the Cre-LoxP system, enabled the generation of tissue-specific PTEN

null mice to study the physiological role of PTEN in different tissues. These studies revealed that loss of PTEN causes hyperproliferation and increased activation of Akt and Erk signalling pathways in the targeted cells, which eventually lead to tissues hyperplasia and carcinoma (Suzuki et al., 2008). Precisely, the role of PTEN in ECs biology and angiogenesis was investigated using Tie2Cre-PTEN$^{Flox/Flox}$ and Tie2Cre-PTEN$^{Flox/+}$ mice. This study demonstrated that the homozygous loss of PTEN in ECs is embryonically lethal, while heterozygous PTEN deficiency is associated with enhanced tumorigenesis due to increase angiogenesis (Hamada et al., 2005). The embryonic lethality of both constitutive and endothelial-tissue specific PTEN mutant mice has hampered the progress in understanding how PTEN regulates vessel growth. However, using a Cre-inducible ECs specific PTEN$^{Flox/Flox}$ model, our group has recently defined the Notch–PTEN signalling axis as an essential mechanism to ensure a normal vessel development and density. Specifically, we have shown that PTEN is crucial for blocking stalk cell proliferation downstream of Notch, therefore endothelial deletion of PTEN results in vascular hyperplasia due to a failure to mediate Notch-induced proliferation arrest. Conversely, overexpression of PTEN reduces vascular density and abrogates the increase in EC proliferation (Serra et al., 2015).

1.3.5 ECs metabolism

The lumen of the blood vessel is formed by a thin, single sheet of ECs separated from the surrounding outer layers by a basal lamina. In healthy adults, ECs remain quiescent for years but if necessary, for example in response to tissue damage, lack of nutrients or oxygen deprivation, as well as in some pathological conditions, ECs can rapidly switch to a proliferative state and form new vessels. This ability to expand the vascular network (angiogenesis) in response to changing metabolic demands is vital for organ growth and function in health and disease. However, the switch from a quiescent to proliferative state has important consequence for ECs metabolism (Figure 1.20). In fact, active ECs must adapt their metabolism to the increasing bioenergetics and biomass demands of proliferating cells, and they must do that in an hostile and hypoxic environment (De Bock et al., 2013a; Potente and Carmeliet, 2017).

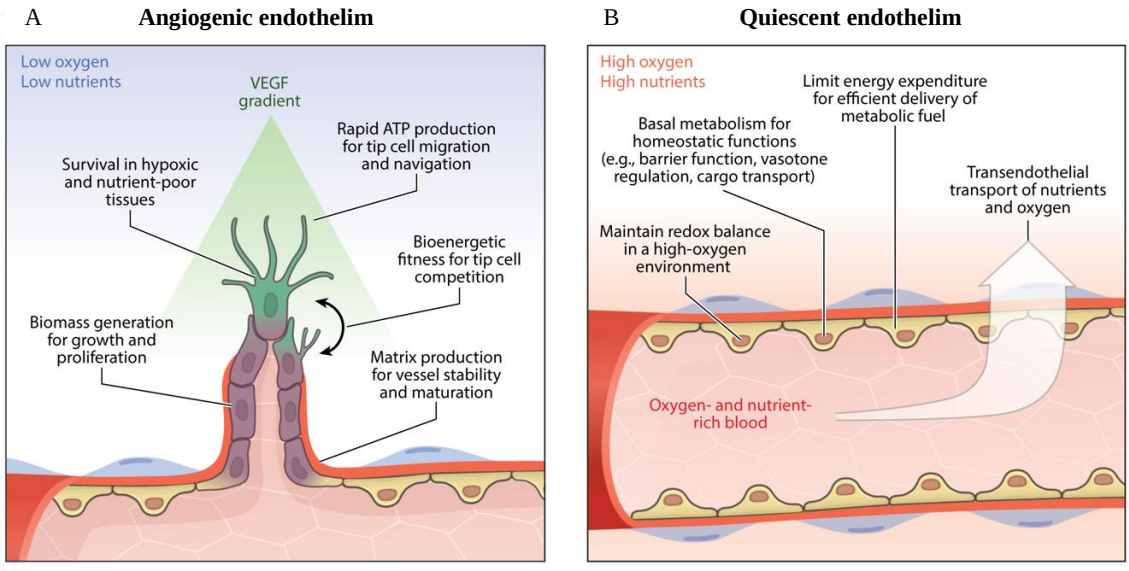

Figure 1.20: Metabolic requirements of growing and quiescent vasculature. A) Activated by VEGF, ECs migrate and proliferate into the hypoxic tissues, all of which are highly energy demanding processes. In addition, angiogenic ECs need biomass for sprout elongation, expansion, and matrix production. B) Quiescent ECs rest in well-perfused vessels and deliver O_2 and nutrients for the oxidative metabolism of the perivascular tissue. To accomplish their function, quiescent ECs only needs a basal metabolic activity that keep them alive, but avoid excessive nutrient and O_2 consumption that would make the delivery process less efficient. Adapted from (Potente and Carmeliet, 2017).

1.3.5.1 Glycolysis and mitochondrial respiration

Despite being directly exposed to oxygen, ECs principally rely on glycolysis to produce ATP. In fact, ECs were found to be “glucose addicted”, generating up to 85% of their ATP by anaerobic glycolysis (De Bock et al., 2013a, 2013b). When angiogenesis is required, proangiogenic molecules, such as VEGF, further enhance glycolysis by increasing glucose uptake and driving expression of key glycolytic enzymes such as phosphofructokinase-2/fructose-2,6-bisphosphatase 3 (PFKFB3). Therefore, active ECs are even more "addicted to" glucose than quiescent ECs, at the extent that these cells die when deprived of glucose or when treated with the glucose analog 2-deoxy-D-glucose (De Bock et al., 2013b; Merchan et al., 2010; Wang et al., 2011). Several reasons may explain why ECs prefer anaerobic glycolysis rather than glucose oxidation, even though the last yields much more ATP per each glucose molecule (2 mol of ATP per mole of glucose versus 36 mol of ATP). First of all, anaerobic glycolysis makes ECs more "hypoxic resistant", thus facilitating ECs sprouting into avascular tissues. Second, it allows to produce more ATP in a short time frame providing ECs with the necessary energy to sprout and form new vessels. Interestingly, several lines of evidence indicate that, during vascular sprouting, glycolytic enzymes compartmentalize with F-actin in

lamellipodia facilitating efficient and rapid local ATP production to fuel migration. Third, by maintaining a low oxidative metabolism, ECs on one side minimize the production of reactive oxygen species and, on the other side, they maximize O_2 delivery to energy-demanding tissues. Finally, the entry of glycolytic metabolites into side pathways ensure the production of macromolecules needed for ECs growth, division, and migration (De Bock et al., 2013b; Vandekeere et al., 2015). Unlike other glycolysis-addicted cell types, such as erythrocytes or embryonic stem cells (Kondoh et al., 2007), ECs have functional active mitochondria, but fewer than oxidative cells (Blouin et al., 1977). In physiological glucose concentration, only a small fraction of pyruvate, derived from glycolysis, enters the TCA-cycle. Nevertheless, when glycolysis is compromised ECs still preserve the ability to adopt an oxidative metabolism (Dranka et al., 2010; Krützfeldt et al., 1990). Importantly, mitochondria in ECs are believed to have functions other than energy production, such as signalling (by the production of ROS and NO) (Davidson, 2010; Davidson and Duchen, 2007) and biomass generation.

1.3.5.2 Fatty Acid Metabolism

ECs express all the enzymes required for FFA synthesis: ACL, ACC and FASN (Wei et al., 2011), but also several proteins involved in FFA uptake like FAT/CD36, FABP4, FATP3, FATP4, FABP3, and FABP5 (Antohe et al., 1998; Elmasri et al., 2009; Greenwalt et al., 1990; Masouyé et al., 1997), suggesting that lipid metabolism might be more important for ECs viability than previously thought. Even though it is generally accepted that ECs generate most of the ATP by anaerobic glycolysis, some studies suggested that FAO can constitute an important energy supply pathway for ECs (especially under stress conditions like glucose deprivation). In fact, it has been reported that cultured Human Umbilical Vein Endothelial Cells (HUVECs) can oxidize both extra- and intra-cellular fatty acids and posses the classic AMPK-ACC-malonyl-CoA-CPT1 system to regulate FAO (Dagher et al., 1999, 2001; Fisslthaler and Fleming, 2009; Hülsmann and Dubelaar, 1988). Besides, it has been recently found that FAO is critical for vessel sprouting *in vivo*, not as energy supplier, but because it provides carbon for *de-novo* synthesis of nucleotide that are indispensable for DNA replication. Basically, it was shown that carbons derived from FAO enter the TCA cycle and are incorporated into aspartate (a nucleotide precursor), uridine monophosphate (a pyrimidine nucleoside triphosphate precursor), and DNA. Accordingly, inhibition of

FAO in ECs was found to be associated with reduced ECs proliferation which, in turn, impairs vessel growth (Schoors et al., 2015).

1.3.5.3 Amino Acids Metabolism

The role of amino acids metabolism in ECs has not been studied extensively, however, a little is known about glutamine and arginine. ECs can import glutamine via Na^+-dependent transport mechanisms or produce it via glutamine synthetase (Lohmann et al., 1999); glutamine taken up by ECs can be converted to glutamate and ammonia (Wu et al., 2000). Glutaminolysis is an important energy source in ECs and its pharmacological inhibition impairs ECs proliferation and induces premature senescence (Unterluggauer et al., 2008). With regard to arginine, it is reported to control angiogenesis by regulating the levels of ROS (Park et al., 2003).

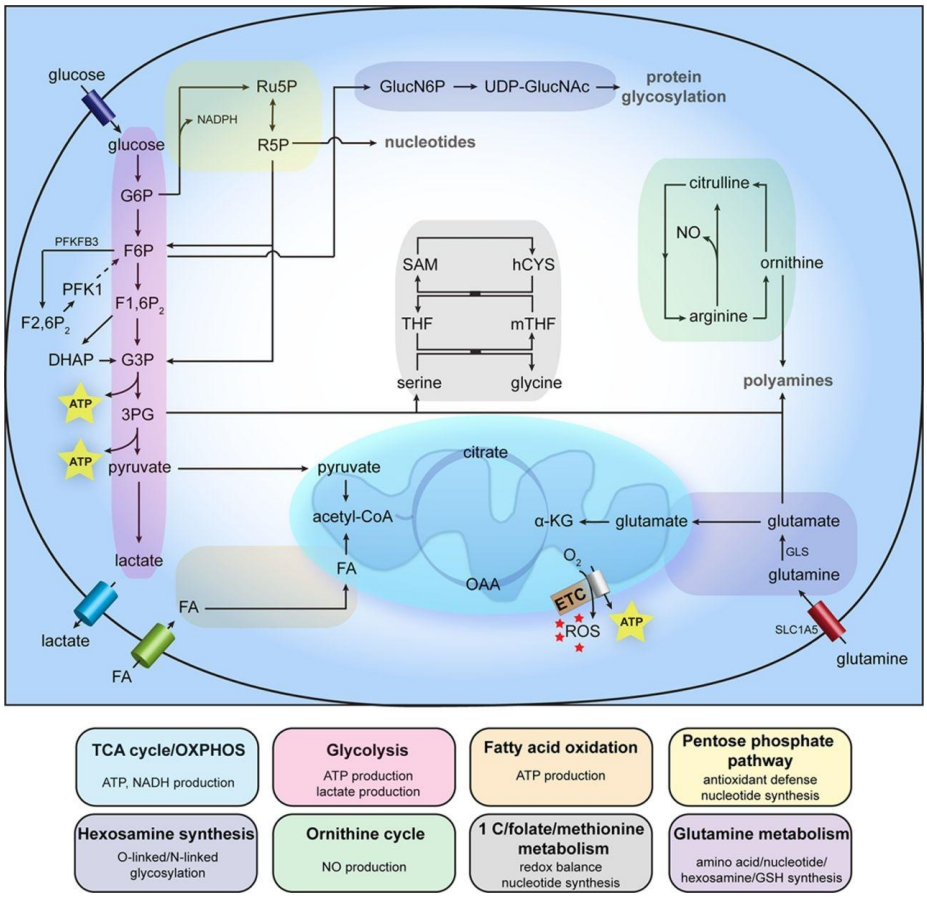

Figure 1.21: General metabolism in healthy endothelial cells (ECs). Schematic and simplified overview of general EC metabolism. PG indicates 3-phosphogylcerate; α-KG, α-ketoglutarate; CoA, coenzyme A; DHAP, dihydroxyacetone phosphate; ETC, electron transport chain; F1,6P2, fructose-1,6-bisphosphate; F2,6P2, fructose-2,6-bisphosphate; F6P, fructose-6-phosphate; FA, fatty acid; G3P, glyceraldehyde-3-phosphate; G6P, glucose-6-phosphate; GLS, glutaminase; GlucN6P, glucosamine-6-phosphate; GSH, reduced glutathione; hCYS, homocysteine; mTHF, 5-methyltetrahydrofolate; NADPH,

nicotinamide adenine dinucleotide phosphate; NO, nitric oxide; OAA, oxaloacetate; OXPHOS, oxidative phosphorylation; PFK1, phosphofructokinase-1; PFKFB3, 6-phosphofructo-2-kinase/fructose-2,6-bisphosphatase 3; R5P, ribose-5-phosphate; ROS, reactive oxygen species; Ru5P, ribulose-5-phosphate; SAM, S-adenosylmethionine; SLC1A5, solute carrier family 1 member 5; TCA, tricarboxylic acid; THF, tetrahydrofolate; and UDP-GlucNAc, uridine diphosphate N-acetylglucosamine. Adapted from (Eelen et al., 2015).

1.3.5.4 Sensing metabolism in the endothelium

In order to dynamically respond to environmental changes, ECs must possess signaling mechanism that sense the energy status of the cells and balance catabolic and anabolic processes to fit with cells requirements. One of this mechanism is the AMP-activated protein kinase (AMPK). AMPK is a heterotrimeric serine/threonine protein kinase that is activated in many different cell types by increased intracellular concentrations of AMP (an indicator of energy shortage), and is generally referred to as a “metabolite-sensing kinase” (Hardie et al., 2016). Once activated, AMPK phosphorylates several metabolic targets, thereby promoting catabolic pathways that generate ATP and inhibit ATP consuming processes (Figure 1.22). Regulation of this kinase thus allows cells to restore their energy balance. In ECs, AMPK is activated by glucose deprivation, hypoxia, and shear stress (blood flow), all of which can affect ECs energy balance (Fisslthaler and Fleming, 2009). AMPK activation in ECs promotes FAO to maintain ATP levels when glucose is limiting (Dagher et al., 2001). In addition, AMPK signalling has been implicated in the regulation of angiogenesis, as it is required for ECs migration and differentiation under hypoxic condition (Nagata et al., 2003).

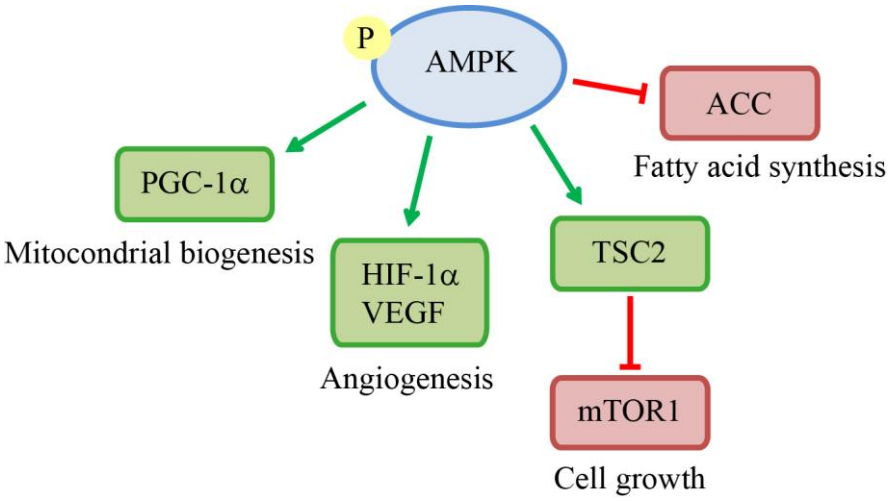

Figure 1.22: Schematic representation of several AMPK targets and the physiological consequences of AMPK activation. In green are proteins that are functionally activated by AMPK; in red are inhibited.

1.4 WAT expansion and obesity

1.4.1 Obesity: a worldwide emergency

Obesity is a medical condition in which excess body fat has accumulated to the extent that it may have an adverse effect on health, leading to reduced life expectancy and/or augmented health problems (Haslam and James, 2005; Peeters et al., 2003). According to a recent report by the World Health Organization (WHO), worldwide obesity has more than doubled since 1980; in 2014 more than 1,9 billion adults were overweight and of these over 600 million were obese. A standard guide to categorise people as overweight or obese is the Body Mass Index (BMI), which is defined as a person's weight in kilograms divided by the square of one's height in meters (kg/m^2). This criterion defines people as overweight, if their BMI is between 25 and 30, and obese if it is more than 30. Nowadays, obesity is a primary public health problem not only confined to developed countries; in fact, in the past 20 years the rates of obesity has tripled in developing country that have been adopted a Western lifestyle. In the majority of the cases, obesity is the outcome of a combination of excessive calories intake, sedentary life style/ lack of physical activity and genetic susceptibility (Hossain et al., 2007). It is well known that being overweight or obese dramatically increases the risk to develop chronic diseases such as cardiovascular diseases, diabetes, musculoskeletal disorders (especially osteoarthritis) and some cancers (endometrial, breast and colon). Furthermore, childhood obesity reduces life expectancy and is associated with higher chance to be disabled in adulthood (Sarnali and Pk, 2010; Tan and Vidal-Puig, 2008).

1.4.2 WAT expansion and metabolic complication

Most of the organs and tissues growth occur during development, and their final size remain relatively constant through adulthood. In contrast, WAT is unique in that it can expand many-fold, in response to excess energy intake, and constitute up to 40% of total body composition in obese subjects. This remarkable plasticity of WAT gives a clear evolutionary advantage enabling survival in time of food scarcity; however, concomitant to WAT expansion, the risk of metabolic dysfunction increases. For example, excessive weight gain is clearly associated with an increase risk to develop diabetes. However, not all obese people become diabetic and interestingly some individuals became diabetic after an only moderate weight gain (Corvera and Gealekman, 2014; Sun et al., 2011). Whereas obesity is related to the expansion of the adipose tissue, it remains unclear why it is associated with the development of

metabolic complications. Two potential mechanisms may explain the onset of metabolic syndromes: lipotoxicity, where excess of lipid cannot be stored in dysfunctional adipocytes, and a specific pattern of adipokines and pro-inflammatory cytokines released from already compromised adipocytes. On those principles is based the hypothesis of "limited adipose tissue expandability", which states that the WAT of each individual has a maximal fixed capacity to safely store fat. This maximal capacity may be determine by several factors including the number of adipocyte precursors, genetic profile and functionality of other cellular components within the adipose tissue. Basically, this hypothesis suggests that an individual will remain metabolically healthy until his/her WAT is able to properly store caloric excess (Tan and Vidal-Puig, 2008). To make the scenario even more complex, the observation that more than the excessive fat mass, per se, is the pattern of fat distribution that influences systemic metabolism, with VIS fat accumulation being more frequently associated with unfavourable metabolic state (Lee et al., 2013).

1.4.2.1 Hypertrophy versus hyperplasia

In response to excessive calories intake, WAT can grow either by hypertrophy (an increase in adipocytes volume) or hyperplasia (an increase in adipocytes number), which are respectively defined as pathological and healthy fat pad expansion (Figure 1.23). Several studies indicate that WAT hypertrophy leads to huge and dysfunctional adipocytes and consequently insulin resistance (Kim et al., 2015; Salans et al., 1968); conversely, hyperplasia provides more, smaller and functional fat cells that protects against obesity induced metabolic diseases (Lee et al., 2010). Typically, hypertrophic adipocytes express and secrete more pro-inflammatory cytokines, including Tumor Necrosis Factor α (TNFα), interleukin (IL)-6, IL-8, and Monocyte Chemoattractant Protein-1 (MCP-1) that, together with increased adipocytes death, enhance inflammation and Macrophages (MΦs) accumulation in WAT. Furthermore, adipocytes hypertrophy leads to local hypoxia, due to impaired angiogenesis, which in turn induces the activation of HIF-1α that, rather than stimulating angiogenesis, accelerates adipose tissue fibrosis (Halberg et al., 2009). Finally, WAT hypertrophy is always associated with increased rates of lipolysis and, consequently, ectopic lipid deposition especially in liver, muscles and pancreas that causes lipotoxicity (Choe et al., 2016).

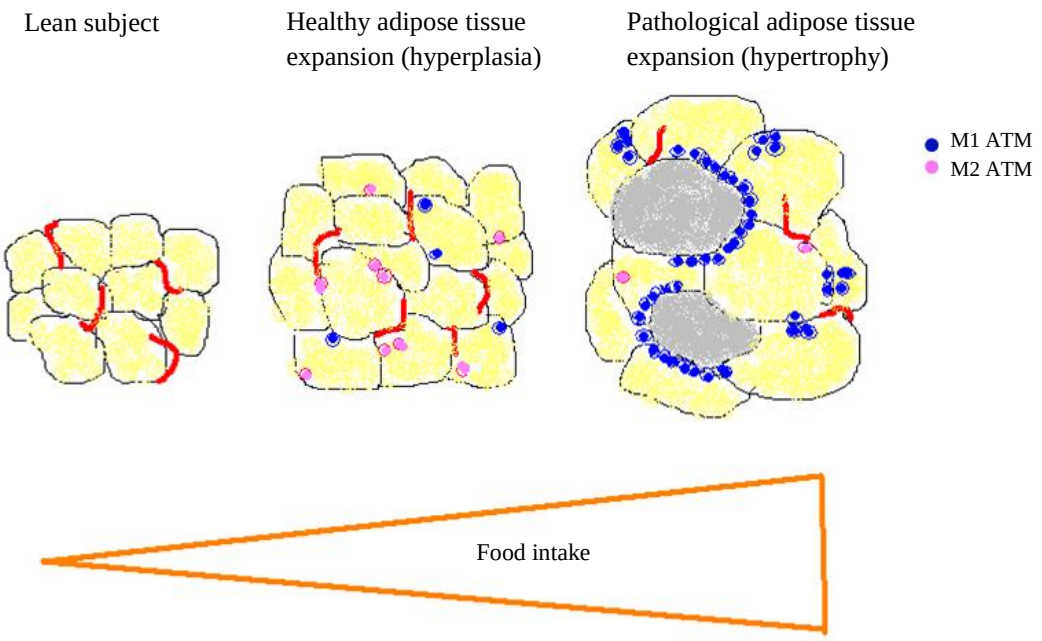

Figure 1.23: Healthy and unhealthy WAT expansion. In physiological condition WAT growth is accompanied by angiogenesis. Chronic over-nutrition leads to excessive WAT expansion not coordinated with angiogenesis and associated with inflammation and adipocytes death.

1.4.3 WAT remodelling

The concept of WAT remodelling refers to the turnover of cells within WAT and the renovation of the ECM in response to requirements for growth and expansion, changes in hormonal milieu, aging or pathologies (Lee et al., 2010). Until recently, mature adipocytes were described as terminally differentiated cells that never die. However, the discovery of structure in WAT named "crown-like structures (CLS)", consisting of Adipose Tissue Macrophages (ATMΦs) surrounding dead adipocytes, proved the existence of an adipocytes turnover at least in the context of obesity (Cinti et al., 2005). The lifespan of adipocytes in rodents has not been directly investigated, but time course studies suggested a huge difference between depots; for example it has been reported that, under HFD, about 80% of gonadal-WAT, but only 3% of SC-WAT, fat cells died and were replaced within few weeks (Strissel et al., 2007). Recent studies estimated that human SC-WAT adipocytes have approximately ~2–3 (Strawford et al., 2004) or 10 (Spalding et al., 2008) years lifespan (a discrepancy likely due to methodological issues). Interestingly, the total number of fat cells, in both lean and obese adults, is constant lifelong indicating that the number of adipocytes is set during childhood and adolescence. Indeed, significant weight gain or loss results, respectively, in increased or

decreased fat mass associated with changes in adipocytes volume rather than adipocytes number (Spalding et al., 2008).

1.4.3.1 ECM and ATMΦ

Within WAT, adipocytes are trapped in a dense network of ECM that not only provides a mechanical support for the fat pad, but also regulates physiological and pathological WAT expansion (Sun et al., 2011). In a condition of a positive energy balance, excessive stiffness of the ECM can limit adipocytes enlargement; conversely weakening of adipose tissue ECM results in unlimited adipocytes expansion and, paradoxically, considerable improvement of the metabolic status (Khan et al., 2009). The ECM composition of WAT is known to be regulated mainly by Matrix MetalloProteinases (MMPs), a family of neutral endopeptidases able to cleave all of the ECM components as well as several non-ECM proteins. Fibrosis and metabolic dysregulation, often observed in obesity, are associated with a differential MMPs expression pattern between healthy and obese subjects (Maquoi et al., 2002; Sun et al., 2013). Other important players in both physiological and pathological WAT remodelling are ATMΦs. Conventionally, MΦs are classified into two functional subtypes: M1 and M2. The M1, or “classically activated” MΦs, are induced by pro-inflammatory mediators and they produce pro-inflammatory cytokines like TNF-α, IL-6, IL-12. On the contrary, M2 or “alternatively activated” MΦs express high levels of anti-inflammatory cytokines as, for example, IL-10 (Sun et al., 2011). Obesity promotes a "phenotypic switch” towards M1 polarized MΦs that positively correlates with systemic inflammation and insulin resistance (Fujisaka et al., 2009). In the lean state, resident MΦs are polarized towards M2 state that help to maintain normal adipocytes function, possibly by promoting tissue repair and angiogenesis. At the onset of obesity the M2 polarized ATMΦs can partially prevents accumulation and activation of M1 MΦs, therefore allowing a healthy WAT expansion. However, with the progression of the disease, the severe pro-inflammatory environment overwhelms the protective effect of M2 ATMΦs, thereby compromising the whole body energy metabolism (Lumeng et al., 2007).

1.4.3.2 Vascular remodelling

The growth of WAT requires continuous remodelling of the vasculature network. WAT expansion can be supported by both neovascularisation (for adipocyte hyperplasia) and dilation and remodelling of existing capillaries (for adipocyte hypertrophy) (Lijnen, 2008). The newly formed vessels provide O_2, nutrients, growth factors, hormones and

inflammatory cells, all indispensable elements to sustain WAT growth. Indeed, several lines of evidence indicate that adipose tissue growth can be limited by its vascular supply (Christiaens and Lijnen, 2010; Crandall et al., 1997). Activated adipocytes produce various angiogenic factors including leptin, angiopoietins, VEGF, FGF-2, and TGF-β, which either alone or collectively stimulate neovascularisation during fat mass expansion (Cao, 2007).

1.4.4 Standard approach to treat obesity

The goal of obesity treatment is to reach and maintain one's healthy weight, however, the complexity and multifactorial nature of this pathology makes this objective difficult to achieve. A predominate challenge is not losing weight, but the long-term maintenance of this weight loss (Jeffery et al., 2000; Wadden et al., 2007). Obesity and overweight can be clinically approached with a diverse array of interventions broadly classified into non-pharmacological, pharmacological and surgical. The first line treatment is almost always a non-pharmacological intervention, also defined as lifestyle modification; it aims at decreasing food intake and increasing energy expenditure through a combination of diet, physical activity and psychological behavior therapy to improve compliance to the treatment ((US), 1998; Wadden et al., 2007). Pharmacological intervention, which includes drugs that inhibit appetite and absorption, is recommended for those patients unable to lose weight with life style modifications alone. The drawbacks of this approach are its short-term effect that makes it necessary a long-term usage, and the possible side effects. Orlistat, the most widely used drug, inhibits pancreatic lipases thereby reducing fat absorption from the gut by ~30% (Borgström, 1988). Unfortunately it causes an only modest weight loss but sufficient to reduce cardiovascular risk and with acceptable side effects. Many other compounds that have been approved in the past were later suspended from the market due to unexpected and intolerable adverse effects (Rodgers et al., 2012). Finally, for the most severe obese patients, the only possibly effective intervention is bariatric surgery. This more drastic intervention encompasses restrictive surgery that limits food intake (e.g. gastric banding), malabsorptive surgery (e.g. intestinal bypass) and mixed interventions (e.g. gastric bypass, duodenal switch). Most of the time bariatric surgery successfully reduces body weight and ameliorates metabolic syndrome and others comorbidities, however it is important to mention that this intervention implies several important risks such as perioperative mortality, surgical complication, vitamin and mineral deficiency and

weight-loss failure (Kral and Näslund, 2007). These traditional interventions (excluding the bariatric surgery) are often insufficient to permanently normalize body weight and prevent metabolic complication, thus novel therapies are urgently needed.

1.4.5 Novel approach: obesity as a vascular disease

Given that obesity and obesity-related complications are associated with pathological angiogenesis (Cao, 2007), modulating angiogenesis has been recently considered as a novel potential therapeutic approach. At first, it has been proposed that angiogenesis inhibition may impair adipose tissue expansion and consequently prevent obesity (hypothesis based on the knowledge that WAT growth is dependent on angiogenesis). Actually, administration of endogenous angiogenesis inhibitors (like angiostatin or endostatin), to ob/ob mice, resulted in a reversible reduction in body weight associated with vascular remodeling (Rupnick et al., 2002). Similarly, treatment with antiangiogenic drugs such as TNP-470 or VEGFR2-specific inhibitors have been shown to prevent obesity in high-fat diet fed mice as well as genetically obese ob/ob mice (Bråkenhielm et al., 2004; Tam et al., 2009). Despite this strategy successfully prevents fat mass expansion; the simultaneous effect of reduced food intake complicate the interpretation of the real beneficial effects of anti-angiogenic drugs per se. Later on, the demonstration that metabolic dysfunction most likely arises from insufficient fat storage and consequent lipotoxicity and inflammation, rather than directly from increased fat accumulation, limited the initial enthusiasm on treatment focused on decreasing fat expansion (Corvera and Gealekman, 2014). Currently, promoting rather than inhibiting WAT angiogenesis is believed to be a promising intervention. Induction of angiogenesis in adipose tissue via VEGF/VEGFR2 has been shown to activate the thermogenic program in brown and white adipose tissues and protect mice from obesity and associated metabolic complications (Elias et al., 2012; Sun et al., 2012, 2014). In analogy, it has been reported that VEGFB gene transduction into mice inhibits obesity-associated inflammation and improves metabolic health without alteration in body weight or ectopic lipid deposition (Robciuc et al., 2016).

2. Objectives

WAT growth is strictly coordinated with angiogenesis; newly formed vessels provide O_2, nutrients, growth factors and hormones, all indispensable elements to sustain WAT expansion. Indeed several lines of evidence indicate that adipose tissue growth can be limited by its vascular supply. WAT produces many proangiogenic factors that alone or collectively stimulate neovascularisation during healthy WAT expansion. Loss of coordination between angiogenesis and adipose tissue growth leads to a dysfunctional tissue which in turns impairs systemic metabolism. However, little is known about the cell intrinsic function of ECs in adipose tissue remodelling. Thus, the objective of this thesis was to study how ECs modulate WAT remodelling in both physiological and pathological condition. Specifically we set up the following aims:

1. Address the relevance of ECs as key modulator of WAT physiology and whole body energy homeostasis.

2. Identify the intrinsic property of ECs that modulate WAT remodelling.

3. Address the impact of differently functional ECs on high fat diet induced obesity.

3. Materials and Methods

3.1 Mice experiment

3.1.1 Mice and breeding conditions

Mice were kept in individually ventilated cages and cared for according to the guidelines and legislation of the Catalan Departament d' Agricultura, Ramaderia i Pesca, with procedures accepted by the Ethics Committees of IDIBELL-CEEA. Specifically, mice were kept in a pathogen-free facility and maintained under a 12-h light–dark cycle at 22°C. Mice were fed ad libitum with a chow diet or an HFD (45% fat enriched diet). When stated, mice were fasted for 6h.

To delete PTEN in postnatal vessels, we crossed the $PTEN^{flox}$ mice (Suzuki et al., 2001) into the transgenic mice expressing the tamoxifen-inducible recombinase CreERT2 under the control of the endothelial specific Pdgfb promoter (Pdgfb-iCre-ERT2) transgenic mice (Claxton et al., 2008). For experiments, breedings were set up between Pdgfb-iCre-ERT2-$PTEN^{Flox/Flox}$ and $PTEN^{Flox}$, thus obtaining Pdgfb-iCre-ERT2-$PTEN^{Flox/Flox}$ (referred $PTEN^{i\Delta EC}$) and $PTEN^{Flox/Flox}$ (referred as control). Cre activity and gene deletion were induced by intraperitoneal injection of 25 mg 4-OH tamoxifen (Sigma, H7904, 10 mg/ml in EtOH) in all pups of the litter at P1 and P2, tissues were collected at 5 and 12 weeks of age.

3.1.2 Mice genotyping

3.1.2.1 Tail digestion

New born mice were weaned once they turned 3-weeks of age. Upon weaning, tail biopsies were kept for genotyping. Tissue was lysed with 600µl of 50mM NaOH (Sigma). Samples were incubated at 100ºC for 15', vortexed and cool down. Next, 100µl of 1M Tris (Sigma) HCL pH 7.4 was added to each sample. Samples were vortexed, centrifuged at maximum speed for 1 min and kept at 4ºC**.**

3.1.2.2 PCR

Polymerase chain reactions (PCR) were performed using the following protocol: PCR reaction mix (to a final volume of 30 µl): 2 µl DNA sample, 15.75 µl H_2O, 3 µl $MgCl_2$ 15mM (diluted from $MgCl_2$ 50 mM Ecogen, #MG-110C), 3 µl of 10X reaction buffer

without Mg (Ecogen), 3 µl of 10M primer pool (forward+reverse), 3 µl dNTPs and 0.35 µl Ecotaq DNA polymerase (Ecogen, #BT-314106).

Gene	Primers sequence (5'-3')	Amplification programme
Pdgfb-iCreERT2	EGFP_3UTR_FW: CCAGCCGCCGTCGCAACT EGFP_3UTR_RV: GCCGCCGGGATCACTCTCG IL-2 FW: CTAGGCCACAGAATTGAAAGATCT IL-2 RV: GTAGGTGGAAATTCTAGCATCATCC	1-94°C - 4' 2- 94°C - 30" 3- 57.5^{o}C - 45" 4- 72°C - 1' 5- From 2 to 4 x 34 cycles 6- 4°C- hold

Table 3.1: PCR condition and primers

Mastercycler (Eppendorf) was used to perform PCRs. PCR reactions were then separated on a 2% agarose (Sigma) gel diluted in TAE buffer 1X (from a TAE 50X stock: 242 g Tris base (Sigma), 57.1 ml acetic acid glacial (Panreac) and 100ml EDTA 0.5 M pH8 (Gibco, #15575) in dH2O) with ethidium bromide (Sigma, E8751).

3.1.3 Pharmacological treatment

3.1.3.1 β-oxidation inhibition

The β-oxidation inhibitor Etomoxir was purchase from Sigma (Sigma, E1905), and dissolved in sterile physiological solution at a concentration of 5mg/ml. Equal number of control and PTEN$^{i\Delta EC}$ mice (5 weeks old) were injected intraperitoneal (ip), day on/ day off with Etomoxir 25mg/kg or vehicle during 5 weeks; afterwards mice were scarified by cervical dislocation, body weight and tissue weight was measured with a standard and precision scale, respectively. Tissues were collected for whole mount blood vessels stain, or embedded in paraffin.

3.1.4 In-vivo metabolic studies

3.1.4.1 Daily food intake

Mice were single housed and acclimatized for 1-week prior to study. Food intake was measured for 5 consecutive days at 4, 8 and 12 weeks of age. A known amount of food

(80g) was given to each mouse and every morning, during 5 days, food was reweighted and the amount consumed was calculated by difference.

3.1.4.2 Glucose Tolerance Test (GTT)

GTTs assess the disposal of a glucose load administered via oral or intragastric dosing (OGTT), intraperitoneal injection (IPGTT) or intravenous injection (IVGTT). The results of a GTT are determined by insulin secretion, insulin action, and 'glucose effectiveness'. The protocol for carrying out a GTT is simple; following a fast (generally an overnight or morning fast), a glucose load is administered and blood glucose is measured over a span of 2 hours. When performing GTT, the standard approach in mice is to base the dose of glucose on the weight of the mouse, usually at 1 or 2 g/kg (Muniyappa et al., 2008). This is reasonable as long as the weight and body composition for different cohorts are similar. However, in obese models, the increased body weight is mainly due to a higher fat mass without a proportionally higher lean mass. This is an important point to keep in mind as lean mass is the primary site of glucose disposal. If glucose dose is calculated on total body weight then the dose given to an obese mouse will be biased by the increase in fat mass, thus obese mice could be misdiagnosed as being glucose intolerant simply because they receive more glucose for the same lean body mass. This bias will be greater with higher glucose dose. If body composition data are available, then it is more appropriate to base the dose of glucose for a GTT on the lean body mass (Ayala et al., 2010). In this study glucose dose was calculated on total body weight, lower glucose dose was administer to HFD feed mice. GTT was carry out with conscious and properly identified mice. Prior the test mice were fasted (always at 8:30 am); after 6h of morning-starvation glucose basal level was measured (t0) and right after D-glucose, diluted in saline solution, was administered intraperitoneal [2g/Kg] or [1.5g/Kg] for mice in chow and HFD respectively. Blood glucose levels were measured, from the tail tip puncture, at 15', 30', 60' and 120' after D-Glucose injection.

3.1.4.3 Insulin Tolerance Test (ITT)

Similarly to GTT, ITT monitors glucose concentration over time, but in response to a bolus of insulin rather than of glucose. The convention is to conduct ITTs in mice following a short (5- to 6-hour) fast to avoid hypoglycaemia. Glucose concentration is monitored every 15 to 30 minutes for 60 to 90 minutes following a bolus of insulin administered by intraperitoneal or intravenous injection. The degree to which glucose

falls following the insulin bolus is indicative of whole-body insulin action. In analogy to GTT, differences in body weight and composition influence the dose of insulin. An obese mouse will receive a larger dose of insulin than a non-obese mouse even though the mass of insulin-sensitive tissue (lean mass) might not differ significantly. ITT was carry out with conscious and properly identified mice. Prior the test mice were fasted (always at 8:30 am) and glucose basal level (t0) was measured 6h later. Right after, insulin (Humulin R 100Ui/mL Regular by Eli Lilly and Company), diluted in saline solution, was administered intraperitoneal [0.4 Ui/Kg] or [0.75 Ui/Kg] for mice in chow and HF diet respectively. Blood glucose levels were measured, from the tail tip puncture, at 15', 30', 60' and 90' after insulin injection.

3.1.4.4 Indirect calorimetry

Indirect calorimetry was assessed using a TSE LabMaster modular research platform (TSE Systems) as previously described (Czyzyk et al., 2012), in collaboration with Rubén Nogueiras' group at department of Physiology (CIMUS University of Santiago de Compostela). Briefly, mice were acclimated for 24h into test chambers and monitored for an additional 48h. Data were collected to calculate several parameters: O_2 consumption, and CO_2 production were measured every 45' during 48h, to indirectly determine Energy Expenditure (EE) utilizing a software provided with the system. Thus, VO_2 (ml/h/Kg) and heat production (Kcal/h/Kg) were measured during the dark and light phase. Heat production was calculated using the Weir equation that describes the relationship between heat produced and oxygen consumption and is equivalent to the resting EE. In the abbreviated Weir equation kcal per day are calculated as follows: $[3.94(VO_2) + 1.11 (VCO_2)]1.44$ (Weir, 1949).

In parallel, Locomotor Activity (LA) was measured using a multidimensional infrared light beam system with installed beams on cage top and bottom levels; thus activity was expressed as beam breaks. The locomotr activity was assesed with the XF, XA and Z parameters defined by the LabMaster software. XA account for the X-beam breaks for ambulatory mouvment, which are breaks of any of two different X-beams of light. Conversely, XF accounts for fine mouvments where two breaks in succession of the same beam of light are registered at the X level.

3.1.5 Histology and Immunohistochemistry (IHC)

3.1.5.1 Paraffin block preparation

Adipose tissue were included in hystological cassettes, fixed over night at 4°C in 4% paraformaldehyde, washed in PBS (3 times 10') and temporarily stored in PBS NaAz 0,005%. Next samples were processed with the TissueTek VIP'5 Jr, applying an optimized protocol for adipose tissue. Any other tissue was fixed over night in formalin at 4°C, washed in PBS and embedded in paraffin with a standard procedure (Table 3.2). Paraffin block were then prepared in a paraffin embedding station.

Adipose tissue		**Other tissues**	
Solution	**Time**	**Solution**	**Time**
EtOH 50%	1h 30'	EtOH 96%	1h x 2
EtOH 70%	1h 30'	EtOH 96%	o/n
EtOH 96%	45' x2	EtOH 100%	1h 30' x 3
EtOH 100%	2h 30' x2	Xilol	1h 30'
Tissue clearer	2h 30' x2	Paraffin	o/n
Parafine	90' x3		
Parafine	4h		

Table 3.2: Paraffin processing of tissue (detailed protocols)

3.1.5.2 Histology

Once embedded in paraffin, 5µm section were cut at the microtome, placed on Poly-L-Lisine treated microscope slide and dried at 37°C o/n. Previous any staining, paraffin was removed and tissue rehydrated following a standard protocol (Table 3.3).

Solution	**Time**
Xilene	10' x3
EtOH 100%	3' x3
EtOH 96%	3' x3
EtOH 70%	3'
EtOH 50%	3'
H_2O	3'

Table 3.3: Standard procedure do clear and rehydrate histological section

After that slides were sunk in haematoxylin for 4', staining was stopped with run tap water, followed by staining with eosin 2'. Then tissue were again dehydrated, cleared and mounted with DPX mounting media (06522 SIGMA). Images were taken at the Nikon microscope 80i using the 20X objective. Adipocytes area was calculated with the MRI_Adipocytes_Tools of Image J software.

3.1.5.3 Immunohistochemistry (IHC)

IHC was performed on 5µm section previously deparaffinized and rehydrated. Most formalin-fixed tissues require an antigen retrieval step before IHC because methylene bridges formed during fixation cross-link proteins and mask antigenic sites. To unmask antigens, samples were heated in a pressure cooker in sodium citrate buffer pH6 during 10'; after that the pressure cooker was place in the sink and cold tap water was run on top of it to slowly cool down samples. Next the endogenous peroxidase was inactivated with H_2O_2 3% in H_2O for 10', followed by 3 washes in PBS 0.05% triton X-100 (from now PBST). To avoid unspecific binding, samples were incubated with blocking solution (PBS 5% goat serum) for 1h at RT in a humid chamber. After that slides were incubated with the primary antibody (Ab) of interest or blocking solution (negative control) o/n at 4°C in humid chamber (to avoid evaporation). In this thesis the Ab utilized for IHC was rabbit anti UCP1 (Abcam, ab10983) or rabbit anti PTEN used at concentration 1:100 in blocking solution. The following day samples were washed in PBST (3x 10') and incubated with the secondary Ab conjugated with HRP, for 1h30' at RT. After that samples were washed as before and HRP activity was detected by adding the substrate diaminobenzidine; the chromogenic reaction was stopped with H_2O, one sample of BAT was utilized as positive control. Finally, sample were counterstained with haematoxylin, dehydrated, cleared and mounted with DPX. Images were taken at the Nikon microscope 80i.

3.1.6 Immunofluorescence (IF)

3.1.6.1 IF on frozen section

Fresh isolated tissue (liver, pancreas, muscle and brain) was snap-frozen, embed in OCT and stored at -80°C. IF was performed on 5µm sections that were cut at the cryostat and placed on Poly-L-Lisine treated microscope slide. First samples were fixed with cold acetone for 10' at 4°C, then acetone was removed and samples were washed 3 times in PBS for 10'. To avoid unspecific signal, samples were incubated with blocking solution (PBS 5% goat serum) for 1h at RT in humid chamber. After that primary Ab anti-CD31was added and samples were kept o/n in humid chamber at 4°C. The next day samples were washed as in the previous step and incubated with secondary Ab goat anti-rat Alexa Fluor 568 (Invitrogen #A11077) 1:200 in blocking solution, for 1h30', at RT in humid dark chamber. Then samples were washed in PBS, incubated 5' with DAPI

1:5000 in PBS (to stain nuclei) and mounted with mounting media composed of mowiol and DABCO.

Images were taken at Nikon microscope 80i. CD31 immunostaining was used to determine vessel density, briefly CD31 positive structure were counted in images of at least 6 controls and 6 $PTEN^{i\Delta EC}$ mice; vessel density was expressed as percentage of control tissue.

3.1.6.1 Whole mount adipose tissue

Fresh isolated adipose tissue were fixed o/n in 4% paraformaldehyde at 4°C, washed in PBS (3 times 10') and stored at 4°C in PBS NaAz 0,005%. Samples were then incubated with blocking solution (PBS 5% goat serum) 2h RT. Incubation with primary Ab was done o/n at RT. Next day samples were washed over day in PBS 0,3% Triton 100x (PBST). Secondary Ab conjugated with Alexa dye 488 was used 1:500 o/n at 4°C. The following day sample were washed in PBST, incubated with DAPI 1:5000 (when required) at RT for 10' and stored in PBS NaAz 0,005% at 4°C covered from light.
Images were taken at the Leica confocal SP5 using 20X objective. All images are maximal z-stack projections. Images were processed using Volocity, Fiji and Adobe Photoshop CS5. Vessel density was quantified by measuring isolectin-B4 positive area, within a fixed square template, using the Image J software. ECs proliferation was quantified by counting the number of Ki65 positive nuclei, which was then normalized with the IB4 positive area.

Primary Ab	Host	Dilution	Company	Catalogue#
CD31	rat	1:100	BD Pharmingen	A11077
Isolectin GS-IB4568	-	1:300	Mol. probes	I21412
Ki65	rabbit	1:100	NeoMarkers	9106-S1

Table 3.4: Antibody utilised for IF staining

3.2 Cell culturing

3.2.1 Endothelial cell isolation from mouse lungs (mlECs) and WAT (adiposeECs)

3.2.1.1 Tissue digestion

Control and $PTEN^{i\Delta EC}$ mice were sacrificed by cervical dislocation and lungs and inguinal-WAT were removed and kept on ice cold Hank's balanced salt solution

(HBSS) (Gibco, #14170-088) containing 1% penicillin/streptomycin (P/S, Gibco). From now on samples were manipulated in sterile cell culture hood. The first step of tissue digestion is slightly different between lungs and inguinal-WAT thus will be explained separately.

Lungs

Lungs were minced with a scalpel, poured through a 40 µm cell strainer, placed on a 50 ml Falcon tube, to remove blood constituents. Tissue pieces were then digested in 5ml digestion buffer composed of HBSS with 4U/ml of dispase II (Gibco, #17105-041) for 1h at 37ºC.

Inguinal-WAT

Inguinal-WAT was minced with scissors and directly placed in a 50ml tube with 5 ml digestion buffer composed of HBSS with 4U/ml of dispase II (Gibco, #17105-041) and collagenase A 0.5 mg/ml (Roche, #10103578001). Digestion was carried out at 37°C during 1h. To facilitate tissue digestion samples were gently vortexed prior digestion.

Thereafter, the suspension containing lung or inguinal-WAT pieces was homogenized by pippetting up and down to release single cells from the tissue pieces. Then, DMEM (Lonza, #BE12-604F) containing 10% of inactivated FBS (Gibco, #10270-106) and 1% P/S (from now on DMEM complete medium) was added to the cell suspension to stop digestion and the homogenate was filtered through a 40 µm cell strainer, to remove indigested tissue, and placed on a 50ml. Cell suspension was centrifuged 10' at 1200rpm. Then, the pellet was washed twice with PBS/BSA (PBS containing 0.5% BSA (PAA, #K11-022)), performing a 5 min centrifugation (1200rpm) after each wash.

3.2.1.2 First selection

The resulting cell pellet was re-suspended in 100µl of PBS/BSA and incubated with previously prepared magnetic beads coated with VE-cadherin (BD Pharmigen, #555289). Beads preparation: beads were prepared as followed described: 8µl/sample of magnetic beads were placed into a 1.5ml eppendorf and were washed five times with PBS/BSA using a Dynal magnet (Dynal, MCP-S). After the last wash, magnetic beads were re-suspended in 6µl of PBS/BSA and finally, 1.25µl/sample of VE-cadherin antibody were added. The mixture of magnetic beads and VE-cadherin was incubated 1h at RT with gentle shaking. Magnetic beads were then washed four times with

PBS/BSA using a magnet for cell separation; next, 100 µl of PBS/BSA for each sample were added. Thus, 100 µl of beads in PBS/BSA was incubated with 100 µl cells suspension for 30 min at RT.

Next, samples were washed 3 times with PBS/BSA using a magnet to separate ECs bound to beads from other unbounded cell type. After the final wash, magnetic beads coupled with ECs were re-suspended in F-12 complete medium containing: DMEM F-12 (Gibco, #21041-025), supplemented with 20% of inactivated FBS (Gibco, #10270-106), 4 ml of endothelial cell growth factor (Promocell, #C-30140) and 1% P/S. Then, the suspension was seeded on 12-well culture dishes coated with 0.5% gelatine (Sigma) in sterile H_2O (this moment is considered as passage 0 (P0)). The following day, the wells were carefully washed twice with PBS/BSA and F-12 complete medium was replaced. Medium was changed every second day.

3.2.1.3 Second selection

Once cells reach the confluence, a second purification step was done. Cell culture media was removed and cells were incubated with magnetic beads coated with Ve-Chaderin (prepared in PBS/BSA as described above) for 1h at RT. Then, cells were trypsinized and centrifuged for 5 min at 1200 rpm. Next, cells were washed three times with PBS/BSA, using a magnet to separate ECs bound to beads from other unbounded cell type. After the final wash, magnetic beads coupled with ECs were re-suspended in F-12 complete medium and seeded on 12-well culture dishes coated with 0.5% gelatine in sterile H_2O. The following day, wells were carefully washed with PBS/BSA and DMEN F-12 complete medium was replaced. From here on, cells were cultured and splitted following standard procedures, always guaranteeing a confluence of at least 70%. All experiments were performed in cells at passage 5.

3.2.2 In vitro assays

3.2.2.1 Glucose consumption

To measure glucose consumption 1 x10^5 primary mlECs or adipose ECs were seeded in 12 wells plate coated with gelatine 0.5%. The next day F12 complete was replaced with DMEM [-glucose, -pyruvate, +glutamine] with 1% penicillin/streptomycin, 10% dialysed inactivated FBS and 1mM or 2mM glucose. After 8h and 24h, medium was collected, centrifuged and froze at -80°C. Duplicate was done for each sample at both time point and condition. Glucose content in the medium was determined with the PGO

Enzyme Preparation (Sigma, P7119) following the protocol recommended by manufacturer. Glucose concentration was normalised with total protein content.

3.2.2.2 Lactate production

To measure lactate production 1 x10^5 primary mlECs or adipose ECs were seeded in 12 wells plate coated with gelatine 0.5%. The next day F12 complete was replaced with DMEM [4,5g/L glucose, +glutamine], 10% dialysed inactivated FBS with 1% penicillin/streptomycin. After 8h and 24h, medium was collected, centrifuged and froze at -80°C. Duplicate was done for each sample at both time point. The concentration of l-lactate was determined using an enzymatic reaction based on the oxidation of l-lactate to pyruvate by lactate dehydrogenase (5 mg of the enzyme (Roche)/mL, 550 U/mg) in the presence of NAD (Sigma-Aldrich). In this assay, the amount of NADH produced is proportional to the amount of l-lactate in the samples. Samples were diluted 1:20 with reaction mix [0.3 M hydrazine sulfate (Merck) and 0.87 M glycine (AppliChem), pH 9.5; 2.5 M NAD+ (Sigma-Aldrich), 0.19 M EDTA (Merck)]. Lactate dehydrogenase was added at a final concentration of 6.9 U/mL. The NADH concentration was determined by using the Fluostar Optima BMG Labtech system to measure absorbance (340 nm) and fluorescence (excitation 340 nm/emission 460 nm) at time 0 and 20 min after the reaction started. The endpoint was set at 20 min and the corresponding values were used in the calculations. Different concentrations of sodium l-lactate (Sigma-Aldrich) served as the standard.

3.2.2.3 FFA oxidation

To measure FFA oxidation 7,5 x10^4 primary ECs were plated in 24 wells plate in F12 complete medium. The next day medium was replaced with culture medium containing 100 μM palmitate (C16:0), 1 mM carnitine and 1.7 μCi [9,10(n)-3H]palmitic acid (GE Healthcare) in the presence or absence of etomoxir (200 μM). After 4h incubation (at 37°C, 5% CO_2) medium was collected to analyze the released $3H_2O$ formed during cellular oxidation of [3H]palmitate (DeBerardinis et al., 2006). Briefly, medium was TCA precipitated, and supernatants were neutralized with NaOH and loaded onto ion exchange columns packed with DOWEX 1X2-400 resin (Sigma-Aldrich). The radioactive product was eluted with water and quantified by liquid scintillation counting. Oxidation of [3H]palmitate was normalized to protein content using Bio-Rad DC Protein Assay. Etomoxir, a specific inhibitor of CPT1A, was used to specifically inhibit mitochondrial FAO.

Compound	Stock solution	Source, product code
Palmitic acid	100mM in DMSO	Sigma, P0500
Etomoxir	20mM in H_2O	Sigma, E1905-5mg
Carnitine	100mM in H_2O	C01518-5g
Dowex 1x2-400	22g in 60ml H_2O	Sigma, 217395-100G
Glass wool		Supelco 2-3084
3H-palmitate	1.7 mCi/ml EtOH	
Scintillation fluid		Fisher scintisafe plus 50%
Scintillation vial		Sigma, V8255-500EA

Table 3.5: Chemical material utilized to perform FFA oxidation assay

3.2.2.4 ECs proliferation

To assess cell proliferation 1 $\times 10^4$ primary mlECs were plated in 12 well plates with F12 complete medium and kept in a standard incubator (37°C, 5% CO_2). Twelve hours later, considered day 0, cells were fixed during 30' in 4% paraformaldehyde and stored in PBS at 4°C. The same procedure was performed at day 3. Cell growth was measured by staining with crystal violet (0.1% in 20% methanol) for 30'. The precipitate was solubilized in 10% acetic acid, and the absorbance was measured at 595 nm.

3.2.3 Stromal Vascular Fraction (SVF) isolation and differentiation

Control and $PTEN^{i\Delta EC}$ mice were sacrificed by cervical dislocation and gonadal and inguinal-WAT were removed and kept on ice cold DMEM containing 1% penicillin/streptomycin (P/S, Gibco). From now on samples were manipulated in sterile cell culture hood. WAT was minced with scissors and placed in a 50ml tube with 10 ml digestion buffer/ g of tissue (Table 3.6). Digestion was carried out at 37°C during 30-45' with continuous shaking. After that collagenase activity was neutralised adding 10ml of DMEM complete medium, then cell suspension was filtered through a 100 µm cell strainer placed on a 50ml, to remove indigested tissue, and allowed to divided into two phases (a process that took about 15'). The lower phase contains the SVF whereas the upper phase mature adipocytes, thus the lower phase was carefully aspirate with a syringe and place in a new 50ml tube. Next cell suspension was centrifuged at 700x g for 10', and cells were seeded in 6 wells plate in DMEM complete medium. 24h after seeding, each well was washes twice with PBS to remove cell debris and floating erythrocytes and medium was replaced with fresh DMEM complete medium. Medium was changed every second day. Differentiation was induced 48h after cells reached 100% confluence by replacing DMEM complete medium with induction medium (DMEM complete plus Insulin 100nM, Dexamethasone 1µM, IBMX 0.5 mM and

Rosiglitazone 1 µM). 48h later, induction medium was replaced with differentiation medium (DMEM complete plus Insulin 100nM). Medium was changed every second day. Within 8-10 days cells were completely differentiated into mature adipocytes.

Reagent	10ml digestion buffer
HEPES 1.5M pH 7.4	667µl
NaCl 5M	246µl
KCl 1M	50µl
$CaCl_2$ 50mM	260µl
Glucose	9mg
BSA (fraction V)	150mg
Collagenase A 0.25 U/mg	10mg
H_2O miliQ	up to 10ml

Table 3.6 Digestion buffer detailed composition

Compound	Stock solution	Source and product code
Insulin solution human	10mg/ml	Sigma, I9278
Dexamethasone	1mM in EtOH	Sigma, D4902
IBMX	50mM in EtOH	Sigma, 858455
Rosiglitazone	1mM in EtOH	Sigma, R2408

Table 3.7 List of compounds utilised to induce SVF differentiation

3.3 Protein extraction and Western Blot

3.3.1 Protein lysis and sample processing

Adipose Tissue

To analyse protein expression frozen WAT was smashed in small pieces, on dry ice to avoid protein degradation, and transferred to a 1,5ml tube. Tissue was homogenized with a pestles in 400-500µl lysis buffer (150 mM NaCl, 1mM EDTA, 50 mM Tris-HCl pH 7.4 and 1% Triton X-100 in H2O) supplemented with 1mM DTT, 2 mg/ml aprotinin, 1 mM pepstatin A, 1 M leupeptin, 10 g/ml TLCK, 1 mM PMSF, 50 mM NaF, 1 mM NaVO3 and 1 µM okadaic acid (further information about the reagents used for lysis buffer preparation can be found in (Table 3.7). Tissue lysates were kept on ice for 15min, next it was centrifuged at maximum speed for 15' at 4°C to pellet cell debris. Supernatants were collected in new ice-cold 1.5ml tubes and keep on ice. Protein content was quantified using the BCA protein assay kit (Pierce) following the instructions recommended by the manufacturer. A protein stock solution [2mg/ml] was prepared by adding the correct volume of sample buffer (250 mM Tris-HCl pH 6.8,

40% glycerol, 8% SDS, 0.04% bromophenol blue and 250mM DTT in H2O) and lysis buffer plus inhibitors to each protein lysate. Samples were boiled at 100ºC for 10', spinned and stored at -20°C.

Primary mlECs and adipose ECs

For western blot analysis of primary ECs, 7 x10^5 cells were seeded in 6 well plates and kept in culture for 24h in F12 complete medium. Next, plates were quickly wash with PBS plus CaMg and stored at -80°C or directly processed. Primary ECs were lysed with the same lysis buffer above described; cell lysates were collected in a 1.5ml tube, kept on ice for 15' and, then, centrifuged for 15min, at maximum speed at 4ºC. Supernatants were collected in new ice-cold 1.5ml eppendorfs and kept on ice. Protein content was quantified using the BCA protein assay kit (Pierce) following the instructions recommended by the manufacturer. Protein samples were then diluted in sample buffer 4X (the same described above) in a proportion of 3 volumes of protein sample: 1 volume of 4X SDS sample buffer. Samples were heated at 100ºC for 10', spinned for 30sec and stored at -20°C.

Product	Company	Catalogue
DL-Dithiothreitol (DTT)	Sigma	D0632
Aprotinin	Sigma	A6279
Pepstatin A	Sigma	P4265
Leupeptin	Sigma	L2884
Na-p-tosyl-L-lysine chloromethyl ketone (TLCK)	Sigma	T7254
Phenylmethylsulfonylfluoride (PMSF)	Sigma	P7626
Sodium fluoride (NaF)	Sigma	S7920
Sodium orthovanadate (NaVO3)	Sigma	S6508
Okadaic acid	Cayman Chemical Company	10011490

Table 3.8: Reducing agents, phosphatase and protease inhibitors used for lysis buffer

3.3.2 Electrophoresis and membrane transference

Protein samples were resolved on 10% SDS poli-acrylamide gel. SDS-PAGE gel was composed of a stacking part (4% acrylamide, 125mM Tris-HCl pH 6.8, 0.4% SDS, 0.1% ammonium persulfate (APS) and 0.1% tetrametiletilendiamina (TEMED) in H_2O) and a resololving part (10% acrylamide, 375mM Tris-HCl pH8.8, 0.4% SDS, 0.1% APS and 0.1% TEMED in H_2O). Samples were runned for 1- 2h at 110V with running buffer 1X (25mM Tris, 192 mM glycine and 0.1% SDS in H_2O). Thereafter, proteins separated

in the acrylamide gels were transferred onto nitrocellulose membranes (Roche). Gel to membrane transference was performed at 4ºC at 200 mA for 2h in Transfer buffer 1X (25mM Tris, 192mM glycine and 20% methanol). After transference, membranes were quickly washed in 1X TBS (For 500mL of TBS 10x: 6g Tris, 43.85 g NaCl, pH7.5) containing 0.05% Tween (referred as TBS-T). Blocking was performed in 5% milk in TBST, next membrane were washed with TBST and incubated with primary Ab (prepared in a solution of 2% BSA in TBS-T with 0.02% sodium azide), o/n at 4°C. Details primary antibodies used for immunoblotting (Table 3.9). The following day, membranes were washed 3 times (10' each) with TBST and were incubated for 1h at RT with secondary Ab 1:5000 in 2.5% milk in TBS-T (Table 3.10). After that membranes were washed 3 times (10' each) with TBS-T and protein detection was performed by enhanced chemiluminescence (ECL) following the protocol described in Table 3.11. Quantification of band intensities by densitometry was carried out using the Image J software.

Primary Ab	Host	Dilution	Company	Catalogue#
Ve-chaderin	Goat	1:500	Santa Cruz	Sc-6458
β-actin	Mouse	1:50000	Abcam	49900
p-Akt Ser473	Rabbit	1:1000	Cell Signalling	4060
t-Akt	Rabbit	1:1000	Cell Signalling	9272
PTEN	Rabbit	1:1000	Cell Signalling	9559
FAS	Rabbit	1:1000	Cell Signalling	3180
pACC	Rabbit	1:1000	Cell Signalling	36615
pAMPK	Rabbit	1:1000	Cell Signalling	2531
UCP1	Rabbit	1:1000	Abcam	ab10983
UCP3	Rabbit	1:1000	Abcam	Ab3477

Table 3.9: Primary antibodies used for immunoblotting

Secondary Ab	Host	Dilution	Company	Catalogue #
Anti-Rabbit HRP	Swine	1:5000	Dako	P 0399
Anti-Mouse HRP	Rabbit	1:5000	Dako	P 0260
Anti-Goat HRP	Rabbit	1:5000	Dako	P 0160

Table 3.10: Secondary antibodies used for immunoblotting

Solution A	Solution B
5 ml 1M Tris pH8.5 45 mL H_2O 110 µl 90mM acid cumaric (Sigma) 250 µl 250mM luminol (Sigma)	100µl H_2O_2 30% 900µl H_2O
Solution A and B need to be mixed following the proportion 1mL A + 3µl B	

Table 3.11: ECL composition

3.4 RNA extraction and quantitative Real Time PCR (qRT-PCR) analysis

3.4.1 RNA extraction

Adipose tissue

To analyse gene expression frozen WAT was cut in small pieces, on dry ice to avoid RNA degradation, and transferred to a 2ml tube. RNA extraction was done with a combined protocol that join the conventional extraction with TRIzol Reagent (Invitrogen, #15596-018) and commercial RNeasy Plus Kit (Qiagen). Briefly, samples were homogenized in 1 ml TRIzol Reagent using a pestle followed by several passages through a syringe with decreasing needle size. Homogenized samples were centrifuged 20' at 12000 rpm, at 4°C, clear supernatant was placed in a new 2 ml tube, 200µl chloroform/ml TRizol was added and samples were vortexed for 15"; after 2'/3' of incubation at RT samples were centrifuged as before. Next the upper aqueous phase (~600 µl) was transferred to a new tube, 1 volume of 70% EtOH was added and samples were vortexed. Then, samples were transferred to RNeasy column of the RNeasy Plus Kit (Qiagen); from now on the extraction was done following the manufacturer instruction of this kit. RNA was eluted in 40 µl nuclease free H_2O and quantified using NanoDrop 1000 (Thermo Scientific).

Primary mlECs and adipose ECs

For gene expression analysis of primary ECs, 7 x10^5 cells were seeded in 6 well plates and kept in culture for 24h in F12 complete medium. Next, plates were quickly wash with PBS plus CaMg and stored at -80°C or directly processed. Total RNA was extracted using the RNeasy Plus Kit (Qiagen) as recommended by manufacturer. RNA

was eluted with nuclease free H_2O in a final volume of 30µl and quantified using NanoDrop 1000 (Thermo Scientific).

3.4.2 cDNA synthesis and qRT-PCR

cDNA was produced from 0.5µg of RNA using the High Capacity cDNA Reverse Transcription Kit (Applied Biosystems) following the protocol recommended by manufacturer. Briefly, 10 µl of reaction mix (Table 3.12) was added to 10 µl of sample (0.5 µg RNA plus H_2O up to 10 µl) in a 0.5ml eppendorf; tubes were placed in a thermal cycle with the following program: 25°C 10', 37°C 2h, 85°C 5', 4°C 2∞.

Reagents	Amount for 20µl reaction
10x RT buffer	2 µl
25X dNTPs mix	0.8 µl
10X Random primers	2 µl
RNase inhibitor	1 µl
Multi Scribe RT	1 µl
Nuclease free H_2O	3.2 µl
Total volume	10 µl

Table 3.12: RT reaction mix composition

Quantitative RT-PCR was performed using two different techniques: SYBR Green I Master Kit (Roche) or Premix Ex Taq ™ by Takara (RR390A) respectively run in LightCycler480 and 7300 Real-Time PCR System. For both strategy 9 µl of reaction mix (Table 3.13) and 1 µl of cDNA diluted 1:10 were used. PCR programs are described in Table 3.14 HPRT1 and mouseL32 were used as houskeeping. Data analysis was done with the ΔΔCT method.

Premix Ex Taq		SYBR Green	
Reagent	Volume for 10µl reaction	Reagent	Volume for 10 µl reaction
Premix Ex Taq 2x	5 µl	Master mix	5 µl
Taqman probe	0,4 µl	Primers	1 µl
ROX Dye 50x	0,2 µl	H_2O	3 µl
H_2O	3,4 µl		

Table 3.13: qRT-PCR reaction mix

TaqMan
Stage 1: initial denaturation
Number of cycles: 1
95 °C 30"
Stage 2: PCR
Number of cycles: 45
95°C 15"
60°C 1'

Table 3.14.A: qRT-PCR program, TaqMan probes

SYBR green				
Stage 1	denaturation			
Cycles	1	Analysis Mode	None	
Target (°C)	Acquisition mode	Hold (hh:mm:ss)	Ramp Rate (°C /s)	Acquisition (per °C)
95	none	00:10:00	4.80	
Stage 2	annealing			
Cycles	45	Analysis Mode	Quantification	
Target (°C)	Acquisition mode	Hold (hh:mm:ss)	Ramp Rate (°C /s)	Acquisition (per °C)
95	none	00:00:04	4.80	
62	none	00:00:30	2.00	
72	single	00:00:30	4.80	
Stage 3	melting			
Cycles	1	Analysis Mode	Melting Curves	
Target (°C)	Acquisition mode	Hold (hh:mm:ss)	Ramp Rate (°C /s)	Acquisition (per °C)
95	none	00:00:10	4.80	
65	none	00:01:00	2.50	
95	continous		0.11	5
Stage 4	cooling			
Cycles	1	Analysis Mode	None	
Target (°C)	Acquisition mode	Hold (hh:mm:ss)	Ramp Rate (°C /s)	Acquisition (per °C)
40	none	00:00:20	2.5	

Table 3.14.B: qRT-PCR programs, SYBR Green

Name	Reference	Company
PGC1α	01208835_m1	Applied Biosystems
PGC1β	01258518_m1	Applied Biosystems
CPT1A	00550438_m1	Applied Biosystems
HPRT1	Mm00446968_m1	Applied Biosystems
PRDM16	Mm00712556_m1	Applied Biosystems
CIDEA	Mm00432554_m1	Applied Biosystems
UCP1	00494069_m1	Applied Biosystems
ACC1	Mm01304277_m1	Applied Biosystems
ACC2	Mm01204678_m1	Applied Biosystems

Table 3.15: Taqman probe FAM

Name	**Forward primer** (5'-3')	**Reverse primer** (5'-3')
mL32	AACCCAGAGGCATTGACAAC	ATT GTGGACCAGGAACTTGC
mCPT1A	CATGTCAAGCCAGAGGAAGA	TGGTAGGAGAGCAGCACCTT
mCPT1B	CCCATGTGCTCCTACCAGAT	CCTTGAAGAAGCGACCTTTG
mAcadm	TCGGAGGCTATGGATTCAAC	CAGCCTCTGAATTTGTGCAG
mACADS	AGGTCCTGGAGGTCTGTGC	CAGTCCCGAACACCGAGA
mUCP1	CTGCCAGGACAGTACCCAAG’	GCCACAAACCCTTTGAAAAA
mACC2	CCCAGCAGAATAAAGCTACTTTGG	TCCTTTTGTGCAACTAGGAACGT
mFatp3	CGCAGGCTCTGAACCTGG	TCGAAGGTCTCCAGACAGGAG
mFatp4	GCAAGTCCCATCAGCAACTG	GGGGGAAATCACAGCTTCTC
mCD36	GATGAGCATAGGACATACTTAGATGTG	CACCACTCCAATCCCAAGTAAG
mFabp3	TTCAGCTGGGAATAGAGTTCG	CTGCACATGGATGAGTTTGC
mAP2	TGTGTGATGCCTTTGTGGGAACC	CTTCACCTTCCTGTCGTCTGCGG
mCBPα	CGCTGTTGCTGAAGGAACTTG	GGCAGACGAAAAAACCCAAAC
mPREF1	CGTCCTCTTGCTCCTGCTGGC	TCCCGTCCCAGCCATCCTTGC
mPPRγ	ATTGAGTGCCGAGTCTGTGGG	AGCAAGGCACTTCTGAAACCG
mGATA2	CACCCCGCCGTATTGAATG	CCTGCGAGTCGAGATGGTTG

Table 3.16 Primers used for qRT-PCR using SYBR Green I Master Kit

3.4.3 RNA sequencing

RNA sequencing was performed in collaboration with Dr. Pau Castel (Memorial Sloan Kettering Cancer Center, New York). After ribogreen quantification and quality control of Agilent BioAnalyzer, 500ng of total underwent polyA selection and Truseq library preparation according to instruction provided by Illumina (TruSeq™ RNA Sample Prep Kit v2), with 6 cycles of PCR. Samples were barcoded and run on a Hiseq 2500 in a 50bp/50bp Paired end run, using the TruSeq SBS Kit v3 (Illumina). An average of 31 million paired reads was generated per sample. At the most the ribosomal reads represented 0.1% and the percent of mRNA bases was closed to 74% on average.

3.5 Mitochondria respirometry

3.5.1 Substrate-Uncopler-Inhibitor Titration (SUIT) protocol

Oxygen consumption was measured with oroboros-2k respirometer (Oroboros Instruments GmbH Corp, Austria). DataLab (Oxygraph-2k associated software) was used to calculate the negative derivative of the oxygen concentration with respect to time, to provide the respiration value.

Substrate-Uncopler-Inhibitor Titration (SUIT) protocol (Cantó and Garcia-Roves, 2015) using Hamilton syringes was performed, the following titrations were given (with a minimum period of 4-5' between titration to allow the stabilisation of the slope): malate [2mM] and pyruvate [5mM] to measure the **LEAK** state of uncouple respiration in the absence of ADP (due to proton leak, electron slip and cation cycling that do not depend on ATP synthase activity). Next **OXPHOS** state was measured by adding ADP+$MgCl_2$ [5mM] and cytochrome C (10mM), to make sure the membrane has not been damage during sample preparation, followed by the addition of glutamate [10mM] to measure the complex I respiration NADH-dependent. Then succinate [10mM] was add to measure the complex II respiration $FADH_2$ dependent along with the respiration of complex I in the **OXPHOS CI+II state**. Next FCCP [0.5µM] was added to evaluate the maximal capacity of the Electron Transporter System (ETS) through the non physiological uncoupling of the mitochondria internal membrane, **ETS CI+II state.** Then rotenone [0.5µM] was used to inhibit CI and measure the maximal respiration of CII, **ETS CII state**; finally antimycin A [2.5µM] was add to inhibit CIII and measure the residual oxygen consumption define **ROX state**, this value represent a non-mitochondrial respiration and will be subtracted to the previous number to analyse any experiment.

3.5.2 Tissue preparation

Fresh isolated gonadal-WAT was collected in MiR05 media and kept on ice. A precision scale was used to weight ~120mg of tissue, then sample were homogenized using a PBI-Schredder SG3 (Pressure Biosciences Inc; South Easton, MA) to obtain a 40mg/ml preparation in MiR05. Next 2,1 ml of the homogenate was place in the O2k chamber (previously filled with MiR05 to calibrate the instrument) to start the experiment. Importantly the measure is automatically normalized to the amount of sample placed in the chamber.

3.5.3 Reagents and media utilized to perform high resolution respirometry

Substrate	Stock solution [mM]	Source and product code
L-Glutamic acid	2000	Sigma, G1626
L-Maltic acid	400	Sigma M1000
Pyruvic acid	2000	Sigma P2256
Succinate	1000	Sigma S2256
Cytochrome c	4	Sigma C7752
ADP	500	Sigma A5285
Uncoupler	**Stock solution [mM]**	**Source and product code**
FCCP	1	SigmaC2920 (10mg)
Inhibitors	**Stock solution [mM]**	**Source and product code**
Antimycin A	5	Sigma A8674 (25mg)
Rotenone	1	Sigma R8875 (1g)
Permeabilisation agent	**Stock solution [mM]**	**Source and product code**
Digitonin	8.1	Fluka 37008 (1g)

Table 3.17: List of substrates, uncoupler, inhibitors and permeabilisation agent.

Compound	Final concentration	Source and product code
EGTA	0.5 mM	Sigma, E 4378
$MgCl_2$	3 mM	Scharlau, MA 0036
K-lactobionate	60 mM	Aldrich, 153516
Taurine	20 mM	Sigma, T 0625
KH_2PO_4	10 mM	Merck, 104873
HEPES	20 mM	Sigma, H 7523
Sucrose	110 mM	Roth, 4621.1
BSA, essential fatty acid free	1g/L	Sigma, A 6003 fractionV

Table 3.18: MiR05 composition

3.6 Statistical analysis

Statistical analysis was performed by nonparametric Mann Whitney's test using Prism 5 (GraphPad Software Inc.) unless indicated otherwise. In all figures across the manuscript, errors bars are standard error of the mean.

4. Results

4.1 Physiological WAT remodelling

In order to investigate the cell intrinsic function of ECs in physiological WAT remodelling, we took advantage of our mouse model of PTEN deletion in ECs to promote vessel growth, in a cell autonomous manner (Serra et al., 2015). We crossed PTEN flox/flox mice with PdgfbiCreERT2 transgenic mice that express a tamoxifen-iducible Cre recombinase in ECs (Claxton et al., 2008). 4-hydroxytamoxifen (4-OH) was administered in vivo at postnatal day 1 (P1) and P2 to activate Cre expression (Figure 4.1); in each litter we got equal proportion of mice that have inherited the Cre (hereafter referred to as PTEN$^{i\Delta EC}$), and mice that have not (hereafter referred to as control).

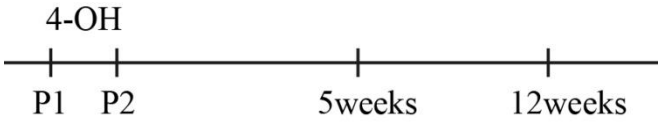

Figure 4.1: In-vivo experimental design. PTEN deletion was induced at postnatal day 1 and 2, WAT was collected and analyzed at 5 and 12 weeks of age.

4.1.1 Vascular characterisation of PTEN$^{i\Delta EC}$ mice

4.1.1.1 Loss of PTEN in ECs promotes vascular hyperplasia exclusively in WAT

To validate the suitability of our mouse model, we first analysed the vasculature in several non-adipose tissues; to this end control and PTEN$^{i\Delta EC}$ male mice were scarified at the age of 12 weeks, several tissues were collected and embedded in OCT. Blood vessels immunostaining on 5µm section, did not point out any differences in either vessels density or size between control and PTEN$^{i\Delta EC}$ mice (Figure 4.2). Conversely, whole-mount staining of gonadal and inguinal WAT disclosed a dramatic vascular hyperplasia already obvious at the age of 5 weeks and exacerbate at 12 weeks (Figure 4.3). Vascular hyperplasia was associated with increased ECs proliferation, evaluated by Ki65 stain of WAT of 5 weeks old mice (Figure 4.4). Based on these results, we

could conclude that PTEN$^{i\Delta EC}$ mice represented a good model to investigate the role of ECs in WAT remodelling.

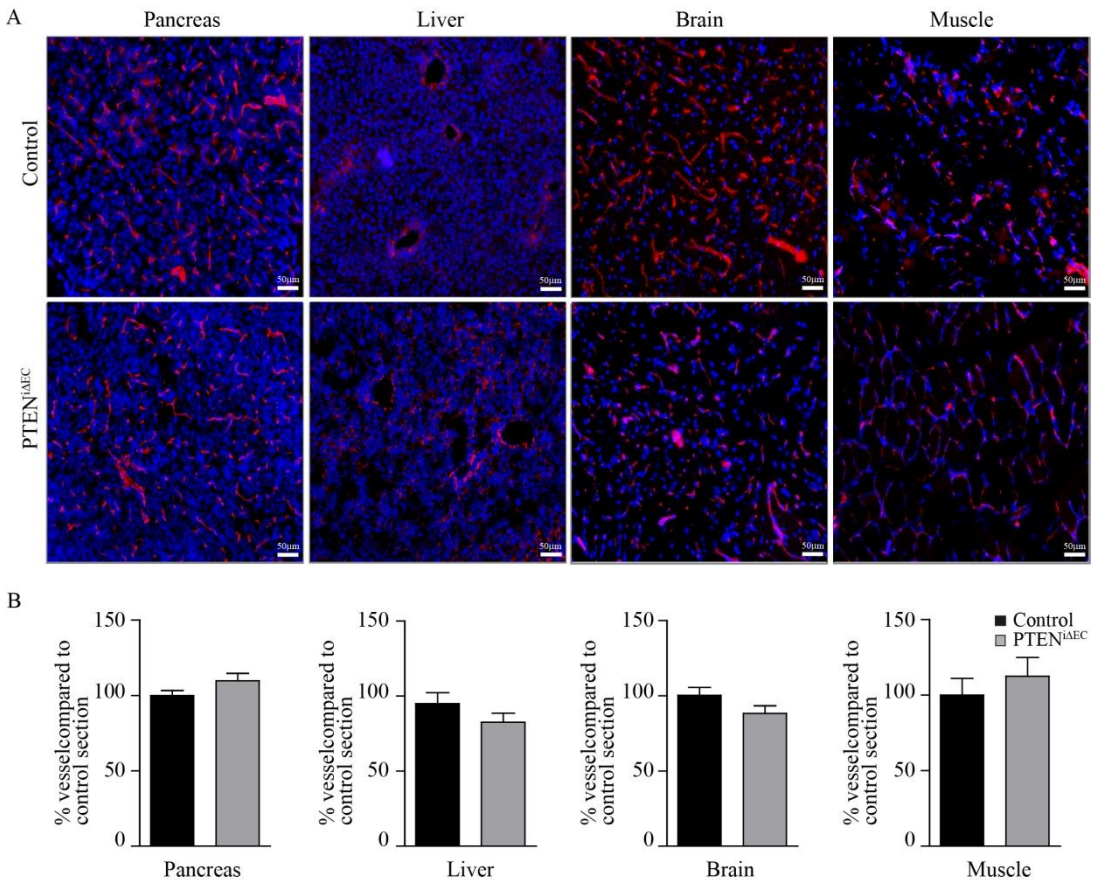

Figure 4.2: PTEN loss in ECs does not affect vascular development. A) Representative IF images of pancreas, liver, brain and muscle sections; blood vessels were stained with anti mouse CD31 (red), nucleus with DAPI (blue); B) Vessel quantification: number of vessels expressed as % of control tissues. Statistical analysis was performed by Mann–Whitney test. Data are expressed as mean ± SEM.

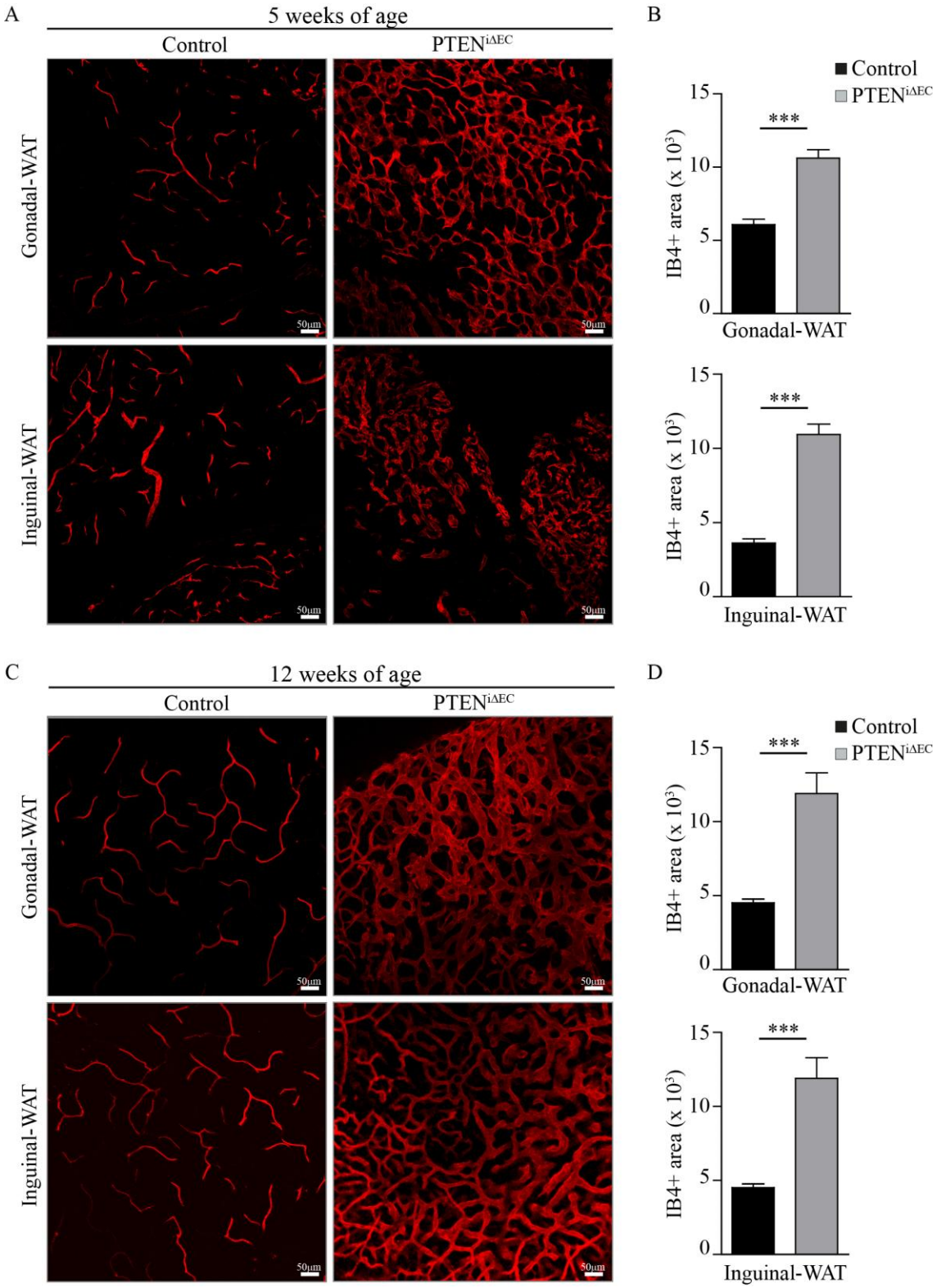

Figure 4.3: Loss of PTEN in ECs results in vascular hyperplasia in WAT. A) Whole-mount visualisation of blood vessel in adipose tissue of 5 and 12 weeks old mice; blood vessel were stained with isolectin B4 (IB4). B) Quantification of vascular density expressed as IB4 positive area, n=6 for each genotype, statistical analysis was performed by Mann–Whitney test. Data are expressed as mean ± SEM. ***P<0.0001.

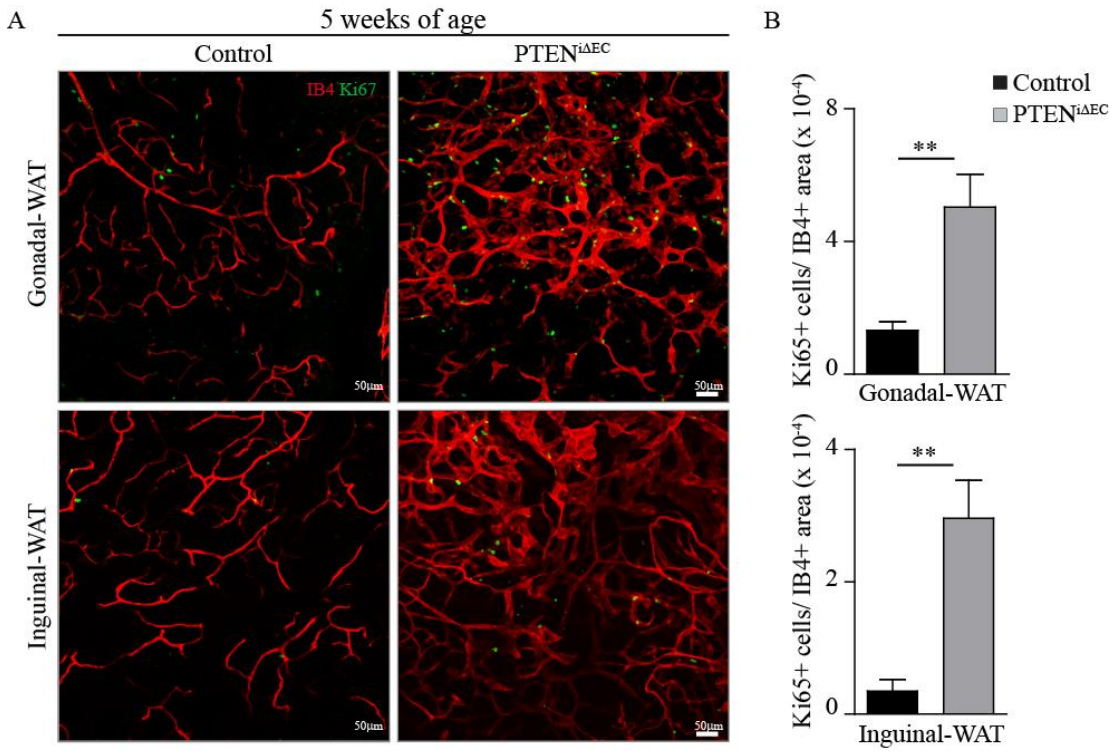

Figure 4.4: Loss of PTEN promotes ECs proliferation. A) Whole-mount visualisation of blood vessel in adipose tissue of 5 weeks old mice; blood vessel were stained with isolectin B4 (IB4) and proliferating nuclei with Ki67. B) Quantification: ECs proliferation was quantified by counting the number of Ki65 positive nuclei, which was then normalized with the IB4 positive area. n=6 for each genotype, statistical analysis was performed by Mann–Whitney test. Data are expressed as mean ± SEM. **P<0.005.

4.1.2 Phenotypic characterisation PTEN$^{i\Delta EC}$ mice

4.1.2.1 PTEN$^{i\Delta EC}$ mice exhibit reduced body weight gain

Body weight was monitored in a time frame of 8 weeks; control and PTEN$^{i\Delta EC}$ mice were systematically weight every Monday from 4 to 12 weeks of age. No differences were observed at 4 and 5 weeks, however, starting from 6 weeks of age PTEN$^{i\Delta EC}$ mice were visibly leaner and this difference became more evident at later time points. Interestingly, we observed that PTEN$^{i\Delta EC}$ mice reach their maximum weight around 8-9 weeks of age, meanwhile control mice keep on growing (Figure 4.5.A). Furthermore we noticed that, by 12 weeks, PTEN$^{i\Delta EC}$ mice suddenly lose weight and eventually die (in a time frame of 4-5 weeks depending on the severity of the phenotype), thus we set the end point of our study at 12 weeks of age. Macroscopic observation of any non-adipose tissue did not show difference in tissue weight and colour (except occasional mice which show splenomegaly) (Figure 4.5.B). Therefore, we focused our attention exclusively on adipose tissue. We choose two time point: i) 5 weeks of age, when the

vascular phenotype is already evident but the difference in body weight is still undetectable, and ii) 12 weeks of age when the vascular phenotype is associated with reduced body weight. At the age of 5 weeks we did not find any difference in gonadal-WAT, inguinal-WAT or BAT weight, but we observed that both WAT depots have already acquired a reddish colour, which reflects increased tissue vascularisation. Instead, at 12 weeks we found a dramatic reduction in both gonadal and inguinal WAT size, and both depots acquired a stronger red colour. Conversely, no macroscopic alteration was observed in BAT (Figure 4.6).

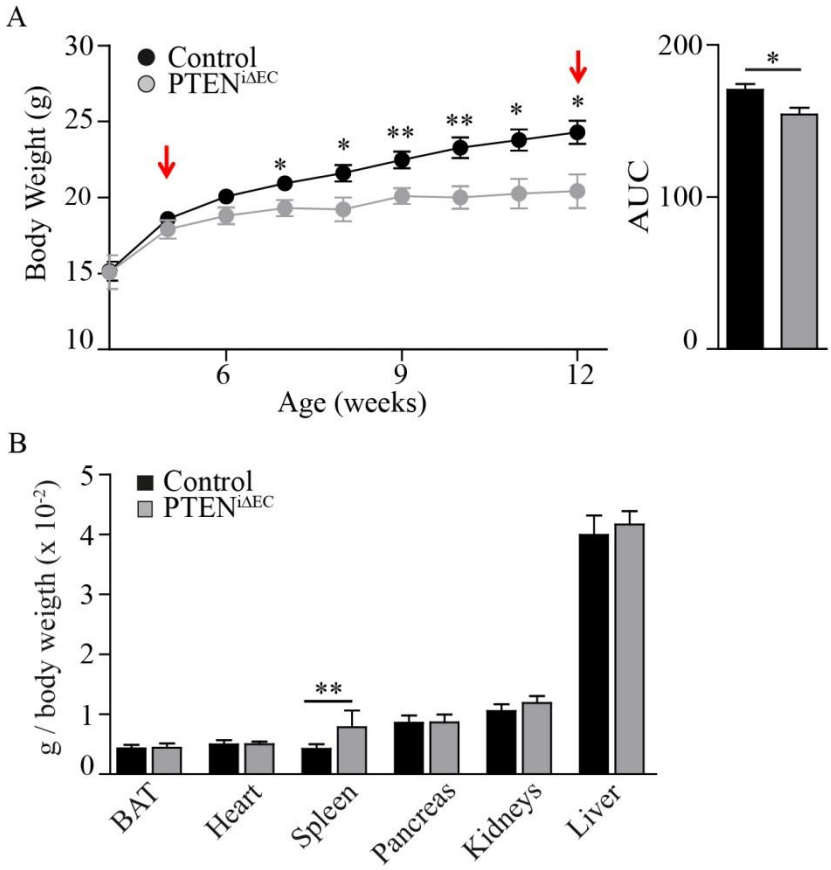

Fig 4.5: Loss of quiescence in ECs resulted in reduced body weight gain. A) Growth curve of control and PTEN$^{i\Delta EC}$ mice, (n≥8 each genotype); B) Tissue weight normalised with total body weight; mice were scarified at 12 weeks of age. Statistical analysis was performed by Mann–Whitney test. Data are expressed as mean ± SEM. *P<0.05; **P<0.005.

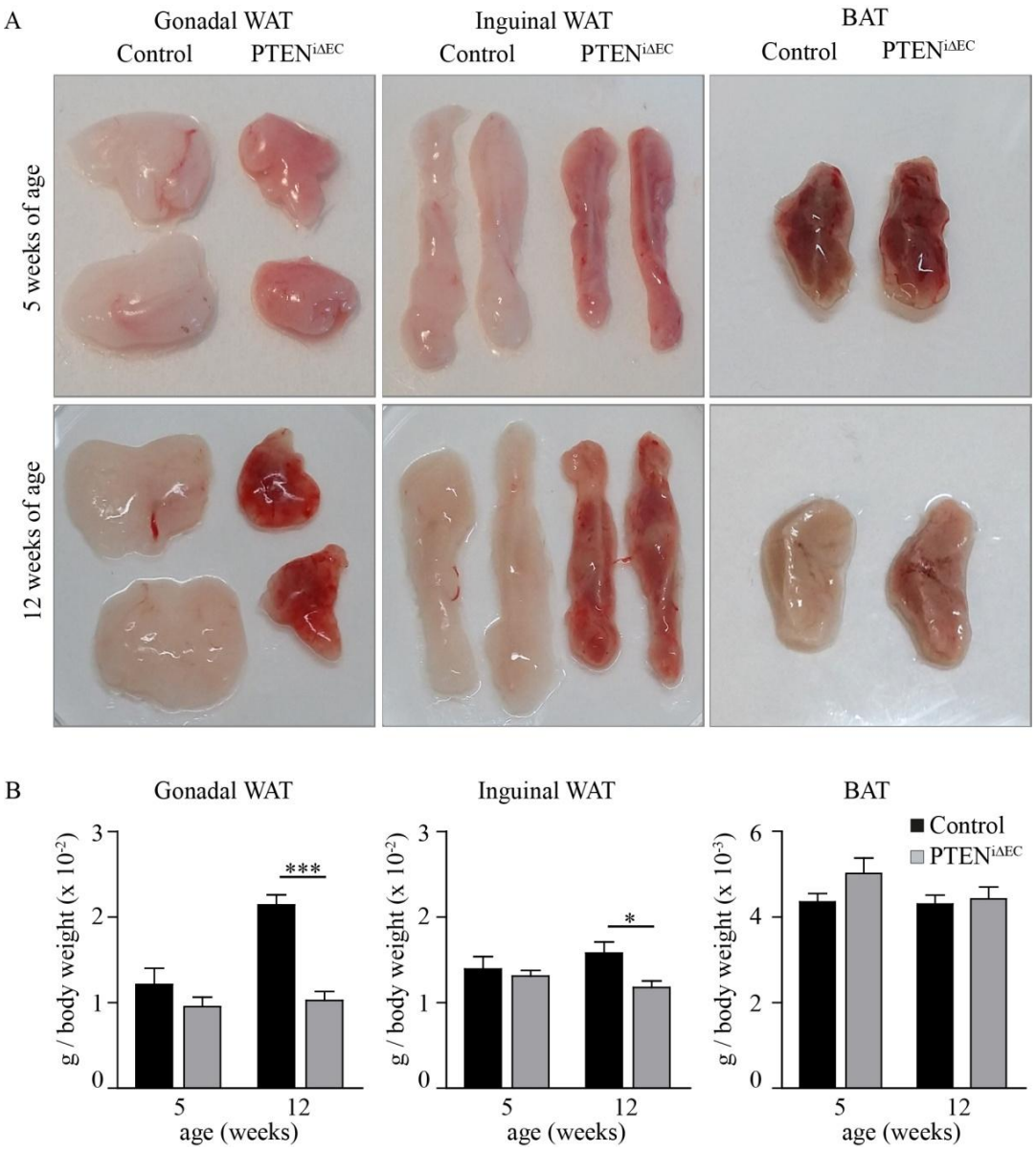

Figure 4.6: Increased vascular density correlates with reduced WAT size. A) Gross morphology of gonadal-WAT, inguinal-WAT and BAT at 5 and 12 weeks of age; B) Quantification: tissue weight normalised with total body weight (n≥7 each genotype). Data are expressed as mean ± SEM. ***P<0.0005, *P<0.05.

4.1.2.2 Enhanced WAT vascularisation is associated with a progressive reduction in adipocytes area

To get a more comprehensive description of the phenotype, we next evaluated the microscopic structure of WAT. According to what we observed macroscopically, histopathological examination of gonadal and inguinal WAT section at 5 weeks of age, underlined the presence of more and larger vessels (vascular hyperplasia) but the overall tissue structure was preserved and adipocytes did not show any anomaly. Later on, at 12 weeks of age, WAT morphology was clearly compromised; examination of gonadal and inguinal WAT section highlighted a dramatic increase in vascular density together with an obvious reduction in adipocytes area (Figure 4.7). Ematoxylin and eosin (H&E) staining of any other analysed tissues did not show morphologic alteration (Figure 4.8).

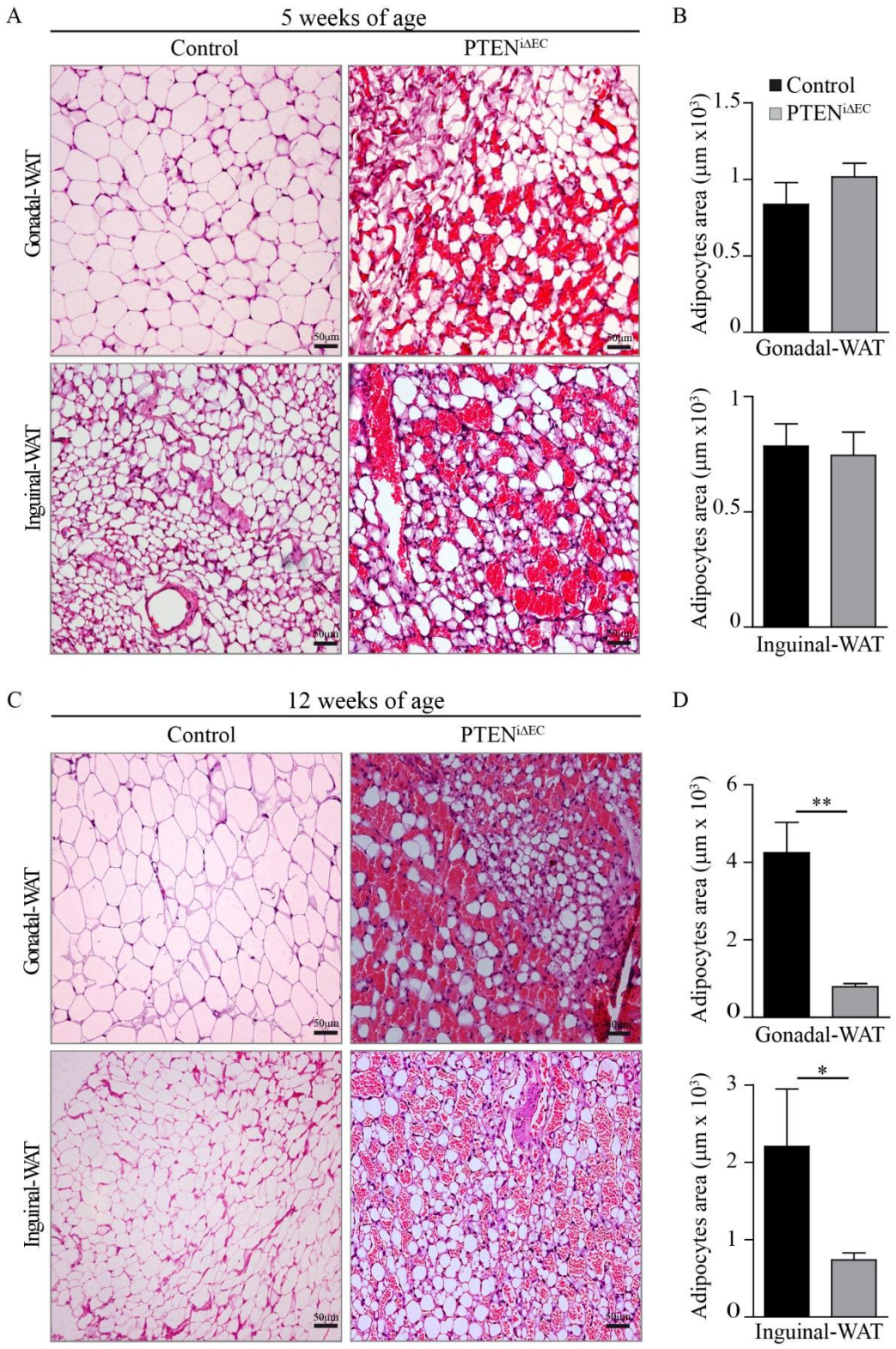

Figure 4.7: Enhanced angiogenesis in WAT leads to a progressive white adipocytes shrinkage. A) H&E staining of 5µm sections of gonadal and inguinal WAT at 5 and 12 weeks of age; B) Quantification of adipocytes area (n≥6), statistical analysis was done with Mann–Whitney test. Data are expressed as mean ± SEM. **P<0.005, *P<0.05.

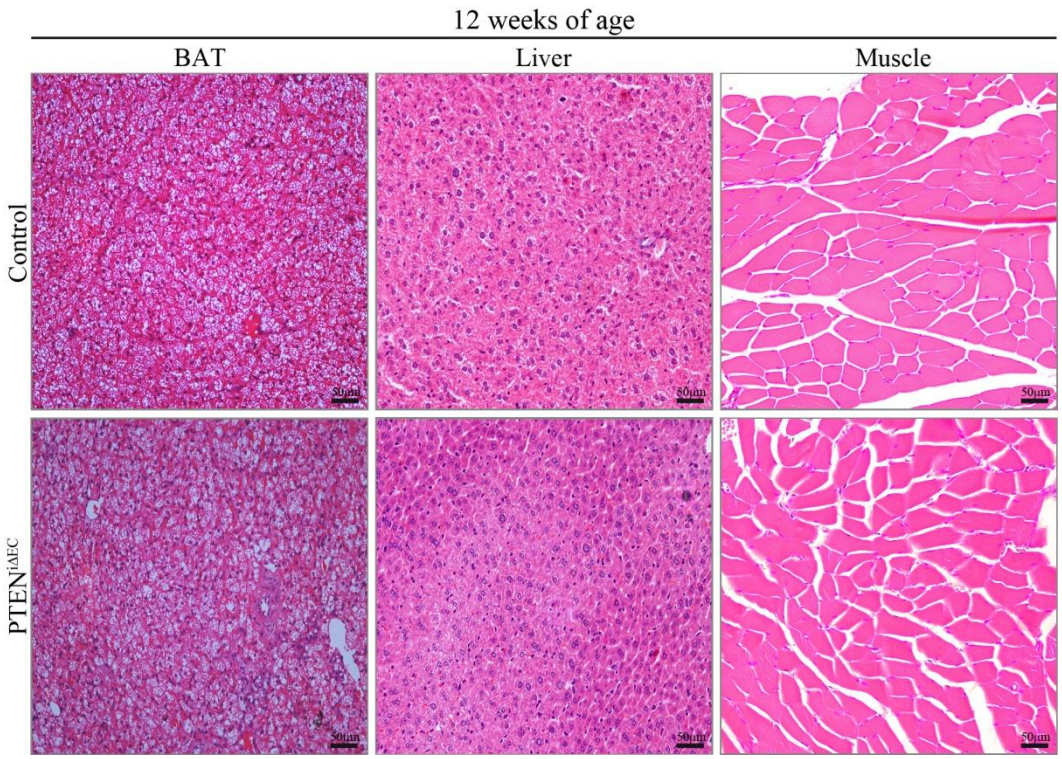

Figure 4.8: Histological analysis of tissues of control and PTEN$^{i\Delta EC}$ mice. Representative images of BAT, liver and muscle of 12 weeks old mice.

4.1.3 Metabolic profile of PTEN$^{i\Delta EC}$ mice

4.1.3.1 Loss of WAT mass does not alter whole body energy homeostasis

Giving that WAT is an endocrine organ essential to preserve whole body energy homeostasis, we were wondering whether the observed remarkable loss of WAT mass could be either cause or consequence of altered systemic metabolism. To this end we measured: Daily Food Intake (DFI), Respiratory Quotient (RQ), Energy Expenditure (EE), Locomotor Activity (LA), glucose homeostasis and insulin resistance. With the exception of DFI, all the experiments were conducted with 12 weeks old mice. DFI was evaluated at three time points: i) 4 weeks of age, before any changes in vascular and adipose structure became detectable; ii) 8 weeks of age, when vessel hyperplasia is already evident together with middle WAT phenotype; and iii) 12 weeks of age, end point of the study. Apart from a slightly food intake reduction, in PTEN$^{i\Delta EC}$ mice, at 4 weeks of age, no other significant differences were found (Figure 4.9).

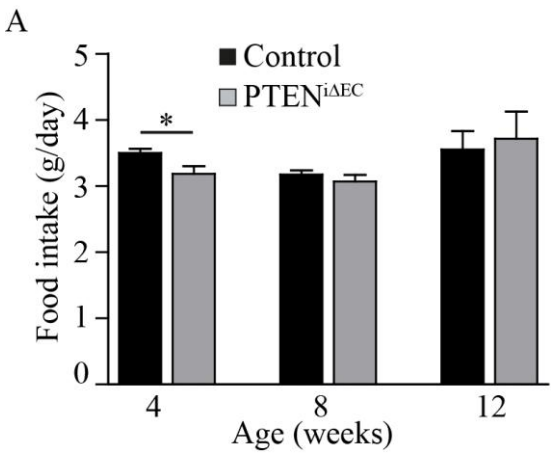

Figure 4.9: Metabolic characterisation of control and PTEN$^{i\Delta EC}$ mice. A) Daily food intake measured at 4, 8 and 12 weeks of age (n=8). Statistical analysis was done with Mann–Whitney test. Data are expressed as mean ± SEM.

RQ is defined as the actual substrate oxidation at the tissue level and it is expressed by the ration between VCO_2 and VO_2. Single housing of mice in metabolic cages allowed the measurement of RQ; no difference was observed between control and PTEN$^{i\Delta EC}$ mice (Figure 4.10).

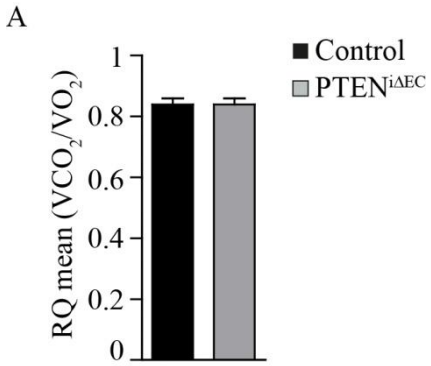

Figure 4.10: Metabolic characterisation of control and PTEN$^{i\Delta EC}$ mice. Respiratory Quotient, measured at 12 weeks of age. Statistical analysis was done with Mann–Whitney test. Data are expressed as mean ± SEM.

Total energy expenditure can be partitioned into different components. These normally include the energy spent on basal metabolism, the thermic effect of food (the increase in energy expenditure following food intake), the energy spent on thermoregulation and the energy spent on physical activity. EE can be measured either by direct or indirect calorimetry; here, it was determined by indirect calorimetry, which did not showed any changes in both dark and light phase (Figure 4.11).

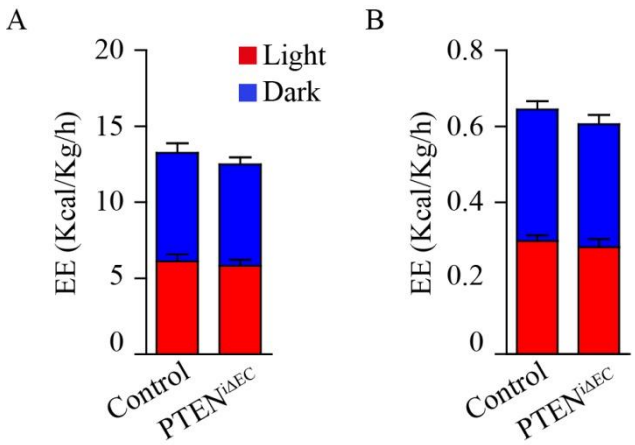

Figure 4.11: Metabolic characterisation of control and PTEN$^{i\Delta EC}$ mice. A) Energy Expenditure and B) EE corrected by total body mass measured at 12 weeks of age. Statistical analysis was done with Mann–Whitney test. Data are expressed as mean ± SEM.

Individual housing of mice in cages with a multidimensional infrared light beam system allowed studying the LA of the animals; no difference were observed in either dark or light phase (Figure 4.12).

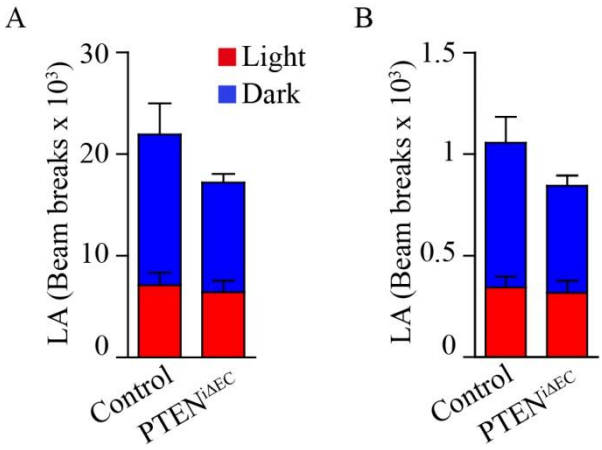

Figure 4.12: Metabolic characterisation of control and PTEN$^{i\Delta EC}$ mice. A) Locomotore Activity and B) LA corrected by total body mass measured at 12 weeks of age. Statistical analysis was done with Mann–Whitney test. Data are expressed as mean ± SEM.

Glucose homeostasis and insulin resistance were assessed by Glucose Tolerance Test (GTT) and Insulin Tolerance Test (ITT) respectively, both experiments were performed after 6h morning starvation. These assays showed that neither glucose tolerance nor insulin sensitivity were impaired in PTEN$^{i\Delta EC}$ mice (Figure 4.13).

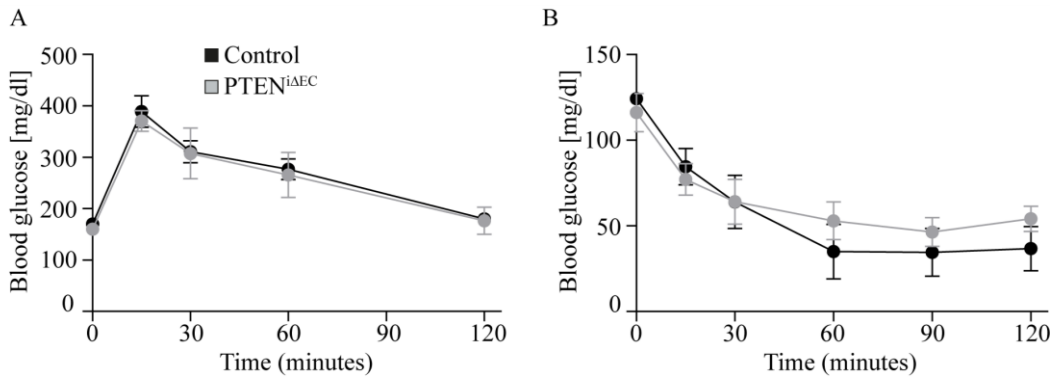

Figure 4.13: Metabolic characterisation of control and PTEN$^{i\Delta EC}$ mice. A) and B) respectively GTT and ITT performed on 12 weeks old mice; glucose or insulin were injected ip at 2 mg/g and 0,4 Ui/Kg respectively. Statistical analysis was done with Mann–Whitney test. Data are expressed as mean ± SEM.

4.1.4 Reduced fat accumulation in gonadal-WAT of PTEN$^{i\Delta EC}$ mice is a direct consequence of enhanced lipid catabolism

4.1.4.1 White adipocytes differentiation is not compromised in PTEN$^{i\Delta EC}$ mice

Based on recent publications, that place adipocytes precursors in the vascular niche (Tang et al., 2008a; Tran et al., 2012a), we were wondering whether the unbalanced microenvironment generated by hyper proliferative ECs might compromise the functionality of fat cell precursors. To address this question we first assessed gene expression of key regulators of adipocytes differentiation. Quantitative PCR on gonadal and inguinal-WAT did not detect statistically significant changes in any analysed gene, with the exception of AP2 (characteristic of mature adipocyte) whose expression is increased in inguinal-WAT of PTEN$^{i\Delta EC}$ mice (Figure 4.14.A and B). Next, to further confirm that the ability of adipocytes precursors to form mature fat cells was not compromised, the SVF of PTEN$^{i\Delta EC}$ WAT was successfully isolated and *in-vitro* differentiated (Figure 4.14.C). In addition, giving that it has been proposed that a subpopulation of endothelial cells might give rise to adipocytes (Gupta et al., 2012a; Tran et al., 2012a), we thought important to assess PTEN expression in adipose tissue to make sure PTEN is lost only in ECs. IHC performed on 5µm section of gonadal-WAT and inguinal-WAT confirmed that PTEN expression is preserved in mature adipocytes (Figure 4.15).

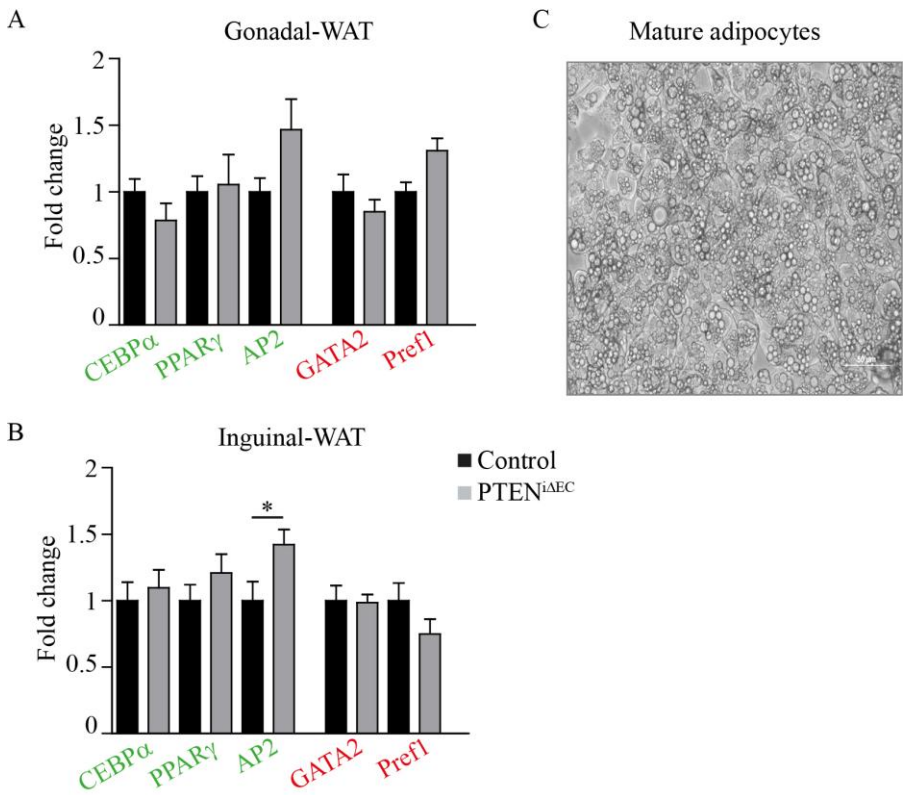

Figure 4.14: Increased ECs proliferation does not impair fat cell differentiation. Gene expression assessed by quantitative PCR (qPCR) in control and PTEN$^{i\Delta EC}$ gonadal-WAT (A) and inguinal-WAT (B) of 12 weeks old mice, n≥5 each genotype; in green pro-differentiation genes, in red negative repressors. Statistical analysis was done with Mann–Whitney test. Data are expressed as mean ± SEM. *P<0.05. C) Live images of mature adipocytes differentiated from the SVF of PTEN$^{i\Delta EC}$ gonadal-WAT (10 days after induction).

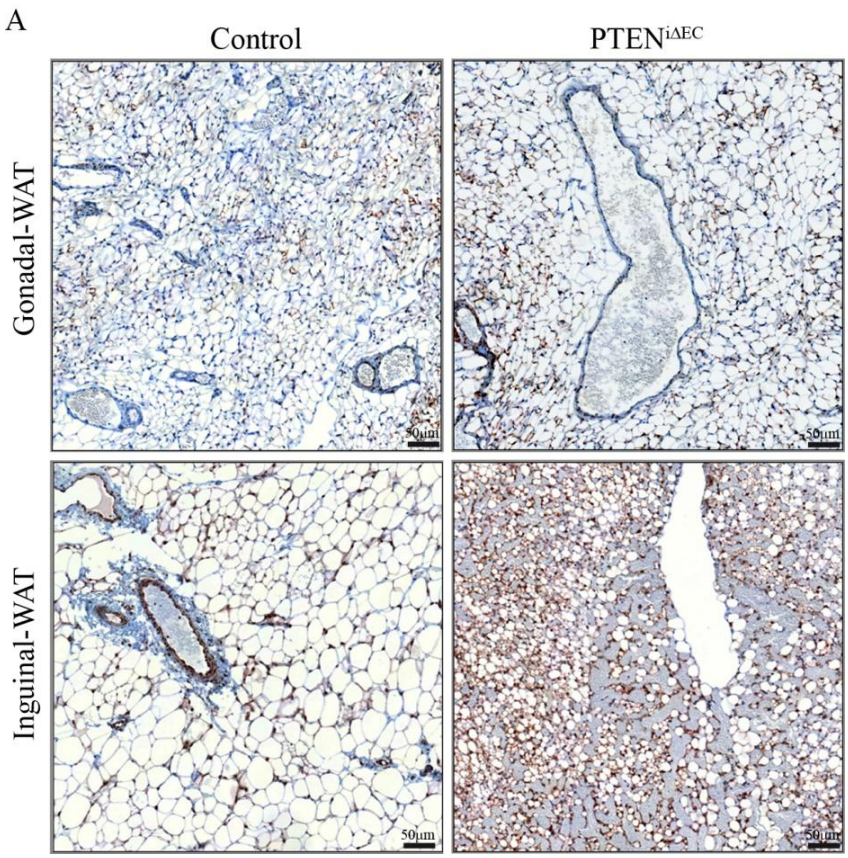

Figure 4.15: Mature adipocytes do express PTEN. A) Representative images of IHC for PTEN performed on 5µm section of gonadal-WAT and inguinal-WAT.

4.1.4.2 WAT of PTEN$^{i\Delta EC}$ mice do not undergo "browning"

Certain depots of WAT, in particular inguinal-WAT, in response to appropriate stimuli, can undergo a process known as browning, where white adipocytes take on characteristics of brown fat cells. Recently it has been described that improved adipose vascularisation activate the thermogenic program in BAT and WAT, thereby protecting mice from obesity and associated metabolic diseases (Elias et al., 2012; Robciuc et al., 2016; Sun et al., 2012, 2014). Based on these data we were wondering whether browning could explain the adipose phenotype of PTEN$^{i\Delta EC}$ mice. To answer this question we first evaluate gene expression of typical markers of BAT in both gonadal and inguinal WAT. QPCR analysis of gonadal-WAT, from 12 weeks old control and PTEN$^{i\Delta EC}$ mice, did not underline any difference in PRDM16, UCP1 and CIDEA expression; with regard to inguinal-WAT we found a significant lower expression of UCP1 in PTEN$^{i\Delta EC}$ mice, with no changes in PRDM16 or CIDEA expression (Figure 4.16.A). Next, we assessed UCP1 protein level in both WAT depots; Western Blot (WB) and IHC on gonadal-WAT form 12 weeks old mice did not detect any UCP1

expression in either control or PTEN$^{i\Delta EC}$ mice. Conversely, according to the qPCR results, we could detect a variable UCP1 expression in inguinal-WAT of few control mice; but no UCP1 was observed in any PTEN$^{i\Delta EC}$ mice (Figure 4.16.B and C). All together these results excluded browning of WAT as putative cause of the observed loss of fat mass.

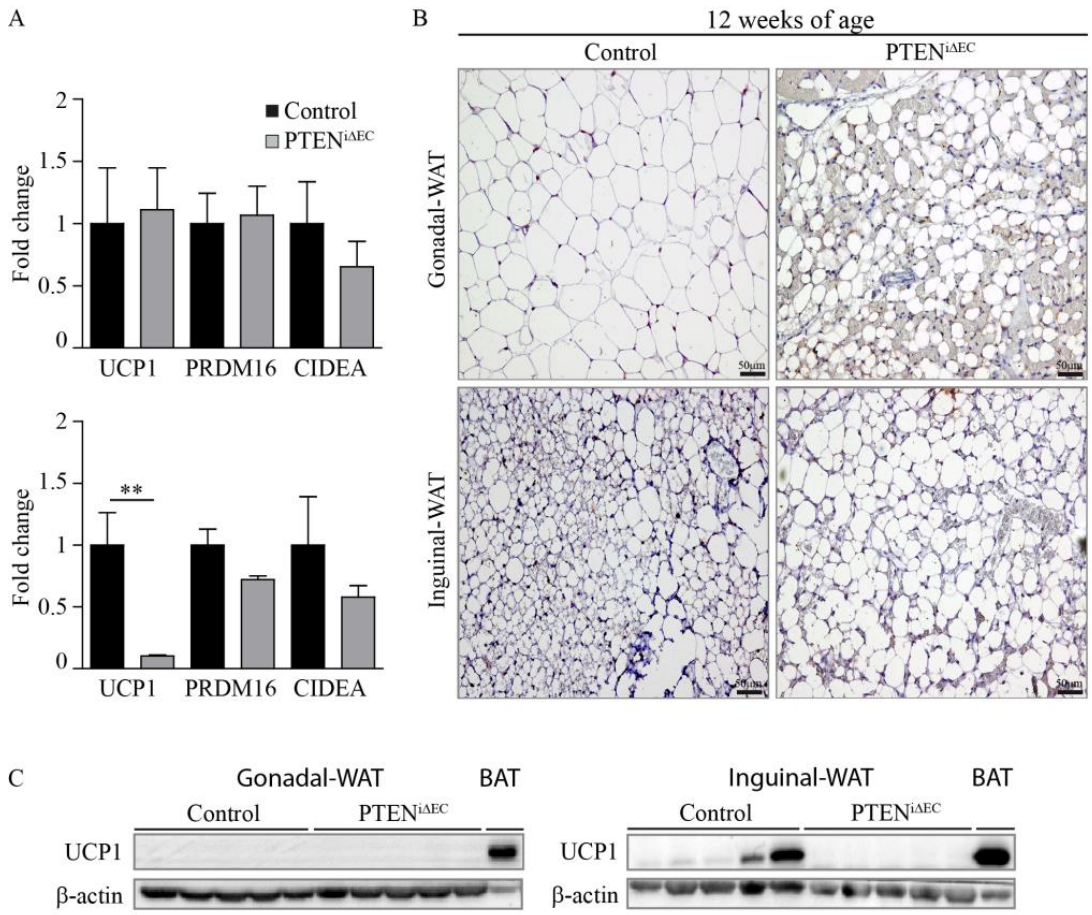

Figure 4.16: **Vascular hyperplasia does not activate a thermogenic program in WAT.** A) Gene expression assessed by qPCR in control and PTEN$^{i\Delta EC}$ gonadal and inguinal-WAT of 12 weeks old mice, n≥5 each genotype; B) representative images of IHC for UCP1 in 5µm section of control and PTEN$^{i\Delta EC}$ WAT; C) Immunoblot analysis of gonadal and inguinal-WAT using the indicated antibody; BAT was used as positive control. Statistical analysis was done with Mann–Whitney test. Data are expressed as mean ± SEM. **P<0.01.

4.1.4.3 Loss of gonadal-WAT mass is driven by enhanced β-oxidation and increased mitochondrial respiration

To get inside into the molecular mechanism that could lead to progressive loss of fat mass, we first performed mRNA sequencing on gonadal-WAT of 12 weeks old control and PTEN$^{i\Delta EC}$ mice. According to our speculation, mRNA sequencing revealed a lipid catabolism signature in gonadal-WAT of PTEN$^{i\Delta EC}$ mice. Next, qPCR validation confirmed, among others, increased expression of PGC1β (master regulator of β-oxidation) and CPT1B (the rate-controlling element for mitochondrial β-oxidation) (Figure 4.17). Conversely, gene expression analysis on inguinal-WAT reflected a quite different scenario (Figure 4.18), suggesting that depot specific responses might control fat mass size. At early time point, when vascular hyperplasia is already present but no difference in body weight are detectable, we could not find any variation in genes related to β-oxidation (Figure 4.19). Afterwards, mitochondrial function was assessed ex-vivo; high resolution respirometry experiments on fresh collected gonadal-WAT showed increased mitochondrial respiration, in all respiratory state, in gonadal-WAT of PTEN$^{i\Delta EC}$ mice (Figure 4.20).

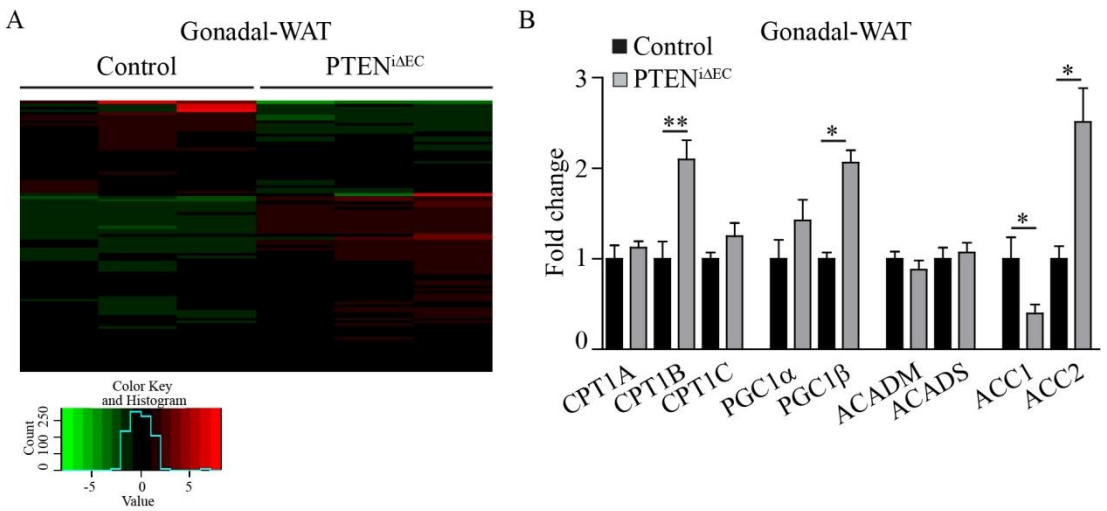

Figure 4.17: Reduced fat mass correlates with enhanced β-oxidation in gonadal-WAT. A) RNA seq. heat map. B) Validation by qPCR of a set of gene related to lipid catabolism, n≥5 each genotype. Statistical analysis was done with Mann–Whitney test. Data are expressed as mean ± SEM. **P<0.005, *P<0.05.

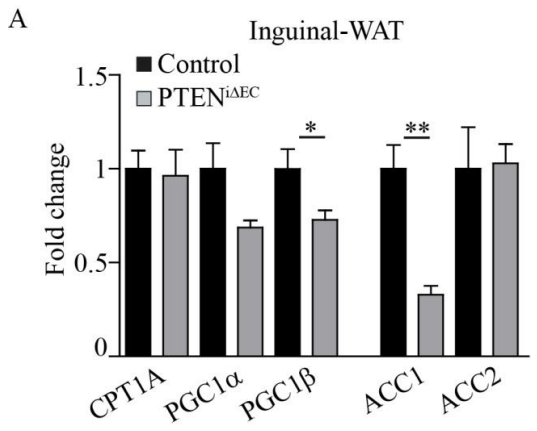

Figure 4.18: Inguinal-WAT did not undergo β-oxidation. A) Gene expression assessed by qPCR in inguinal-WAT of control and PTEN$^{i\Delta EC}$ mice at 12 weeks of age, n≥5 each genotype. Statistical analysis was done with Mann–Whitney test. Data are expressed as mean ± SEM. **P<0.005, *P<0.05.

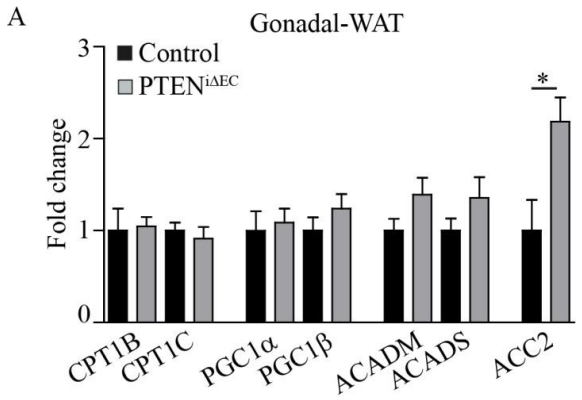

Figure 4.19: No indication of lipid catabolism at 5 weeks of age. Gene expression assessed by qPCR in gonadal-WAT of control and PTEN$^{i\Delta EC}$ mice at 5 weeks of age, n=6 each genotype. Data are expressed as mean ± SEM. *P<0.05.

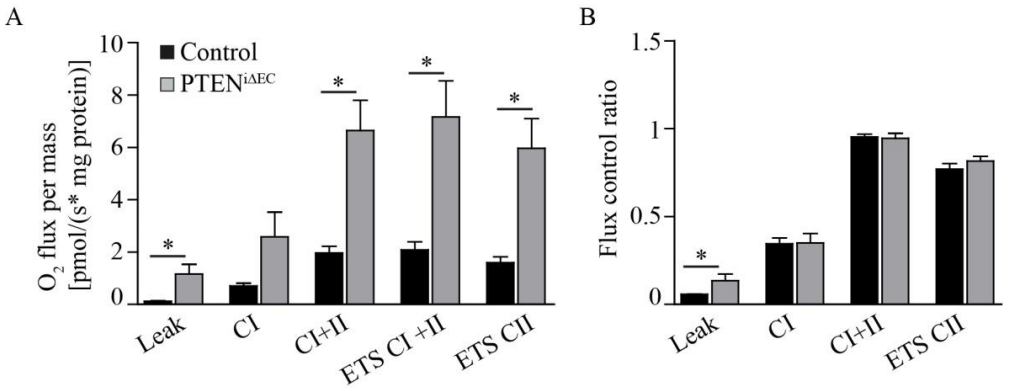

Figure 4.20: Enhanced mitochondrial function in gonadal-WAT of PTEN$^{i\Delta EC}$ mice. A) Oxygen flux normalized by tissue weight. B) Flux control ratio; oxygen flux in each respiratory state normalized by ETS CI +CII state, n≥3 each genotype. Statistical analysis was done with Mann–Whitney test. Data are expressed as mean ± SEM. *P<0.05.

4.1.5 Etomoxir treatment completely reverts vascular hyperplasia and prevents loss of fat mass

According to our results, the progressive diminution of gonadal-WAT was likely to be mediated by increased β-oxidation rate. If this was the case we would expect blockage of β-oxidation to prevent loss of fat mass. To test this hypothesis control and PTEN$^{i\Delta EC}$ mice were treated with Etomoxir (irreversible CPT-1 inhibitor) or vehicle for 5 weeks, day on/ day off, from 5 to 10 weeks of age (Figure 4.21). Adipose tissue vasculature and structure were then analyzed. Surprisingly, Etomoxir treatment alone was sufficient to completely revert vascular hyperplasia in gonadal-WAT and partially in inguinal-WAT (Figure 4.22). This normalization of the adipose vessel network was nicely associated with an almost complete rescue of WAT size, gross morphology and histological structure (Figure 4.23), (Figure 4.24). Necropsy analysis did not point out differences in size between any other examined tissues (Figure 4.25).

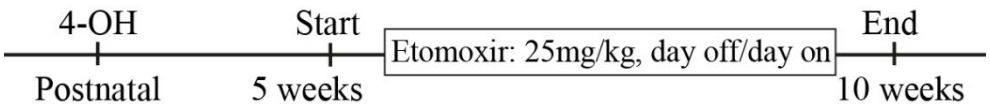

Figure 4.21: *In-vivo* experimental design. PTEN deletion was induced at postnatal day 1 and 2; afterwards, mice were treated day off/day on with Etomoxir, 25mg/Kg, or vehicle from 5 to 10 weeks of age.

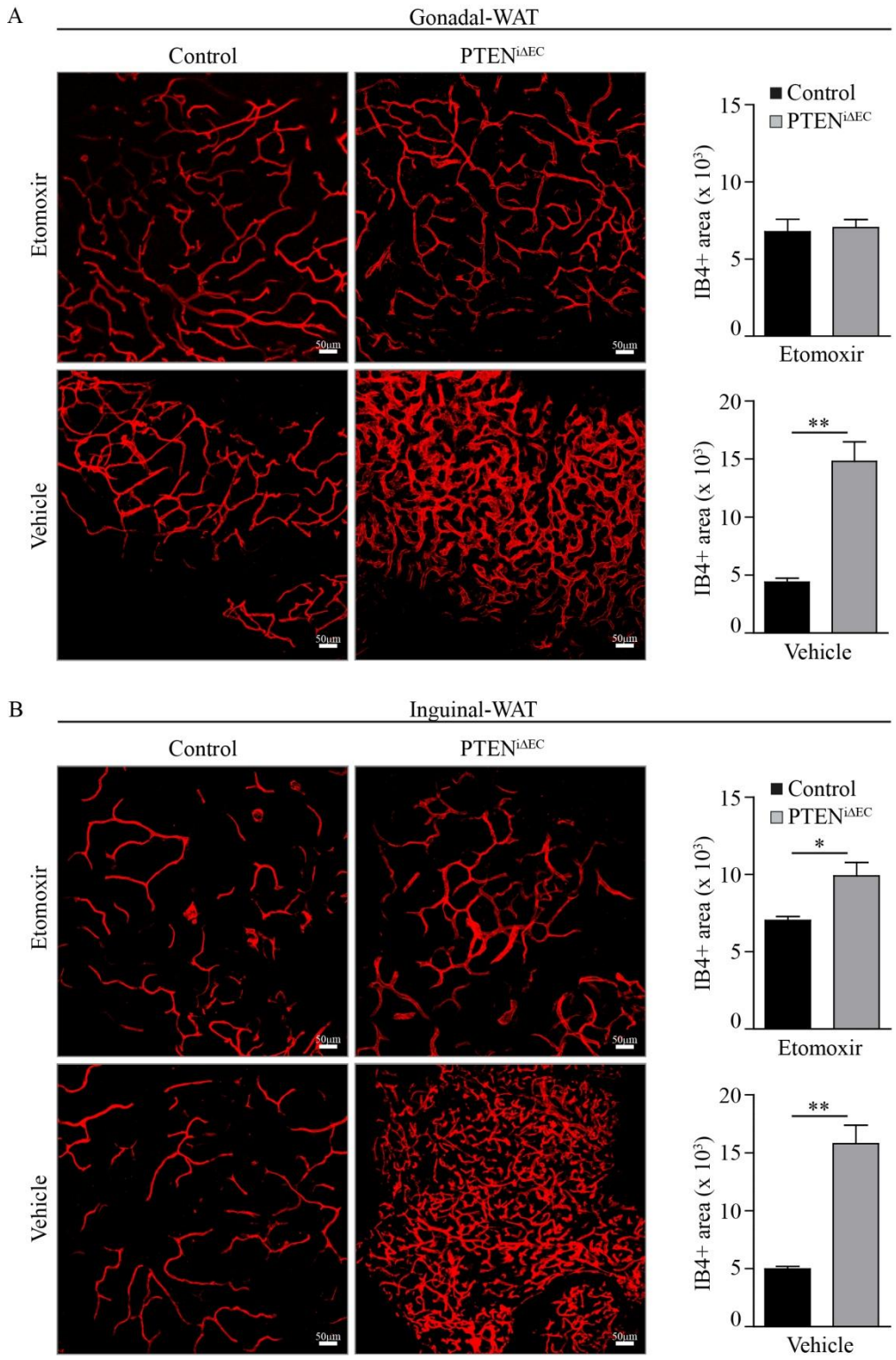

Figure 4.22: Blockade of β-oxidation reverts vascular hyperplasia. Whole-mount visualisation of blood vessel in gonadal-WAT (A) and inguinal-WAT (B) of Etomoxir and vehicle treated mice. Vessels density was quantified as IB4 positive area, n≥6 for each genotype and treatment, statistical analysis was performed by Mann–Whitney test. Data are expressed as mean ± SEM. *P<0.05, **P<0.005.

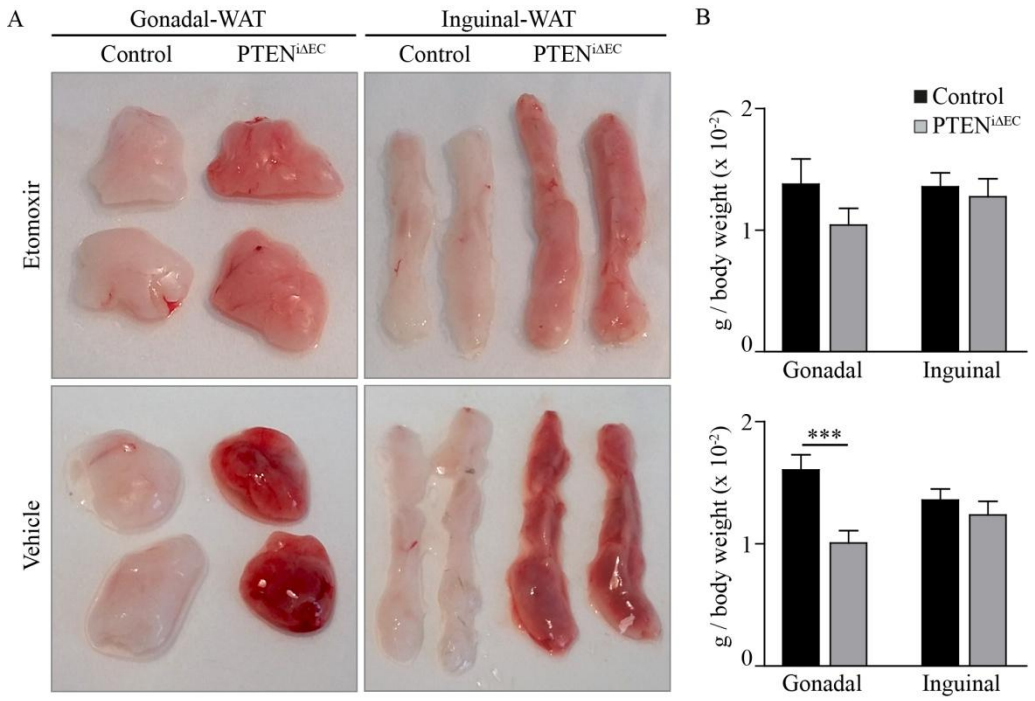

Figure 4.23: **Inhibition of β-oxidation prevents loss of fat mass.** A) Gross morphology of control and PTEN$^{i\Delta EC}$ mice treated with Etomoxir or vehicle; vascular density is reflected in the different color of WAT. B) Quantification: tissue weight normalised with total body weight (n≥6 each genotype and treatment). Data are expressed as mean ± SEM. ***P<0.0005.

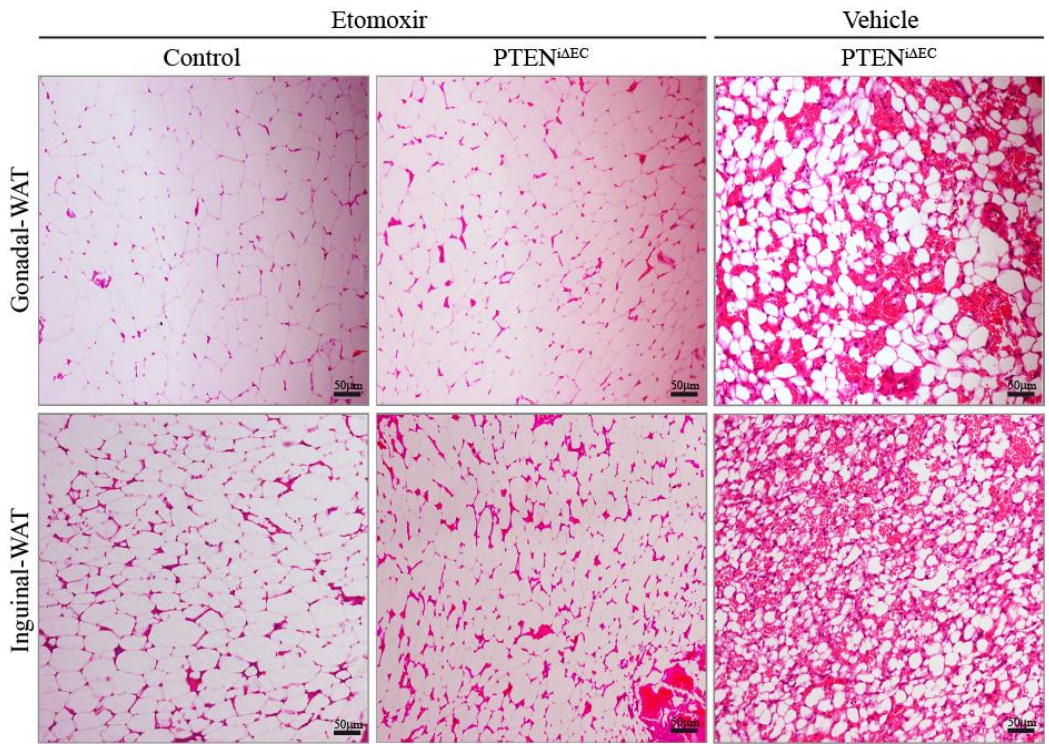

Figure 4.24: Inhibition of β-oxidation prevents white adipocytes shrinkage. H&E staining, of 5µm sections of gonadal and inguinal WAT after 5 weeks of treatment with Etomoxir or vehicle.

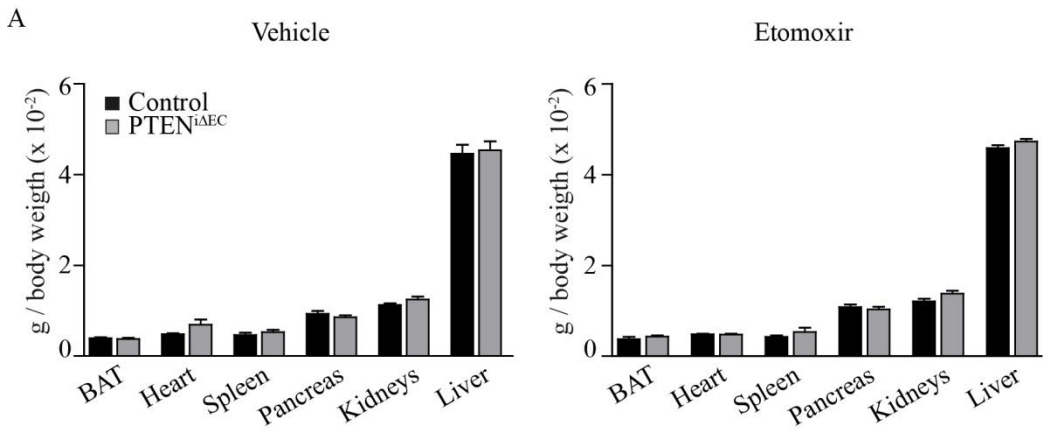

Figure 4.25: Etomoxir treatment does not affect other tissues. A) Tissue weight normalised with total body weight; mice were scarified at 10 weeks of age. Statistical analysis was performed by Mann–Whitney test. Data are expressed as mean ± SEM.

4.1.6 In-vitro characterisation of control and PTEN null ECs

Next we were interested in identifying features that differ between control and PTEN null ECs, which could determine the impact of ECs on WAT. Based on the observation that: i) activation of ECs respectively promotes vessel growth and restrains fat accumulation, and ii) inhibition of β-oxidation normalizes adipose vasculature which in turns prevents fat loss; we focused our attention on ECs metabolism. Specifically we hypothesised that PTEN null ECs (active ECs) need lipids to proliferate and to expand the vascular network.

4.1.6.1 PTEN null ECs are highly proliferative

In order to explore this hypothesis mouse primary lungs endothelial cells (mlECs) and primary adipose tissue ECs (adipose ECs) were isolated from control and PTEN$^{i\Delta EC}$ mice and expanded *in-vitro*. Most of the experiments were performed with mlECs and some were then repeated with adipose ECs, the results obtained were always comparable and in general differences became more evident with adipose ECs. To assess the efficiency of recombination, and the consequent activation of the PI3K pathway, respectively PTEN and pAkt levels were evaluated. Immunoblot analysis showed a concomitant loss of PTEN expression and increased pAkt level (Figure 4.26.A). Next, assessment of ECs proliferation in-vitro, revealed a 2 fold increased upon loss of PTEN, which partially explained the observed vascular hyperplasia in-vivo (Figure 4.26.B).

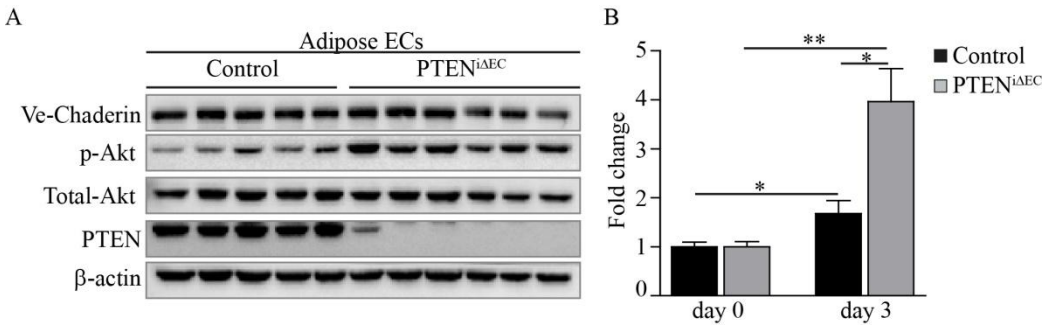

Figure 4.26: PTEN loss in ECs promotes cell proliferation. A) Immunoblot analysis of adipose ECs, plated for 24h in basal condition, using the indicated antibody (n≥5). Similar results were obtained with mlECs (data not shown). B) Proliferation of control and PTEN null ECs, in basal condition, evaluated by crystal violet staining. Data are expressed as mean ± SEM. *P<0.05, **P<0.005.

4.1.6.2 PTEN null ECs undergoes a metabolic switch towards a more oxidative metabolism

Next, we analyzed expression profile of lipid catabolic genes in mlECs and adipose ECs, in particular we centred on genes related to FFA transport and β-oxidation. We found that loss of PTEN in ECs increased the expression of: FATP3, FABP3 and CD36 (which suggested enhanced FFA uptake), PGC1β and CPT1A, (Figure 4.27.A). Notably, this oxidative gene expression profile was associated with enhanced *in-vitro* β-oxidation (Figure 4.27.B). According to these results, western blot analysis of control and PTEN null ECs showed significant increased phosphorylation of ACC (negative regulator of CPT1, whose activity is inhibited by phosphorylation) and a tendency of enhanced AMPK phosphorylation (considered a sensor of cell energy status, activated by phosphorylation when ATP level drops). Furthermore, the observed reduction in FAS and UCP3 expression suggested that FFAs are not used either for de novo lipogenesis or mitochondrial uncoupled respiration (Figure 4.27.C and D). Based on the higher proliferation rate and according to literature (De Bock et al., 2013a; Eelen et al., 2015), we would have expected PTEN null ECs to be more glycolytic then control cells. However, surprisingly, glucose consumption and lactate production assays, performed with mlECs and adipose ECs, did not point out any differences between control and PTEN null ECs (Figure 4.28).

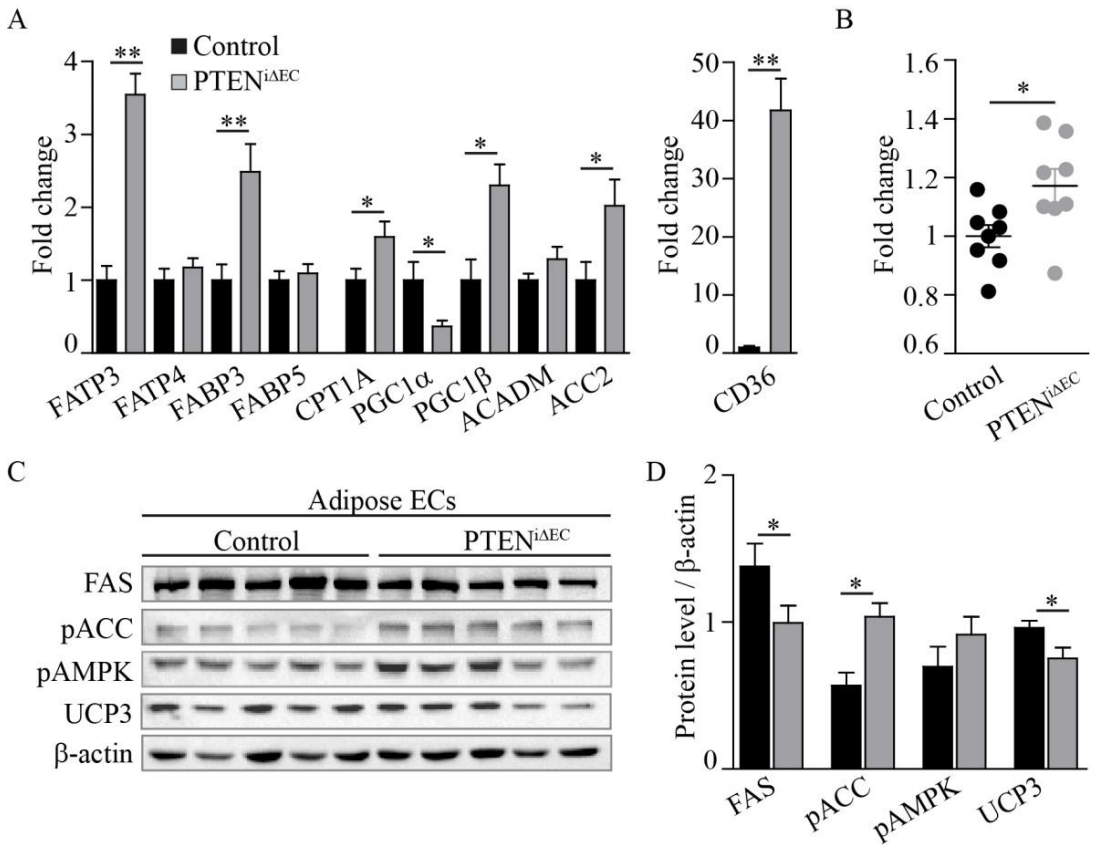

Figure 4.27: Active ECs display an oxidative metabolism. A) Gene expression evaluated by quantitative PCR in primary control and PTEN null mlECs. B) In-vitro evaluation of β-oxidation rate, measured by the dehydrogenation of [3H]-palmitate, n=8 each genotype. C) Immunoblot analysis of adipose ECs using the indicated antibody (n=5 each genotype). D) Quantification of the relative immunoreactivity normalized to β-actin. Data are expressed as mean ± SEM. **P<0.005, *P<0.05.

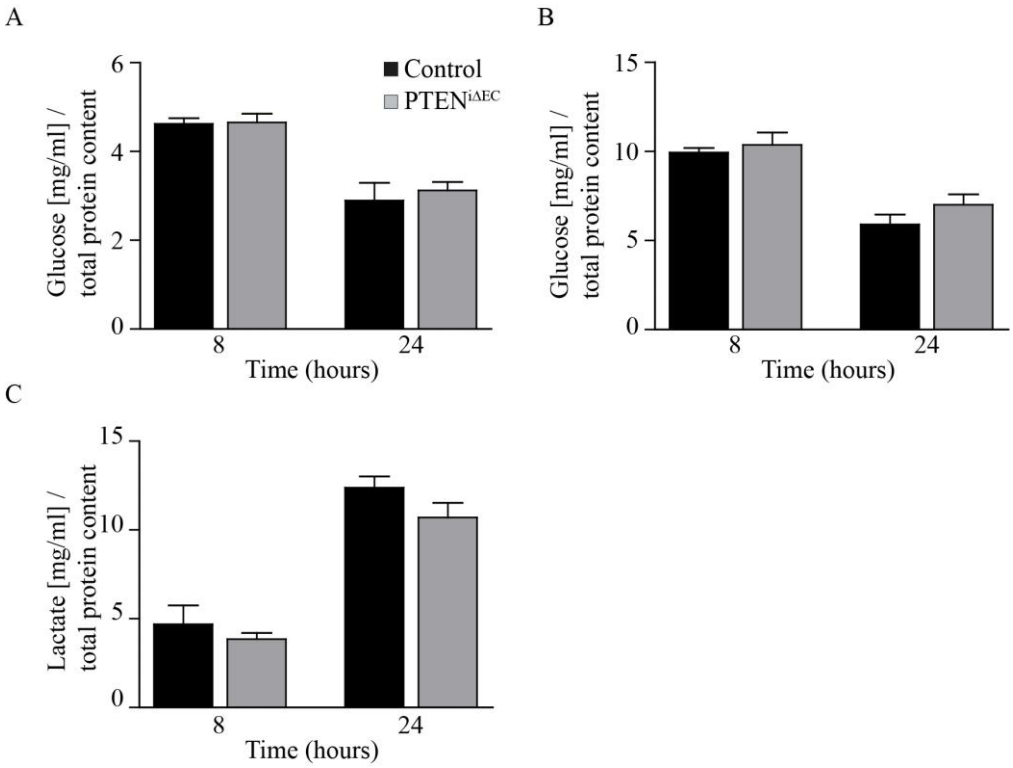

Figure 4.28: PTEN loss in ECs do not alter glucose metabolism. To evaluate glucose consumption glucose was added at the concentration of 1mM (A) or 2mM (B); glucose concentration in the media was measured after 8 and 24 hours and normalised with total protein content. C) Lactate production was measured 8 and 24 hours post seeding and normalised with total protein content. Data are expressed as mean ± SEM. (n≥6).

4.2 Pathological WAT remodelling: diet induced obesity

The second objective of this thesis was to decipher the role of ECs in pathological WAT expansion; specifically we focused on diet induced obesity. To this end control and PTEN$^{i\Delta EC}$ mice were exposed to 45% fat enriched diet (HFD) for 8 consecutive weeks (starting at 6 weeks of age) (Figure 4.29). Adipose vascular network, body weight, adipose tissue morphology and glucose homeostasis were then evaluated.

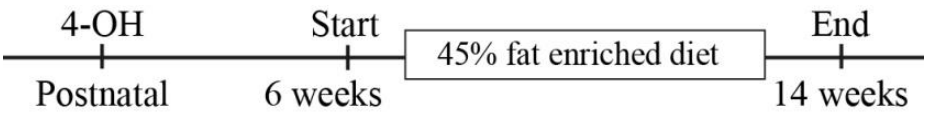

Figure 4.29: In-vivo experimental design. PTEN deletion was induced at postnatal day 1 and 2; afterwards, 6 weeks old control and PTEN$^{i\Delta EC}$ mice were exposed to 45% fat enriched diet for 8 consecutive weeks.

4.2.1 Loss of PTEN in ECs improves WAT vascularisation

Excessive WAT expansion is normally associated with insufficient angiogenesis that leads to hypoxia, adipocytes death and inflammation. Given that PTEN null ECs are highly proliferative and display an oxidative metabolism, we speculated that these active ECs, when exposed to obesogenic microenvironment, might preserve the ability to efficiently expand the adipose tissue vascular network. Hence, we analysed WAT vasculature, after 8 weeks of HFD, and we found increased vascular density in both gonadal and inguinal WAT of PTEN$^{i\Delta EC}$ mice (Figure 4.30).

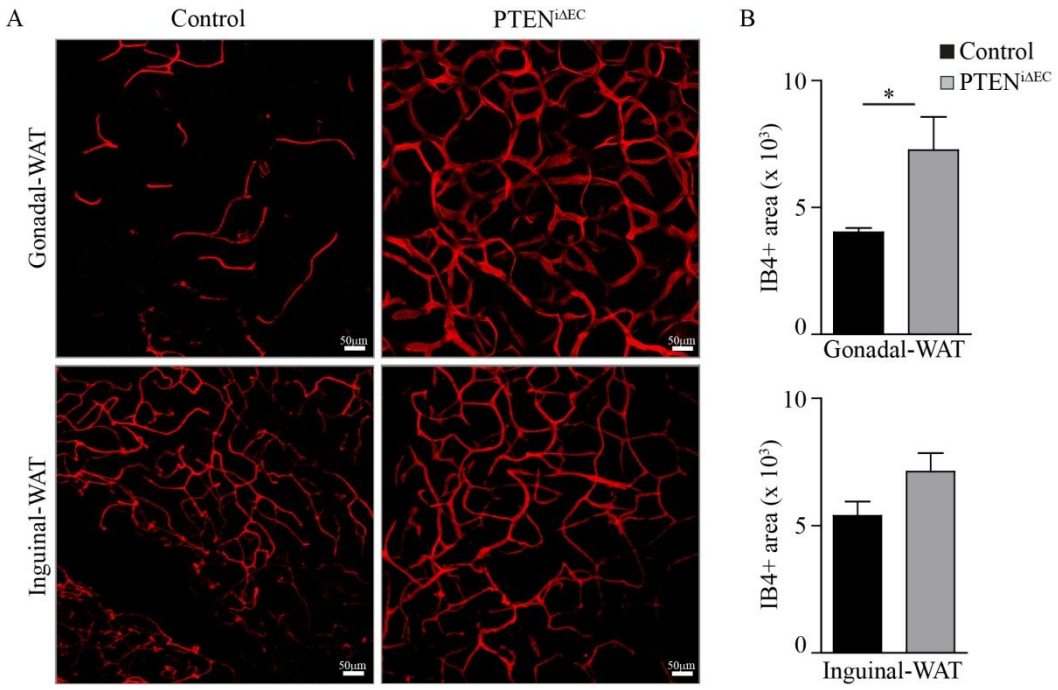

Figure 4.30: In an obesogenic context, more functional ECs ensure a better vascularisation of the expanding WAT. A) Whole-mount visualisation of blood vessel by IB4 staining. B) Quantification of vessel density represented as IB4 positive area. Data are expressed as mean ± SEM. *P<0.05.

4.2.2 PTEN$^{i\Delta EC}$ mice showed reduced body weight gain and WAT mass

To assess whether improved ECs function is protective against HFD induced obesity we first evaluated body weight, to this end control and PTEN$^{i\Delta EC}$ mice were systematically weight every Monday from 5 to 14 weeks of age; we observed that PTEN$^{i\Delta EC}$ mice stay leaner, thus suggesting that improved ECs activity reduces fat accumulation also in a context of high calorie intake (Figure 4.31). Consistent with this data, macroscopic observation of WAT showed an obvious reduction in gonadal fat mass (less evident in the inguinal depot) (Figure 4.32). Conversely, necropsy analysis did not point out

differences in size between any other examined tissue (except occasional mice which show splenomegaly) (Figure 4.33).

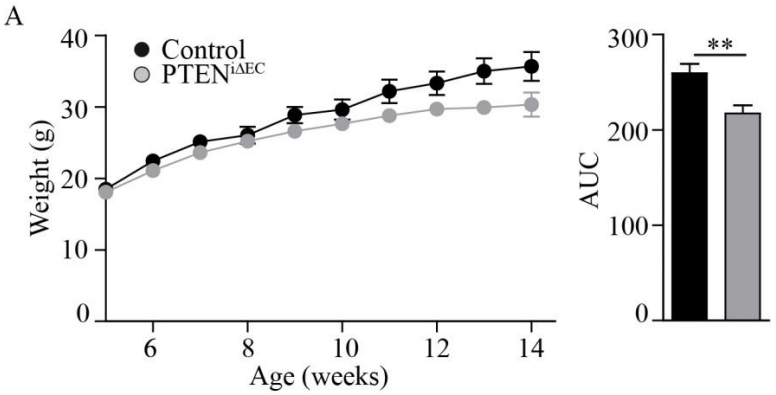

Figure 4.31: PTEN$^{i\Delta EC}$ mice are less sensitive to diet induced obesity. A) Growth curve of control and PTEN$^{i\Delta EC}$ mice feed with HFD, (n≥6 each genotype). Statistical analysis was performed by Mann–Whitney test. Data are expressed as mean ± SEM. **P<0.005.

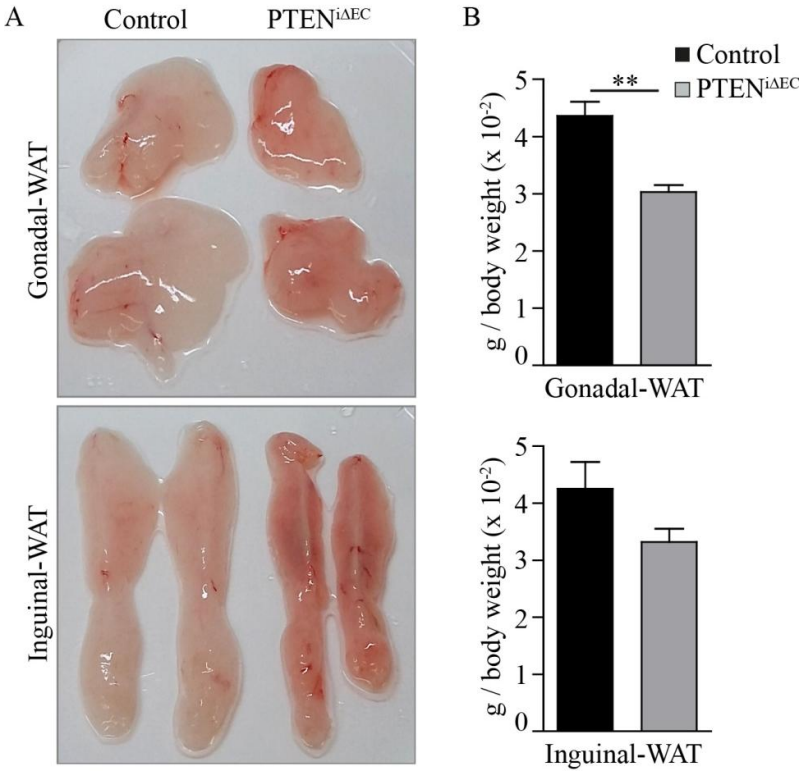

Figure 4.32: A functional vascular network is associated with reduced WAT expansion. A) Gross morphology of gonadal-WAT and inguinal-WAT of control and PTEN$^{i\Delta EC}$ mice after 8 weeks of HFD. B) Quantification: tissue weight normalised with total body weight (n≥5 each genotype). Data are expressed as mean ± SEM. **P<0.005.

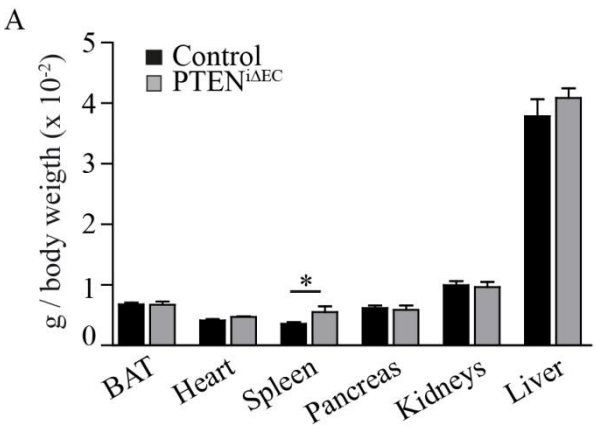

Figure 4.33: Post mortem analysis of control and PTEN$^{i\Delta EC}$ mice do not reveal differences in any tissue but WAT. A) Tissue weight normalised with total body weight. Statistical analysis was performed by Mann–Whitney test. Data are expressed as mean ± SEM. *P<0.05.

4.2.3 Improved ECs function prevents from adipocytes hypertrophy and ectopic lipid deposition

In response to excessive calories intake, WAT can expand either by hypertrophy or hyperplasia, respectively defined as pathological and healthy fat pad expansion. Giving that hypertrophic adipocytes generate a hostile and proinflammatory microenvironment that facilitate the onset of metabolic complication, we next characterised the microscopic structure of WAT. Histopathological examination of gonadal and inguinal WAT section showed that, concomitant with reduced weight gain and decreased fat mass, adipocytes mean area was smaller in PTEN$^{i\Delta EC}$ mice (Figure 4.34), therefore suggesting that improved ECs activity attenuates HFD induced adipocytes hypertrophy. Notably, histological sections of liver and BAT showed that, despite reduction in WAT depot dimension, lipids deposition in hepatocytes or brown adipocytes is not augmented in PTEN$^{i\Delta EC}$ mice (Figure 4.35).

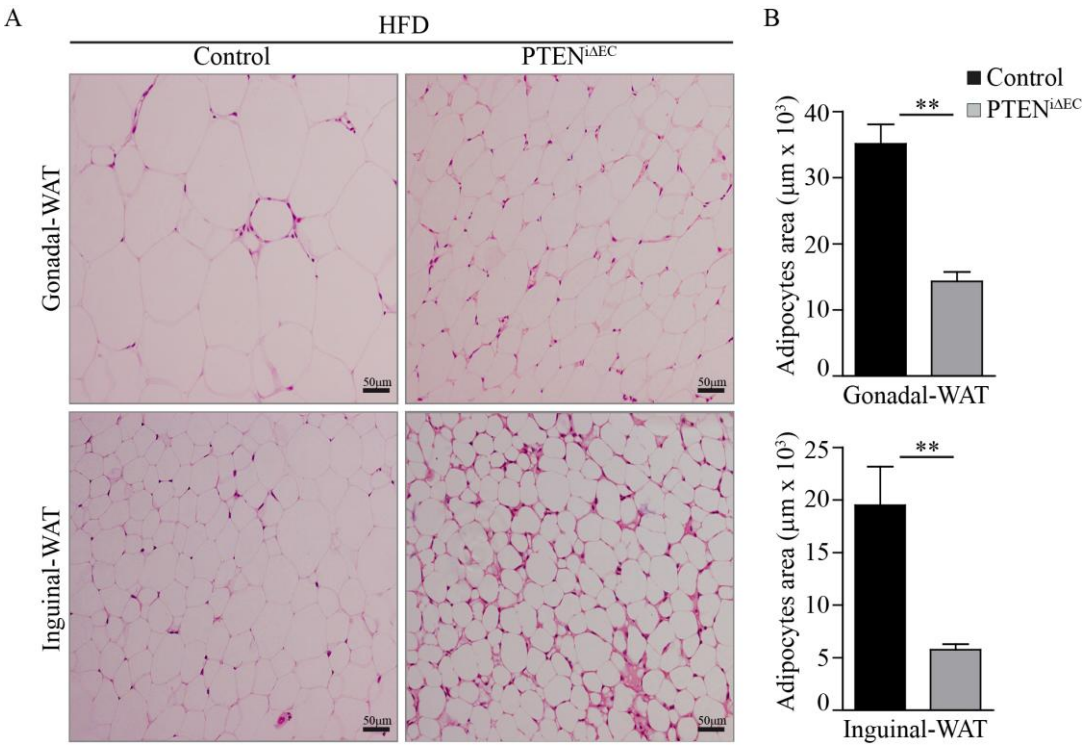

Figure 4.34: Improved ECs function prevents the formation of hypertrophic adipocytes. A) H&E staining on 5µm sections of gonadal and inguinal WAT. B) Quantification of adipocytes area, statistical analysis was done with Mann–Whitney test. Data are expressed as mean ± SEM. **P<0.005.

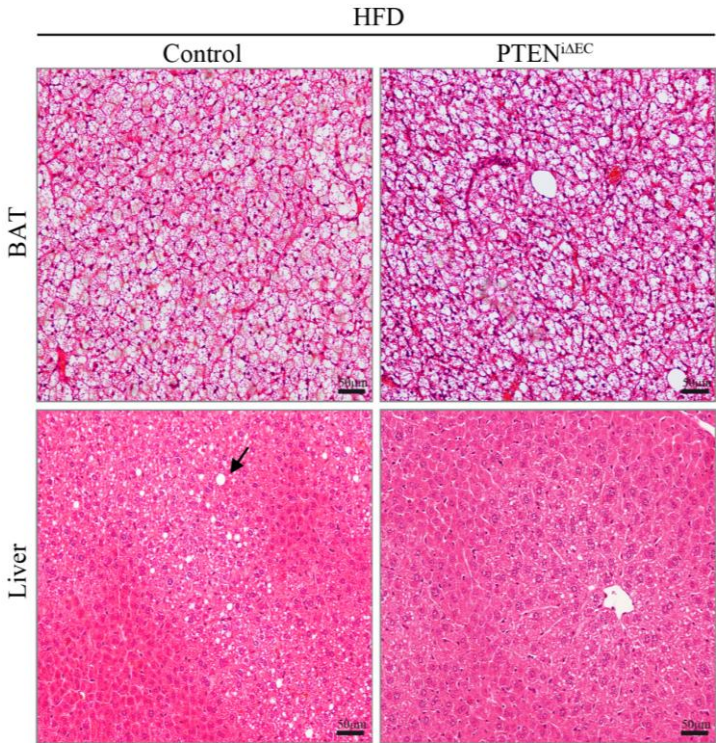

Figure 4.35: Decreased WAT dimension did not results in ectopic lipid deposition. Representative images of liver and BAT of control and PTEN$^{i\Delta EC}$ mice; the arrow indicates a small lipid droplet.

4.2.4 Activation of adipose ECs improves glucose tolerance

To evaluate the potential beneficial effect of more functional ECs on obesity related metabolic diseases, glucose tolerance and insulin sensitivity were analysed. Together with lower basal glucose level, PTEN$^{i\Delta EC}$ mice displayed significant improved glucose tolerance compared to control mice (measured by GTT). A tendency of improved insulin sensitivity was also observed in PTEN$^{i\Delta EC}$ mice (measured by ITT) (Figure 4.36).

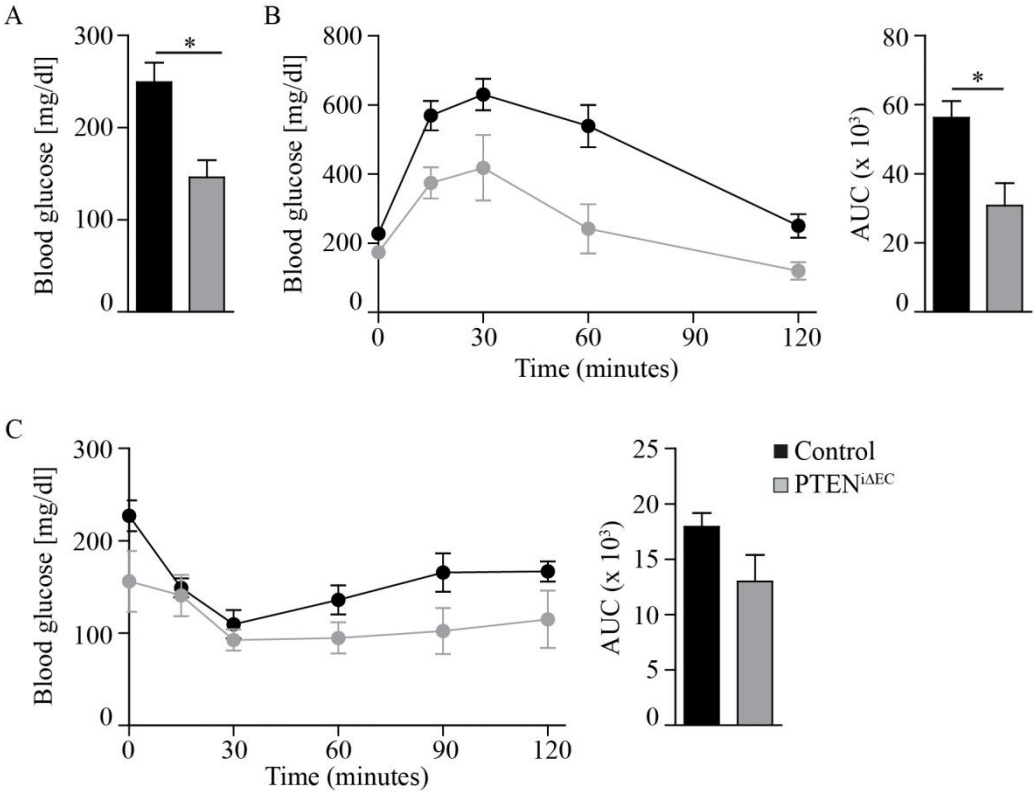

Figure 4.36: PTEN$^{i\Delta EC}$ mice exhibit improved glucose homeostasis. A) Basal blood glucose level measured after 6h morning starvation (n≥4). B) and C) GTT and ITT in control and PTEN$^{i\Delta EC}$ mice after 8 weeks of HFD (n≥4); glucose and insulin were injected ip respectively 1,5 mg/g and 0,75 Ui/Kg, after 6h morning starvation. Data are expressed as mean ± SEM. *P<0.05.

5. Discussion

WAT growth is strictly coordinated with angiogenesis; newly formed vessels provide O_2, nutrients, growth factors and hormones, all indispensable elements to sustain WAT expansion. Indeed several lines of evidence indicate that adipose tissue growth can be limited by its vascular supply (Christiaens and Lijnen, 2010; Crandall et al., 1997). WAT produces many proangiogenic factors that alone or collectively stimulate neovascularisation during healthy WAT expansion (Cao, 2007). However, chronic over-nutrition determines excessive WAT expansion which is not coordinated with vascular remodelling, and consequently leads to a dysfunctional tissue. Despite it is broadly accepted that blood vessels are essential to preserve a healthy WAT, little is known about the mechanisms involved.

The objective of this thesis was to study how ECs intrinsic properties modulate WAT remodelling in both physiological and pathological condition. To this end we took advantage of a mouse model of PTEN deletion in ECs, which allow us to promote angiogenesis in a cell intrinsic manner.

5.1 Physiological WAT remodelling

Previous data from our group identified PTEN as key regulator of vascular development. Specifically, we demonstrated that loss of endothelial PTEN led to the development of severe vascular defects that principally included increased vascular branching, enhanced vessel diameter and profound changes in the sprouting front morphology (Serra et al., 2015). However, this study did not explore the long term effects of endothelial PTEN loss in whole body angiogenesis; therefore, we first characterised the vasculature of adult $PTEN^{i\Delta EC}$ mice. Interestingly, we found an adipose tissue specific vascular phenotype characterized by an early onset of vascular hyperplasia that got worse over time. This observation raise a key question: why only adipose tissue is affected if PTEN is lost anywhere in ECs? Based on our results we can speculate that loosing PTEN is the "initial event" that predisposes ECs to undergo unrestrained proliferation. Although, in developing retinas loss of PTEN alone is sufficient to promote vascular hyperplasia, in adult mice there is a quite different scenario; that is ECs are normally quiescent so this "initiating factor" alone is not enough to promote proliferation. A secondary determinant element is required and we hypothesise it is the availability of fuel (which is unlimited in adipose tissue). If this is

the case it also implies another important and provocative concept that is the ability of ECs to sense the presence of lipids (fuel) in the surrounding environment and, consequently, to adapt their proliferative behaviour to the context in which those cells are located. Intriguingly, primary PTEN null ECs, independently from which tissue come from (lungs or adipose tissue) behave the same *in vitro*, where nutrient are equally available, thus further reinforcing our hypothesis.

Bearing in mind the aim of this thesis, and the observation that $PTEN^{i\Delta EC}$ mice show a tissue specific vascular phenotype, we conclude this could be a valuable model to study the impact of ECs on WAT remodelling. WAT is highly vascularised, to the extent that each adipocyte is surrounded by capillaries that provide oxygen and nutrients. One of the most remarkable features of WAT is its capacity to expand in a non-neoplastic manner. WAT expansion depends on angiogenesis, and conditions that impair angiogenesis hamper adipose tissue enlargement (Nishimura et al., 2007; Rupnick et al., 2002); impaired expandability leads to ectopic accumulation of lipids in liver and muscle, insulin resistance and metabolic disease. However, the underlying mechanisms by which angiogenesis modulate physiologic and pathologic adipose tissue expansion are largely unknown. Here we found that loss of PTEN in ECs results in adipose tissue vascular hyperplasia associated with reduced body weight gain and followed by progressive loss of fat mass. Taking into account that vascular hyperplasia always came first we hypothesised that, in this permissive environment (that is adipose tissue), PTEN loss in ECs determines a switch from a quiescent endothelium to a proliferative one, which is associated with an increased energy demand. Therefore, to guarantee a positive energy balance, ECs start to uptake and consume lipids, stored in white adipocytes, which obviously hamper fat mass accumulation.

WAT is considered a key regulator of whole body energy homeostasis; both excessive WAT expansion (obesity) and WAT regression or redistribution (lipodistrophy) contribute to metabolic disease (Capeau et al., 2005; Han and Lean, 2016). However, in our model loss of WAT was not associated with metabolic alteration suggesting that targeting ECs could be an effective strategy to reduce fat expansion without altering whole body energy homeostasis. The fact that mice lose fat mass but do not develop metabolic complication might be a consequence of a coordinated fat release and local lipid consumption which avoids fat redistribution in non-adipose tissue (like liver or muscle); in fact the onset of metabolic disease is more related to lipotoxicity rather than the amount of fat mass por se.

5.1.1 Enhanced adipose angiogenesis promotes lipids utilization

WAT is a dynamic organ that preserves the ability to expand and regress lifelong.WAT expansion can occur either by hyperplasia or hypertrophy; WAT hyperplasia rely on the existence of fat cell precursors able to differentiate into mature adipocytes. Recent publications placed adipocytes precursors within the vascular niche, even though the identity and origin of this cells is still controversial (Berry and Rodeheffer, 2013; Gupta et al., 2012b; Tang et al., 2008b; Tran et al., 2012b). Here we demonstrated that although loss of PTEN promotes ECs proliferation, which quite likely alter the microenvironment where adipocytes precursors are located, adipocytes differentiation was not compromised. In addition, we were able to reproduce the same vascular and adipose phenotype by inducing endothelial PTEN deletion in 8 weeks old mice (data not shown); this result further confirmed that the phenotype was not caused by the early post-natal PTEN deletion (which, potentially, could have been interfering with adipocytes differentiation).

Adipose tissue is traditionally divided into brown and white AT, that burn and store energy respectively. However, it has been recently discovered that certain depots, in particular inguinal WAT, when subjected to specific stimuli, could behave like BAT; a phenomenon defined browning of WAT. How browning is regulated is an intense topic of investigation as it has the potential to turn the energy balance from storage to expenditure, a strategy that could represent a new tool to combat obesity and metabolic syndrome (Lo and Sun, 2013). Browning of WAT has been associated with increased energy expenditure, reduced body weight gain and improved glucose tolerance in response to high fat diet (Cederberg et al., 2001; Seale et al., 2011). Furthermore, a phenotypic switch from white to beige fat was also described in the initial stages of cancer-associated cachexia, where it contributes to body weight loss and adipose tissue atrophy, typical of this wasting syndrome (Petruzzelli et al., 2014). Besides, it has been shown that improved adipose vasculature, due to VEGF over-expression in adipose tissue, increases the thermogenic capacity of inguinal-WAT (Elias et al., 2012). Therefore, we thought of primary importance to evaluate browning in our mouse model. Interestingly, we found that promoting angiogenesis by primary stimulating endothelial cell proliferation in a cell intrinsic manner, apparently, has a different impact on WAT: it leads to loss of fat mass without inducing browning of WAT. Hence, other mechanisms must be involved.

Lipogenesis (fatty acid synthesis and storage) and lipolysis (mobilization or hydrolysis of TGs) are considered the primary metabolic activities of WAT. Both process are regulated by the integration of endocrine and neural mechanisms, which cooperate in order to maintain a relatively constant body fat mass, under normal condition (Proença et al., 2014). It has been described that overexpression of ATGL (rate limiting enzyme for lipolisis), in a context of high fat diet, increments lipolisis which results in less body weight gain, decreased adipose tissue TGs content and reduced adipocytes size without ectopic lipid deposition (Ahmadian et al., 2009). In analogy with this data, even though in a context of normal diet, we found a comparable, but stronger, adipose phenotype in $PTEN^{i\Delta EC}$ mice (leaner mice, reduced fat mass, smaller adipocytes and absence of ectopic lipid deposition) which prompted us to hypothesised lipolisis could be involved. In fact mRNA sequencing, of gonadal-WAT of 12 weeks old mice, confirmed a lipid catabolism signature; then, validation by qPCR of several genes identified a β-oxidation profile. Mitochondrial β-oxidation is a cyclic process that breaks down a long acyl-CoA molecule into acetyl-CoA units that can enter the Krebs cycle or can be used to form ketone bodies. The most important checkpoint to control β-oxidation rates consist in the uptake of acyl-CoA mediated by CPT1. Here, we found that Etomoxir (specific CPT1 inhibitor) treatment in vivo efficiently reverts WAT vascular hyperplasia and, consequently, prevents loss of fat mass and adipocytes shrinkage. Hence, we hypothesized that, upon PTEN loss, ECs acquire an oxidative metabolism and rely on FFAs in order to proliferate and form new vessels. Given that the transcriptome analysis, among others, showed a significant up-regulation of PGC1β (broadly considered a master regulator of β-oxidation), we are now crossing $PGC1\beta^{flox/flox}$ mice (Enguix et al., 2013) with our model Pdgfb-iCre-ERT2-$PTEN^{Flox/Flox}$ to assess *in vivo*, with a genetic approach, the reversibility of the $PTEN^{i\Delta EC}$ phenotype. We expect that loss of endothelial PGC1β should prevent vascular hyperplasia and fat mass loss by preventing ECs from acquiring an oxidative metabolism.

In contrast to what we found at 12 weeks of age, at early time point, when vascular hyperplasia was already present but no difference in body weight was detectable, we did not notice a lipid catabolic profile. This data could be explained by the fact that, at 5 weeks of age, the ratio between ECs and adipocytes is lower which makes difficult to detect a ECs specific change in gene expression. To solve this issue we crossed the RiboTag model with our Pdgfb-iCreER^{T2}- $PTEN^{flox/flox}$ mice; this allow us to efficiently

and selectively isolate the translatome of adipose ECs, that will be then analysed by quantitative PCR (for detailed information regarding the RiboTag model see the reference (Sanz et al., 2009)). Unfortunately this is an ongoing work, thus we haven't analysed the sample yet. In addition, we found increased mitochondria respiration in gonadal-WAT of 12 weeks old $PTEN^{i\Delta EC}$ mice which suggested that FFA mobilised from adipocytes are consumed locally and, at least partially, feed into the respiratory chain to generate ATP. Remarkably, the rate of mitochondrial respiration positively correlates with the severity of the vascular phenotype (evaluated by macroscopic observation). All together these results suggested that in our model, enhanced angiogenesis promotes lipid catabolism (particularly FFA oxidation) and eventually exhausts fat depots.

5.1.2 PTEN null ECs utilize FFA to proliferate

PTEN is a tumour suppressor gene mutated in many human sporadic cancers and in hereditary cancer syndromes such as Cowden disease. In mice, PTEN null mutation results in early embryonic lethality; therefore, to investigate the physiological functions of PTEN in viable mice, several groups have utilized the Cre-loxP system to generate several tissue-specific PTEN mutations. From these studies came out that loss of PTEN promotes hyper-proliferation and increased activation of Akt and Erk signalling pathways in the targeted cells. The abnormal function of the tissue-specific PTEN null cells resulted in a variety of consequences in the targeted tissues, including hyperplasia and carcinoma development (Suzuki et al., 2008). Consistent with these results we observed that, in vitro, PTEN loss in ECs resulted in enhanced Akt activation and significantly increased cells proliferation. However, quite surprisingly, ECs hyperproliferation was not associated with any vascular anomalies (VAs). VAs represents a broad spectrum of lesions which are commonly subgrouped into vascular tumours and vascular malformations. Vascular tumours include benign hemangioma (the most common one), Kaposiform hemangioendothelioma and angiosarcoma (AS) which is the most aggressive one. Conversely to what has been described for other tissues, loss of PTEN in ECs did not lead to malignant endothelial tumours. This result is not completely surprisingly, since it has been already described that, in contrast with other sarcomas with complex genomics, PTEN is neither deleted nor mutated in AS (Italiano et al., 2012). Vascular malformations are composed of collections of abnormal vessels, with simple lesions having a predominant vessel type, that can be classified into

capillary malformations, venous malformations (VMs), lymphatic malformations (LMs) and arteriovenous malformations (AVMs). Mutations in the PIK3CA (the gene encoding for p110α), especially the activating mutation $PIK3CA^{H1047R}$, have been observed in one of four human VMs, suggesting a causative role of PIK3CA in this type of vascular malformation (Castillo et al., 2016a). Accordingly, inactivation of the PI3K pathway, either by p110α or mTOR inhibition, leads to regression of PIK3CA-mutant VMs in mice (Castel et al., 2016; Castillo et al., 2016b). Intriguingly, patients affected by Bannayan–Riley–Ruvalcaba syndrome and Cowden syndrome, two disorders caused by germline inactivating mutation of PTEN, also display a spectrum of VAs, with the prevalence of AVMs and VMs (Tan et al., 2007). All together, these data indicate that activating-mutations in the PIK3CA and inactivating-mutations of the principal PI3K inhibitor (PTEN), are both associated with vascular malformations. Based on this knowledge we would have expected $PTEN^{i\Delta EC}$ mice to develop vascular lesions but this is not the case. At least two reasons may explain this result: i) first of all in our model PTEN deletion is induced after birth, which is obviously quite different from having germline mutations. It is possible that in order to develop vascular malformations, PTEN need to be lost or mutated earlier during embryo development. ii) Second, it is conceivable that mutations in PIK3CA determine a more robust activation of the PI3K pathway compared to PTEN loss, and consequently a stronger vascular phenotype.

In healthy adults, ECs remain quiescent for years but, if necessary, they can rapidly switch to a proliferative state. Despite being directly exposed to oxygen, transported in the blood stream, ECs principally rely on glucose to produce ATP. In fact, ECs were found to be “glucose addicted,” generating up to 85% of their ATP via glycolysis (De Bock et al., 2013a, 2013b). However, recent findings suggested that FFA metabolism in ECs is more important than originally expected. Indeed, it has been found that endothelial CPT1a loss causes vascular defects due to impaired ECs proliferation without defects in cell migration. Moreover it has been suggested that FAO in ECs does not contribute to energy production but it provides carbons for de novo nucleotide synthesis, essential for DNA replication (Schoors et al., 2015). Many evidences currently indicate that metabolism influence several aspects of angiogenesis, affecting proliferation and growth, signalling, and gene expression of ECs. However, our understanding of EC metabolism is incomplete, and many questions are still open. Here we identify PTEN as potential regulator of ECs metabolism. We found that loss of

PTEN in ECs is associated with increased expression of key genes regulating FFA uptake, transport and oxidation; in particular, we observed a notable increment of CD36 expression. CD36 is a glycoprotein that binds long-chain fatty acids and facilitates their transport into cells. Recently it has been suggested a direct correlation between PI3K activity and CD36 expression and function in macrophages (Michael et al., 2015). This study showed that treatment of human macrophages with the pan PI3K inhibitor LY294002 or isoform specific PI3K inhibitors, attenuated receptor-mediated uptake of modified LDL and macropinocytosis and reduced CD36 and scavenger receptors-A expression (the molecular mechanism was not investigated). This study, together with our results, prompts us to think that CD36 expression in ECs might be regulated by PI3K as well, and CD36 up-regulation could be a key initial event that converts ECs in "lipids consuming" cells. We are currently testing whether a pan PI3K inhibitor or p110α specific inhibitor, affect CD36 expression in primary adipose ECs *in vitro*; if this is the case it would be interesting to see whether ECs proliferation is dependent on CD36 mediated lipids uptake.

Remarkably, in agreement with the increased expression of β-oxidation-related genes, we observed a significant increase in β-oxidation rate, thus indicating that loss of PTEN determines a metabolic switch toward a highly oxidative metabolism that in turn allows ECs to switch from a quiescent to an active proliferative state. Moreover, in line with these results, we found enhanced ACC phosphorylation; ACC is the main CPT1 inhibitor whose activity is inhibited by phosphorylation. The major kinase responsible for ACC phosphorylation and inactivation is AMPK, which is considered a master sensor for energy level in the cell, (Hardie and Pan, 2002). When activated by ATP depletion, AMPK switches off ATP-consuming processes, while switching on catabolic pathways that generate ATP. Even though we couldn't find a statistically significant difference in pAMPK protein level, we do observe a tendency of increased pAMPK in PTEN null ECs that might contribute to promote β-oxidation. Despite PTEN null ECs displayed enhanced oxidative metabolism, we haven't observed changes in glucose consumption and lactate production. Although further studies need to be done to better characterise glucose metabolism, based on our results we hypothesized that PTEN null ECs are high energy demanding so that any metabolic pathway that could give ATP and/or biomass is accelerated or at least not diminished.

Here, we demonstrated that PTEN null ECs uptake more lipids than wild type cells, and they also breakdown lipids thus generating FFAs, but what we still don't know is where these FFAs are going. Within cells, FFAs can have many fates including: i) being directed to the Endoplasmic Reticulum (ER) to build up membrane or signalling lipids, ii) being stored in lipids droplets, iii) feed into the TCA cycle to generate ATP or iiii) provide carbons to generate biomass (for example nucleotides). It has been recently described that carbons derived from FFAs oxidation in ECs enter the TCA cycle and are used for de novo synthesis of nucleotides (Schoors et al., 2015), required for ECs to proliferate during sprouting angiogenesis. In analogy we can hypothesise that since PTEN null ECs are rapidly proliferating, FFAs might be essential to replenish the nucleotide pool. However, it is also true that proliferating cells needs to synthesised lipids to build up membrane, thus it is also possible that FFAs are mainly diverted to the ER. Additionally, activated ECs need more energy than quiescent ECs, so giving that we did not observed increased glucose consumption and lactate production it is possible that FFAs are also utilized for ATP production. Indeed, oxidative metabolism is more efficient to generate ATP than anaerobic glycolysis, even though it is slower. In conclusion, more experiments need to be done to determine which is the destiny of FFAs once inside the cells, and to understand for which cellular process (proliferation, migration...) they are indispensable.

Other important point we need to determine is the molecular link between loss of PTEN and increased oxidative metabolism. It has been recently reported that the forkhead box O (FOXO) transcription factor FOXO1 is an essential regulator of vascular growth that couples metabolic and proliferative activities in ECs. Specifically, it has been shown that FOXO1 deletion promotes ECs proliferation thereby causing vascular hyperplasia and vessel enlargement. Conversely, FOXO1 forced expression restricts vascular expansion and leads to vessel thinning and hypobranching. Importantly, it has been proposed that FOXO1 contributes to preserve ECs quiescence by decelerating cell metabolism (both glycolysis and oxidative respiration) (Wilhelm et al., 2016). It is well established that FOXOs transcription factors are effectors of the PI3K/AKT pathway that links growth and metabolism (Vander Heiden et al., 2009; Ward and Thompson, 2012). The PI3K signalling inhibits FOXOs through AKT-mediated phosphorylation which leads to their nuclear exclusion (Salih and Brunet, 2008). Considering that in PTEN null ECs the PI3K-Akt pathway is constitutive active we expect FOXO1 to be

inactivated. Constitutive inhibition of FOXO1 could, at least partially, explain the observed metabolic changes. In addition, as mentioned before, CD36 upregulation might be, as well, a direct consequence of PI3K unrestrained activity, and a key molecules responsible for converting glycolytic quiescent cells into lipids consuming active cells.

5.2 Pathological WAT remodelling: obesity

Most of the organs and tissues growth occurs during development, and their final size remains relatively constant through adulthood. In contrast WAT is unique in that it can expand many-fold, in response to excess energy intake, and constitute up to 40% of total body composition in obese subjects. Nowadays obesity is a primary public health problem in both developed and developing countries that have been adopted a Western lifestyle. Standard intervention (excluded bariatric surgery) are often insufficient to permanently normalize body weight and to prevent metabolic complication, thus novel therapy are urgently needed. Considering that WAT growth is coordinated with, and requires, angiogenesis it has been recently proposed to hamper excessive WAT expansion using angiogenesis inhibitors such as TNP-470, endostatin or VEGFR2-specific inhibitors (Bråkenhielm et al., 2004; Rupnick et al., 2002; Tam et al., 2009). Those studies have shown that angiogenesis inhibitors successfully prevent the development of obesity in genetic mouse models and studies based on HF diet induced obesity. Body weight loss was mainly due to reduced food intake and/or an increased metabolic rate, however the mechanism by which limiting vascular supply in fat affects these parameters has not been explained. The initial enthusiasm for treatments that hamper WAT growth through angiogenesis inhibitors was then limited by important doubts concerning the safety of this approach. First of all it is well known that metabolic diseases are mostly caused by ectopic lipid deposition rather than excessive expansion of WAT, therefore strategies that hamper WAT expansion are not applicable for long time treatment as lipids will be directed somewhere else (Corvera and Gealekman, 2014). Second, other side effects of angiogenesis inhibition, that are not metabolically related, might include an impaired process of wound healing and tissue repair, both of which are angiogenesis dependent. This is particularly important in patients with type 2 diabetes, who often develops chronic foot ulcers that in some cases might lead to limb amputation (Alexiadou and Doupis, 2012). Considering that pathological WAT expansion is always associated with suboptimal angiogenesis which in turn cause

hypoxia, adipocytes death and inflammation (all hallmark of obesity); it seems more reasonable that improved rather than reduced angiogenesis could be an effective novel approach to deal with obesity. Recent publications took advantage of the most common proangiogenic signalling pathway, the VEGFA-VEGFR, to promote vessels growth in BAT and/or WAT in a cell extrinsic manner. These studies showed that improved angiogenesis activate the thermogenic program in brown and white adipose tissue and protect mice from obesity and associated metabolic complications (Elias et al., 2012; Sun et al., 2012, 2014). In analogy it has been reported that VEGFB gene transduction inhibits obesity-associated inflammation and improves metabolic health without alteration in body weight or ectopic lipid deposition (Robciuc et al., 2016). All together these results strongly support the hypothesis that in the context of obesity having more vessels is beneficial. However little is known about the intrinsic property of ECs that trigger this beneficial effect. To shed a light on this issue we challenged $PTEN^{i\Delta EC}$ and control mice with 45% fat enriched diet for 8 weeks. As mentioned before this mouse model allow us to induce angiogenesis in a cell intrinsic manner, which make our study different from the ones based on the pro-angiogenic effect of VEGF. In agreement with the above mentioned studies, we found that active ECs (PTEN null ECs) efficiently vascularised the expanding WAT which results in healthier WAT growth; in addition, we showed that these oxidative ECs limits fat mass expansion and prevents adipocytes hypertrophy. Conversely to what have been described with the use of angiogenesis inhibitors, this reduction in fat mass expansion did not result in ectopic lipid deposition in liver or muscle (the principal tissues where lipids tend to accumulate), and was associated with an improved metabolic profile. Thus, we conclude that ECs are not simply spectators but active modulator of WAT remodelling; specifically ECs intrinsic properties determine WAT expandability in both physiological and pathological conditions. Here, we suggest ECs metabolism to be a key element determining how those cells will respond when challenged with obesogenic stimuli. Besides, we propose two novel concepts: i) "unfit ECs" characterised by their inability to adapt and respond to nutritional changes, and ii) "fit ECs" characterised by their intrinsic capability to sense lipids and modify their behaviour to fit with fuel availability. We suggest that fit ECs when exposed to obesogenic microenvironment, preserve the ability to efficiently expand the adipose tissue vascular network, thereby preserving a healthy WAT. Conversely, unfit ECs, in the same microenvironment, are unable to sustain an optimal coordination between vessels growth and adipose tissue expansion which results in

unhealthy WAT (Figure 5.1). Moreover, we claim that fit ECs not only guarantee an adequate vascularisation, but they also exert an anti-obesity activity by consuming lipids. Therefore we suggest that strategies directed to implement ECs fitness represent a valuable and innovative tool to prevent or revert aberrant WAT expansion in obesity.

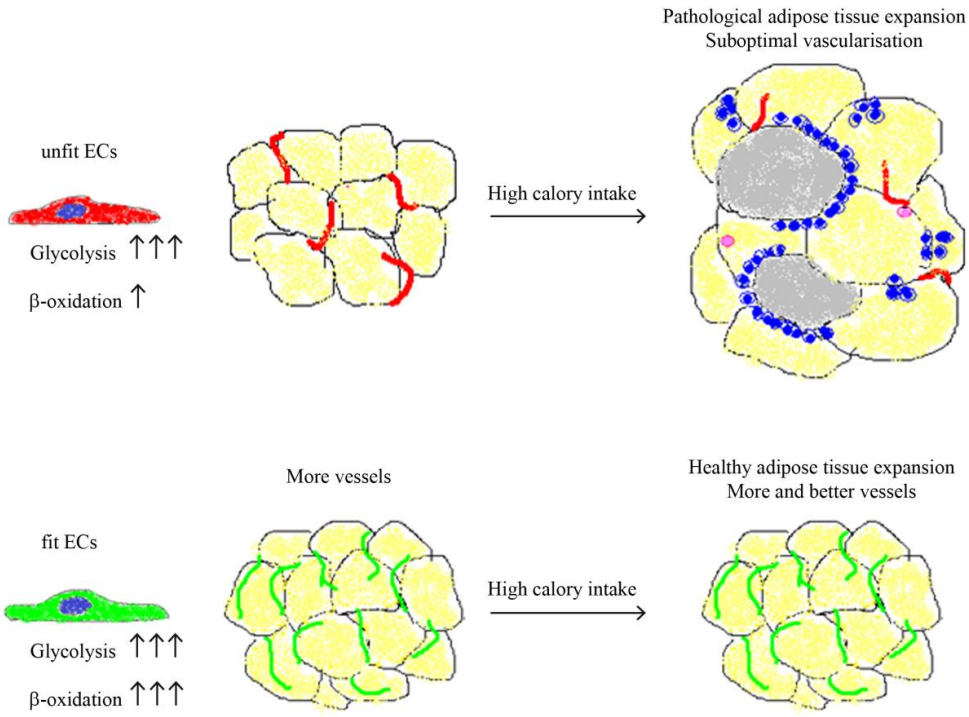

Figure 5.1: Schematic diagram representing the concept of fit and unfit ECs.

6. Conclusions

1. Post-natal deletion of PTEN in ECs causes an adipose tissue specific vascular hyperplasia associated with increased ECs proliferation.

2. Loss of quiescence in ECs leads to a progressive reduction of WAT mass, especially gonadal-WAT, without obvious alteration in any other tissue.

3. Loss of PTEN in ECs has a dramatic impact on WAT morphology: the first visible defect is vascular hyperplasia, followed by progressive adipocytes shrinkage.

4. Loss of fat mass is not caused by reduced food intake and does not impair systemic metabolism.

5. Loss of fat mass is not caused by defects in adipocytes differentiation.

6. Loss of fat mass is not caused by "browining" of WAT.

7. Loss of gonadal-WAT mass is driven by enhanced β-oxidation and increased mitochondrial respiration.

8. In vivo inhibition of β-oxidation is sufficient to revert vascular hyperplasia, thus suggesting that PTEN null ECs depend on FFAs to proliferate, and it prevents loss of fat mass.

9. PTEN negatively regulates ECs proliferation.

10. PTEN, directly or indirectly, modulates ECs metabolism; so that when PTEN is lost ECs adopt a more oxidative metabolism.

11. More active ECs preserve the ability to proliferate and generate functional vessels even when exposed to an obesogenic environment.

12. More functional ECs prevent unhealthy WAT expansion and consequently the onset of obesity related comorbidity.

7. Bibliography

Adams, R.H., and Alitalo, K. (2007). Molecular regulation of angiogenesis and lymphangiogenesis. Nat. Rev. Mol. Cell Biol. *8*, 464–478.

Ahmadian, M., Duncan, R.E., Jaworski, K., Sarkadi-Nagy, E., and Sul, H.S. (2007). Triacylglycerol metabolism in adipose tissue. Future Lipidol. *2*, 229–237.

Ahmadian, M., Duncan, R.E., Varady, K.A., Frasson, D., Hellerstein, M.K., Birkenfeld, A.L., Samuel, V.T., Shulman, G.I., Wang, Y., Kang, C., et al. (2009). Adipose Overexpression of Desnutrin Promotes Fatty Acid Use and Attenuates Diet-Induced Obesity. Diabetes *58*, 855–866.

Alexiadou, K., and Doupis, J. (2012). Management of Diabetic Foot Ulcers. Diabetes Ther. *3*.

Alimonti, A., Carracedo, A., Clohessy, J.G., Trotman, L.C., Nardella, C., Egia, A., Salmena, L., Sampieri, K., Haveman, W.J., Brogi, E., et al. (2010). Subtle variations in Pten dose determine cancer susceptibility. Nat. Genet. *42*, 454–458.

Ameer, F., Scandiuzzi, L., Hasnain, S., Kalbacher, H., and Zaidi, N. (2014). De novo lipogenesis in health and disease. Metab. - Clin. Exp. *63*, 895–902.

Antohe, F., Popov, D., Rădulescu, L., Simionescu, N., Börchers, T., Spener, F., and Simionescu, M. (1998). Heart microvessels and aortic endothelial cells express the 15 kDa heart-type fatty acid-binding proteins. Eur. J. Cell Biol. *76*, 102–109.

Augustin, H.G., Young Koh, G., Thurston, G., and Alitalo, K. (2009). Control of vascular morphogenesis and homeostasis through the angiopoietin–Tie system. Nat. Rev. Mol. Cell Biol. *10*, 165–177.

Ayala, J.E., Samuel, V.T., Morton, G.J., Obici, S., Croniger, C.M., Shulman, G.I., Wasserman, D.H., and McGuinness, O.P. (2010). Standard operating procedures for describing and performing metabolic tests of glucose homeostasis in mice. Dis. Model. Mech. *3*, 525–534.

Banerjee, R.R., Rangwala, S.M., Shapiro, J.S., Rich, A.S., Rhoades, B., Qi, Y., Wang, J., Rajala, M.W., Pocai, A., Scherer, P.E., et al. (2004). Regulation of Fasted Blood Glucose by Resistin. Science *303*, 1195–1198.

Bartlett, K., and Eaton, S. (2004). Mitochondrial beta-oxidation. Eur. J. Biochem. *271*, 462–469.

Bazzoni, G., and Dejana, E. (2004). Endothelial Cell-to-Cell Junctions: Molecular Organization and Role in Vascular Homeostasis. Physiol. Rev. *84*, 869–901.

Beenken, A., and Mohammadi, M. (2009). The FGF family: biology, pathophysiology and therapy. Nat. Rev. Drug Discov. *8*, 235–253.

Benedito, R., Rocha, S.F., Woeste, M., Zamykal, M., Radtke, F., Casanovas, O., Duarte, A., Pytowski, B., and Adams, R.H. (2012). Notch-dependent VEGFR3 upregulation allows angiogenesis without VEGF-VEGFR2 signalling. Nature *484*, 110–114.

Bergers, G., and Song, S. (2005). The role of pericytes in blood-vessel formation and maintenance. Neuro-Oncol. *7*, 452–464.

Bermúdez Brito, M., Goulielmaki, E., and Papakonstanti, E.A. (2015). Focus on PTEN Regulation. Front. Oncol. *5*.

Berry, R., and Rodeheffer, M.S. (2013). Characterization of the adipocyte cellular lineage in vivo. Nat. Cell Biol. *15*, 302–308.

Bhaskar, P.T., and Hay, N. (2007). The two TORCs and Akt. Dev. Cell *12*, 487–502.

Birsoy, K., Berry, R., Wang, T., Ceyhan, O., Tavazoie, S., Friedman, J.M., and Rodeheffer, M.S. (2011). Analysis of gene networks in white adipose tissue development reveals a role for ETS2 in adipogenesis. Dev. Camb. Engl. *138*, 4709–4719.

Bisht, M., Dhasmana, D.C., and Bist, S.S. (2010). Angiogenesis: Future of pharmacological modulation. Indian J. Pharmacol. *42*, 2–8.

Blanco, R., and Gerhardt, H. (2013). VEGF and Notch in Tip and Stalk Cell Selection. Cold Spring Harb. Perspect. Med. *3*.

Blouin, A., Bolender, R.P., and Weibel, E.R. (1977). Distribution of organelles and membranes between hepatocytes and nonhepatocytes in the rat liver parenchyma. A stereological study. J. Cell Biol. *72*, 441–455.

Blüher, S., and Mantzoros, C.S. (2009). Leptin in humans: lessons from translational research. Am. J. Clin. Nutr. *89*, 991S–997S.

Bononi, A., Bonora, M., Marchi, S., Missiroli, S., Poletti, F., Giorgi, C., Pandolfi, P.P., and Pinton, P. (2013). Identification of PTEN at the ER and MAMs and its regulation of Ca2+ signaling and apoptosis in a protein phosphatase-dependent manner. Cell Death Differ. *20*, 1631–1643.

Borgström, B. (1988). Mode of action of tetrahydrolipstatin: a derivative of the naturally occurring lipase inhibitor lipstatin. Biochim. Biophys. Acta BBA - Lipids Lipid Metab. *962*, 308–316.

Bråkenhielm, E., Cao, R., Gao, B., Angelin, B., Cannon, B., Parini, P., and Cao, Y. (2004). Angiogenesis Inhibitor, TNP-470, Prevents Diet-Induced and Genetic Obesity in Mice. Circ. Res. *94*, 1579–1588.

Brasaemle, D.L. (2007). Thematic review series: Adipocyte Biology. The perilipin family of structural lipid droplet proteins: stabilization of lipid droplets and control of lipolysis. J. Lipid Res. *48*, 2547–2559.

Campbell, S.E., Tandon, N.N., Woldegiorgis, G., Luiken, J.J.F.P., Glatz, J.F.C., and Bonen, A. (2004). A Novel Function for Fatty Acid Translocase (FAT)/CD36 INVOLVEMENT IN LONG CHAIN FATTY ACID TRANSFER INTO THE MITOCHONDRIA. J. Biol. Chem. *279*, 36235–36241.

Cannon, B., and Nedergaard, J. (2012). Cell biology: Neither brown nor white. Nature *488*, 286–287.

Cantó, C., and Garcia-Roves, P.M. (2015). High-Resolution Respirometry for Mitochondrial Characterization of Ex Vivo Mouse Tissues. Curr. Protoc. Mouse Biol. *5*, 135–153.

Cao, Y. (2007). Angiogenesis modulates adipogenesis and obesity. J. Clin. Invest. *117*, 2362–2368.

Capeau, J., Magré, J., Lascols, O., Caron, M., Béréziat, V., Vigouroux, C., and Bastard, J.P. (2005). Diseases of adipose tissue: genetic and acquired lipodystrophies. Biochem. Soc. Trans. *33*, 1073–1077.

Carmeliet, P. (2000). Mechanisms of angiogenesis and arteriogenesis. Nat. Med. *6*, 389–395.

Carmeliet, P. (2003). Angiogenesis in health and disease. Nat. Med. *9*, 653–660.

Carmeliet, P., and Jain, R.K. (2011). Molecular mechanisms and clinical applications of angiogenesis. Nature *473*, 298–307.

Carmeliet, P., Ferreira, V., Breier, G., Pollefeyt, S., Kieckens, L., Gertsenstein, M., Fahrig, M., Vandenhoeck, A., Harpal, K., Eberhardt, C., et al. (1996). Abnormal blood vessel development and lethality in embryos lacking a single VEGF allele. Nature *380*, 435–439.

Carracedo, A., Alimonti, A., and Pandolfi, P.P. (2011). PTEN level in tumor suppression: How much is too little? Cancer Res. *71*, 629–633.

Castel, P., Carmona, F.J., Grego-Bessa, J., Berger, M.F., Viale, A., Anderson, K.V., Bague, S., Scaltriti, M., Antonescu, C.R., Baselga, E., et al. (2016). Somatic PIK3CA mutations as a driver of sporadic venous malformations. Sci. Transl. Med. *8*, 332ra42.

Castillo, S.D., Vanhaesebroeck, B., and Sebire, N.J. (2016a). Phosphoinositide 3-kinase: a new kid on the block in vascular anomalies. J. Pathol. *240*, 387–396.

Castillo, S.D., Tzouanacou, E., Zaw-Thin, M., Berenjeno, I.M., Parker, V.E.R., Chivite, I., Milà-Guasch, M., Pearce, W., Solomon, I., Angulo-Urarte, A., et al. (2016b). Somatic activating mutations in Pik3ca cause sporadic venous malformations in mice and humans. Sci. Transl. Med. *8*, 332ra43.

Cederberg, A., Grønning, L.M., Ahrén, B., Taskén, K., Carlsson, P., and Enerbäck, S. (2001). FOXC2 Is a Winged Helix Gene that Counteracts Obesity, Hypertriglyceridemia, and Diet-Induced Insulin Resistance. Cell *106*, 563–573.

Chappell, W.H., Green, T.D., Spengeman, J.D., McCubrey, J.A., Akula, S.M., and Bertrand, F.E. (2005). Increased Protein Expression of the PTEN Tumor Suppressor in the Presence of Constitutively Active Notch-1. Cell Cycle *4*, 1389–1395.

Chen, Y., Siegel, F., Kipschull, S., Haas, B., Fröhlich, H., Meister, G., and Pfeifer, A. (2013). miR-155 regulates differentiation of brown and beige adipocytes via a bistable circuit. Nat. Commun. *4*, 1769.

Choe, S.S., Huh, J.Y., Hwang, I.J., Kim, J.I., and Kim, J.B. (2016). Adipose Tissue Remodeling: Its Role in Energy Metabolism and Metabolic Disorders. Front. Endocrinol. *7*.

Christiaens, V., and Lijnen, H.R. (2010). Angiogenesis and development of adipose tissue. Mol. Cell. Endocrinol. *318*, 2–9.

Chung, A.S., and Ferrara, N. (2011). Developmental and pathological angiogenesis. Annu. Rev. Cell Dev. Biol. *27*, 563–584.

Chung, J.-H., Ginn-Pease, M.E., and Eng, C. (2005). Phosphatase and tensin homologue deleted on chromosome 10 (PTEN) has nuclear localization signal-like sequences for nuclear import mediated by major vault protein. Cancer Res. *65*, 4108–4116.

Cinti, S. (2009). Transdifferentiation properties of adipocytes in the adipose organ. Am. J. Physiol. - Endocrinol. Metab. *297*, E977–E986.

Cinti, S. (2011). Between brown and white: Novel aspects of adipocyte differentiation. Ann. Med. *43*, 104–115.

Cinti, S. (2012). The adipose organ at a glance. Dis. Model. Mech. *5*, 588–594.

Cinti, S., Cigolini, M., Bosello, O., and Björntorp, P. (1984). A morphological study of the adipocyte precursor. J. Submicrosc. Cytol. *16*, 243–251.

Cinti, S., Mitchell, G., Barbatelli, G., Murano, I., Ceresi, E., Faloia, E., Wang, S., Fortier, M., Greenberg, A.S., and Obin, M.S. (2005). Adipocyte death defines macrophage localization and function in adipose tissue of obese mice and humans. J. Lipid Res. *46*, 2347–2355.

Claxton, S., Kostourou, V., Jadeja, S., Chambon, P., Hodivala-Dilke, K., and Fruttiger, M. (2008). Efficient, inducible Cre-recombinase activation in vascular endothelium. Genesis *46*, 74–80.

Corvera, S., and Gealekman, O. (2014). Adipose Tissue Angiogenesis: Impact on Obesity and Type-2 Diabetes. Biochim. Biophys. Acta *1842*, 463–472.

Crandall, D.L., Hausman, G.J., and Kral, J.G. (1997). A Review of the Microcirculation of Adipose Tissue: Anatomic, Metabolic, and Angiogenic Perspectives. Microcirculation *4*, 211–232.

Cristofano, A.D., and Pandolfi, P.P. (2000). The Multiple Roles of PTEN in Tumor Suppression. Cell *100*, 387–390.

Cunningham, S.A., Waxham, M.N., Arrate, P.M., and Brock, T.A. (1995). Interaction of the Flt-1 Tyrosine Kinase Receptor with the p85 Subunit of Phosphatidylinositol 3-Kinase MAPPING OF A NOVEL SITE INVOLVED IN BINDING. J. Biol. Chem. *270*, 20254–20257.

Cypess, A.M., Lehman, S., Williams, G., Tal, I., Rodman, D., Goldfine, A.B., Kuo, F.C., Palmer, E.L., Tseng, Y.-H., Doria, A., et al. (2009). Identification and Importance of Brown Adipose Tissue in Adult Humans. N. Engl. J. Med. *360*, 1509–1517.

Cypess, A.M., White, A.P., Vernochet, C., Schulz, T.J., Xue, R., Sass, C.A., Huang, T.L., Roberts-Toler, C., Weiner, L.S., Sze, C., et al. (2013). Anatomical localization, gene expression profiling and functional characterization of adult human neck brown fat. Nat. Med. *19*, 635–639.

Czyzyk, T.A., Romero-Picó, A., Pintar, J., McKinzie, J.H., Tschöp, M.H., Statnick, M.A., and Nogueiras, R. (2012). Mice lacking δ-opioid receptors resist the development of diet-induced obesity. FASEB J. *26*, 3483–3492.

Dagher, Z., Ruderman, N., Tornheim, K., and Ido, Y. (1999). The effect of AMP-activated protein kinase and its activator AICAR on the metabolism of human umbilical vein endothelial cells. Biochem. Biophys. Res. Commun. *265*, 112–115.

Dagher, Z., Ruderman, N., Tornheim, K., and Ido, Y. (2001). Acute Regulation of Fatty Acid Oxidation and AMP-Activated Protein Kinase in Human Umbilical Vein Endothelial Cells. Circ. Res. *88*, 1276–1282.

Davidson, S.M. (2010). Endothelial mitochondria and heart disease. Cardiovasc. Res. *88*, 58–66.

Davidson, S.M., and Duchen, M.R. (2007). Endothelial Mitochondria. Circ. Res. *100*, 1128–1141.

Dayanir, V., Meyer, R.D., Lashkari, K., and Rahimi, N. (2001). Identification of Tyrosine Residues in Vascular Endothelial Growth Factor Receptor-2/FLK-1 Involved in Activation of Phosphatidylinositol 3-Kinase and Cell Proliferation. J. Biol. Chem. *276*, 17686–17692.

DeBerardinis, R.J., Lum, J.J., and Thompson, C.B. (2006). Phosphatidylinositol 3-Kinase-dependent Modulation of Carnitine Palmitoyltransferase 1A Expression Regulates Lipid Metabolism during Hematopoietic Cell Growth. J. Biol. Chem. *281*, 37372–37380.

De Bock, K., Georgiadou, M., and Carmeliet, P. (2013a). Role of Endothelial Cell Metabolism in Vessel Sprouting. Cell Metab. *18*, 634–647.

De Bock, K., Georgiadou, M., Schoors, S., Kuchnio, A., Wong, B.W., Cantelmo, A.R., Quaegebeur, A., Ghesquière, B., Cauwenberghs, S., Eelen, G., et al. (2013b). Role of PFKFB3-Driven Glycolysis in Vessel Sprouting. Cell *154*, 651–663.

Deng, Y., and Scherer, P.E. (2010). Adipokines as novel biomarkers and regulators of the metabolic syndrome. Ann. N. Y. Acad. Sci. *1212*, E1–E19.

Denning, G., Jean-Joseph, B., Prince, C., Durden, D.L., and Vogt, P.K. (2007). A short N-terminal sequence of PTEN controls cytoplasmic localization and is required for suppression of cell growth. Oncogene *26*, 3930–3940.

Denzel, M.S., Scimia, M.-C., Zumstein, P.M., Walsh, K., Ruiz-Lozano, P., and Ranscht, B. (2010). T-cadherin is critical for adiponectin-mediated cardioprotection in mice. J. Clin. Invest. *120*, 4342–4352.

Ding, L., Chen, S., Liu, P., Pan, Y., Zhong, J., Regan, K.M., Wang, L., Yu, C., Rizzardi, A., Cheng, L., et al. (2014). CBP loss cooperates with PTEN haploinsufficiency to drive prostate cancer: implications for epigenetic therapy. Cancer Res. *74*, 2050–2061.

Dranka, B.P., Hill, B.G., and Darley-Usmar, V.M. (2010). Mitochondrial reserve capacity in endothelial cells: The impact of nitric oxide and reactive oxygen species. Free Radic. Biol. Med. *48*, 905–914.

Dudek, J., Rehling, P., and van der Laan, M. (2013). Mitochondrial protein import: Common principles and physiological networks. Biochim. Biophys. Acta BBA - Mol. Cell Res. *1833*, 274–285.

Duncan, R.E., Ahmadian, M., Jaworski, K., Sarkadi-Nagy, E., and Sul, H.S. (2007). Regulation of Lipolysis in Adipocytes. Annu. Rev. Nutr. *27*, 79–101.

Eelen, G., de Zeeuw, P., Simons, M., and Carmeliet, P. (2015). Endothelial cell metabolism in normal and diseased vasculature. Circ. Res. *116*, 1231–1244.

Eilken, H.M., and Adams, R.H. (2010). Dynamics of endothelial cell behavior in sprouting angiogenesis. Curr. Opin. Cell Biol. *22*, 617–625.

Elias, I., Franckhauser, S., Ferré, T., Vilà, L., Tafuro, S., Muñoz, S., Roca, C., Ramos, D., Pujol, A., Riu, E., et al. (2012). Adipose Tissue Overexpression of Vascular Endothelial Growth Factor Protects Against Diet-Induced Obesity and Insulin Resistance. Diabetes *61*, 1801–1813.

Elmasri, H., Karaaslan, C., Teper, Y., Ghelfi, E., Weng, M., Ince, T.A., Kozakewich, H., Bischoff, J., and Cataltepe, S. (2009). Fatty acid binding protein 4 is a target of VEGF and a regulator of cell proliferation in endothelial cells. FASEB J. *23*, 3865–3873.

Enguix, N., Pardo, R., González, A., López, V.M., Simó, R., Kralli, A., and Villena, J.A. (2013). Mice lacking PGC-1β in adipose tissues reveal a dissociation between mitochondrial dysfunction and insulin resistance. Mol. Metab. *2*, 215–226.

F, R., and M, D. (2013). Role of Adipose Tissue in Metabolic System Disorders- Adipose Tissue is the Initiator of Metabolic Diseases. J. Diabetes Metab. 1–8.

Fantin, A., Vieira, J.M., Gestri, G., Denti, L., Schwarz, Q., Prykhozhij, S., Peri, F., Wilson, S.W., and Ruhrberg, C. (2010). Tissue macrophages act as cellular chaperones for vascular anastomosis downstream of VEGF-mediated endothelial tip cell induction. Blood *116*, 829–840.

Febbraio, M., Hajjar, D.P., and Silverstein, R.L. (2001). CD36: a class B scavenger receptor involved in angiogenesis, atherosclerosis, inflammation, and lipid metabolism. J. Clin. Invest. *108*, 785–791.

Ferrara, N., Carver-Moore, K., Chen, H., Dowd, M., Lu, L., O'Shea, K.S., Powell-Braxton, L., Hillan, K.J., and Moore, M.W. (1996). Heterozygous embryonic lethality induced by targeted inactivation of the VEGF gene. Nature *380*, 439–442.

Ferrara, N., Gerber, H.-P., and LeCouter, J. (2003). The biology of VEGF and its receptors. Nat. Med. *9*, 669–676.

Finck, B.N., and Kelly, D.P. (2006). PGC-1 coactivators: inducible regulators of energy metabolism in health and disease. J. Clin. Invest. *116*, 615–622.

Fischer, J., Lefèvre, C., Morava, E., Mussini, J.-M., Laforêt, P., Negre-Salvayre, A., Lathrop, M., and Salvayre, R. (2007). The gene encoding adipose triglyceride lipase (PNPLA2) is mutated in neutral lipid storage disease with myopathy. Nat. Genet. *39*, 28–30.

Fisslthaler, B., and Fleming, I. (2009). Activation and Signaling by the AMP-Activated Protein Kinase in Endothelial Cells. Circ. Res. *105*, 114–127.

Frontini, A., and Cinti, S. (2010). Distribution and Development of Brown Adipocytes in the Murine and Human Adipose Organ. Cell Metab. *11*, 253–256.

Fujisaka, S., Usui, I., Bukhari, A., Ikutani, M., Oya, T., Kanatani, Y., Tsuneyama, K., Nagai, Y., Takatsu, K., Urakaze, M., et al. (2009). Regulatory Mechanisms for Adipose Tissue M1 and M2 Macrophages in Diet-Induced Obese Mice. Diabetes *58*, 2574–2582.

Furuhashi, M., and Hotamisligil, G.S. (2008). Fatty acid-binding proteins: role in metabolic diseases and potential as drug targets. Nat. Rev. Drug Discov. *7*, 489.

Garg, A. (2004). Acquired and Inherited Lipodystrophies. N. Engl. J. Med. *350*, 1220–1234.

Gerber, H.-P., McMurtrey, A., Kowalski, J., Yan, M., Keyt, B.A., Dixit, V., and Ferrara, N. (1998a). Vascular Endothelial Growth Factor Regulates Endothelial Cell Survival through the Phosphatidylinositol 3′-Kinase/Akt Signal Transduction Pathway REQUIREMENT FOR Flk-1/KDR ACTIVATION. J. Biol. Chem. *273*, 30336–30343.

Gerber, H.-P., Dixit, V., and Ferrara, N. (1998b). Vascular Endothelial Growth Factor Induces Expression of the Antiapoptotic Proteins Bcl-2 and A1 in Vascular Endothelial Cells. J. Biol. Chem. *273*, 13313–13316.

Gerber, H.P., Hillan, K.J., Ryan, A.M., Kowalski, J., Keller, G.A., Rangell, L., Wright, B.D., Radtke, F., Aguet, M., and Ferrara, N. (1999). VEGF is required for growth and survival in neonatal mice. Development *126*, 1149–1159.

Gerhardt, H., and Betsholtz, C. (2003). Endothelial-pericyte interactions in angiogenesis. Cell Tissue Res. *314*, 15–23.

Geudens, I., and Gerhardt, H. (2011). Coordinating cell behaviour during blood vessel formation. Development *138*, 4569–4583.

Giannotta, M., Trani, M., and Dejana, E. (2013). VE-cadherin and endothelial adherens junctions: active guardians of vascular integrity. Dev. Cell *26*, 441–454.

Gil, A., Andrés-Pons, A., Fernández, E., Valiente, M., Torres, J., Cervera, J., and Pulido, R. (2006). Nuclear localization of PTEN by a Ran-dependent mechanism enhances apoptosis: Involvement of an N-terminal nuclear localization domain and multiple nuclear exclusion motifs. Mol. Biol. Cell *17*, 4002–4013.

Gimm, O., Perren, A., Weng, L.P., Marsh, D.J., Yeh, J.J., Ziebold, U., Gil, E., Hinze, R., Delbridge, L., Lees, J.A., et al. (2000). Differential nuclear and cytoplasmic expression of PTEN in normal thyroid tissue, and benign and malignant epithelial thyroid tumors. Am. J. Pathol. *156*, 1693–1700.

Ginn-Pease, M.E., and Eng, C. (2003). Increased Nuclear Phosphatase and Tensin Homologue Deleted on Chromosome 10 Is Associated with G0-G1 in MCF-7 Cells. Cancer Res. *63*, 282–286.

Glatz, J.F.C., Luiken, J.J.F.P., and Bonen, A. (2010). Membrane Fatty Acid Transporters as Regulators of Lipid Metabolism: Implications for Metabolic Disease. Physiol. Rev. *90*, 367–417.

Govender, D., and Chetty, R. (2012). Gene of the month: PTEN. J. Clin. Pathol. *65*, 601–603.

Graupera, M., and Potente, M. (2013). Regulation of angiogenesis by PI3K signaling networks. Exp. Cell Res. *319*, 1348–1355.

Graupera, M., Guillermet-Guibert, J., Foukas, L.C., Phng, L.-K., Cain, R.J., Salpekar, A., Pearce, W., Meek, S., Millan, J., Cutillas, P.R., et al. (2008). Angiogenesis selectively requires the p110alpha isoform of PI3K to control endothelial cell migration. Nature *453*, 662–666.

Greenwalt, D.E., Watt, K.W., Hasler, T., Howard, R.J., and Patel, S. (1990). Structural, functional, and antigenic differences between bovine heart endothelial CD36 and human platelet CD36. J. Biol. Chem. *265*, 16296–16299.

Gupta, R.K., Arany, Z., Seale, P., Mepani, R.J., Ye, L., Conroe, H.M., Roby, Y.A., Kulaga, H., Reed, R.R., and Spiegelman, B.M. (2010). Transcriptional control of preadipocyte determination by Zfp423. Nature *464*, 619–623.

Gupta, R.K., Mepani, R.J., Kleiner, S., Lo, J.C., Khandekar, M.J., Cohen, P., Frontini, A., Bhowmick, D.C., Ye, L., Cinti, S., et al. (2012a). Zfp423 Expression Identifies Committed Preadipocytes and Localizes to Adipose Endothelial and Perivascular Cells. Cell Metab. *15*, 230–239.

Gupta, R.K., Mepani, R.J., Kleiner, S., Lo, J.C., Khandekar, M.J., Cohen, P., Frontini, A., Bhowmick, D.C., Ye, L., Cinti, S., et al. (2012b). Zfp423 Expression Identifies Committed

Preadipocytes and Localizes to Adipose Endothelial and Perivascular Cells. Cell Metab. *15*, 230–239.

Haemmerle, G., Zimmermann, R., Strauss, J.G., Kratky, D., Riederer, M., Knipping, G., and Zechner, R. (2002). Hormone-sensitive Lipase Deficiency in Mice Changes the Plasma Lipid Profile by Affecting the Tissue-specific Expression Pattern of Lipoprotein Lipase in Adipose Tissue and Muscle. J. Biol. Chem. *277*, 12946–12952.

Haemmerle, G., Lass, A., Zimmermann, R., Gorkiewicz, G., Meyer, C., Rozman, J., Heldmaier, G., Maier, R., Theussl, C., Eder, S., et al. (2006). Defective Lipolysis and Altered Energy Metabolism in Mice Lacking Adipose Triglyceride Lipase. Science *312*, 734–737.

Halberg, N., Khan, T., Trujillo, M.E., Wernstedt-Asterholm, I., Attie, A.D., Sherwani, S., Wang, Z.V., Landskroner-Eiger, S., Dineen, S., Magalang, U.J., et al. (2009). Hypoxia-Inducible Factor 1α Induces Fibrosis and Insulin Resistance in White Adipose Tissue. Mol. Cell. Biol. *29*, 4467–4483.

Hamada, K., Sasaki, T., Koni, P.A., Natsui, M., Kishimoto, H., Sasaki, J., Yajima, N., Horie, Y., Hasegawa, G., Naito, M., et al. (2005). The PTEN/PI3K pathway governs normal vascular development and tumor angiogenesis. Genes Dev. *19*, 2054–2065.

Han, T.S., and Lean, M.E. (2016). A clinical perspective of obesity, metabolic syndrome and cardiovascular disease. JRSM Cardiovasc. Dis. *5*.

Han, J., Lee, J.-E., Jin, J., Lim, J.S., Oh, N., Kim, K., Chang, S.-I., Shibuya, M., Kim, H., and Koh, G.Y. (2011). The spatiotemporal development of adipose tissue. Development *138*, 5027–5037.

Hansen, J.B., and Kristiansen, K. (2006). Regulatory circuits controlling white versus brown adipocyte differentiation. Biochem. J. *398*, 153–168.

Hardie, D.G., and Pan, D.A. (2002). Regulation of fatty acid synthesis and oxidation by the AMP-activated protein kinase. Biochem. Soc. Trans. *30*, 1064–1070.

Hardie, D.G., Schaffer, B.E., and Brunet, A. (2016). AMPK: An Energy-Sensing Pathway with Multiple Inputs and Outputs. Trends Cell Biol. *26*, 190–201.

Harper, S.J., and Bates, D.O. (2008). VEGF-A splicing. Nat. Rev. Cancer *8*, 880–887.

Haslam, D.W., and James, W.P.T. (2005). Obesity. The Lancet *366*, 1197–1209.

Hassan, M., Latif, N., and Yacoub, M. (2012). Adipose tissue: friend or foe? Nat. Rev. Cardiol. *9*, 689–702.

Hellström, M., Phng, L.-K., Hofmann, J.J., Wallgard, E., Coultas, L., Lindblom, P., Alva, J., Nilsson, A.-K., Karlsson, L., Gaiano, N., et al. (2007). Dll4 signalling through Notch1 regulates formation of tip cells during angiogenesis. Nature *445*, 776–780.

Hopkins, B.D., Fine, B., Steinbach, N., Dendy, M., Rapp, Z., Shaw, J., Pappas, K., Yu, J.S., Hodakoski, C., Mense, S., et al. (2013). A Secreted PTEN Phosphatase That Enters Cells to Alter Signaling and Survival. Science *341*, 399–402.

Hossain, P., Kawar, B., and El Nahas, M. (2007). Obesity and Diabetes in the Developing World — A Growing Challenge. N. Engl. J. Med. *356*, 213–215.

Houck, K.A., Ferrara, N., Winer, J., Cachianes, G., Li, B., and Leung, D.W. (1991). The Vascular Endothelial Growth Factor Family: Identification of a Fourth Molecular Species and Characterization of Alternative Splicing of RNA. Mol. Endocrinol. *5*, 1806–1814.

Houten, S.M., and Wanders, R.J.A. (2010). A general introduction to the biochemistry of mitochondrial fatty acid β-oxidation. J. Inherit. Metab. Dis. *33*, 469–477.

Hu, E., Tontonoz, P., and Spiegelman, B.M. (1995). Transdifferentiation of myoblasts by the adipogenic transcription factors PPAR gamma and C/EBP alpha. Proc. Natl. Acad. Sci. U. S. A. *92*, 9856–9860.

Huang, J., and Manning, B.D. (2008). The TSC1-TSC2 complex: a molecular switchboard controlling cell growth. Biochem. J. *412*, 179–190.

Hue, L., and Taegtmeyer, H. (2009). The Randle cycle revisited: a new head for an old hat. Am. J. Physiol. - Endocrinol. Metab. *297*, E578–E591.

Hülsmann, W.C., and Dubelaar, M.-L. (1988). Aspects of fatty acid metabolism in vascular endothelial cells. Biochimie *70*, 681–686.

Huss, J.M., and Kelly, D.P. (2004). Nuclear Receptor Signaling and Cardiac Energetics. Circ. Res. *95*, 568–578.

Hüttemann, M., Lee, I., Samavati, L., Yu, H., and Doan, J.W. (2007). Regulation of mitochondrial oxidative phosphorylation through cell signaling. Biochim. Biophys. Acta BBA - Mol. Cell Res. *1773*, 1701–1720.

Iijima, M., Huang, Y.E., Luo, H.R., Vazquez, F., and Devreotes, P.N. (2004). Novel mechanism of PTEN regulation by its phosphatidylinositol 4,5-bisphosphate binding motif is critical for chemotaxis. J. Biol. Chem. *279*, 16606–16613.

Inoki, K., Li, Y., Zhu, T., Wu, J., and Guan, K.-L. (2002). TSC2 is phosphorylated and inhibited by Akt and suppresses mTOR signalling. Nat. Cell Biol. *4*, 648–657.

Iruela-Arispe, M.L., and Davis, G.E. (2009). Cellular and Molecular Mechanisms of Vascular Lumen Formation. Dev. Cell *16*, 222–231.

Iso, T., Kedes, L., and Hamamori, Y. (2003). HES and HERP families: Multiple effectors of the notch signaling pathway. J. Cell. Physiol. *194*, 237–255.

Italiano, A., Chen, C.-L., Thomas, R., Breen, M., Bonnet, F., Sevenet, N., Longy, M., Maki, R.G., Coindre, J.-M., and Antonescu, C.R. (2012). Alterations of p53 and PIK3CA/AKT/mTOR Pathways in Angiosarcomas: A Pattern Distinct from Other Sarcomas with Complex Genomics. Cancer *118*, 5878–5887.

Jakobsson, L., Franco, C.A., Bentley, K., Collins, R.T., Ponsioen, B., Aspalter, I.M., Rosewell, I., Busse, M., Thurston, G., Medvinsky, A., et al. (2010). Endothelial cells dynamically compete for the tip cell position during angiogenic sprouting. Nat. Cell Biol. *12*, 943–953.

Jeffery, R.W., Drewnowski, A., Epstein, L.H., Stunkard, A.J., Wilson, G.T., Wing, R.R., and Hill, D.R. (2000). Long-term maintenance of weight loss: current status. Health Psychol. Off. J. Div. Health Psychol. Am. Psychol. Assoc. *19*, 5–16.

Jenkins, C.M., Mancuso, D.J., Yan, W., Sims, H.F., Gibson, B., and Gross, R.W. (2004). Identification, Cloning, Expression, and Purification of Three Novel Human Calcium-

independent Phospholipase A2 Family Members Possessing Triacylglycerol Lipase and Acylglycerol Transacylase Activities. J. Biol. Chem. *279*, 48968–48975.

Jimenez, M.A., Åkerblad, P., Sigvardsson, M., and Rosen, E.D. (2007). Critical Role for Ebf1 and Ebf2 in the Adipogenic Transcriptional Cascade. Mol. Cell. Biol. *27*, 743–757.

Johnsson, P., Ackley, A., Vidarsdottir, L., Lui, W.-O., Corcoran, M., Grandér, D., and Morris, K.V. (2013). A pseudogene long-noncoding-RNA network regulates PTEN transcription and translation in human cells. Nat. Struct. Mol. Biol. *20*, 440–446.

Jones, N., Master, Z., Jones, J., Bouchard, D., Gunji, Y., Sasaki, H., Daly, R., Alitalo, K., and Dumont, D.J. (1999). Identification of Tek/Tie2 binding partners. Binding to a multifunctional docking site mediates cell survival and migration. J. Biol. Chem. *274*, 30896–30905.

Kang, S., Akerblad, P., Kiviranta, R., Gupta, R.K., Kajimura, S., Griffin, M.J., Min, J., Baron, R., and Rosen, E.D. (2012). Regulation of Early Adipose Commitment by Zfp521. PLOS Biol. *10*, e1001433.

Kazantzis, M., and Stahl, A. (2012). Fatty Acid transport Proteins, implications in physiology and disease. Biochim. Biophys. Acta *1821*, 852–857.

Kersten, S. (2001). Mechanisms of nutritional and hormonal regulation of lipogenesis. EMBO Rep. *2*, 282–286.

Khan, T., Muise, E.S., Iyengar, P., Wang, Z.V., Chandalia, M., Abate, N., Zhang, B.B., Bonaldo, P., Chua, S., and Scherer, P.E. (2009). Metabolic Dysregulation and Adipose Tissue Fibrosis: Role of Collagen VI. Mol. Cell. Biol. *29*, 1575–1591.

Kim, J.I., Huh, J.Y., Sohn, J.H., Choe, S.S., Lee, Y.S., Lim, C.Y., Jo, A., Park, S.B., Han, W., and Kim, J.B. (2015). Lipid-Overloaded Enlarged Adipocytes Provoke Insulin Resistance Independent of Inflammation. Mol. Cell. Biol. *35*, 1686–1699.

Knittle, J.L., Timmers, K., Ginsberg-Fellner, F., Brown, R.E., and Katz, D.P. (1979). The growth of adipose tissue in children and adolescents. Cross-sectional and longitudinal studies of adipose cell number and size. J. Clin. Invest. *63*, 239–246.

Kondoh, H., Lleonart, M.E., Nakashima, Y., Yokode, M., Tanaka, M., Bernard, D., Gil, J., and Beach, D. (2007). A High Glycolytic Flux Supports the Proliferative Potential of Murine Embryonic Stem Cells. Antioxid. Redox Signal. *9*, 293–299.

Kopan, R., and Ilagan, M.X.G. (2009). The Canonical Notch Signaling Pathway: Unfolding the Activation Mechanism. Cell *137*, 216–233.

Kral, J.G., and Näslund, E. (2007). Surgical treatment of obesity. Nat. Clin. Pract. Endocrinol. Metab. *3*, 574–583.

Krützfeldt, A., Spahr, R., Mertens, S., Siegmund, B., and Piper, H.M. (1990). Metabolism of exogenous substrates by coronary endothelial cells in culture. J. Mol. Cell. Cardiol. *22*, 1393–1404.

Kwon, J., Lee, S.-R., Yang, K.-S., Ahn, Y., Kim, Y.J., Stadtman, E.R., and Rhee, S.G. (2004). Reversible oxidation and inactivation of the tumor suppressor PTEN in cells stimulated with peptide growth factors. Proc. Natl. Acad. Sci. U. S. A. *101*, 16419–16424.

Lago, F., Gómez, R., Gómez-Reino, J.J., Dieguez, C., and Gualillo, O. (2009). Adipokines as novel modulators of lipid metabolism. Trends Biochem. Sci. *34*, 500–510.

Lange, C., Storkebaum, E., de Almodóvar, C.R., Dewerchin, M., and Carmeliet, P. (2016). Vascular endothelial growth factor: a neurovascular target in neurological diseases. Nat. Rev. Neurol. *12*, 439–454.

Lass, A., Zimmermann, R., Oberer, M., and Zechner, R. (2011). Lipolysis – A highly regulated multi-enzyme complex mediates the catabolism of cellular fat stores. Prog. Lipid Res. *50*, 14–27.

Lee, M.-J., Wu, Y., and Fried, S.K. (2010). Adipose tissue remodeling in pathophysiology of obesity. Curr. Opin. Clin. Nutr. Metab. Care *13*, 371–376.

Lee, M.-J., Wu, Y., and Fried, S.K. (2013). Adipose Tissue Heterogeneity: Implication of depot differences in adipose tissue for Obesity Complications. Mol. Aspects Med. *34*, 1–11.

Leslie, N.R., Bennett, D., Lindsay, Y.E., Stewart, H., Gray, A., and Downes, C.P. (2003). Redox regulation of PI 3-kinase signalling via inactivation of PTEN. EMBO J. *22*, 5501–5510.

Li, J., Yen, C., Liaw, D., Podsypanina, K., Bose, S., Wang, S.I., Puc, J., Miliaresis, C., Rodgers, L., McCombie, R., et al. (1997). PTEN, a Putative Protein Tyrosine Phosphatase Gene Mutated in Human Brain, Breast, and Prostate Cancer. Science *275*, 1943–1947.

Lijnen, H.R. (2008). Angiogenesis and obesity. Cardiovasc. Res. *78*, 286–293.

Liu, F., Wagner, S., Campbell, R.B., Nickerson, J.A., Schiffer, C.A., and Ross, A.H. (2005). PTEN enters the nucleus by diffusion. J. Cell. Biochem. *96*, 221–234.

Lo, K.A., and Sun, L. (2013). Turning WAT into BAT: a review on regulators controlling the browning of white adipocytes. Biosci. Rep. *33*.

Lohmann, R., Souba, W.W., and Bode, B.P. (1999). Rat liver endothelial cell glutamine transporter and glutaminase expression contrast with parenchymal cells. Am. J. Physiol. - Gastrointest. Liver Physiol. *276*, G743–G750.

Lubarsky, B., and Krasnow, M.A. (2003). Tube morphogenesis: making and shaping biological tubes. Cell *112*, 19–28.

Lumeng, C.N., Bodzin, J.L., and Saltiel, A.R. (2007). Obesity induces a phenotypic switch in adipose tissue macrophage polarization. J. Clin. Invest. *117*, 175–184.

Maccario, H., Perera, N.M., Davidson, L., Downes, C.P., and Leslie, N.R. (2007). PTEN is destabilized by phosphorylation on Thr366. Biochem. J. *405*, 439–444.

Majka, S.M., Fox, K.E., Psilas, J.C., Helm, K.M., Childs, C.R., Acosta, A.S., Janssen, R.C., Friedman, J.E., Woessner, B.T., Shade, T.R., et al. (2010). De novo generation of white adipocytes from the myeloid lineage via mesenchymal intermediates is age, adipose depot, and gender specific. Proc. Natl. Acad. Sci. U. S. A. *107*, 14781–14786.

Manning, B.D., and Cantley, L.C. (2007). AKT/PKB Signaling: Navigating Downstream. Cell *129*, 1261–1274.

Maquoi, E., Munaut, C., Colige, A., Collen, D., and Lijnen, H.R. (2002). Modulation of Adipose Tissue Expression of Murine Matrix Metalloproteinases and Their Tissue Inhibitors With Obesity. Diabetes *51*, 1093–1101.

Masouyé, I., Hagens, G., Kuppevelt, T.H.V., Madsen, P., Saurat, J.-H., Veerkamp, J.H., Pepper, M.S., and Siegenthaler, G. (1997). Endothelial Cells of the Human Microvasculature Express Epidermal Fatty Acid–Binding Protein. Circ. Res. *81*, 297–303.

Mattson, M.P. (2010). Does Brown Fat Protect Against Diseases of Aging? Ageing Res. Rev. *9*, 69.

Mayo, L.D., and Donner, D.B. (2001). A phosphatidylinositol 3-kinase/Akt pathway promotes translocation of Mdm2 from the cytoplasm to the nucleus. Proc. Natl. Acad. Sci. U. S. A. *98*, 11598–11603.

Merchan, J.R., Kovács, K., Railsback, J.W., Kurtoglu, M., Jing, Y., Piña, Y., Gao, N., Murray, T.G., Lehrman, M.A., and Lampidis, T.J. (2010). Antiangiogenic Activity of 2-Deoxy-D-Glucose. PLOS ONE *5*, e13699.

Michael, D.R., Davies, T.S., Laubertová, L., Gallagher, H., and Ramji, D.P. (2015). The Phosphoinositide 3-Kinase Signaling Pathway is Involved in the Control of Modified Low-Density Lipoprotein Uptake by Human Macrophages. Lipids *50*, 253–260.

Minokoshi, Y., Kim, Y.-B., Peroni, O.D., Fryer, L.G.D., Müller, C., Carling, D., and Kahn, B.B. (2002). Leptin stimulates fatty-acid oxidation by activating AMP-activated protein kinase. Nature *415*, 339–343.

Miyoshi, H., Souza, S.C., Zhang, H.-H., Strissel, K.J., Christoffolete, M.A., Kovsan, J., Rudich, A., Kraemer, F.B., Bianco, A.C., Obin, M.S., et al. (2006). Perilipin Promotes Hormone-sensitive Lipase-mediated Adipocyte Lipolysis via Phosphorylation-dependent and -independent Mechanisms. J. Biol. Chem. *281*, 15837–15844.

Montague, C.T., Farooqi, I.S., Whitehead, J.P., Soos, M.A., Rau, H., Wareham, N.J., Sewter, C.P., Digby, J.E., Mohammed, S.N., Hurst, J.A., et al. (1997). Congenital leptin deficiency is associated with severe early-onset obesity in humans. Nature *387*, 903–908.

Mori, M., Nakagami, H., Rodriguez-Araujo, G., Nimura, K., and Kaneda, Y. (2012). Essential Role for miR-196a in Brown Adipogenesis of White Fat Progenitor Cells. PLOS Biol. *10*, e1001314.

Muniyappa, R., Lee, S., Chen, H., and Quon, M.J. (2008). Current approaches for assessing insulin sensitivity and resistance in vivo: advantages, limitations, and appropriate usage. Am. J. Physiol. Endocrinol. Metab. *294*, E15-26.

Myers, M.G., Leibel, R.L., Seeley, R.J., and Schwartz, M.W. (2010). Obesity and Leptin Resistance: Distinguishing Cause from Effect. Trends Endocrinol. Metab. TEM *21*, 643–651.

Nagata, D., Mogi, M., and Walsh, K. (2003). AMP-activated Protein Kinase (AMPK) Signaling in Endothelial Cells Is Essential for Angiogenesis in Response to Hypoxic Stress. J. Biol. Chem. *278*, 31000–31006.

Newcomer, M.E., and Ong, D.E. (2000). Plasma retinol binding protein: structure and function of the prototypic lipocalin. Biochim. Biophys. Acta BBA - Protein Struct. Mol. Enzymol. *1482*, 57–64.

Nielsen, T.S., Jessen, N., Jørgensen, J.O.L., Møller, N., and Lund, S. (2014). Dissecting adipose tissue lipolysis: molecular regulation and implications for metabolic disease. J. Mol. Endocrinol. *52*, R199–R222.

Nishimura, S., Manabe, I., Nagasaki, M., Hosoya, Y., Yamashita, H., Fujita, H., Ohsugi, M., Tobe, K., Kadowaki, T., Nagai, R., et al. (2007). Adipogenesis in Obesity Requires Close Interplay Between Differentiating Adipocytes, Stromal Cells, and Blood Vessels. Diabetes *56*, 1517–1526.

Oellerich, M.F., and Potente, M. (2012). FOXOs and Sirtuins in Vascular Growth, Maintenance, and Aging. Circ. Res. *110*, 1238–1251.

Okumura, K., Mendoza, M., Bachoo, R.M., DePinho, R.A., Cavenee, W.K., and Furnari, F.B. (2006). PCAF modulates PTEN activity. J. Biol. Chem. *281*, 26562–26568.

Olsson, A.-K., Dimberg, A., Kreuger, J., and Claesson-Welsh, L. (2006). VEGF receptor signalling ? in control of vascular function. Nat. Rev. Mol. Cell Biol. *7*, 359–371.

Osuga, J., Ishibashi, S., Oka, T., Yagyu, H., Tozawa, R., Fujimoto, A., Shionoiri, F., Yahagi, N., Kraemer, F.B., Tsutsumi, O., et al. (2000). Targeted disruption of hormone-sensitive lipase results in male sterility and adipocyte hypertrophy, but not in obesity. Proc. Natl. Acad. Sci. U. S. A. *97*, 787–792.

Otrock, Z.K., Mahfouz, R.A.R., Makarem, J.A., and Shamseddine, A.I. (2007). Understanding the biology of angiogenesis: Review of the most important molecular mechanisms. Blood Cells. Mol. Dis. *39*, 212–220.

Ouchi, N., Parker, J.L., Lugus, J.J., and Walsh, K. (2011). Adipokines in inflammation and metabolic disease. Nat. Rev. Immunol. *11*, 85–97.

Palomero, T., Sulis, M.L., Cortina, M., Real, P.J., Barnes, K., Ciofani, M., Caparros, E., Buteau, J., Brown, K., Perkins, S.L., et al. (2007). Mutational loss of PTEN induces resistance to NOTCH1 inhibition in T-cell leukemia. Nat. Med. *13*, 1203–1210.

Park, I.-S., Kang, S.-W., Shin, Y.-J., Chae, K.-Y., Park, M.-O., Kim, M.-Y., Wheatley, D.N., and Min, B.-H. (2003). Arginine deiminase: a potential inhibitor of angiogenesis and tumour growth. Br. J. Cancer *89*, 907–914.

Patel, L., Pass, I., Coxon, P., Downes, C.P., Smith, S.A., and Macphee, C.H. (2001). Tumor suppressor and anti-inflammatory actions of PPARgamma agonists are mediated via upregulation of PTEN. Curr. Biol. CB *11*, 764–768.

Peeters, A., Barendregt, J.J., Willekens, F., Mackenbach, J.P., Al Mamun, A., Bonneux, L., and NEDCOM, the Netherlands Epidemiology and Demography Compression of Morbidity Research Group (2003). Obesity in adulthood and its consequences for life expectancy: a life-table analysis. Ann. Intern. Med. *138*, 24–32.

Peirce, V., Carobbio, S., and Vidal-Puig, A. (2014). The different shades of fat. Nature *510*, 76–83.

Pelleymounter, M.A., Cullen, M.J., Baker, M.B., Hecht, R., Winters, D., Boone, T., and Collins, F. (1995). Effects of the obese gene product on body weight regulation in ob/ob mice. Science *269*, 540–543.

Perren, A., Komminoth, P., Saremaslani, P., Matter, C., Feurer, S., Lees, J.A., Heitz, P.U., and Eng, C. (2000). Mutation and Expression Analyses Reveal Differential Subcellular Compartmentalization of PTEN in Endocrine Pancreatic Tumors Compared to Normal Islet Cells. Am. J. Pathol. *157*, 1097–1103.

Petruzzelli, M., Schweiger, M., Schreiber, R., Campos-Olivas, R., Tsoli, M., Allen, J., Swarbrick, M., Rose-John, S., Rincon, M., Robertson, G., et al. (2014). A Switch from White to Brown Fat Increases Energy Expenditure in Cancer-Associated Cachexia. Cell Metab. *20*, 433–447.

Poissonnet, C.M., Burdi, A.R., and Bookstein, F.L. (1983). Growth and development of human adipose tissue during early gestation. Early Hum. Dev. *8*, 1–11.

Poissonnet, C.M., Burdi, A.R., and Garn, S.M. (1984). The chronology of adipose tissue appearance and distribution in the human fetus. Early Hum. Dev. *10*, 1–11.

Poliseno, L., Salmena, L., Zhang, J., Carver, B., Haveman, W.J., and Pandolfi, P.P. (2010). A coding-independent function of gene and pseudogene mRNAs regulates tumour biology. Nature *465*, 1033–1038.

Potente, M., and Carmeliet, P. (2017). The Link Between Angiogenesis and Endothelial Metabolism. Annu. Rev. Physiol. *79*, 43–66.

Potente, M., Gerhardt, H., and Carmeliet, P. (2011). Basic and Therapeutic Aspects of Angiogenesis. Cell *146*, 873–887.

Proença, A.R.G., Sertié, R. a. L., Oliveira, A.C., Campaãa, A.B., Caminhotto, R.O., Chimin, P., Lima, F.B., Proença, A.R.G., Sertié, R. a. L., Oliveira, A.C., et al. (2014). New concepts in white adipose tissue physiology. Braz. J. Med. Biol. Res. *47*, 192–205.

Puigserver, P., and Spiegelman, B.M. (2003). Peroxisome Proliferator-Activated Receptor-γ Coactivator 1α (PGC-1α): Transcriptional Coactivator and Metabolic Regulator. Endocr. Rev. *24*, 78–90.

Putz, U., Howitt, J., Doan, A., Goh, C.-P., Low, L.-H., Silke, J., and Tan, S.-S. (2012). The Tumor Suppressor PTEN Is Exported in Exosomes and Has Phosphatase Activity in Recipient Cells. Sci Signal *5*, ra70-ra70.

Qi, Y., Nie, Z., Lee, Y.-S., Singhal, N.S., Scherer, P.E., Lazar, M.A., and Ahima, R.S. (2006). Loss of Resistin Improves Glucose Homeostasis in Leptin Deficiency. Diabetes *55*, 3083–3090.

Rahimi, N. (2006). VEGFR-1 and VEGFR-2: two non-identical twins with a unique physiognomy. Front. Biosci. J. Virtual Libr. *11*, 818–829.

Rigamonti, A., Brennand, K., Lau, F., and Cowan, C.A. (2011). Rapid Cellular Turnover in Adipose Tissue. PLoS ONE *6*.

Robciuc, M.R., Kivelä, R., Williams, I.M., de Boer, J.F., van Dijk, T.H., Elamaa, H., Tigistu-Sahle, F., Molotkov, D., Leppänen, V.-M., Käkelä, R., et al. (2016). VEGFB/VEGFR1-Induced Expansion of Adipose Vasculature Counteracts Obesity and Related Metabolic Complications. Cell Metab. *23*, 712–724.

Roca, C., and Adams, R.H. (2007). Regulation of vascular morphogenesis by Notch signaling. Genes Dev. *21*, 2511–2524.

Rodgers, R.J., Tschöp, M.H., and Wilding, J.P.H. (2012). Anti-obesity drugs: past, present and future. Dis. Model. Mech. *5*, 621–626.

Rosen, E.D., and MacDougald, O.A. (2006). Adipocyte differentiation from the inside out. Nat. Rev. Mol. Cell Biol. *7*, 885–896.

Rosen, E.D., and Spiegelman, B.M. (2014). What We Talk About When We Talk About Fat. Cell *156*, 20–44.

Rosenwald, M., Perdikari, A., Rülicke, T., and Wolfrum, C. (2013). Bi-directional interconversion of brite and white adipocytes. Nat. Cell Biol. *15*, 659–667.

Rousset, S., Alves-Guerra, M.-C., Mozo, J., Miroux, B., Cassard-Doulcier, A.-M., Bouillaud, F., and Ricquier, D. (2004). The Biology of Mitochondrial Uncoupling Proteins. Diabetes *53*, S130–S135.

Rupnick, M.A., Panigrahy, D., Zhang, C.-Y., Dallabrida, S.M., Lowell, B.B., Langer, R., and Folkman, M.J. (2002). Adipose tissue mass can be regulated through the vasculature. Proc. Natl. Acad. Sci. U. S. A. *99*, 10730–10735.

Saely, C.H., Geiger, K., and Drexel, H. (2010). Brown versus White Adipose Tissue: A Mini-Review. Gerontology *58*, 15–23.

Salans, L.B., Knittle, J.L., and Hirsch, J. (1968). The role of adipose cell size and adipose tissue insulin sensitivity in the carbohydrate intolerance of human obesity. J. Clin. Invest. *47*, 153–165.

Salih, D.A.M., and Brunet, A. (2008). FoxO transcription factors in the maintenance of cellular homeostasis during aging. Curr. Opin. Cell Biol. *20*, 126–136.

Salmena, L., Carracedo, A., and Pandolfi, P.P. (2008). Tenets of PTEN tumor suppression. Cell *133*, 403–414.

Sanchez-Gurmaches, J., and Guertin, D.A. (2014). Adipocyte Lineages: Tracing Back the Origins of Fat. Biochim. Biophys. Acta *1842*, 340–351.

Sanz, E., Yang, L., Su, T., Morris, D.R., McKnight, G.S., and Amieux, P.S. (2009). Cell-type-specific isolation of ribosome-associated mRNA from complex tissues. Proc. Natl. Acad. Sci. *106*, 13939–13944.

Saponaro, C., Gaggini, M., Carli, F., and Gastaldelli, A. (2015). The Subtle Balance between Lipolysis and Lipogenesis: A Critical Point in Metabolic Homeostasis. Nutrients *7*, 9453–9474.

Sarjeant, K., and Stephens, J.M. (2012). Adipogenesis. Cold Spring Harb. Perspect. Biol. *4*.

Sarnali, T.T., and Pk, M.M. (2010). Obesity and Disease Association: A Review. Anwer Khan Mod. Med. Coll. J. *1*, 21–24.

Savage, D.B., Sewter, C.P., Klenk, E.S., Segal, D.G., Vidal-Puig, A., Considine, R.V., and O'Rahilly, S. (2001). Resistin / Fizz3 Expression in Relation to Obesity and Peroxisome Proliferator–Activated Receptor-γ Action in Humans. Diabetes *50*, 2199–2202.

Schoors, S., Bruning, U., Missiaen, R., Queiroz, K.C.S., Borgers, G., Elia, I., Zecchin, A., Cantelmo, A.R., Christen, S., Goveia, J., et al. (2015). Fatty acid carbon is essential for dNTP synthesis in endothelial cells. Nature *520*, 192–197.

Schreurs, M., Kuipers, F., and Van Der Leij, F.R. (2010). Regulatory enzymes of mitochondrial β-oxidation as targets for treatment of the metabolic syndrome. Obes. Rev. *11*, 380–388.

Seale, P., Bjork, B., Yang, W., Kajimura, S., Chin, S., Kuang, S., Scimè, A., Devarakonda, S., Conroe, H.M., Erdjument-Bromage, H., et al. (2008). PRDM16 controls a brown fat/skeletal muscle switch. Nature *454*, 961–967.

Seale, P., Conroe, H.M., Estall, J., Kajimura, S., Frontini, A., Ishibashi, J., Cohen, P., Cinti, S., and Spiegelman, B.M. (2011). Prdm16 determines the thermogenic program of subcutaneous white adipose tissue in mice. J. Clin. Invest. *121*, 96–105.

Sekimoto, T., Fukumoto, M., and Yoneda, Y. (2004). 14-3-3 suppresses the nuclear localization of threonine 157-phosphorylated p27(Kip1). EMBO J. *23*, 1934–1942.

Semenza, G.L. (2003). Targeting HIF-1 for cancer therapy. Nat. Rev. Cancer *3*, 721–732.

Senger, D.R., and Davis, G.E. (2011). Angiogenesis. Cold Spring Harb. Perspect. Biol. *3*.

Serra, H., Chivite, I., Angulo-Urarte, A., Soler, A., Sutherland, J.D., Arruabarrena-Aristorena, A., Ragab, A., Lim, R., Malumbres, M., Fruttiger, M., et al. (2015). PTEN mediates Notch-dependent stalk cell arrest in angiogenesis. Nat. Commun. *6*, 7935.

Shen, W.H., Balajee, A.S., Wang, J., Wu, H., Eng, C., Pandolfi, P.P., and Yin, Y. (2007). Essential Role for Nuclear PTEN in Maintaining Chromosomal Integrity. Cell *128*, 157–170.

Shi, Y., Paluch, B.E., Wang, X., and Jiang, X. (2012). PTEN at a glance. J Cell Sci *125*, 4687–4692.

Shin, I., Yakes, F.M., Rojo, F., Shin, N.-Y., Bakin, A.V., Baselga, J., and Arteaga, C.L. (2002). PKB/Akt mediates cell-cycle progression by phosphorylation of p27Kip1 at threonine 157 and modulation of its cellular localization. Nat. Med. *8*, 1145–1152.

Silverstein, R.L., and Febbraio, M. (2009). CD36, a Scavenger Receptor Involved in Immunity, Metabolism, Angiogenesis, and Behavior. Sci. Signal. *2*, re3.

Song, L.-B., Li, J., Liao, W.-T., Feng, Y., Yu, C.-P., Hu, L.-J., Kong, Q.-L., Xu, L.-H., Zhang, X., Liu, W.-L., et al. (2009). The polycomb group protein Bmi-1 represses the tumor suppressor PTEN and induces epithelial-mesenchymal transition in human nasopharyngeal epithelial cells. J. Clin. Invest. *119*, 3626–3636.

Song, M.S., Carracedo, A., Salmena, L., Song, S.J., Egia, A., Malumbres, M., and Pandolfi, P.P. (2011). Nuclear PTEN regulates the APC-CDH1 tumor-suppressive complex in a phosphatase-independent manner. Cell *144*, 187–199.

Spalding, K.L., Arner, E., Westermark, P.O., Bernard, S., Buchholz, B.A., Bergmann, O., Blomqvist, L., Hoffstedt, J., Näslund, E., Britton, T., et al. (2008). Dynamics of fat cell turnover in humans. Nature *453*, 783–787.

Stahl, A., Gimeno, R.E., Tartaglia, L.A., and Lodish, H.F. (2001). Fatty acid transport proteins: a current view of a growing family. Trends Endocrinol. Metab. *12*, 266–273.

Stambolic, V., MacPherson, D., Sas, D., Lin, Y., Snow, B., Jang, Y., Benchimol, S., and Mak, T.W. (2001). Regulation of PTEN transcription by p53. Mol. Cell *8*, 317–325.

Steck, P.A., Pershouse, M.A., Jasser, S.A., Yung, W.K.A., Lin, H., Ligon, A.H., Langford, L.A., Baumgard, M.L., Hattier, T., Davis, T., et al. (1997). Identification of a candidate tumour suppressor gene, MMAC1, at chromosome 10q23.3 that is mutated in multiple advanced cancers. Nat. Genet. *15*, 356–362.

Stephens, J.M. (2012). The Fat Controller: Adipocyte Development. PLoS Biol. *10*.

Steppan, C.M., and Lazar, M.A. (2004). The current biology of resistin. J. Intern. Med. *255*, 439–447.

Strawford, A., Antelo, F., Christiansen, M., and Hellerstein, M.K. (2004). Adipose tissue triglyceride turnover, de novo lipogenesis, and cell proliferation in humans measured with 2H2O. Am. J. Physiol. - Endocrinol. Metab. *286*, E577–E588.

Stremmel, W., Pohl, J., Ring, A., and Herrmann, T. (2001). A new concept of cellular uptake and intracellular trafficking of long-chain fatty acids. Lipids *36*, 981–989.

Strissel, K.J., Stancheva, Z., Miyoshi, H., Perfield, J.W., DeFuria, J., Jick, Z., Greenberg, A.S., and Obin, M.S. (2007). Adipocyte Death, Adipose Tissue Remodeling, and Obesity Complications. Diabetes *56*, 2910–2918.

Stump, D.D., Zhou, S.L., and Berk, P.D. (1993). Comparison of plasma membrane FABP and mitochondrial isoform of aspartate aminotransferase from rat liver. Am. J. Physiol. - Gastrointest. Liver Physiol. *265*, G894–G902.

Su, X., and Abumrad, N.A. (2009). Cellular Fatty Acid Uptake: A Pathway Under Construction. Trends Endocrinol. Metab. TEM *20*, 72–77.

Suchting, S., Freitas, C., Noble, F. le, Benedito, R., Bréant, C., Duarte, A., and Eichmann, A. (2007). The Notch ligand Delta-like 4 negatively regulates endothelial tip cell formation and vessel branching. Proc. Natl. Acad. Sci. *104*, 3225–3230.

Sun, L., and Trajkovski, M. (2014). MiR-27 orchestrates the transcriptional regulation of brown adipogenesis. Metab. - Clin. Exp. *63*, 272–282.

Sun, K., Kusminski, C.M., and Scherer, P.E. (2011). Adipose tissue remodeling and obesity. J. Clin. Invest. *121*, 2094–2101.

Sun, K., Asterholm, I.W., Kusminski, C.M., Bueno, A.C., Wang, Z.V., Pollard, J.W., Brekken, R.A., and Scherer, P.E. (2012). Dichotomous effects of VEGF-A on adipose tissue dysfunction. Proc. Natl. Acad. Sci. U. S. A. *109*, 5874–5879.

Sun, K., Tordjman, J., Clément, K., and Scherer, P.E. (2013). Fibrosis and Adipose Tissue Dysfunction. Cell Metab. *18*, 470–477.

Sun, K., Kusminski, C.M., Luby-Phelps, K., Spurgin, S.B., An, Y.A., Wang, Q.A., Holland, W.L., and Scherer, P.E. (2014). Brown adipose tissue derived VEGF-A modulates cold tolerance and energy expenditure. Mol. Metab. *3*, 474–483.

Suzuki, A., Yamaguchi, M.T., Ohteki, T., Sasaki, T., Kaisho, T., Kimura, Y., Yoshida, R., Wakeham, A., Higuchi, T., Fukumoto, M., et al. (2001). T Cell-Specific Loss of Pten Leads to Defects in Central and Peripheral Tolerance. Immunity *14*, 523–534.

Suzuki, A., Nakano, T., Mak, T.W., and Sasaki, T. (2008). Portrait of PTEN: Messages from mutant mice. Cancer Sci. *99*, 209–213.

Symonds, M.E. (2013). Brown Adipose Tissue Growth and Development. Scientifica *2013*, e305763.

Taanman, J.-W. (1999). The mitochondrial genome: structure, transcription, translation and replication. Biochim. Biophys. Acta BBA - Bioenerg. *1410*, 103–123.

Tam, J., Duda, D.G., Perentes, J.Y., Quadri, R.S., Fukumura, D., and Jain, R.K. (2009). Blockade of VEGFR2 and Not VEGFR1 Can Limit Diet-Induced Fat Tissue Expansion: Role of Local versus Bone Marrow-Derived Endothelial Cells. PLOS ONE *4*, e4974.

Tan, C.Y., and Vidal-Puig, A. (2008). Adipose tissue expandability: the metabolic problems of obesity may arise from the inability to become more obese. Biochem. Soc. Trans. *36*, 935–940.

Tan, W., Baris, H.N., Burrows, P.E., Robson, C.D., Alomari, A.I., Mulliken, J.B., Fishman, S.J., and Irons, M.B. (2007). The spectrum of vascular anomalies in patients with PTEN mutations: implications for diagnosis and management. J. Med. Genet. *44*, 594–602.

Tang, W., Zeve, D., Suh, J.M., Bosnakovski, D., Kyba, M., Hammer, R.E., Tallquist, M.D., and Graff, J.M. (2008a). White Fat Progenitors Reside in the Adipose Vasculature. Science *322*, 583–586.

Tang, W., Zeve, D., Suh, J.M., Bosnakovski, D., Kyba, M., Hammer, R.E., Tallquist, M.D., and Graff, J.M. (2008b). White Fat Progenitors Reside in the Adipose Vasculature. Science *322*, 583–586.

Tansey, J., Sztalryd, C., Hlavin, E., Kimmel, A., and Londos, C. (2004). The Central Role of Perilipin A in Lipid Metabolism and Adipocyte Lipolysis. IUBMB Life *56*, 379–385.

Tolkacheva, T., Boddapati, M., Sanfiz, A., Tsuchida, K., Kimmelman, A.C., and Chan, A.M.-L. (2001). Regulation of PTEN Binding to MAGI-2 by Two Putative Phosphorylation Sites at Threonine 382 and 383. Cancer Res. *61*, 4985–4989.

Tontonoz, P., Hu, E., and Spiegelman, B.M. (1994). Stimulation of adipogenesis in fibroblasts by PPAR gamma 2, a lipid-activated transcription factor. Cell *79*, 1147–1156.

Trajkovski, M., and Lodish, H. (2013). MicroRNA networks regulate development of brown adipocytes. Trends Endocrinol. Metab. *24*, 442–450.

Tran, K.-V., Gealekman, O., Frontini, A., Zingaretti, M.C., Morroni, M., Giordano, A., Smorlesi, A., Perugini, J., De Matteis, R., Sbarbati, A., et al. (2012a). The vascular endothelium of the adipose tissue give rise to both white and brown fat cells. Cell Metab. *15*, 222–229.

Tran, K.-V., Gealekman, O., Frontini, A., Zingaretti, M.C., Morroni, M., Giordano, A., Smorlesi, A., Perugini, J., De Matteis, R., Sbarbati, A., et al. (2012b). The vascular endothelium of the adipose tissue give rise to both white and brown fat cells. Cell Metab. *15*, 222–229.

Trotman, L.C., Wang, X., Alimonti, A., Chen, Z., Teruya-Feldstein, J., Yang, H., Pavletich, N.P., Carver, B.S., Cordon-Cardo, C., Erdjument-Bromage, H., et al. (2007). Ubiquitination Regulates PTEN Nuclear Import and Tumor Suppression. Cell *128*, 141–156.

Turer, A.T., and Scherer, P.E. (2012). Adiponectin: mechanistic insights and clinical implications. Diabetologia *55*, 2319–2326.

Tzivion, G., Dobson, M., and Ramakrishnan, G. (2011). FoxO transcription factors; Regulation by AKT and 14-3-3 proteins. Biochim. Biophys. Acta BBA - Mol. Cell Res. *1813*, 1938–1945.

Unterluggauer, H., Mazurek, S., Lener, B., Hütter, E., Eigenbrodt, E., Zwerschke, W., and Jansen-Dürr, P. (2008). Premature senescence of human endothelial cells induced by inhibition of glutaminase. Biogerontology *9*, 247–259.

(US), N.O.E.I.E.P. on the I., Evaluation, and Treatment of Obesity in Adults (1998). Clinical Guidelines on the Identification, Evaluation, and Treatment of Overweight and Obesity in Adults (National Heart, Lung, and Blood Institute).

Vandekeere, S., Dewerchin, M., and Carmeliet, P. (2015). Angiogenesis Revisited: An Overlooked Role of Endothelial Cell Metabolism in Vessel Sprouting. Microcirculation *22*, 509–517.

Vander Heiden, M.G., Cantley, L.C., and Thompson, C.B. (2009). Understanding the Warburg Effect: The Metabolic Requirements of Cell Proliferation. Science *324*, 1029–1033.

Vanhaesebroeck, B., Guillermet-Guibert, J., Graupera, M., and Bilanges, B. (2010). The emerging mechanisms of isoform-specific PI3K signalling. Nat. Rev. Mol. Cell Biol. *11*, 329–341.

Vanhaesebroeck, B., Whitehead, M.A., and Piñeiro, R. (2016). Molecules in medicine mini-review: isoforms of PI3K in biology and disease. J. Mol. Med. *94*, 5–11.

Vasudevan, K.M., Gurumurthy, S., and Rangnekar, V.M. (2004). Suppression of PTEN Expression by NF-κB Prevents Apoptosis. Mol. Cell. Biol. *24*, 1007–1021.

Vaughan, M., Berger, J.E., and Steinberg, D. (1964). Hormone-sensitive Lipase and Monoglyceride Lipase Activities in Adipose Tissue. J. Biol. Chem. *239*, 401–409.

Vazquez, F., Matsuoka, S., Sellers, W.R., Yanagida, T., Ueda, M., and Devreotes, P.N. (2006). Tumor suppressor PTEN acts through dynamic interaction with the plasma membrane. Proc. Natl. Acad. Sci. U. S. A. *103*, 3633–3638.

Vega, R.B., Huss, J.M., and Kelly, D.P. (2000). The Coactivator PGC-1 Cooperates with Peroxisome Proliferator-Activated Receptor α in Transcriptional Control of Nuclear Genes Encoding Mitochondrial Fatty Acid Oxidation Enzymes. Mol. Cell. Biol. *20*, 1868–1876.

Villena, J.A., Roy, S., Sarkadi-Nagy, E., Kim, K.-H., and Sul, H.S. (2004). Desnutrin, an Adipocyte Gene Encoding a Novel Patatin Domain-containing Protein, Is Induced by Fasting and Glucocorticoids ECTOPIC EXPRESSION OF DESNUTRIN INCREASES TRIGLYCERIDE HYDROLYSIS. J. Biol. Chem. *279*, 47066–47075.

Virolle, T., Adamson, E.D., Baron, V., Birle, D., Mercola, D., Mustelin, T., and de Belle, I. (2001). The Egr-1 transcription factor directly activates PTEN during irradiation-induced signalling. Nat. Cell Biol. *3*, 1124–1128.

Wadden, T.A., Butryn, M.L., and Wilson, C. (2007). Lifestyle Modification for the Management of Obesity. Gastroenterology *132*, 2226–2238.

Wakil, S.J., and Abu-Elheiga, L.A. (2009). Fatty acid metabolism: target for metabolic syndrome. J. Lipid Res. *50*, S138–S143.

Wallez, Y., and Huber, P. (2008). Endothelial adherens and tight junctions in vascular homeostasis, inflammation and angiogenesis. Biochim. Biophys. Acta *1778*, 794–809.

Wang, Q., Liang, B., Shirwany, N.A., and Zou, M.-H. (2011). 2-Deoxy-D-glucose treatment of endothelial cells induces autophagy by reactive oxygen species-mediated activation of the AMP-activated protein kinase. PloS One *6*, e17234.

Wang, S.P., Laurin, N., Himms-Hagen, J., Rudnicki, M.A., Levy, E., Robert, M.-F., Pan, L., Oligny, L., and Mitchell, G.A. (2001). The Adipose Tissue Phenotype of Hormone-Sensitive Lipase Deficiency in Mice. Obes. Res. *9*, 119–128.

Ward, P.S., and Thompson, C.B. (2012). Metabolic Reprogramming: A Cancer Hallmark Even Warburg Did Not Anticipate. Cancer Cell *21*, 297–308.

Warren, C.M., and Iruela-Arispe, M.L. (2010). Signaling circuitry in vascular morphogenesis. Curr. Opin. Hematol. *17*, 213–218.

Wei, X., Schneider, J.G., Shenouda, S.M., Lee, A., Towler, D.A., Chakravarthy, M.V., Vita, J.A., and Semenkovich, C.F. (2011). De Novo Lipogenesis Maintains Vascular Homeostasis through Endothelial Nitric-oxide Synthase (eNOS) Palmitoylation♦. J. Biol. Chem. *286*, 2933–2945.

Weir, J.B. de V. (1949). New methods for calculating metabolic rate with special reference to protein metabolism. J. Physiol. *109*, 1–9.

Whelan, J.T., Forbes, S.L., and Bertrand, F.E. (2007). CBF-1 (RBP-Jk) Binds to the PTEN Promoter and Regulates PTEN Gene Expression. Cell Cycle *6*, 80–84.

Whiteman, D.C., Zhou, X.-P., Cummings, M.C., Pavey, S., Hayward, N.K., and Eng, C. (2002). Nuclear PTEN expression and clinicopathologic features in a population-based series of primary cutaneous melanoma. Int. J. Cancer *99*, 63–67.

Wilhelm, K., Happel, K., Eelen, G., Schoors, S., Oellerich, M.F., Lim, R., Zimmermann, B., Aspalter, I.M., Franco, C.A., Boettger, T., et al. (2016). FOXO1 couples metabolic activity and growth state in the vascular endothelium. Nature *529*, 216–220.

Wong, K.-K., Engelman, J.A., and Cantley, L.C. (2010). Targeting the PI3K signaling pathway in cancer. Curr. Opin. Genet. Dev. *20*, 87.

Wu, G., Haynes, T.E., Li, H., and Meininger, C.J. (2000). Glutamine metabolism in endothelial cells: ornithine synthesis from glutamine via pyrroline-5-carboxylate synthase. Comp. Biochem. Physiol. A. Mol. Integr. Physiol. *126*, 115–123.

Wu, J., Boström, P., Sparks, L.M., Ye, L., Choi, J.H., Giang, A.-H., Khandekar, M., Nuutila, P., Schaart, G., Huang, K., et al. (2012). Beige Adipocytes are a Distinct Type of Thermogenic Fat Cell in Mouse and Human. Cell *150*, 366–376.

Xu, K., and Cleaver, O. (2011). Tubulogenesis during blood vessel formation. Semin. Cell Dev. Biol. *22*, 993–1004.

Yan, Q.-W., Yang, Q., Mody, N., Graham, T.E., Hsu, C.-H., Xu, Z., Houstis, N.E., Kahn, B.B., and Rosen, E.D. (2007). The Adipokine Lipocalin 2 Is Regulated by Obesity and Promotes Insulin Resistance. Diabetes *56*, 2533–2540.

Yang, X., Lu, X., Lombès, M., Rha, G.B., Chi, Y.-I., Guerin, T.M., Smart, E.J., and Liu, J. (2010). The G0/G1 Switch Gene 2 Regulates Adipose Lipolysis through Association with Adipose Triglyceride Lipase. Cell Metab. *11*, 194–205.

Yoshimi, A., Goyama, S., Watanabe-Okochi, N., Yoshiki, Y., Nannya, Y., Nitta, E., Arai, S., Sato, T., Shimabe, M., Nakagawa, M., et al. (2011). Evi1 represses PTEN expression and activates PI3K/AKT/mTOR via interactions with polycomb proteins. Blood *117*, 3617–3628.

Yu, Z., Fotouhi-Ardakani, N., Wu, L., Maoui, M., Wang, S., Banville, D., and Shen, S.-H. (2002). PTEN associates with the vault particles in HeLa cells. J. Biol. Chem. *277*, 40247–40252.

Zechner, R., Kienesberger, P.C., Haemmerle, G., Zimmermann, R., and Lass, A. (2009). Adipose triglyceride lipase and the lipolytic catabolism of cellular fat stores. J. Lipid Res. *50*, 3–21.

Zhang, Y., Proenca, R., Maffei, M., Barone, M., Leopold, L., and Friedman, J.M. (1994). Positional cloning of the mouse obese gene and its human homologue. Nature *372*, 425–432.

Zhou, G.-L., Tucker, D.F., Bae, S.S., Bhatheja, K., Birnbaum, M.J., and Field, J. (2006). Opposing Roles for Akt1 and Akt2 in Rac/Pak Signaling and Cell Migration. J. Biol. Chem. *281*, 36443–36453.

Zhu, Y., Hoell, P., Ahlemeyer, B., and Krieglstein, J. (2006). PTEN: A crucial mediator of mitochondria-dependent apoptosis. Apoptosis *11*, 197–207.

Zimmermann, R., Strauss, J.G., Haemmerle, G., Schoiswohl, G., Birner-Gruenberger, R., Riederer, M., Lass, A., Neuberger, G., Eisenhaber, F., Hermetter, A., et al. (2004). Fat Mobilization in Adipose Tissue Is Promoted by Adipose Triglyceride Lipase. Science *306*, 1383–1386.